Radical grafting of polyolefins onto multi-walled carbon nanotubes : model study and application to manufacture PE & PP composites

Sohaib Akbar

N° d'ordre : 151-2010 Année 2010

THESE

Présentée

Devant l'UNIVERSITE CLAUDE BERNARD - LYON 1

Pour l'obtention

Du DIPLOME DE DOCTORAT

Spécialité « MATERIAUX POLYMERES ET COMPOSITES »

(Arrêté du 7 août 2006)

Présentée et soutenue publiquement le

16 septembre 2010

Par

Sohaib Akbar

Ingénieur Chimiste

Greffage radicalaire de polyoléfines sur les nanotubes de carbone multi-parois : l'étude modèle et l'application pour la fabrication de composites PE et PP

Radical grafting of polyolefins onto multi-walled carbon nanotubes: Model study and application to manufacture PE & PP composites

JURY :

Prof. Philippe Cassagnau, *Université Lyon 1*, Président

Dr. Emmanuel Beyou, *Université Lyon 1*, Directeur de thèse

Prof. Philippe Chaumont, *Université Lyon 1*, Co-directeur

Dr. Didier Gigmes, *Université Aix-Marseille I*, Rapporteur

Dr. Philippe Poulin, *Centre de Recherche Paul Pascal, Bordeaux*, Rapporteur

Dr. Jean-Jacques Flat, *ARKEMA-Serquigny*, Examinateur

UNIVERSITE CLAUDE BERNARD - LYON 1

Président de l'Université	**M. le Professeur L. Collet**
Vice-président du Conseil Scientifique	M. le Professeur J-F. Mornex
Vice-président du Conseil d'Administration	M. le Professeur G. Annat
Vice-président du Conseil des Etudes et de la Vie Universitaire	M. le Professeur D. Simon
Secrétaire Général	M. G. Gay

COMPOSANTES SANTE

Faculté de Médecine Lyon Est – Claude Bernard	Directeur : M. le Professeur J. Etienne
Faculté de Médecine Lyon Sud – Charles Mérieux	Directeur : M. le Professeur F-N. Gilly
UFR d'Odontologie	Directeur : M. le Professeur D. Bourgeois
Institut des Sciences Pharmaceutiques et Biologiques	Directeur : M. le Professeur F. Locher
Institut des Sciences et Techniques de Réadaptation	Directeur : M. le Professeur Y. Matillon
Département de Biologie Humaine	Directeur : M. le Professeur P. Farge

COMPOSANTES ET DEPARTEMENTS DE SCIENCES ET TECHNOLOGIE

Faculté des Sciences et Technologies	Directeur : M. le Professeur F. Gieres
Département Biologie	Directeur : M. le Professeur C. Gautier
Département Chimie Biochimie	Directeur : Mme le Professeur H. Parrot
Département GEP	Directeur : M. N. Siauve
Département Informatique	Directeur : M. le Professeur S. Akkouche
Département Mathématiques	Directeur : M. le Professeur A. Goldman
Département Mécanique	Directeur : M. le Professeur H. Ben Hadid
Département Physique	Directeur : Mme S. Fleck
Département Sciences de la Terre	Directeur : M. le Professeur P. Hantzpergue
UFR Sciences et Techniques des Activités Physiques et Sportives	Directeur : M. C. Collignon
Observatoire de Lyon	Directeur : M. B. Guiderdoni
Ecole Polytechnique Universitaire de Lyon 1	Directeur : M. le Professeur J. Lieto
Institut Universitaire de Technologie de Lyon 1	Directeur : M. le Professeur C. Coulet
Institut de Science Financière et d'Assurance	Directeur : M. le Professeur J-C. Augros
Institut Universitaire de Formation des Maîtres	Directeur : M R. Bernard

"Il n'existe pas une catégorie de sciences auxquelles on puisse donner le nom de sciences appliquées. Il y a la science et les applications de la science, liées entre elles comme le fruit à l'arbre qui l'a porté"

Louis Pasteur (1822–95)

"The important thing in science is not so much to obtain new facts as to discover new ways of thinking about them."

Sir William Henry Bragg (1862–1942)

TABLE OF CONTENTS

ABSTRACT

Carbon nanotubes (CNTs) as filler are particularly interesting because they possess very high aspect ratio (length/diameter), typically up to 10,000. Hence, they can form conductive path in polymer matrix at much lower concentrations (below 5%), whereas in case of carbon black filler more than 20wt% loading is needed. However, the development of applications based on nanotubes with high value addition has been hampered by processing limitations resulting from the difficulty of dispersing in a polymeric medium. The formation of aggregates or bundles of nanotubes into host polymer do not allow obtaining homogeneous mixtures. The solution lies in the functionalisation of nanotubes with polymer chains to reduce the effect of interactions between CNTs and better compatibility with the host polymer in the mixture. Here, in this study, we aim to functionalise carbon nanotubes by using a polyolefin grafting procedure involving radical 'grafting onto'. The radical grafting reaction was performed in the presence of dicumyl peroxide used as a hydrogen abstracter. The major drawback of this strategy is its radical grafting selectivity associated with a very short lifetime of radicals which leads coupling reactions and β-scission. We, therefore, carried out a study with pentadecane as a model compound to facilitate analysis of reaction products by conventional techniques. The radical grafting of pentadecane on carbon nanotubes has been verified by Raman spectroscopy and quantitatively confirmed by elemental and thermogravimetric analysis (30% grafting of pentadecane on nanotubes by weight). The state of dispersion of functionalised carbon nanotubes was investigated by transmission electron microscopy and we have shown an improvement in the stability of suspensions of pentadecane grafted carbon nanotubes in solvents such as DMF, toluene, dichlorobenzene, and xylene. For a grafting density of 1.464 mmol/g, solubility ranged from 1.1mg/mL to 19.2mg/mL depending on the type of the solvent used. The highest solubility was obtained in dichlorobenzene (i.e. 19.2mg/mL). The introduction of nitroxyl radical (TEMPO) in the grafting reaction increased the grafting density of pentadecane onto nanotubes by reducing the coupling reactions which has been shown by gas chromatography coupled with mass spectrometry. In polyethylene medium, the grafting density was evaluated to be around 0.015 $\mu mol.m^{-2}$ at 160°C; and strongly enhanced by the use of oligomers of nitroxide- and thiol-end-functionalised polyethylene. With same procedure, polypropylene has been grafted on the CNTs and the study of nanocomposite containing 3wt% PP grafted nanotubes by TEM did not show any significant improvement in the dispersion of nanotubes in the PP matrix; however, it was observed that aggregate size of CNTs in PP reduced.

ACKNOWLEDGEMENTS

First and foremost, I would like to express my sincere thanks to my principal advisor, Dr Emmanuel Beyou, for his valuable guidance and support throughout my PhD study. From the design of experiments to writing down the manuscript for publication, I've always found him dynamic, energetic and tireless. Without him, this dissertation would not have been possible to complete.

Special thanks to Prof Philippe Cassagnau for his valuable comments, suggestion, ideas and discussion. His passion for research has always remained a source of inspiration for me. My deep gratitude goes to Prof Philippe Chaumont and Dr Royaud-Stevenson Isabelle for very useful discussions. I also appreciate Dr Franck D'Agosto and his team for their cooperation and collaboration which led to interesting findings in this work.

I would like to thank Flavien Melis, Agnès Crépet and Pierre Alcouffe for their invaluable technical assistance. But for their help, I would not have succeeded in doing intricate experiments safely and perfectly.

Big Thanks also go to my friends who stood always by me — come rain or shine — and made this stint unforgettable. I would always cherish these pleasant memories.

I find no words to express gratitude to my family for their never ending support, sacrifice and motivation to achieve this formidable task.

Finally I would like acknowledge support of French embassy in Pakistan, SFERE and Higher Education Commission of Pakistan for providing me this great opportunity that has cultivated in me an aspiration to consistently work hard and to always aim and strive for the best. This experience has not only groomed me as a researcher and empowered me professionally; it has made me a better person.

LIST OF SYMBOLS AND ACRONYMS

2p2p	2-phenyl-2-propanol
ABS	Acrylonitrile–butadiene–styrene
Aceto	Acetophenone
AIBN	1,1'-azobisisobutyronitrile
AIBN	1,1'-azobisisobutyronitrile
BA	n-butyl acrylate
CCVD	Catalytic chemical vapour deposition
CNTs	Carbon nanotubes
Cumyl-g-MWCNTs	Cumyloxyl radicals grafted multi walled carbon nanotutbes
Cumyloxyl.TEMPO-g-MWCNTs	Cumyloxyl and TEMPO radicals grafted multi walled carbon nanotutbes
DCB	1,2-Dichlorobenzene
DMF	N,N-dimethylformamide
DT	dodecanethiol
DWCNTs	Double walled carbon nanotubes
EA	Elemental analysis
FETs	field effect transistors
f-MWCNTs	Functionalised multi walled carbon nanotutbes
FTIR	Fourier transform infrared spectroscopy
GC	Gas chromatography
GC-MS	Gas chromatography mass spectroscopy
HiPCO	High-Pressure CO Conversion
MMA	methyl methacrylate
MWCNTs	Multi walled carbon nanotubes
PE	Polyethylene
PE.TEMPO-g-MWCNTs	MWCNTs functionalisation by LDPE using DCP and TEMPO
$PE_{f\text{-}SH}$-g-MWCNTs	MWCNTs grafted via SH functionalised PE
$PE_{f\text{-}TEMPO}$-g-MWCNTs	MWCNTs grafted via TEMPO functionalised PE
PE-g-MWCNTs	MWCNTs functionalisation by LDPE using DCP
PEI	polyethylene imine
Penta.TEMPO-g-MWCNTs	Pentadecane and TEMPO grafted multi walled carbon nanotubes
Pent-g-MWCNTs	Pentadecane grafted multi walled carbon nanotubes
p-MWCNTs	Pristine multi walled carbon nanotutbes
PP	Polypropylene
PSS	polystyrene sulfonate
PVP	polyvinyl pyrrolidone
SWCNTs	Single wall carbon nanotubes
SWCNTs	Single walled carbon nanotubes
TEM	Transmission electron microscopy
TGA	Thermogravimetric analysis
THF	Tetrahydrofuran, Oxacyclopentane
TMP	Tetramethylpentadecane

Introduction

Polymer systems are widely used due to their unique attributes; however, polymers have lower modulus and strength as compared to metals and ceramics. One way to improve their mechanical properties is to reinforce polymers with inclusions (fibres, whiskers, platelets, or particles). The embedding of inclusions in a host matrix to make composites or filled polymer systems, which gives material properties not achieved by either phase alone, has been a common practice for many years. Using this approach, polymer properties can be improved while maintaining their light weight and ductile nature. Traditionally, composites were reinforced with micron-sized inclusions or fillers. Recently, processing techniques have been developed to allow the size of inclusions to go down to nanoscale. Through alteration/control of the additives at nanoscale level, one is able to maximise the property enhancement of selected polymer system to meet the requirement of current commercial, military and aerospace applications.

Polymer nanocomposites or the more inclusive term, polymer nanostructured materials, represents a radical alternative to these traditional filled polymer systems where the reinforcement is of the order of microns. Among these nanofillers, carbon nanotubes (CNTs) has taken a prominent position in modern filled systems, since the introduction of Carbon nanotubes (CNTs) as additive into polymer systems has resulted in composites exhibiting multifunctional, high performance polymer characteristics beyond what traditional polymeric systems possess.

Nanotubes were first documented in 1991, and the first report on polymer nanocomposites using carbon nanotubes as a filler were published in 1994. Earlier nanocomposites used nanoscale fillers such as carbon blacks, silicas, clays, and carbon nanofibres to improve the mechanical, electrical, and thermal properties of polymers. Carbon nanotubes possess high flexibility, low mass density, and large aspect ratio. CNT have a unique combination of mechanical, electrical, and thermal properties that make nanotubes excellent candidates to substitute or complement the conventional nanofillers in the fabrication of multifunctional polymer nanocomposites. Some nanotubes are stronger than steel, lighter than aluminium, and more conductive than copper. Because of these extraordinary properties of

isolated carbon nanotubes, great enthusiasm exists among researchers around the world as they explore the immense potential of these nanofillers.

These documents address various aspects of nanotubes production, purification, suspension, filling, functionalisation, and applications as well as the fabrication and characterization of polymer nanocomposites with various types of nanotubes. However, there are only a few nanotube-based commercial products in the market at present.

In conclusion, nanotubes/polymer composites offer both great potential and great challenges, marking it as a vibrant area of work for years to come. The improvement and application of these composites will depend on how effectively we can handle the challenges. The significant progress in the understanding of these composite systems within the past few years points towards a bright future.

The most common method for preparing polymer nanotubes composites has been to mix the nanotubes and polymer in a suitable solvent and to evaporate the solvent to form composite film. But to gain the advantages at its best, one needs: (i) high interfacial area between nanotubes and polymer; and, (ii) strong interfacial interaction. Unfortunately this solvent technique does not help much in achieving these targets; and as a result a nanocomposite having properties much inferior to theoretical expectations are obtained.

In order to obtain higher contact area between nanotubes and polymer, the issue of dispersion needs to be addressed. Uniform dispersion of these nanotubes produces immense internal interfacial area, which is the key to enhancement of properties of interest. On the other hand modification of nanotubes surface through functionalisation is required for creating an effective interaction with the host matrix and to make nanotubes soluble and dispersible [1].

Despite the availability of considerable research work (figure 1), one of the greatest impediments to progress is that all known preparations of CNT give mixtures of nanotube chiralities, diameters, and lengths along with different amount of impurities and structural defects. These parameters vary significantly both within a

[1] Polymer Nanocomposites by Joseph H Koo. McGraw-Hill Ed 1st (2006).

sample and between samples from different batches and laboratories. Thus, it is very difficult to conduct reproducible controlled experiments with these inconsistent nanofillers and virtually impossible to compare results between different researchers [1].

Polyethylene (PE) is one of the most common materials in our daily lives and accounts for 40% of the total volume of world production of plastic materials. From the chemical point of view, it is a basic material, or better a semi-finished industrial material used as a raw material by companies that transform it into a range of finished goods, form the most basic to the highly sophisticated. The addition of nanotubes to PE would results in widening the range of its application in high-tech products and cutting-edge technology.

We selected 'grafting onto' approach to covalently bond PE on the surface of nanotubes which would assist in achieving the goals of a high degree of dispersion and a robust interfacial interaction between the two phases of the composite. We employed a systematic model compound study, prior to surface modification of nanotubes with PE, because of the following motives:

- To establish an optimised model for PE grafting onto nanotubes.
- To foresee the extent of side reactions and attempt to minimise it.
- To check the effects of reaction conditions on the degree of grafting.
- To perform extensive characterisation, which might be difficult in case of PE.
- To examine the compatibility of surface modified nanotubes with various organic solvents.

For this purpose we selected pentadecane as our model compound, which offers ease in experimentation and represents the characteristics of PE. After this simulation study with pentadecane, we employed this model for PE grafting onto nanotubes.

In the course of experimentation with model compound, we thoroughly investigated the undesired reactions taking place on the sidelines of the main reaction. We examined the radical preferences for combination and addition to gain a better understanding of the radical chemistry of the grafting reaction. Some blank samples were also prepared to use as reference to verify some crucial findings.

The literature review carried out in chapter 1 outlines the research work carried out in the field of filled polymer systems and gives an insight into the methods adopted to make filled polymer systems more efficient. It also presents a comprehensive overview of the emerging techniques for preparing nanotubes/polymer composites which are believed to broaden the use of polymer nanocomposites' in high-tech applications.

The idea of Polyolefin's grafting on nanotubes is implemented stepwise in chapter 2. Starting with a simple model compound approach in chapter 2, we attempted to restrain the undesired side reactions by means of a radical scavenger (TEMPO) in chapter 3. Chapter 4 applies the established model in chapter 2 and 3 for PE grafting to nanotubes. Chapter 5 presents a parallel study on the similar lines for polypropylene (PP) grafting on nanotubes. This study was carried out with the participation of a post-doc researcher.

Finally, chapter 6 presents the original contribution of this dissertation and also outline the future work and application of this piece of research. A comprehensive summary of the thesis in French has been added at the end of the thesis.

Chapter 1

Literature review

This review is written with purpose to obtain a general understanding of various techniques used for the functionalisation of carbon nanotubes (CNTs) with polymers. An overview of nanofillers in the field of developing polymer filled nanocomposites, followed by a short glimpse of properties of polymer/CNTs composites is presented. General comprehension of the surface chemistry and modification of nanotubes is also summarised by reviewing recent research work.

1.1 Nanofillers

Nanoscience and nanotechnology include the areas of synthesis, characterisation, exploration, and application of nanostructured and nanosize materials. A decrease in grain size, equivalent to an increase in specific area of the system, indicates not only increase in reactivity but also those physical properties are no longer dominated by the physics of the bulk materials. Therefore individual nanofillers exhibit greater mechanical and electrical properties [1].

Dimensionally there different types of nanofillers are generally used in preparation of polymer nanocomposites. The first type of nanofillers has only one dimension may be in the nanometre range. They possess a platelet like structure. The lateral dimension may be in the range of several hundred nanometres to microns, while the thickness is usually less than 100 nm. Nanoclay is the example of this type of nanofillers.

The second type of nanofillers has two dimensions in the nanometre scale while the third dimension is larger than few hundred nanometres in size. They possess an elongated structure. Carbon nanotubes and nanocellulose fibre belong to this group. The third type of nanofillers has all three dimensions in the nanometre scale, for example, spherical silica and metals nanoparticles. The nanoparticles can also be classified into two different classes based on their aspect ratio. Theses are high- and low- aspect ratio nanoparticles. High aspect ratio nanoparticles include nanotubes and

nanowires, with various shapes, such as helices, zigzags, belts, rod, etc. Small-aspect ratio morphologies include spherical, oval, cubic, prism, helical, or pillar. Collections of many particles exist as powders, suspensions, or colloids. Thus nanosize thin layered aluminonsilicates or nanoclays, a large number of nanometals and their oxides, carbon nanotubes, cellulose nanofibre, etc are used as nanofillers for the preparation of polymer nanocomposites.

1.1.1 Carbon nanotubes

The discovery of carbon nanotubes were reported by Iijima *et al* in 1993 [2]. Remarkable progress has been made in the ensuing years from the discovery of two basic types of nanotubes (single-walled and multi-walled) to realistic practical application.

1.1.1.1 Types and manufacturing

They are generally prepared by high temperature processes such as arc discharge, laser ablation [3,4], and low temperature processes such as chemical vapour deposition techniques [5]. Nanotubes can be single-walled or multi-walled (figure 1-1).

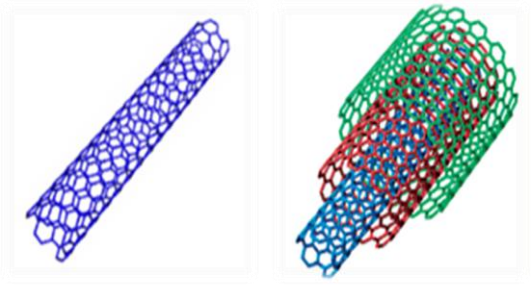

Figure 1-1: Structure of carbon nanotubes: single-walled (a); multi-walled (b).

Various techniques are used for the preparation of nanotubes; each having its own positive and negative aspects. The following table (1-1) summarises these techniques.

Table 1-1: Preparation Techniques of Carbon Nanotubes.

Nanotubes	Technique	Final Product Characteristics
Multiwalled	Carbon arc [6]	Fractal structure consisting of aligned fibers made of aligned nanotubes and nanotubes bundles (low yield)
Multiwalled	Catalytic vapour deposition [7]	Curved and entangled nanotubes with good uniformity of size (higher yield than carbon arc)
Multiwalled	Microwave plasma-enhanced CVD [8]	Aligned nanotubes
Multiwalled	Hot-filament-enhanced CVD [9]	Aligned nanotubes
Single walled	Electric arc [10]	Web-like structure
Single walled	Laser ablation [11]	Hexagonal ropes arrangement (70–90 vol%)
Single walled	Solar furnace [12]	Structure similar to the electric arc with purity level depending on the furnace power
Single walled	Catalytic CVD [13]	Straight and open-ended short nanotubes

Among these techniques, arc discharge method is widely used and it produces good quality CNTs. In this technique a current of 50 amperes between two graphite electrodes in a helium atmosphere is applied. This causes the graphite to vaporise, parts of which are condensed on the walls on reaction vessel and parts are condensed on the cathode. This cathode condensed vapour is MWCNTs. The SWCNTs are produced similarly when Co and Ni or some other metals are used to the anode.

CVD is a common method for the commercial production of carbon nanotubes. For this purpose, the metal nanoparticles (Co, Fe, Ni) are mixed with a catalyst support such as MgO or Al_2O_3 to increase the surface area for higher yield of the catalytic reaction of the carbon feedstock with the metal particles [14]. One issue in this synthesis route is the removal of the catalyst support via an acid treatment, which sometimes could destroy the original structure of the carbon nanotubes. Different modifications in CVD process have shown potential for improving manufacturing process. For instance, plasma enhanced chemical vapour deposition process ensures the vertical aligned growth of nanotubes [15] and water-assisted chemical vapour deposition process in which the activity and life of the catalyst are enhanced by addition of water into the CVD reactor.

In 2007, researchers at the University of Cincinnati developed a process to grow aligned carbon nanotubes arrays of 18 mm length in their carbon nanotubes growth system.

Carbon nanotubes are cylindrical sheets of carbon atom and can be thought of as a rolled up sheet of graphite. Depending on how the sheet is rolled into a tube, different nanotube structures are produced. Figure 1-2 shows several types of nanotubes, each with a different atomic structure.

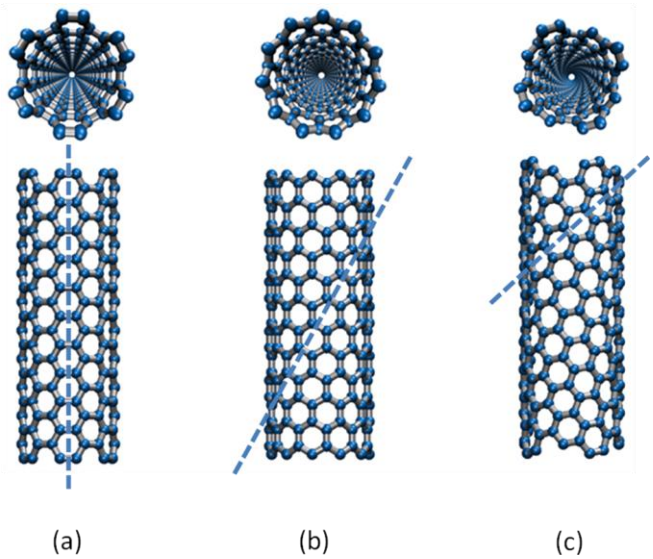

Figure 1-2: Based on the rolling angle, three types of nanotubes are possible: armchair (a); zigzag (b); and chiral (c).

The structures can be clearly distinguished by looking at the cross-section or along the axis of the nanotube. The structure of a SWCNT can be conceptualised by wrapping a one-atom-thick layer of graphite called graphene into a seamless cylinder. The nanotube's chirality, along with its diameter, determines its electrical properties. The armchair structure has metallic characteristics. Both zigzag and chiral structures produce band gaps, making these nanotubes semiconductors. Most SWCNTs have a diameter of close to 1 nanometre, with a tube length that can be many thousands of times longer. A MWCNT consist of multiple rolled layers (concentric tubes) of graphite. There are two models which can be used to describe the structures of multi-walled nanotubes. In the Russian Doll model, sheets of graphite are arranged in concentric cylinders, e.g. a (0,8)

SWCNT within a larger (0,10) single-walled nanotube. In the Parchment model, a single sheet of graphite is rolled in around itself, resembling a scroll of parchment or a rolled newspaper. The interlayer distance in multi-walled nanotubes is close to the distance between graphene layers in graphite, approximately 3.4 Å.

The special place of double-walled carbon nanotubes (DWNTs) must be emphasised here because their morphology and properties are similar to SWCNTs but their resistance to chemicals is significantly improved. This is especially important when functionalisation is required (this means grafting of chemical functions at the surface of the nanotubes) to add new properties to the CNT. In the case of SWCNTs, covalent functionalisation will break some C=C double bonds, leaving 'holes' in the structure on the nanotube and thus modifying both its mechanical and electrical properties.

1.1.1.2 Characteristics

Nanotubes bear unique properties that make them an extremely important class of nanostructured materials. Some important electrical and mechanical characteristics of carbon nanotubes are shown in Table 1-2.

Table 1-2: Theoretical and experimental properties of carbon nanotubes [16].

Property	CNTs	Graphite
Specific gravity	0.8 g/cm^3 for SWCNT; 1.8 g/cm^3 for MWCNT (theoretical)	1.16 g/cm^3
Elastic modulus	≈1 TPa for SWCNT; ≈0.3–1 TPa for MWCNT	1 TPa (in-plane)
Strength	50–500 GPa for SWCNT; 10–60 GPa for MWCNT	
Resistivity	5–50 μΩ cm	50 μΩ cm (in-plane)
Thermal conductivity	3000 W m^{-1} K^{-1} (theoretical)	3000 W m^{-1} K^{-1} (in-plane), 6 W m^{-1} K^{-1} (*c*-axis)
Magnetic susceptibility	11 × 10^6 EMU/g (perpendicular with plane), 0.5 × 10^6 EMU/g (parallel with plane)	
Thermal expansion	Negligible (theoretical)	−1 × 10^{-6} K^{-1} (in-plane), 19 × 10^{-6} K^{-1} (*c*-axis)
Thermal stability	>700 °C (in air); 1800 °C (in vacuum)	

It is clear that CNTs have unique mechanical, electrical, magnetic, optical and thermal properties. In some special applications, such as space explorations, high-performance lightweight structural materials are required, and they can be developed by adding CNTs to polymers or other matrix materials. Moreover, although graphite is a semi-metal, CNTs can be either metallic or semi-conducting due to the topological defects from the fullerene-like end caps in CNTs (pentagons in a hexagonal lattice). Thus, the physico-mechanical properties of CNTs are dependent upon their dimensions, helicity or chirality.

1.1.1.3 End and defect-site Chemistry

The end caps of nanotubes (when not closed by the catalyst particle) tend to be composed of highly curved (and hence, unstable) fullerene like hemispheres, which are therefore highly reactive, as compared with the sidewalls [17,18]. The sidewalls themselves contain defect sites (figure 1-3) such as pentagon-heptagon pairs called Stone-Wales defects, sp hybridized defects, and vacancies in the nanotube lattice [19]. Frequently, these intrinsic defects are supplemented by oxidative damage to the nanotube framework by strong acids which leave holes functionalised with oxygenated functional groups such as carboxylic acid, ketone, alcohol, and ester groups [20].

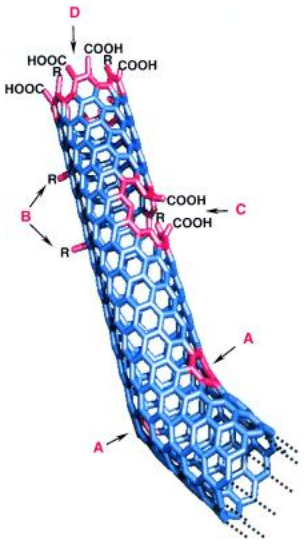

Figure 1-3: Typical defects in a SWNT. A) Five-or seven-membered rings in the carbon framework, instead of the normal six-membered ring, leads to a bend in the tube. B) sp^3-hybridized defects (R = H and OH). C) Carbon framework damaged by oxidative conditions, which leaves a hole lined with -COOH groups. D) Open end of the SWNT, terminated with COOH groups. Besides carboxy termini, the existence of which has been unambiguously demonstrated, other terminal groups such as —NO_2, OH, H, and ═O are possible [21].

1.1.1.4 Covalent sidewall functionalisation

Whereas fullerenes have a well developed addition chemistry [22], sidewall functionalisation of carbon nanotubes has only been achieved relatively recently [23]. In CNTs the chemical reactivity in strained carbon systems arises from two factors: a) pyramidalisation at the carbon atom, and b) n-orbital misalignment between adjacent carbon atoms [24]. Smaller diameter tubes are expected to be more reactive than larger diameter tubes. The high degree of chemical functionalisation possible through covalent sidewall derivatisation makes these routes ideal for applications such as composite formation. However, one disadvantage of these reactions is that they usually result in the loss of the intrinsic electronic structure.

It has been predicted that covalent chemical attachments can decrease the maximum buckling force of SWCNTs by as much as 15%, regardless of tube helical structure or radius [25]. A threefold decrease in thermal conductivity, due to a decrease in the phononscattering length, was calculated to occur upon 1% sidewall functionalisation of

SWCNTs with phenyl groups [26]. Numerous diverse ways of nanotubes functionalisation have been reported in literature (figure 1-4).

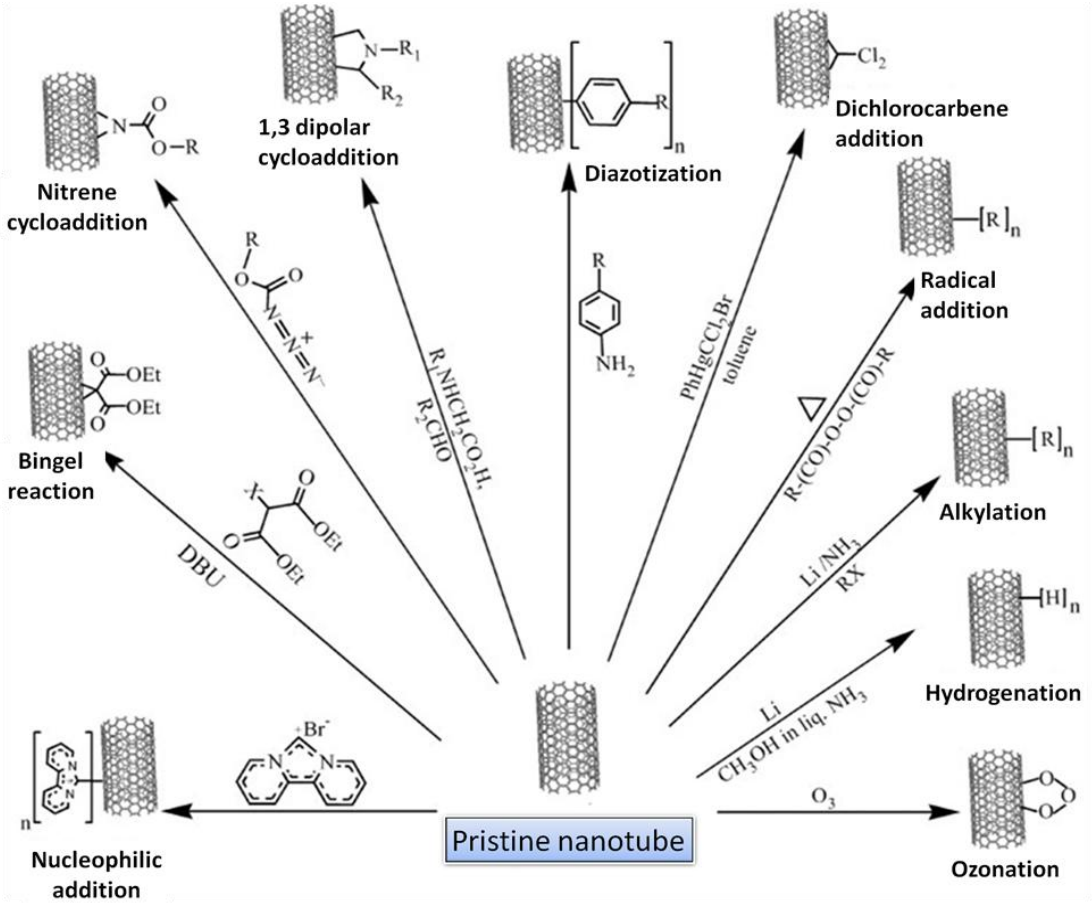

Figure 1-4: Schematic describing some covalent sidewall functionalisation reactions of nanotubes. Some typical examples are: ozonation [27], hydrogenation [28], alkylation [29], radical addition [30], dichlorocarbene addition [31], diazotization [32], 1,3 dipolar cycoladdition [33], nitrene cycloaddition [34], Bingel reaction [35], nucleophilic addition [36].

1.1.1.5 Price, production and safety aspects

The safety and bio-compatibility of nanotubes is a debatable question. However, nanotubes cytotoxic properties appear situational, depending highly on the degree and type of functionalisation, aggregation state and the presence of metal catalyst particles remaining from synthesis [37]. Fortunately, nanotubes may be toxic in the free state but they are not at all toxic in the fixed structured or in bound state. As in polymer

nanocomposites, the nanotubes are in bound state so they are not toxic. But they could release and become harmful because of the decomposition, degradation or wear and tear of nanocomposites .However the preparation processes should ensure minimum exposure to nanotubes. MWCNTs are generally easier to make at large scale and thus less expensive as compared to single walled. Product developers are using MWCNTs for their high thermal conductivity and to add mechanical strength and electrical conductivity to polymer composites [38]. A decade ago, carbon nanotubes were sold primarily in tiny research quantities for hundreds or thousands of dollars per gram. By 2005, MWCNTs prices had come down to several hundred dollars per kilogram. Prices are expected to fall even further as capacity continues to rise.

There are over 85 companies in the carbon nanotubes market, making it extremely competitive. Several major players are building commercial levels of capacity and bringing prices down significantly. Major market players are Hyperion Catalysis, Arkema, Thomas Swan, Bayer Material Science, and Showa Denko. All these companies are large materials and chemicals companies. The main markets at present are electronics and data storage, defence, aerospace and automotive. Arkema is one of the biggest producers of nanotubes. Their recent R&D activity and patents show worldwide interest in large-scale manufacturing for commercial products [39,40,41].

1.2 Polymer Carbon nanotubes composites

1.2.1 Need for surface modification of nanotubes

Despite many advantages such as high mechanical, electrical, and thermal properties of nanotubes, their homogeneous dispersion in polymer matrix has been a problem to get high performance nanocomposites. This is because of strong interfacial interactions in the form of electrostatic and van der Waals interactions between the layers of CNTs. The poor dispersion leads to rope like aggregates or bundles of nanotubes, which slide

against each other instead of enhancing a load transfer capacity to the host polymer. As nanotubes do not have any functionality and surface is very uniform, so it is difficult to get any interaction with polymer matrix as well as a uniform dispersion. So to overcome these problems, they need to be modified. They are generally modified to generate some functional groups on their outer surface without much damaging the structure. These surface modified nanotubes could further be used to attach other chemical moieties of interest for different purposes. Different strategies have been adopted to integrate nanotubes into different host systems. The main approaches for modification can be grouped into two main categories: (a) the covalent attachment of chemical groups through reactions onto the π-conjugated skeleton of CNT; (b) the noncovalent adsorption or wrapping of various functional molecules. SWCNTs generally have a higher degree of perfection than MWCNTs; however, apart from different physical properties, both types are believed to respond equally to chemical surface modifications (covalent or noncovalent).

The covalent attachment of functional groups to the surface of nanotubes can improve the efficiency of load transfer. However, it must be noted that these functional groups might introduce defects on the walls of the perfect structure of the nanotubes. These defects will lower the strength of the reinforcing component. Therefore, there will be a trade-off between the strength of the interface and the strength of the nanotube filler. The functional groups attached could be small molecules or polymer chains. The chemical functionalisation is an especially attractive target, as it can improve solubility and processibility and allows the unique properties of CNTs to be coupled to those of other types of materials.

1.2.2 Composites processing

Fabrication methods have overwhelmingly focused on improving nanotube dispersion because better nanotube dispersion in the polymer matrices has been found to improve

properties [42]. Similar to the case of nanotube/solvent suspensions, pristine nanotubes have not yet been shown to be soluble in polymers illustrating the extreme difficulty of overcoming the inherent thermodynamic drive of nanotubes to bundle [43]. The methods of solution blending, melt blending, and in situ polymerisation are widely applied to produce nanotube/polymer composites (figure 1-5) [44].

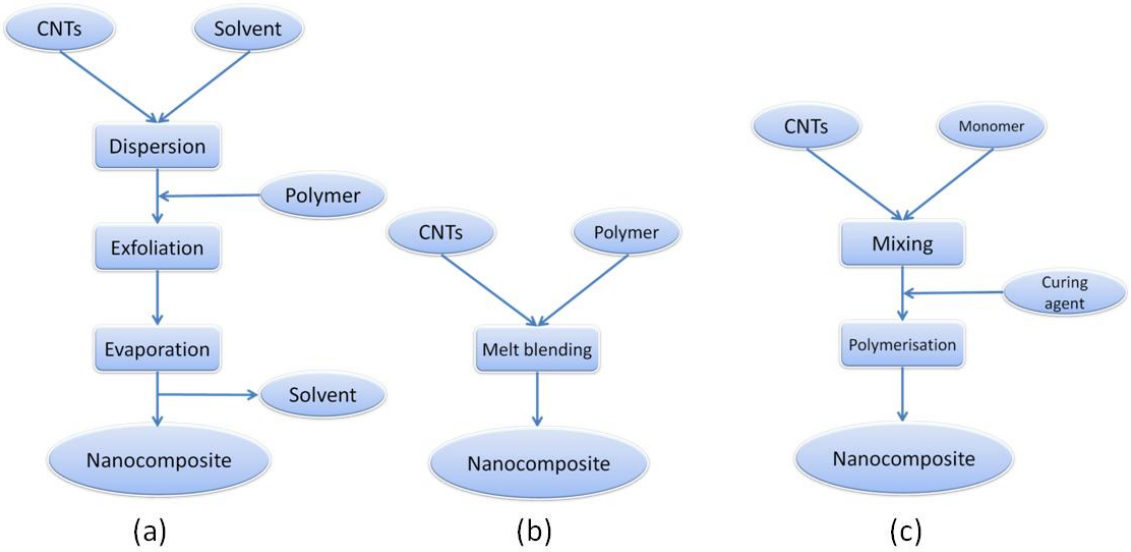

Figure1- 5: Schematic representation of different steps of polymer/CNTs composite processing: solution mixing (a); melt mixing (b); *in situ* polymerisation (c).

1.2.2.1 Solution blending

Perhaps the most common method for preparing polymer nanotube composites has been to mix the nanotubes and polymer in a suitable solvent before evaporating the solvent to form a composite film. One of the benefits of this method is that agitation of the nanotubes powder in a solvent facilitates nanotubes' de-aggregation and dispersion. Almost all solution processing methods are based on a general theme which can be summarised as:

1. Dispersion of nanotubes in either a solvent or polymer solution by energetic agitation.
1. Mixing of nanotubes and polymer in solution by energetic agitation.
3. Controlled evaporation of solvent leaving a composite film.

In general, agitation is provided by magnetic stirring, shear mixing, reflux or ultrasonication. Sonication can be provided in two forms, mild sonication in a bath or high-power sonication using a tip or horn. An early example of solution based composite formation is described by Jin *et al* [45]. By this method, high loading levels of up to 50 wt% and reasonably good dispersions were achieved.

A number of papers have discussed dispersion of nanotubes in polymer solutions [46,47]. This can result in good dispersion even when the nanotubes cannot be dispersed in the neat solvent. Coleman *et al* used sonication to disperse catalytic MWCNT in polyvinylalcohol/H_2O solutions, resulting in a MWCNT dispersion that was stable indefinitely. Films could be easily formed by drop-casting with microscopy studies showing very good dispersion. Cadek *et al* [48] showed that this procedure could also be applied to arc discharge MWCNTs, double walled nanotubes (DWNTs) and High-Pressure CO Conversion (HiPCO) SWCNTs. They also showed that this procedure could be used to purify arc-MWCNTs by selective sedimentation during composite production.

1.2.2.2 Melt mixing

While solution processing is a valuable technique for both nanotube dispersion and composite formation, it is completely unsuitable for the many polymer types that are insoluble. Melt processing is a common alternative method, which is particularly useful for dealing with thermoplastic polymers. This range of techniques makes use of the fact that thermoplastic polymers soften when heated. Amorphous polymers can be processed above their glass transition temperature while semi-crystalline polymers need to be heated above their melt temperature to induce sufficient softening. Advantages of this technique are its speed and simplicity, not to mention its compatibility with standard industrial techniques [49,50].

In general, melt processing involves the melting of polymer pellets to form a viscous liquid. Any additives, such as carbon nanotubes can be mixed into the melt by shear mixing. Bulk samples can then be fabricated by techniques such as compression moulding, injection moulding or extrusion. However it is important that processing conditions are optimised, not just for different nanotube types, but for the whole range of polymer–nanotube combinations. This is because nanotubes can affect melt properties such as viscosity, resulting in unexpected polymer degradation under high shear rates [51].

In two papers in 2001 Andrews and co-workers [52] showed that commercial polymers such as high impact polystyrene, polypropylene and acrylonitrile–butadiene–styrene (ABS) could be melt processed with CVD-MWCNT to form composites. The polymers were blended with nanotubes at high loading level in a high shear mixer to form master batches. A similar combination of shear mixing and compression moulding was also used by a number of other groups [53,54]. Injection moulding has also been used to fabricate composites. Meincke *et al* [55] mixed polyamide-6, ABS and CVD-MWCNT in a twin screw extruder at 160 °C. Another example of using combined techniques was demonstrated by Tang *et al* [56]. High density polyethylene pellets and nanotubes were melted in a beaker, then mixed and compressed. The resulting solid was broken up and added to a twin screw extruder at 170 °C and extruded through a slit die. The resulting film was then compression moulded to form a thin film.

1.2.2.3 In Situ Polymerisation

This fabrication strategy starts by dispersing nanotubes in monomer followed by polymerising the monomers. As with solution blending, functionalised nanotubes can improve the initial dispersion of the nanotubes in the liquid (monomer, solvent) and consequently in the composites. Furthermore, in situ polymerisation methods enable covalent bonding between functionalised nanotubes and the polymer matrix using

various condensation reactions. Initially, in situ radical polymerisation was applied for the synthesis of PMMA composites by Jia *et al* [54]. In this work, the reaction was performed using radical initiator 1,1'-azobisisobutyronitrile (AIBN). The authors suggested that π-bonds of the CNT graphitic network were opened by the radical fragments of initiator and therefore the carbon nanostructures could participate in PMMA polymerisation by acting as efficient radical scavengers. If all reactants were mixed simultaneously, the growth of polymer chains was inhibited since many of the initiator molecules would be consumed by the CNTs.

By using an improved in situ process [57,58], in which CNT material is added a little time after the mixing of initiator and monomer, longer polymer chains were obtained in the resulting composite, giving rise to better mechanical properties of the composites. Concerning the preparation of anisotropic CNT–polymer composites, Kimura *et al* [59] have mixed styrene monomer with nanotubes and subjected the suspension to a constant magnetic field of 10 T. By polymerising the mixture, the nanotubes were found to be kept aligned within the polymer matrix.

Epoxy nanocomposites comprise the majority of reports using in situ polymerisation methods [60,61], where the nanotubes are first dispersed in the resin followed by curing the resin with the hardener. Zhu *et al* [62] prepared epoxy nanocomposites by this technique using end-cap carboxylated SWCNTs and an esterification reaction to produce a composite with improved tensile modulus (E is 30% higher with 1 wt % SWCNT). Note that as polymerisation progresses and the viscosity of the reaction medium increases, the extent of *in situ* polymerisation reactions might be limited. Noteworthy extensions of *in situ* polymerisation include infiltration methods in which the reactive agents are introduced into a nanotube structure and subsequently polymerised [63,64].

1.2.2.4 Novel methods

Rather than avoid the high viscosities of nanotube/polymer composites, some researchers have decreased the temperature to increase viscosity to the point of processing in the solid state. Solid-state mechanochemical pulverisation processes (using pan milling [65] or twin-screw pulverisation [66]) have mixed MWCNT with polymer matrices. Pulverisation methods can be used alone or followed by melt mixing. Nanocomposites prepared in this manner have the advantage of possibly grafting the polymer on the nanotubes, which account in part for the observed good dispersion, improved interfacial adhesion, and improved tensile modulus.

An innovative latex fabrication method for making nanotube/polymer composites disperses nanotubes in water (SWCNT require a surfactant, MWCNT do not) and then adds a suspension of latex nanoparticles [67,68]. Freeze-drying and subsequent processing of this colloidal mixture produces composites with uniform dispersion of nanotubes even in a highly viscous matrix like high molecular weight polystyrene. This promising method can be applied to polymers that can be synthesised by emulsion polymerisation or formed into artificial latexes, e.g., by applying high-shear conditions [41].

Finally, to obtain nanotube/polymer composites with very high nanotube loadings, Vigolo *et al* [69] developed a 'coagulation spinning' method to produce composite fibers comprising predominately nanotubes. This method disperses SWCNT using a surfactant solution, coagulates the nanotubes into a mesh by wet spinning it into an aqueous poly(vinyl alcohol) solution, and converts the mesh into a solid fiber by a slow draw process. In addition, Mamedov *et al* [70] developed a fabrication method based on sequential layering of chemically modified nanotubes and polyelectrolytes to reduce phase separation and prepared composites with SWCNT loading as high as 50 wt %. In conclusion, interest in polyolefin composites is growing and will continue to grow as new polyolefins are made and as new applications are source for these materials.

1.3 Functionalisation of carbon nanotubes with polymers

CNT are considered ideal materials for reinforcing fibres due to their exceptional mechanical properties. Therefore, nanotube-polymer composites have potential applications in aerospace science, where lightweight robust materials are needed [71]. It is widely recognised that the fabrication of high performance nanotube-polymer composites depends on the efficient load transfer from the host matrix to the tubes. The load transfer requires homogeneous dispersion of the filler and strong interfacial bonding between the two components [72]. To address these issues, several strategies for the synthesis of such composites have been developed. Currently, these strategies involve physical mixing in solution, *in situ* polymerisation of monomers in the presence of nanotubes, surfactant-assisted processing of composites, and chemical functionalisation of the incorporated tubes. As mentioned earlier, in many applications it is necessary to tailor the chemical nature of the nanotube's walls in order to take advantage of their unique properties. For this purpose, two main approaches for the surface modification of CNTs are adopted i.e. covalent and noncovalent. Figure 1-6 depicts a typical representation of such surface modifications.

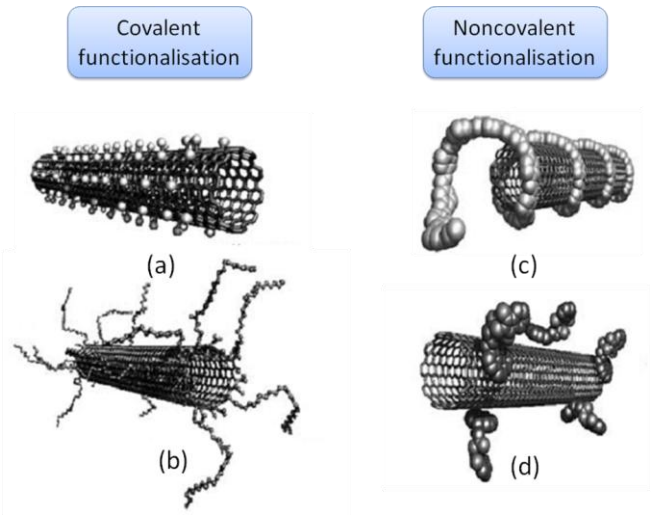

Figure 1-6: Different possibilities for nanotubes' functionalisation: sidewall covalent functionalisation (a); defect-group covalent functionalisation (b); noncovalent polymer wrapping (c); noncovalent pi-stacking (d).

1.3.1 Noncovalent attachment of polymers

The noncovalent attachment, controlled by thermodynamic criteria [73], which for some polymer chains is called wrapping, can alter the nature of the nanotube's surface and make it more compatible with the polymer matrix. The advantage of noncovalent attachment is that the perfect structure of the nanotube is not altered, thus its mechanical properties should not change. The main potential disadvantage of noncovalent attachment is that the forces between the wrapping molecule and the nanotube might be weak, thus as a filler in a composite the efficiency of the load transfer might be low.

1.3.1.1 Polymer wrapping

Bahr *et al* [74] reported that nanotubes could be reversibly solubilised in water by noncovalently associating them with a variety of linear polymers such as polyvinyl pyrrolidone (PVP) and polystyrene sulfonate (PSS). They demonstrated that the association between the polymer and the nanotubes is robust, not dependent upon the presence of excess polymer in solution, and is uniform along the sides of the tubes. Conjugated luminescent polymer poly-{(m-phenylenevinylene)-co-[(1,5-dioctyloxy-p-phenylene)-vinylene]} (PmPV) and its derivatives [75,76,77] have been successfully used for the wrapping around nanotubes on account of stabilising noncovalent bonding interactions, presumably as a result of π–π stacking and van der Waals interactions between PmPV and the surfaces of the nanotubes. Stoddart *et al* [78] also synthesised the Stilbenoid dendrimers, a hyperbranched variant of the PmPV polymer, which exhibits an appropriate degree of branching, and it was found to be more efficient at breaking up nanotube bundles, provided it is employed at higher polymer-to-nanotube ratios than was the 'parent' PmPV polymer. The following figure (1-7) gives an idea of polymer wrapping around nanotubes.

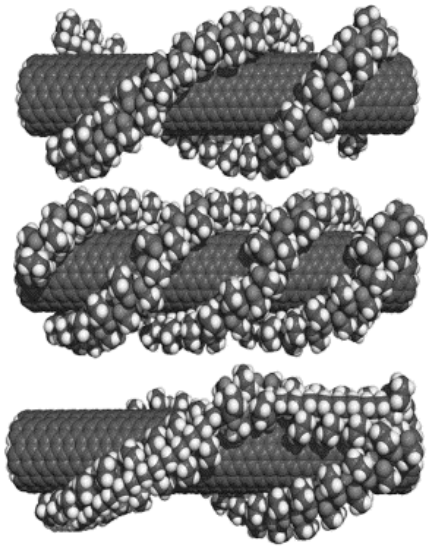

Figure 1-7: Some possible wrapping arrangements of PVP on an 8,8 SWNT. A double helix (top) and a triple helix (middle). Backbone bond rotations can induce switch-backs, allowing multiple parallel wrapping strands to come from the same polymer chain (bottom) [79].

Gum Arabic has also been used to exfoliate the bundles, and stabilise individual carbon nanotubes in aqueous dispersions [80]. It is clear from theses accounts that noncovalent functionalisation of carbon nanotubes can be achieved without disrupting the primary structure of the nanotubes themselves.

1.3.1.2 Polymer absorption

Xia *et al* [81] devised a method to prepare polymer-encapsulated MWCNTs had been successfully prepared through ultrasonically initiated *in situ* emulsion polymerisations of n-butyl acrylate (BA) and methyl methacrylate (MMA) in presence of MWCNT. Another noncovalent method of modifying SWCNTs was developed by encasing the SWCNTs within crosslinked, amphiphilic copolymer micelles [82]. SWCNTs were dispersed in the dimethylformamide (DMF) solutions of amphiphilic poly(styrene)-block-poly(acrylic acid) copolymer. Water was added to the solutions and the poly(styrene)-block-poly(acrylic acid) copolymer wrapped the SWCNTs and formed micelle. Then the PAA blocks of the micellar shells were permanently crosslinked by addition of a water-soluble diamine linker and a carbodiimide activator. This encapsulation significantly enhances the

dispersion of SWCNTs in a wide variety of polar and nonpolar solvents and polymer matrices. In addition, because the copolymer shell is permanently fixed, the encapsulated SWCNTs are stabilised with respect to typical polymer processing and recovery from the polymer matrix.

Moreover, n-Doping of carbon nanotubes by functionalisation of SWCNTs' sidewalls with polymers was prepared by submerging SWCNT in a 10 wt% solution of polyethylene imine (PEI) in methanol for use as field effect transistors (FETs) [83]. Zhang *et al* [84] reported the synthesis of tubular composite of doped polyaniline (PANI) core (c-MWCNTs)-shell (doped-PANI) structures by *in situ* polymerisation of aniline monomers adsorbed on the surface of carboxylic groups contained MWCNT (c-MWCNT). The conductivities of these tubular composites are several times higher than that of PANI without MWCNTs, which will offer new application possibilities. In addition, MWCNTs had been solubilised in water and in various organic solvents by noncovalent side-wall functionalisation by pyrene containing polymers [85].

1.3.2 Covalent attachment of polymers

Covalent functionalisation and surface chemistry of single-walled carbon nanotubes have been envisaged as very important factors for nanotubes processing and applications. Recently, many efforts on polymer composites reinforcement have been focused on an integration of chemically modified nanotubes containing different functional groups into the polymer matrix.

Covalent functionalisation can be realised by either modification of surface-bound carboxylic acid groups on the nanotubes or direct addition of reagents to the sidewalls of nanotubes. As discussed previously, *in situ* polymerisation is also one of the main approaches for the preparation of polymer grafted nanotubes. Therefore, work on the

preparation of polymer grafted nanotubes frequently overlaps with *in situ* polymerisation processing [86].

The covalent reaction of CNT with polymers is important because the long polymer chains help to dissolve the tubes into a wide range of solvents even at a low degree of functionalisation. There are two main methodologies for the covalent attachment of polymeric substances to the surface of nanotubes, which are defined as 'grafting to' and 'grafting from' methods. The former relies on the synthesis of a polymer with a specific molecular weight followed by end group transformation. Subsequently, this polymer chain is attached to the graphitic surface of CNT. A disadvantage of this method is that the grafted polymer contents are limited because of high steric hindrance of macromolecules. The 'grafting from' method is based on the covalent immobilisation of the polymer precursors on the surface of the nanotubes and subsequent propagation of the polymerisation in the presence of monomeric species.

1.3.2.1 'Grafting from' method

The 'grafting from' approach, in general, involves the polymerisation of monomers from surface-derived initiators on either MWCNTs or SWCNTs. These initiators are covalently attached using the various functionalisation reactions developed for small molecules, including acid-defect group chemistry and sidewall functionalisation of CNTs. The advantage of 'grafting from' approach is that the polymer growth is not limited by steric hindrance, allowing high molecular weight polymers to be efficiently grafted. In addition, nanotube–polymer composites with quite high grafting density can be prepared. However, this method requires strict control of the amounts of initiator and substrate as well as accurate control of conditions required for the polymerisation reaction [87].

1.3.2.1.1 Cationic/anionic polymerisation

In situ anionic polymerisation of styrene in the presence of modified SWCNTs was developed by Viswanathan *et al* [88]. Carbanions were introduced onto the SWCNT surface by treatment with the anionic initiator (*sec*-butyllithium) that served to exfoliate the bundles and to provide initiating sites for the polymerisation of styrene (figure 1-8). The PS content in grafted SWCNTs was about 10 wt%, while the PDI of the polymer was about 1.01. A similar method was used for PMMA [89], where PMMA content was around 45 wt% determined by TGA.

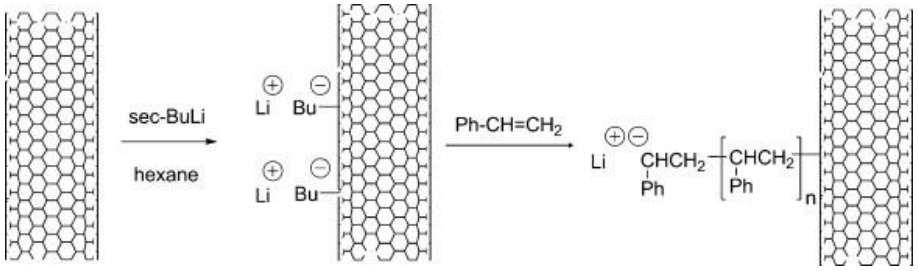

Figure 1-8: Anionic polymerisation of styrene onto carbon nanotubes.

PEI was also grafted onto the surface of MWCNTs by performing a cationic polymerisation of aziridine in the presence of amine-functionalised MWCNTs [90]. The obtained PEI had a dendritic structure with primary, secondary, and tertiary amines in a molar ratio of about 1:1:1.

Moreover, polytetramethylene ether was chemically anchored to the surface of MWCNTs by cationic polymerisation of THF starting from acyl chloride-functionalised MWCNTs [91]. The polymer had $M_w \approx 1000$ and PDI of 1.0 after cleaving from nanotube surface. DSC measurements showed a huge increase of the T_g (about 65 °C) in the composite sample, which was attributed to the immobilization of polymer chains onto the CNT sidewalls.

1.3.2.1.2 Metallocene catalysis polymerisation

Anchored Ziegler–Natta catalyst ($MgCl_1/TiCl_4$) at the surface of oxidized SWCNTs was used for *in situ* polymerisation of ethylene monomer [92]. The prepared SWCNT-PE samples contained 94 wt% of polymer. Similarly, *in situ* polymerisation of ethylene by a highly active metallocene complex anchored onto the nanotube surface was reported [93]. It was observed that by supporting the catalytic system onto MWCNTs, an increase of the ethylene polymerisation rate was seen. The prepared MWCNT–PE composites contained up to 83 wt% of polymer. This method was also used for surface coating of MWCNTs by *in situ* copolymerisation of ethylene and 1-norbornene. Depending on the experimental conditions used (ethylene pressure, solvent, feed 1-norbornene concentration), the relative quantity of ethylene-1-norbornene copolymer could be tuned, as well as the 1-norbornene content in the formed copolymers and accordingly their T_g. Two independent groups used MWCNT-Cp_2ZrCl_2 as catalyst to produce PE by *in situ* polymerisation [94,95]. PDI was determined to be 1.95 with a unimodal curve by GPC. The melting temperature indicated that the obtained PE was high-density polyethylene.

Li *et al* [96] first functionalised SWCNTs with α-alkene groups on their sidewalls and consequently performed metallocene catalysed copolymerisation of ethylene- and alkene-functionalised SWCNTs. The polymer-grafted SWCNTs contained 91.5 wt% of PE. In a similar approach, the preparation of isotactic polypropylene nanocomposites filled with pristine, purified and oxidized MWCNTs was accomplished by polymerisation of propylene with a metallocene/methylaluminiumoxane catalyst [97].

1.3.2.1.3 Free radical polymerisation

MWCNTs purified by oxidative treatment were modified with PMMA chains via an *in situ* radical polymerisation [98,99]. During polymerisation, MWCNTs consumed initiator-

derived radicals which were added to π-bonds of CNT network. As a result, the molecular weight of PMMA increased with the MWCNT content, as the possibility of primary termination reactions were diminished appreciably. The bonding between MWCNTs and PMMA chains was supported by FT-IR spectroscopy. Later on, this procedure was modified, using CNTs as macroinitiator [100]. In the first step, an amount of potassium persulfate was dissolved in hydrogen peroxide solution to obtain grafting of initiator on the CNT surface. In the second step, MMA monomer containing vinyl benzene as crosslinking agent were emulsified and added to solution of activated MWCNTs. In an analogous manner, PMMA chains were grafted on SWCNTs by *in situ* free radical polymerisation in a poor solvent (methanol) for the polymer [101]. The weight loss of PMMA-g-SWCNTs measured by TGA and the solubility in ethyl acetate suggests that an appreciable amount of PMMA (up to 17 wt%) was successfully grafted on SWCNTs after a 3 h reaction. Alternatively, Yue *et al* [102] performed *in situ* polymerisation of MMA in supercritical CO_2. The surfaces of the SWCNTs were first functionalised with amino ethyl methacrylate by amidation of oxidized nanotubes. The supercritical fluid enhanced the diffusivity of monomer and facilitated the growth of tethered PMMA chains. The grafting of oxidized MWCNTs with PS molecules using an *in situ* radical polymerisation reaction was reported by Shaffer and Koziol [103]. The water dispersion of oxidized MWCNTs was combined with styrene monomer and a radical initiator. TEM micrographs of grafted nanotubes revealed a thin polymer coating (figure 1-9).

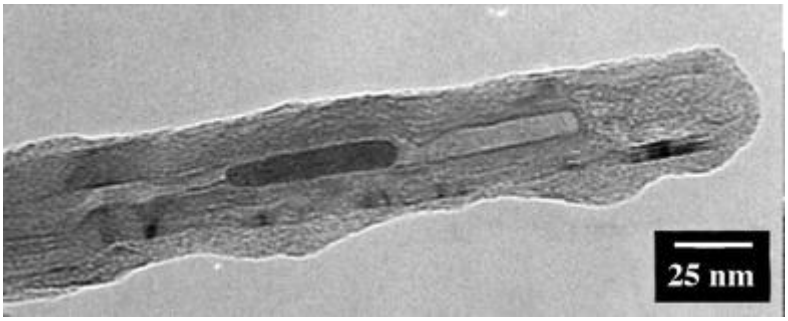

Figure 1-9: TEM micrograph of a typical grafted nanotube where a thin polystyrene coating (5–10 nm) can be seen [100].

Grafting ratios of 50–90% were observed depending on initial nanotube concentration. The grafting efficiency was around 0.5% for the benzoyl peroxide system, but reached 18% in the case of the potassium persulfate initiator. The different grafting efficiencies observed for the two initiators were explained in terms of their solubilities in the organic phase.

In another attempt, an easy method for preparing polymer-grafted multi-walled carbon nanotubes (MWCNTs) with high graft yields was developed by using free radical graft polymerisation from photoinduced surface initiating groups on MWCNTs [104]. Polystyrene, poly(butyl acrylate), poly(methyl methacrylate), and poly(2-hydroxyethyl methacrylate) were successfully grafted onto the surface of MWCNTs with graft yields of 46, 26, 37, and 53 wt.%, respectively, after 15 h of free radical graft polymerisation. Figure 1-10 shows a high resolution TEM image for a polystyrene grafted MWCNT.

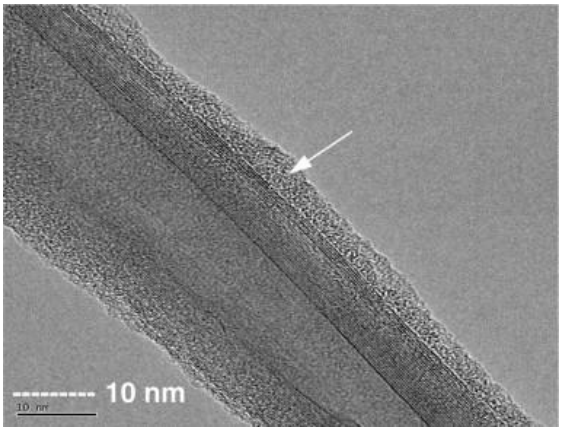

Figure 1-10: Surface of PS-g-MWCNT covered with 4–5 nm thick amorphous polystyrene layer observed via high resolution TEM [101].

In the work of Yang *et al* [105], vinyl modified MWCNTs were synthesized by the amidation of acyl chloride-functionalised MWCNTs and allylamine, followed by the *in situ* free radical polymerisation of styrene to produce MWCNT-g-PS with hairy rod structures. The results showed that 1 of every 100 carbon atoms of MWCNTs was functionalised and grafted by PS with M_w=9800 g/mol (PDI ≈ 1.8). A similar approach was used by Kim *et al* [106] in which vinyl functionalised MWCNTs were obtained by

reaction of hydroxyl terminated MWCNTs with methacryloxypropyl trimethoxysilane. The amount of PS content was estimated by TGA to be about 14%.

PAM was grafted to oxidized MWCNT by an *in situ* UV radiation-initiated polymerisation [107]. The diameter of MWCNT–PAM hybrid nanostructures increased 3–8 times. Qin *et al* [108] reported grafting of P4VP to SWCNTs by *in situ* free radical polymerisation. The composite contained 39 wt% of P4VP, determined by TGA. In the same year, Qin *et al* [109] reported the grafting of SWCNTs by poly(sodium 4-styrenesulfonate) (PSS) using radical polymerisation (figure 1-11). TGA analysis determined 45 wt% of PSS.

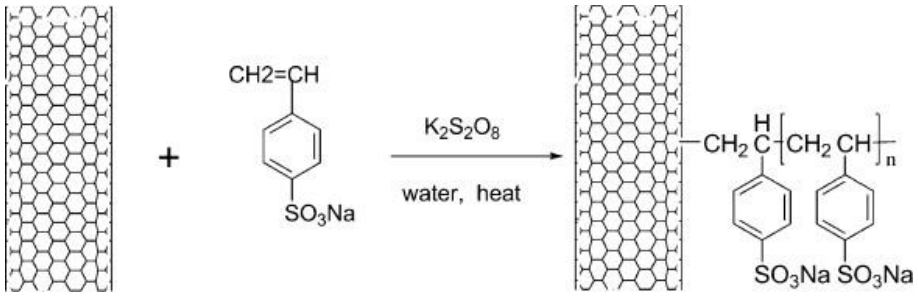

Figure 1-11: Grafting of polystyrene derivate by *in situ* radical polymerisation.

In another account Kumar *et al* [110] oxidised MWCNTs and reacted with HEMA via esterification reaction followed by free radical polymerisation of HEMA. Weight loss measurements in TGA showed that a moderated amount of 10% of PHEMA was grafted by this technique.

A facile strategy to prepare water-soluble MWCNTs by γ-radiation was developed by Chen *et al* [111]. First, MWCNTs were irradiated in ethanol. The radiolysis of ethanol produced many active species such as $\cdot CH_2CH_2OH$ and $\cdot CH(CH_3)OH$ which can react with carbon ethylene bonds on the surface of MWCNTs. Afterwards, PAA was covalently grafted to the surface of modified MWCNTs by radiation in the presence of the vinyl monomer. TEM images provided direct evidence of the formation of a core–shell

structure, and the external diameter of resultant MWCNTs was increased remarkably. The amount of grafted polymer was determined to be about 10 wt%.

Polyvinyltriethoxysilane was grafted to MWCNTs by free radical polymerisation of vinyltriethoxysilane by using benzoyl peroxide as radical initiator [112]. The weight fraction of polymer in functionalised MWCNTs was 35%. In the work of Maity *et al* [113], the different degree of MWCNT and SWCNT efficiency to N-vinyl carbazole polymerisation has been demonstrated. Analyses revealed that under the same experimental conditions, the ability of SWCNTs to initiate the *in situ* polymerisation of the monomer was higher compared to that of MWCNTs. The morphology of resultant nanocomposites revealed wrapping and grafting of some PVK chains on SWCNTs, whereas only wrapping of outer surfaces of MWCNTs by PVK chains.

1.3.2.1.4 Controlled radical polymerisation

Atom transfer radical polymerisation (ATRP)

An *in situ* polymerisation process using modified CNTs as the initiating species was developed by Yao *et al* [114]. Initially, the SWCNT sidewalls were functionalised with alkyl bromide moieties using a two-step procedure involving first a 1,3-dipolar cycloaddition to introduce phenol functionalities, followed by an esterification with 1-bromoisobutyryl bromide. The prepared surface modified CNTs served as macroinitiator for ATRP of MMA and tBA (figure 1-12).

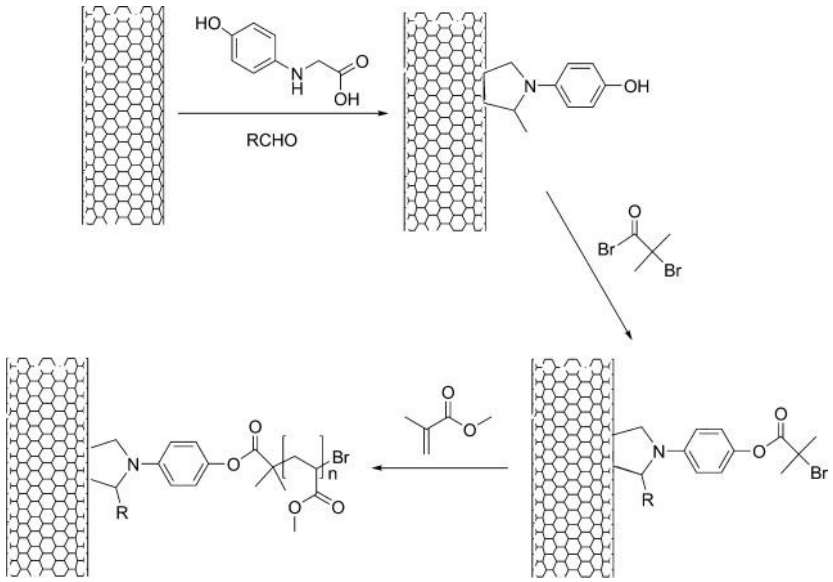

Figure 1-12: ATRP 'grafting from' modification approach of carbon nanotubes.

In the case of PMMA-based composites it was observed that the glass transition temperature (T_g) of the polymer increased from 111 °C in the bulk to 118 °C when attached to the nanotubes. Surprising, no solubility enhancement was observed for these samples in a mixture of H_2O/CH_2Cl_2. In the case of PtBA-functionalised nanotubes, DSC showed slight increasing for T_g. After acidic hydrolysis of the tert-butyl groups to PAA-functionalised SWCNTs, an enhanced solubility in aqueous solution was observed and no solubility in organic solvents.

The ATRP technique was used by independent groups [115,116] for grafting PMMA chains to MWCNTs. It was observed by TEM that the average thickness of the polymer layer increased with increasing feed ratio of monomer and nanotube initiator. The weight fraction of the polymer layer ranged from 31% to 81%. In a subsequent step, a block copolymer with 1-hydroxyethyl methacrylate (HEMA) was prepared [117]. The molar ratio of PHEMA to PMMA calculated from ^{1}H NMR was 1.1:1, while the ratio calculated from TGA was only 0.55:1.

The grafting of PMMA and PS brushes by ATRP from surface of aligned MWCNTs was reported by Matrab *et al* [118]. In the first step, the ATRP initiator was grafted to the nanotube surface by electrochemical treatment with diazonium salts.

Baskaran *et al* [119] reported ATRP of styrene and MMA from MWCNTs. The amount of PMMA covalently attached in MWCNT-g-PMMA was determined by TGA (≈70 wt%), while in the case of MWCNT-g-PS it varied from 18 to 33 wt% depending on the initiator concentration. The discovery of a correlation between the concentration of initiator on nanotubes and the amount of polymer present on the surface, allows control of the molecular weight of the growing polymer chains. Surface grafted copolymer MWCNT-g-(PS-*co*-PMMA) was also synthesized in this work. Large increase in the glass transition temperature (T_g) of the grafted PMMA and PS ($15 < \Delta T_g < 30$ °C) was observed due to tethering. In a later work, Liu *et al* [120] reported ATRP polymerisation of MMA with SWCNTs, in which the relative amount of polymer was determined by TGA to be about 17 wt%.

The grafting of styrene-*co*-acrylonitrile (SAN) copolymer from MWCNTs was carried out through the introduction of ATRP initiator onto the surface of CNTs [121]. For comparison, PS- and PAN-grafted MWCNTs were prepared. The amount of PS, SAN and PAN covalently bound to MWCNTs were estimated to be 63.4, 45.5 and 64.5 wt%, respectively. A significant increase of T_g of grafted polymer was observed, indicating an enhanced immobilization of chains due to adsorption onto the CNTs.

As demonstrated in a number of the aforementioned studies, a general conclusion is that nanotubes can influence the progress of solution-phase ATRP, although the precise mechanism is not clear. It may be possible that initiating radicals and propagating polymer chains undergo radical coupling to CNT sidewalls, thereby quenching the polymerisation and increasing the molecular weight distribution.

Reversible addition-fragmentation chain transfer (RAFT)

The grafting of MWCNTs by PS via a reversible addition-fragmentation chain transfer (RAFT) polymerisation process was performed by Cui *et al* [122]. In the first step the authors immobilized a thiocarbonylthio RAFT agent to the surface of oxidized nanotubes. In the next step, the styrene was polymerised in the presence of RAFT agent and using 1,1′-azobisisobutyronitrile (AIBN) as an initiator (figure 1-13).

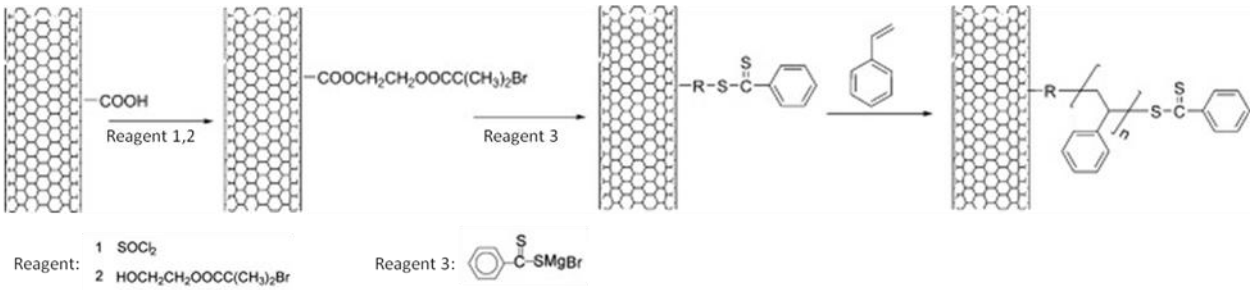

Figure 1-13: RAFT polymerisation of styrene from nanotube's surface.

TGA analysis determined the amount of PS ranged from 31.5 to 61.1 wt% depending on reaction conditions. The same procedure was used for grafting the PNIPAAM, a temperature-responsive polymer [123,124]. The molecular weight of PNIPAAM chains on MWCNTs increased linearly with NIPAAM conversion. The amount of PNIPAAM attached to MWCNTs determined by TGA varies from 35 to 87 wt% as the polymerisation time increased from 9 to 36 h. Water-soluble polyacrylamide (PAM) was also grafted by RAFT polymerisation to SWCNTs [125]. The RAFT agents were covalently attached to the SWCNT sidewalls by *in situ* generated diazonium chemistry. As the polymerisation time increased from 11 to 50 h, the amount of PAM attached onto nanotube surface, determined by means of TGA, varied from 46.3% to 77.9%. The amount of PAM exhibited a linear increase with increasing polymerisation time, indicating the 'living' characteristics of the RAFT polymerisation. Amphiphilic polymer brushes consisting of a MWCNT hard core and a relatively soft shell of PS-b-PNIPAAM was easily constructed by *in situ* RAFT polymerisation of styrene followed by NIPAAM on

the modified convex surfaces of MWCNT–PS [126]. The amount of PS-b-PNIPAAM attached to MWCNTs varied from 56 to 86 wt% when the polymerisation time increased from 10 to 36 h. The prepared MWCNT–PS-b-PNIPAAM was very sensitive to temperature, due to the thermoresponsive properties of PNIPAAM.

Similarly, the diblock polymer PMMA-b-PS was attached onto MWCNTs by *in situ* RAFT polymerisation [127,128]. The results showed that both styrene and acrylate monomers can be easily initiated and then propagate from the MWCNT sidewalls via the radical polymerisation method.

The RAFT method was also used for grafting different kind of water-soluble ionic polymers, such as poly[1-(dimethylamino)ethyl methacrylate] (PDMEMA), poly(acrylic acid) (PAA) and poly[3-(N-(3-methacrylamidopropyl)-N,N-dimethyl)ammoniopropanate sulfonate] (PMDMAS) onto the MWCNTs surface [129]. The amount of PMDMAS attached to the MWCNTs determined by TGA was about 78 wt% after 10 h polymerisation (70 wt% for PDMA and 50 wt% for PAA after 15 h polymerisation). Other methacrylate polymer grafted by RAFT on the nanotube surface was poly(1-diethylaminoethyl methacrylate) (PDEAEMA) [130]. The polymer content determined by TGA was 60 wt%. In the final step, PDEAEMA-grafted MWCNTs were quaternised with methyl iodide, resulting in cationic polyelectrolyte-grafted MWCNTs.

Nitroxide-mediated radical polymerisation

Datsyuk *et al* [131] reported an *in situ* nitroxide-mediated polymerisation (NMP) of MMA onto double-walled carbon nanotubes (DWCNTs). The main advantage of this two-step synthetic route is that it does not involve any CNT pre-treatment or functionalisation. In the first step, short chains of PAA or PS were polymerised *in situ* in the presence of NMP initiator. A pre-composite (DWCNT-PAA or DWCNT-PS) was thus obtained. In the second step, the presence of the stable nitroxide radical on CNTs

surface makes it possible to reinitiate the polymerisation of different monomers. The authors did not perform any relevant analytical measurements to confirm chemical bonding. The final composites namely DWCNT-PAA-PMA and DWCNT-PS-PMA were prepared with CNT content varied between 0.3 and 4.7 wt%. The same procedure was applied later for the grafting of PAA-b-PMA or PAA-b-PS to MWCNTs and DWCNTs [132].

NMP of styrene was carried out on the surfaces of MWCNTs initiated by an MWCNT-supported initiator (MWCNT-TEMPO) [133]. A copolymer, PS-b-P4VP, was also grafted to MWCNTs by further polymerisation of 4-vinylpyridine initiated by MWCNT–PS. According to the polymerisation results with the same ratio of MWCNT-TEMPO to styrene (w/w), the weight percentage of PS increased from 36.7 to 56.6% when the polymerisation reaction time increased from 14 to 48 h; it is worth mentioning that the weight percentage of PS varied from 0 to 61.4% when MWCNT-TEMPO/styrene (w/w) ratio varied from 1/7.5 to 1/60. A similar experiment was performed on N-doped MWCNTs with polystyrene [134], in which authors grafted 35 wt% of polymer. In the work of Fan *et al* [135] MWCNT–PS composites were prepared by NMP of MWCNT-TEMPO and styrene. The maximal weight percentage of the polymer was estimated to be 30.7%. The molecular weight increased almost linearly with monomer conversion.

1.3.2.2 'Grafting to' method

The 'grafting to' method means that the readymade polymers with reactive end groups reacted with the functional groups on the nanotubes' surfaces. It is the reaction between the surface groups of nanotubes and readymade polymers. The main approaches exploited in this functionalisation strategy are radical or carbanion additions as well as cycloaddition reactions to the CNT double bonds. Since the curvature of the carbon nanostructures imparts a significant strain upon the sp^2 hybridised carbon atoms that make up their framework, the energy barrier required to convert these atoms to sp^3 hybridisation is lower than that of the flat graphene sheets, making

them susceptible to various addition reactions. Therefore, to exploit this chemistry, it is only necessary to produce a polymer-centred transient in the presence of CNT material. Alternatively, defect sites on the surface of oxidized CNTs, as open-ended nanostructures with terminal carboxylic acid groups, allow covalent linkages of oligomer or polymer chains. The 'grafting to' method onto CNT defect sites means that the ready-made polymers with reactive end groups can react with the functional groups on the nanotube surfaces. In most cases, polymer chains terminated with amino or hydroxyl moieties are attached by amidation or esterification reactions with the nanotube surface-bound carboxylic acid groups.

1.3.2.2.1 Nucleophilic addition/coupling reactions

Wu *et al* [136] reported a functionalisation methodology based on the nucleophilic addition reaction of polymer carbanions generated from hydrids and/or organometallic reagents, such as sodium hydride or butyllithium. In their experiments, polyvinylcarbazole (PVK)- and polybutadiene (PB)-modified SWCNTs were obtained. TGA analysis determined the polymer contents in the composites to be around 5 wt% for PVK and 8 wt% for PB. Living polystyryllithium anions prepared by anionic polymerisation were covalently bonded to MWCNT-COCl by a nucleophilic substitution reaction (figure 1-14) [137].

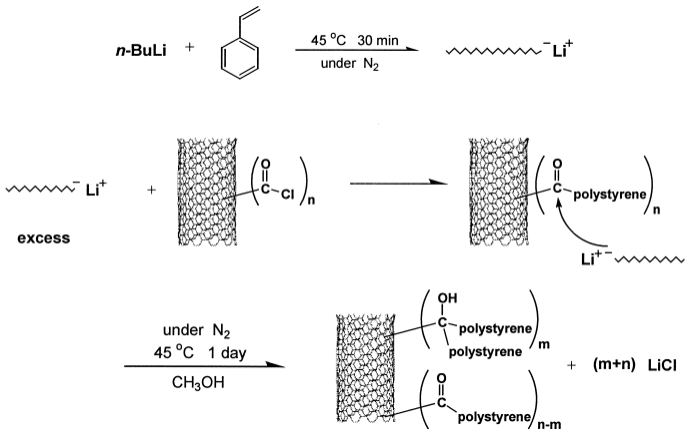

Figure 1-14: Nucleophilic substitution reaction of living polystyryllithium anions with acyl choride-modified CNTs.

The PS content in the MWCNT–PS sample was nearly 40%. TEM images clearly showed an uneven distribution of PS on the surface of MWCNTs. Analogous results were observed by Baskaran *et al* [138] with living polystyryllithium and polybutadienyllithium grafted at fractions up to 15%. The percentage of PS grafted onto the MWCNTs increased with decreasing molecular weight of the precursor living polymer.

Blake *et al* [139] used an alternative approach for the preparation of chlorinated polypropylene (PP)-modified MWCNTs. Butyllithium-functionalised MWCNTs have been reacted with chlorinated PP to give nanotubes covalently bonded to polymer chains. According to TGA, the estimated polymer content was 31 wt%. Using a different approach, Xie *et al* [140] first introduced alkynyl groups onto the SWCNT surface followed by reaction with chlorinated polymers. A number of phenylalkyne groups were bonded to the SWCNT surface via diazonium salt chemistry [141], which can further react with the benzyl chlorine groups appended on the polymer chains. The diblock polymers used were polystyrene-*co*-poly(*p*-chloromethylstyrene) and polystyrene-*co*-poly(*p*-chloromethylstyrene)-*b*-polystyrene and were synthesized by the living free radical polymerisation. The palladium-catalysed coupling reaction between benzyl chloride moieties and alkyne-modified SWCNTs could be completed under relatively mild conditions. The contents of the polymer layers calculated from TGA were 53 and 81 wt% for polystyrene-*co*-poly(*p*-chloromethylstyrene) and polystyrene-*co*-poly(*p*-chloromethylstyrene)-*b*-polystyrene, respectively.

Similarly, You *et al* [142] decorated the MWCNT sidewalls and tips with a thiol-reactive-functionality by amidation reaction. In a subsequent step, the modified tubes were reacted with a thiol-terminated poly[N-(1-hydroxypropyl)methacrylamide] (PHPMA) by a coupling reaction. FT-IR, HRTEM, NMR and TGA results showed that this thiol-coupling reaction is effective to produce water-soluble polymer-modified MWCNTs under mild conditions.

In addition, Oxidized MWCNTs were chemically modified by a ligand exchange reaction of ferrocene [143]. The modified MWCNTs underwent a direct monolithiation at the ferrocene moieties by tert-butyllithium and were terminated with *p*-chloromethylstyrene. The *p*-chloromethylstyrene-terminated species were then functionalised with living polystyryllithium chains. According to TGA traces, the polymer content in MWCNT–PS was approximately 80 wt%.

1.3.2.2.2 Condensation

Poly(urea-urethanes) end-capped with aminopropyltriethoxysilane were covalently bonded to MWCNTs functionalised with alkoxysilane by hydrolytic condensation of alkoxy groups of silane (figure 1-15) [144].

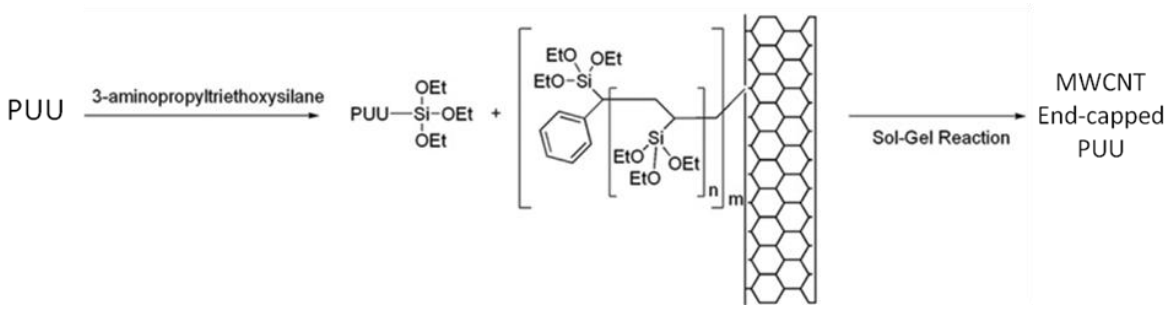

Figure 1-15: Siloxane bonding between nanotube and silane terminated polymer.

An analogous approach was used for the grafting of vinyltrimethoxysilane-modified MWCNTs with linear low density polyethylene (LDPE) terminated by silanol group [145] , as well as the crosslinking of 3-isocyanato-propyltriethoxysilane-modified MWCNTs with vinyltriethoxy silane-capped PMMA [146].

Jung *et al* [147] crosslinked polyurethane (PU) chains to MWCNTs by a reaction between carboxylic acid groups of oxidized MWCNTs and isocyanate groups (NCO) of prepolyurethane (figure 1-16).

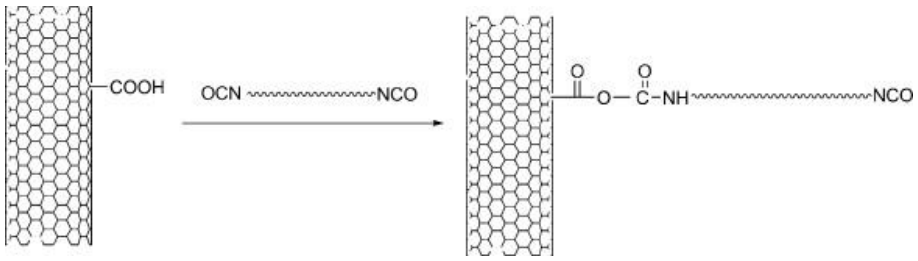

Figure 1-16: Crosslinking of polyurethanes chains with carbon nanotubes.

Similarly, waterborne polyurethane terminated with isocyanate group was grafted to amino-functionalised MWCNTs [148]. The copolymerisation of short carboxylic acid functionalised SWCNTs with poly(p-phenylene benzobisoxazole) oligomers terminated by aminophenol group was successfully carried out in a mixed solvent of polyphosphoric acid and methanesulfonic acid in the presence of P_2O_5 [149]. The degree of functionalisation was estimated from elemental composition, assuming that the average number of monomer units was 15 (one PBO oligomer for about 150 CNT carbons).

1.3.2.2.3 Cycloaddition

The cycloaddition reaction of azide-terminated PS and SWCNTs in inert atmosphere was performed by Qin *et al* [150] (figure 1-17).

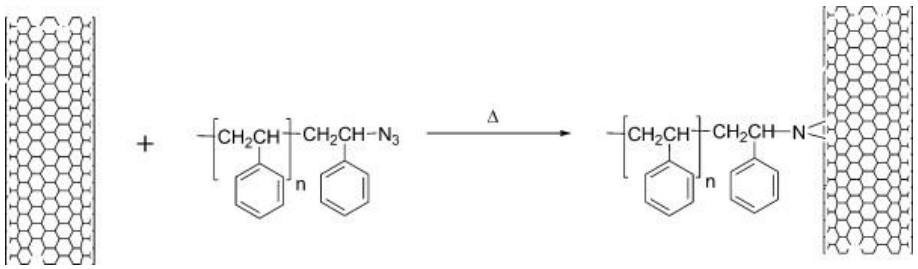

Figure 1-17: Cycloaddition reaction of azide-terminated polystyrene onto CNTs surface.

The degree of functionalisation was estimated to be one polymer chain per 48 CNT carbons calculated from the molecular weight of PS and the TGA result (85% weight loss of polymer).

Wang *et al* [151] observed that the amount of PS on the surface of SWCNTs first increased with increasing molecular weight of PS, followed by a gradual decrease. In an analogous approach, a well-defined azide-terminated PS was used for cycloaddition reaction to alkyne-decorated SWCNTs [152], in which alkyne-functionalised SWCNTs and PS-N_3 were coupled via [3 + 1] Huisgen cycloaddition between the alkyne and azide end groups. TGA measurements indicated that the SWCNT-PS consisted of 45wt% polymer.

In a subsequent work, the same group performed a sulfonation reaction to the grafted PS chains [153]. The degree of PS sulfonation could be controlled by the amount of the sulfonation reagent (acetyl sulfate) used in the reaction mixture and ranged from 10 to 33 mol%.

1.3.2.2.4 By amide linkage

Sun and co-workers [154,155,156] reported the grafting of poly(propionylethylenimine-*co*-ethylimine) (PPEI-EI) to acyl-activated tubes by direct heating or carbodiimide-assisted amidation. The polymer-bound nanotubes were found to be luminescent with quantum yields up to 11%. The luminescence properties were found to be independent from the chemical grafting approach [157]. Scanning tunneling microscopy (STM) images confirmed that the polymer interacts with the whole length of the tube and not just at the CNT ends [158]. TGA measurements determined approximately 30 wt% content of polymer for the 'acylation-amidation' route and about 40 wt% of polymer for the 'heating' method [159].

Hu *et al* [160] grafted branched polyethyleneimine (PEI) to acyl chloride-modified CNTs and they used the CNT adduct as a substrate for neurite outgrowth and branching. Two

independent techniques (UV–vis–NIR and TGA) indicated that SWCNTs constitute about 10% by weight of the graft copolymer SWCNT-PEI. Neurons grown on SWCNT-PEI showed more branched neurites than those grown on the as-prepared MWCNTs.

Ge *et al* [161] grafted oxidized MWCNTs with a non-fluorinated polyetherimide. The reaction occurred in the solid state at high temperatures under inert atmosphere without the addition of a catalyst or force fields. The authors speculated that the polymer was grafted onto MWCNTs via not only the amide but also the imide linkages. They grafted about 30 wt% of polymer. Sano *et al* [162] grafted monoamine-terminated poly(ethylene oxide) (PEO) (M_w ≈5000) to acyl-activated SWCNTs. The amidation reaction time was dramatically reduced by using microwave radiation conditions [163].

In a different approach, Chattopadhyay *et al* [164] prepared CNT salts by treating SWCNTs with lithium in liquid ammonia. Subsequently, these anionic tubes reacted with ω-bromocarboxylic acid to yield sidewall-derivatised SWCNTs with pendant carboxylic acid groups. Such derivatised SWCNTs reacted with amine-terminated PEG chains by carbodiimide-activated reaction to yield water-soluble PEGylated SWCNTs. The group of Tour and co-workers [165] grafted ultra-short carboxylated SWCNTs with amino-terminated PEG by carbodiimide-activated reaction. These water-soluble nanotubes underwent further functionalisation with diazonium salts in order to produce multifunctional CNT-based material.

The carboxylic acid groups of oxidized SWCNTs were converted into acyl chlorides and were then treated with the tenth generation G10 of poly(amidoamine) (PAMAM) starburst dendrimer [166]. Oxidized SWCNTs were grafted with amino-terminated poly(N-isopropylacrylamide) (PNIPAAm) by carbodiimide-activated reaction, which yielded a 8wt% polymer content [167]. In a different approach, oxidized MWCNTs were attached onto polyacrylonitrile (PAN) nanoparticles through the reaction of the reduced cyano-groups of the polymer and the carboxylic moieties of CNT surface [168] . In

addition, the amidation reaction was used for grafting of oligohydroxyamides to MWCNTs as described in figure 1-18 [169]. This adduct was covalently incorporated in a poly(phenylenebenzobisoxazole) (PBO) matrix during the *in situ* polymerisation process.

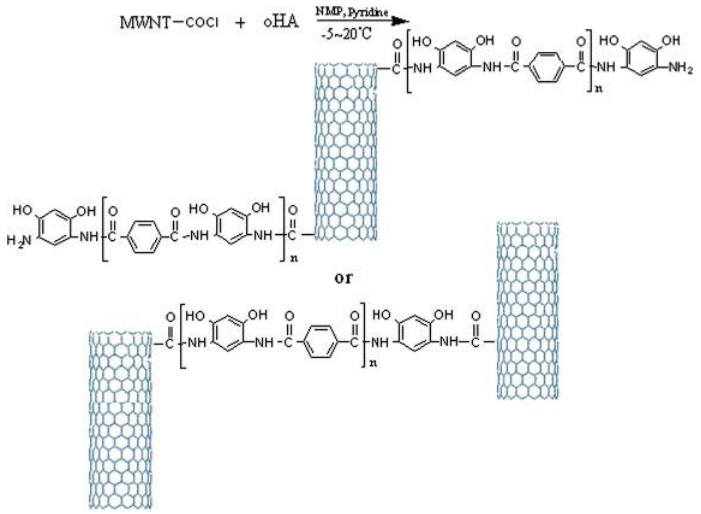

Figure 1-18: Synthesis of oligo-HA-grafted MWNT (MWNT-oHA)

1.3.2.2.5 By ester linkage

The grafting of both oxidized SWCNTs and MWCNTs with a polystyrene (PS) copolymer was reported by Sun and co-workers [170] , where a solution of poly(styrene-*co*-p-(4-(4′-vinylphenyl)-3-oxobutanol)) (PSV) in tetrahydrofuran (THF) was mixed with acyl chloride-activated nanotubes. According to thermogravimetric analysis (TGA), the CNT contents in the PSV-functionalised SWCNT and MWCNT samples are approximately 11wt% and 18wt%, respectively. Similarly, Zehua and co-workers [171] grafted a styrene–maleic anhydride copolymer (SMA) onto MWCNTs and the modified material was incorporated into poly(vinyl chloride) (PVC) matrix. Mechanical testing showed significant enhancements of the elongation at break and the impact strength. Alternatively, the reaction of hydroxy-terminated PS with thionyl chloride treated MWCNTs was performed by Baskaran *et al* [172], resulting in a hybrid containing 86 wt% of CNTs.

Poly(vinyl alcohol) (PVA) was grafted by carbodiimide-activated esterification reactions of oxidized SWCNTs and MWCNTs [173]. Riggs *et al* [174] reported the grafting of poly(vinyl acetate-*co*-vinyl alcohol) (PVAc-VA) via ester linkages to acyl-activated SWCNTs for measurement of the optical properties of the prepared modified nanotubes. Other PVA-based copolymers used for functionalisation of nanotubes was poly(ethylene-*co*-vinyl alcohol) (EVOH) copolymer under carbodiimide-activated esterification reaction conditions [175]. Nuclear magnetic resonance (NMR) spectra showed that nanotube content in the SWCNT-EVOH is about 14 wt%, whereas thermogravimetric analysis showed 10 wt%.

Silicone-functionalised CNT derivatives were prepared by opening terminal epoxy groups of functionalised polydimethylsiloxanes (PDMS) by the carboxylic groups of acid-treated MWCNTs [176]. The esterification reaction was used for grafting polyethylene glycol (PEG) chains to acyl chloride-activated SWCNTs [177]. Such modified nanotubes were found to modulate neurite outgrowth, indicating a potential application in nerve regeneration [178]. In the absence of solvent medium, a grafting reaction of hydroxy-terminated PEG with thionyl chloride treated MWCNTs was performed at temperatures above the melting point of the polymer[179]. However, grafting efficiency was low, as the TGA analysis showed the presence of 93 wt% of nanotubes.
Both oxidized SWCNT and MWCNT material were targeted for carbodiimide-activated esterifications with a derivatised polyimide endcapped with alkoxysilane groups [180,181] or having pendant hydroxyl groups [182].

Grafting reactions of hydroxyl terminated poly(methyl methacrylate) (PMMA-OH) and poly[(methyl methacrylate)-*co*-(1-hydroxyethyl methacrylate)] (PMMAHEMA) with acyl chloride-activated MWCNTs were carried out in different solvents at various temperatures [183]. It was found that at higher temperatures and longer reaction times favoured the grafting reaction. Increasing the concentration ratio of hydroxyl groups to acid-chloride groups did not improve the grafting efficiency. Other examples of

esterification reactions include the grafting of poly(bisphenol-A-*co*-epichlorohydrin) chains to oxidized MWCNTs [184] by a reactive blending process and the grafting of hyperbranched polyester based on 1,1-bis(methylol)propionic acid to the surfaces of MWCNTs [185].

1.3.2.2.6 By radical chemistry

Lou and co-workers [186] studied the attachment of poly(1-vinylpyridine) (P1VP) of controlled molecular weight end-capped by 1,1,6,6-tetramethylpiperidinyl-1-oxyl (TEMPO) group to MWCNT sidewalls (figure 1-19).

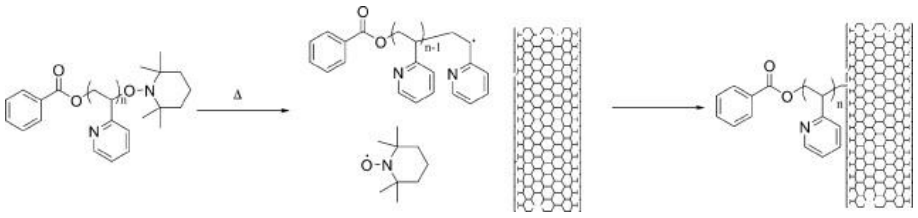

Figure 1-19: TEMPO-terminated polymer thermal dissociation and radical grafting of polymer radical to CNTs.

Heating of TEMPO-terminated P1VP chains (at 140°C) causes the TEMPO group to dissociate, resulting in radical-terminated chains which were grafted to CNTs. The grafting ratio was found to be in the 6–11% range. The same approach used by the same authors for grafting PS, polycaprolactone (PCL) and the corresponding block copolymer (PCL-*b*-PS) [187]. Changing the dormant end group to benzyl-alkyl-N-oxide led the authors to the conclusion that the efficiency of grafting is independent of the alkoxyamine moiety. In addition, it was found that longer polymer chains covered a larger surface and the grafting density decreased.

Adronov and co-workers [188] functionalised shortened SWCNTs with PS and poly[(tert-butyl acrylate)-*b*-styrene] (PtBA-*b*-PS) through a radical coupling reaction involving

thermal loss of a nitroxide capping agent. TGA analysis indicated that samples with PS were composed of 13tw% CNTs by weight, whereas the (PtBA-*b*-PS)-SWCNT sample contained approximately 38 wt% of CNTs. In a subsequent step, SWCNT-(PtBA-*b*-PS) sample was hydrolysed to yield SWCNT-(PAA-*b*-PS). The same approach was used for grafting PS, poly(4-vinylpyridine) (P4VP) and their random and block copolymers terminated with TEMPO onto MWCNTs [189]. The authors observed a non-uniform coating of CNT sidewalls with PS and their copolymers, but in the case of P4VP they observed complete and continuous surface coating. It is interesting to note that this composite was tested as a sensor for organic vapour detection.

A diazo-carrying macroinitiator of polyvinylpyrrolidone (PVP), PEG and dextran was used for radical grafting of oxidized SWCNTs [190]. PVA and its two derivates (dimethylketal and polyvinylacetone) were grafted onto MWCNTs by γ-ray irradiation [191]. The content of grafted PVA was about 38wt%, whereas the weight fraction of PVA derivatives was in the range between 13wt% and 31wt%.

1.3.3 Recent patents on polymer carbon nanotubes composites

Patents are rich sources of technical and commercial information. Analysis of patents provides information on the nature and growth of the inventive activity; its international comparison; the active players from industry, academia and government; co-inventorship; linkages with science; and technological trends [192].

The number of patents in the field of polymer/CNTs composites is rising every passing year. This shows the interest in transforming basic research into application. A number of patents can be cited in this connection. For instance, Thomas *et al* [193] invented a polymer/CNT composite electrochemical actuator. A series of uniform composites was prepared by dispersing purified single walled nanotubes with varying weight percents

into a polymer matrix (NAFION®), followed by solution casting. The resulting Polymer/CNTs composite was found successful for use as electrochemical actuator.

Nadia *et al* [194] invented a processing method for fine dispersion of nanotubes in a water-soluble polymer using high shear in an aqueous medium first, and then evaporating water. This method is claimed to lower the percolation threshold, at the same time further improving the conductivity of CNT reinforced polymers. Richard invented a method to functionalise nanotubes with m-phenylenevinylene-1,5-disubstituted-p-phenylenevinylene polymers.

These polymer grafted nanotubes are reported to be advantageous in dispersing into other polymer matrix as a master batch. Exemplary base polymers include epoxy, polyester, or nylon [195]. Michael *et al* [196] invented methods of selectively functionalising carbon nanotubes of a specific type, based on their electronic properties, using diazonium chemistry. They claimed that this invention is also directed toward methods of separating carbon nanotubes into populations of specific types via selective functionalisation and electrophoresis, and also to the novel compositions generated by such separations. Valerie *et al* [197] in a recent patent application described a procedure to prepare toners comprising functionalized CNTs in a suspension of wax, colorant and surfactant etc. This toner exhibits increased conductivity, and is thus suitable for conductive developing methods.

1.3.4 Properties of polymer/carbon nanotubes composites

1.3.4.1 Mechanical Properties

The outstanding potential of CNTs as reinforcements in polymer composites is evident from different accounts available. Composite films consisting of alternating layers of CNTs and polyelectrolyte have shown great promise as high strength light weight

materials [198,199]. Composites containing 50 wt% SWCNTs were estimated to have modulus and strength values of about 11 GPa and 315 MPa, respectively, which are one order higher than the corresponding values for the neat matrix. The structural integrity of the films was greatly enhanced by chemical crosslinking reactions between the components of the composite. In the category of solution-based bulk composites, the most obvious conclusion is that matrices filled with CNTs bearing covalently attached polymer chains show enhanced mechanical properties [200,201,202,203]. This is not surprising since polymer grafting should significantly improve both CNT dispersion and stress transfer to the matrix. Regarding the blending of unmodified CNTs with polymers by a solution-phase protocol, PVA shows significant reinforcement after incorporation of CNT material [204,205]. This can be explained by the fact that CNT sidewalls nucleate the crystallization of the polymer, thus leading to stiffer composite.

Similarly, *in situ* polymerisation has presented a number of advantages over other composite processing methods [206,207,208]. This is because it is easier to get strong interactions between polymer and nanotube during the growth stage rather than mixing the constituents by various means. A salient message is the low reinforcement observed for the melt processed bulk composites. On the contrary, microfibers produced by melt spinning/drawing techniques display better reinforcement compared to the bulk, due to CNT alignment effects [209,210]. Spitalsky *et al* [211] concluded that CNT reinforcement is much more effective for ductile matrices, whereas for brittle polymers the CNT filler does not seem to improve considerably the mechanical properties of the matrix.

1.3.4.2 Electrical properties

Literature survey reveals a large variation of the electrical properties values as a function of the polymer matrix, processing method and CNT type. Nanocomposites based on PMMA and MWCNTs as a filler show a significant enhancement in the electrical conductivity. Kim *et al* [212] reported a value of ≈3000 S/m at 0.4 wt% for

extremely low percolation threshold (≈0.003 wt%) prepared by the solution mixing method. Furthermore, the addition of MWCNTs to polycarbonate by the melt mixing technique induces a dramatic increase of about 16 orders of magnitude in the maximum conductivity; reaching the value of ≈1000 S/m at 15 wt% [213].

According to Koerner *et al* [214] a σ_{max} value of 1000 S/m is observed for PU filled with 17 wt% MWCNTs using the solution casting technique. The same conductivity value has been achieved for SWCNTs/PANI composite prepared by solution mixing at 15 wt% loading. Composite fibres SWCNTs/PEI prepared by means of the coagulation fibre spinning process exhibit a considerably high σ_{max} value of 1×10^4 S/m.

Concerning Φ_c polymer hosts such as PI, PMMA, epoxy and PS exhibit extremely low percolation threshold values. It is important to stress the recently reported ultra low Φ_c value of 0.000846 wt% for MWCNTs/PVC composites [215]. As a general statement, the excellent electrical properties of composites containing MWCNTs are promising for the design of low cost polymer composites for numerous future applications.

1.3.4.3 Other properties

The viscoelastic properties of nanotube/polymer composites have both practical importance related to composite processing and scientific importance as a probe of the composite dynamics and microstructure. As with electrical percolation, the rheological percolation is found to depend on nanotube dispersion, aspect ratio, and alignment. Mitchell *et al* [216] improved dispersion by functionalising SWNTs, such that the rheological percolation threshold dropped from 3 wt% when using pristine SWNT to 1.5 wt% in functionalised SWNT/polystyrene composites. The values of *G*‘ at low frequencies were also higher for the functionalized composites, indicating better load transfer between the nanotube network and the polymer. The effect of aspect ratio

(shape) was illustrated by comparing nanotube and layered silicate nanofillers, which are disk-shaped and require a higher loading to form a percolated network [217].

The thermal conductivity, κ, of carbon materials is dominated by atomic vibrations or phonons. Nanocomposites with good thermal conductivity have potential applications in printed circuit boards, connectors, thermal interface materials, heat sinks, and other high-performance thermal management systems. The excellent thermal conductivity of individual nanotubes led to early expectations that it will enhance the thermal conductivity of polymer nanocomposites, as nanotubes do with the electrical conductivity. Choi *et al* [218] reported a 300% increase in thermal conductivity at room temperature with 3 wt % SWNT in epoxy. Optical properties of polymer/nanotubes composites have also been explored for various applications [219,220].

1.3.5 Polyolefins

Polyolefins are synthetic polymers obtained from olefinic monomers. They are the biggest polymer family by volume of production and consumption. Several million metric tons of polyolefins are produced and consumed globally each year, and they are regarded as commodity polymers. Figure 1-20 shows a break-up of different types of polyolefins consumed in 2009.

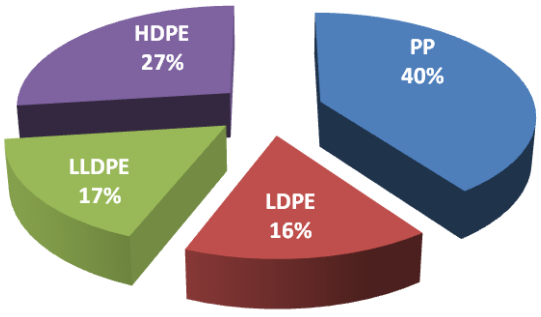

Figure 1-20: Global polyolefin consumption reported for 2009 [221].

Polyolefins have enjoyed great success due to many application opportunities, relatively low cost, and wide range of properties. Polyolefins are recyclable and significant improvement in properties is available through blending and composite manufacturing technologies. Polyolefins may be classified based on their monomeric unit and chain structures as ethylene-based polyolefins (contain mostly ethylene units), propylene-based polyolefins (contain mostly propylene units), higher polyolefins (contain mostly higher olefin units), and polyolefin elastomers. Today polyolefins and polyolefin-based materials are used in main many applications. Theses applications include transportation (automotive, aerospace), packaging, medical, consumer products (toys, appliances, etc.), electronics, cable and wire coating, thermal and acoustic insulation, and building and construction. Polyolefins can be extruded as filament (fibres), films (cast and blown), and pipes/profiles. They can be moulded into parts of various shapes. They can be foamed with physical and chemical foaming/blowing or/and can be coasted onto other materials. And what's more, incorporation of reinforcement materials can expand their application to sophisticated and customised applications.

1.4 Nanocomposites based on Polyolefins

Polyolefins are today the most used thermoplastic materials thanks to the high technology and sustainability of the polymerisation process, their excellent thermomechanical properties and their good environmental compatibility, including easy recycling. In the last few decades much effort has been devoted worldwide to extend the applications of polyolefins by conferring on them new properties through mixing and blending with different materials. In this latter context, nanocomposites have recently offered new exciting possibilities. This has been made possible on the basis of the improvement of polyolefin functionalisation processes with the availability of several olefin homo- and copolymers bearing a small (generally less than 1 mol%) amount of backbone grafted polar groups. These are indeed adequate to endow

favourable interface interactions with polar macromolecules and inorganic compounds, leading first to compatible blends and then to microcomposites.

Literature review shows that researchers have adopted various routes to prepare nanostructured biphase materials having the typical structural properties of polyolefins (continuous matrix) but showing enhanced thermomechanical properties, thermostability, lower flammability, lower gas permeability and electrical and optical properties, thanks to the presence of an extended interphase interaction with very different nanodispersed species [222].

Additives in polyolefin composites may be classified according to their functions as modifiers (e.g. fillers, plasticizers, blowing agents, coupling agents, impact modifier, and nucleating/clarifying agents), property extenders (e.g. heat stabiliser, antioxidants, flame retardants, light stabilisers, antistatic agents, and biocides), and processing aids (e.g. lubricants, slip agents, and antiblocking agent). In terms of specific chemical names, additives used in polyolefin composites include, but not limited to, the following: glass fibres, hollow glass bubbles, clay minerals, carbon black, carbon nanotubes, carbon fibres, graphite, magnesium hydroxide, aluminium trithydroxide, titanium dioxide, calcium carbonate, silica, and natural fibres.

In a recent account Ling *et al* [223] prepared a microwave absorbing composite by melt blending MWCNTs in LLDPE and Ethylene-octene copolymer matrix. This composite containing 30wt% MWCNTs showed strong absorbance of microwave at 4.4 GHz and the maximum reflection loss achieved was -11.15 dB.

Isaji *et al* [224] manufactured composite films with a mixture of MWCNTs in low and ultra high molecular weight PE by gelation/crystallisation from a dilute decalin solution. The filler content was 10 wt% of MWCNTs. The temperature dependence of electrical conductivities measured from 25 to 220°C shows that the conductivity increased slowly

and had small jump-down near to the melting point matrix, and then increased again till to the 220°C. The jump-down associated with the thermal expansion of polymer happened near melting points of matrix ≈ 127 °C and ≈ 100 °C corresponding to the melting points of UHMWPE and LMWPE respectively.

In another work, Prashantha *et al* [225] obtained an effective dispersion of nanotubes via extrusion process by master batch dilution technique to prepare PP/CNTs composite. They concluded that preparation of nanocomposites by master batch dilution technique is an excellent method to obtain well-dispersed CNTs, while limiting the handling difficulties (potential health and safety hazards) in plastics processing industrial workshops and also offering a greater flexibility and cost-effective adaptation ability of the nanofiller content to focused applications.

1.5 Trends and future perspectives

Basically nanotubes are incorporated into a polymer matrix to enhance electrical, mechanical, and thermal or a combination of theses properties. In polymer nanocomposites, properties such as strength and stiffness, flam retardation/char formation, barrier, heat distortion temperature, electrical and thermal conductivities can be improved significantly at low (typically < 5 wt%) nanotubes loading. However studies are now more focused on nanocomposites with lower nanotubes content and more efforts are being made to achieve a perfect dispersion of nanotubes in host matrix [226,227,228].

Reinforced/filled polyolefin composites with improved impact are increasingly replacing low end engineering polymers such as ABS and polyamides. Attempts are being made to prepare textile weaved with polymer CNTs composite fibres (by melt spinning on large scale) which have shown promising results [229]. Carbon nanotubes are a model system for nanoelectronics [230] and a huge part of the nanotechnology research is devoted

towards practical applications like sensors [231,232], conduction composites [233,234], electromegnetic shielding [235], antistatic coatings [236] etc. Interests in hybrid nanocomposites are also growing owing to its potential applications. Recently Liao *et al* [237] have reported that double walled carbon nanotube–Fullerene hybrids exhibit superior optical limiting performance to those of Fullerenes and CNTs. Another study reports that functionalised nanotubes in an electroactive fullerene-based (C_{60}–Pd) polymer film markedly increases the capacitance and decreases the resistance of the electrode [238]. Engineering of CNTs into microwires can open up new synthetic routes for novel electrodes that overcome mass transport limitations and provide high specific areas [239].

New approaches are being introduced to stabilise nanotubes in polymer suspensions. Saint-Aubin *et al* [240] has recently prepared stable aqueous solution of nanotubes in Poly(acrylic acid). Such formulation could be used for manufacturing conductive inks, paints etc. Polymer/CNTs composites are also being investigated for space suit reinforcements, radar absorbance material for stealth applications [241]. Most of the reported work on polymer nanocomposites is based on experimental studies; however, some researchers are concentrating on theatrical work [242,243] to develop mathematical models to estimate the properties of nanocomposites and characteristics of interface between the nanotubes and polymer. The establishment of such models would help in future in preparing polymer nanocomposites with tailored properties. Another prospective trend is particularly important from the standpoint of the development of nanotubes composites that are environmentally sustainable, recyclable, renewable and reusable. This last factor could define the future of wider applications of polymer/CNTs composites. Moreover new functional polymers [244] could also provide further opportunities for nanocomposite manufacturing.

1.6 Summary

Nanotubes are a tiny miracle. But perhaps they are useless, unless incorporated in some host matrices in order to make functional materials that are fit to be used for specific purposes. A review of research work presented in this chapter shows that carbon nanotubes are promising candidates for developing high-performance functional materials. But the structure and chemistry of nanotubes make it a challenging task. Its tendency to agglomerate in bundles is a major obstacle in achieving homogenous composites that could be used for different applications. To reap the full benefits of this wonderful discovery, it has to be integrated in various other materials especially polymers.

Functionalisation of nanotubes generally has two motives: 1) to facilitate the dispersion of nanotubes by surface modification that minimise the possibility of bundling (e.g. in solvents or polymer melts); and 2) to incorporate such chemical moieties onto nanotubes' surface that can further attached to other species (e.g. polymers).

Researchers have discovered various routes to facilitate the incorporation of CNTs into polymer host matrix, ranging from noncovalent (such as solvent evaporation, melt mixing, polymer wrapping and absorption, and in situ polymerisation) to covalent (such as 'grafting from' and 'grafting to'). All these routes have their own upside and downside and selected according to the limitations/requirements related to product, processing, cost, scale of production, yield and other feasibility parameters. CNTs have been dispersed in a variety of polymer matrices using solution processing, melt processing, or in situ polymerisation using pristine, functionalised (with polymer or other chemical moieties). Literature presents processing of CNTs composites with different polymers including semicrystalline, amorphous, liquid crystalline, conjugated, and solvent-processable polymer, as well as thermosetting resins. Property enhancement include strength, stiffness, thermal stability, solvent resistance, glass

transition temperature, crystallisation time, crystallinity, electrical conductivity, reduced thermal shrinkage and optical anisotropy.

In order to covalently attach polyolefin onto nanotubes two potential approaches can be considered: (i) 'Grafting to' approach through radical chemistry and (ii) via functional polyolefins. The former approach is simple in terms of large scale application as radicals have short life times which make this kind of processing possible in an extruder; however, control of side reactions is complicated as radicals have limited selectivity. The latter approach requires the synthesis of end-functionalisation polyolefin which is a complex way, moreover the degree of functionalisation of these polyolefins is in the range of 50-75%.

Carbon nanotubes can lend new functionality to polymer, metal, or carbon matrices and therefore with the discovery of new methods of incorporation of nanotubes in these matrices is believed to further widen the scope of such nanocomposites.

1.7 References

1 N Karak; Fundamentals of Polymers, 1st ed.; PHI learning ltd.: New-Delhi, India, (2009) pp. 235–236.

2 S Iijima, T Ichihashi. Nature Mater 363(1993), pp. 603-605.

3 W Krastchmer, L Lamb, K Fostiropoulos, D Huffman. Nature 347 (1990), pp. 354.

4 T Guo, P Nikolaev, A Rinzler, D Tomanek, D Colbert, R Smalley. J Phys Chem 99 (1995), pp. 10694.

5 N Rodriguez. J Mater Res 8 (1993), pp. 3233.

6 H Zhang, X Xue, D Wang, Y He, S Peng. Mater Chem Phys 58 (1999), pp. 1–5.

7 M Yudasaka, R Kikuchi, T Matsui, Y Ohki, S Yoshimura, E Ota. Appl Phys Lett 67 (1995), pp. 2477–2479.

8 YC Choi, DJ Bae, TH Lee, BS Lee, IT Han, WB Choi, NS Lee, JM Kim. Synth Metals 108 (2000), pp. 159–163.

9 YL Chen, GS Patel, DT Shaw. J Mater Sci 35 (2000), pp. 5517–5521.

10 WT Ebbesen, Carbon Nanotubes Preparation, Properties, 1st ed., CRC Press, Boca Raton, FL, (1997).

11 J Liu, AG Rinzler, H Dai, JH Hafner, RK Bradley, PJ Boul, A Lu, T Iverson, K Shelimov, CB Huffman, F Rodriguez-Macias, YS Sheon, LT Randall, DT Colbert, RE Smalley. Science 280 (1998), pp. 1253.

12 E Anglaret, N Bendiab, T Guillard, C Journet, G Flamant, D LaPlaze, P Bernier, JL Sauvajol. Carbon 36 (1998), pp. 1815–1820.

13 M Zhang, CL Xu, DH Wu, LM Cao, WK Wang. J Mater Sci Lett 19 (2000), pp. 511–514.

14 C Kocabas, SH Hur, A Gaur, MA Meitl, M Shim, JA Rogers. Small 1 (2005), pp. 1110–1116.

15 ZF Ren, ZP Huang, JW Xu, JH Wang, P Bush, MP Siegal, PN Provencio. Science 282 (1998), pp. 1105–1107.

16 X Xiao-Lin, M Yiu-Wing, Z Xing-Ping. Mater Sci Eng R 49 (2005), pp. 89-112.

17 S Niyogi, MA Hamon, H Hu, B Zhao, P Bhowmik, R Sen, M E Itkis, RC Haddon. Acc Chem Res 35 (2002), pp. 1105.

18 SB Sinnott, J Nanosci Nanotechnol 2 (2002), pp. 113.

19 RJ Chen, Y Zhang, D Wang, H Dai. J Am Chem Soc 123 (2001), pp. 3838.

20 J Chen, MA Hamon, H Hu, Y Chen, AM Rao, PC Eklund, RC Haddon. Science 282 (1998), pp. 95.

21 A Hirsch. Angew Chem Int Ed 41 (2002), pp. 1853-1859.

22 A Hirsch. The Chemistry of the Fullerenes, Thieme, Stuttgart, Germany (1994).

23 J Bahr, JM Tour. J Mater Chem 12 (2002), pp. 1952.

24 J Sloan, AI Kirkland, J L Hutchison, MLH Green. Acc Chem Res 35 (2002), pp. 1054.

25 A Garg, SB Sinnott. Chem Phys Lett 295 (1998), pp. 273.

26 CW Padgett, DW Brenner. Nano Lett 4 (2004), pp. 1051.

27 L Cai, JL Bahr, Y Yao, J M Tour. *Chem Mater 14* (2002), pp. 4235–4241.

28 A Nikitin, H Ogasawara, D Mann, R Denecke, Z Zhang, H Dai, K Cho, A Nilsson. Phys Rev Lett 95 (2005), pp. 225507 [4 pages].

29 X Li, J Shi, Y Qin, Q Wang, H Luo, P Zhang, ZX Guo, HS Woo, DK Park. Chem Phys Lett 444 (2007), pp. 258-262.

30 C Klinke, JB Hannon, A Afzali, P Avouris. Nano Lett 6 (2006), pp. 906-910.

31 ML Usrey, ES Lippmann, MS Strano. J Ame Chem Soc 127 (2005), pp. 16129-16135.

32 N Chimot, V Derycke, MF Goffman, JP Bourgoin, H Happy, G Dambrine. Appl Phys Lett 91 (2007-153111.

33 J Borghetti, V Derycke, S Lenfant, P Chenevier, A Filoramo, M Goffman. Adv Mater 18 (2006), pp. 2535.

34 J Cabana, R Martel. J Am Chem Soc 129 (2007), pp. 2244-2245.

35 CA Dyke, MP Stewart, F Maya, JM Tour. Synlett 1 (2004), pp. 155-160.

36 O Byl, P Kondratyuk, JT Yates. J Phys Chem B 107 (2003), pp. 4277–4279.

37 Jorio A. In Carbon nanotubes: Advanced topics in the synthesis, structure, properties, application, 1st ed.; Editor: Dresselhaus G, Dresselhaus M S; Springer: Heidelberg, Germany (2008), pp. 45-46.

38 MA Thayer. Chemical & Engineering News 85 (2007), pp. 29-35.

39 D Plee. US2010/0038602 A1 (2010).

40 S Bordere , P Gaillard, C baddour. US7622059 B2 (2009).

41 T Mcandrew, C Roger, E Bressand, P Laurent. WO/2008/106572 (2008).

42 JN Coleman, U Khan, WJ Balu, YK Gun'ko. Carbon 44 (2006), pp. 16224-52.

43 O Breuer, U Sundararaj. Polym Compos 25 (2004), pp. 630-645.

44 M Moniruzzaman, KI Winey. Macromoleucles 39 (2006), pp. 5194-204.

45 L Jin, CL Bower, O Zhou. Appl Phys Lett 73 (1998), pp. 1197–1199.

46 JN Coleman, M Cadek, R Blake, V Nicolosi, KP Ryan, C Belton. Adv Funct Mater 14 (2004), pp. 791–798.

47 M Cadek, JN Coleman, KP Ryan, V Nicolosi, G Bister, A Fonseca. Nano Letters 4 (2004), pp. 353–356.

48 M Cadek, JN Coleman, V Barron, K Hedicke, WJ Blau. Appl Phys Lett 81 (2002), pp. 5123–5125.

49 R,rews, D Jacques, M Minot, T Rantell. Macromol Mater Eng 287 (2002), pp. 395–403.

50 O Breuer, U Sundararaj. Polym Compos 25 (2004), pp. 630–645.

51 P Potschke, AR Bhattacharyya, A Janke, H Goering. Compos Interf 10 (2003), pp. 389–404.

52 R,rews, D Jacques, DL Qian, T Rantell. Acc Chem Res 35 (2002), pp. 1008–1017.

53 TX Liu, IY Phang, L Shen, SY Chow, WD Zhang. Macromolecules 37 (2004), pp. 7214–7222.

54 P Potschke, AR Bhattacharyya, A Janke. Euro Polym J 40 (200), pp. 137-148.

55 O Meincke, D Kaempfer, H Weickmann, C Friedrich, M Vathauer, H Warth. Polymer 45 (2004), pp. 739–748.

56 W Tang, MH Santare, SG Advani. Carbon 41 (2003), pp. 2779–2785.

57 Z Jia, Z Wang, C Xu, J Liang, B Wei, D Wu. Mater Sci Eng A 271 (1999), pp. 395–400.

58 C Velasco-Santos, AL Martinez-Hernandez, FT Fisher, R Ruoff, VM Castano. Chem Mater 15 (2003), pp. 4470–4475.

59 T Kimura, H Ago, M Tobita, S Ohshima, M Kyotani, M Yumura. Adv Mater 14 (2002), pp. 1380–1383.

60 MB Bryning, DE Milkie, MF Islam, JM Kikkawa, AG Yodh. Appl Phys Lett 87 (2005), pp. 161909 [3 pages].

61 M Moniruzzaman, F Du, N Romero, KI Winey. Polymer 47 (2006), pp. 293−298.

62 J Zhu, J Kim, H Peng, JL Margrave, VN Khabashesku, Barrera EV. Nano Lett 3 (2003), pp. 1107−1113.

63 NR Raravikar, LS Schadler, A Vijayaraghavan, Y Zhao, B Wei, PM Ajayan. Chem Mater 17 (2005), pp. 974−983.

64 F Du, C Guthy. T Kashiwagi, JE Fischer, KI Winey. J Polym Sci Part B: Polym Phys 44 (2006), pp. 1513−1519.

65 H Xia, Q Wang, K Li, GH Hu. J Appl Polym Sci 93 (2004), pp. 378−386.

66 KG Kasimatis, JA Nowell, LM Dykes, WR Burghardt, R Thillalyan, LC Brinson, R,rews, JM Torkelson. PMSE Prepr 92 (2005), pp. 255−256.

67 O Regev, PNB ElKati, J Loos, CE Koning. Adv Mater 16 (2004), pp. 248−251.

68 A Dufresne, M Paillet, JL Putaux, R Canet, F Carmona, P Delhaes, S Cu. J Mater Sci 37 (2002), pp. 3915−3923.

69 B Vigolo, A Penicaud, C Coulon, C Sauder, R Pailler, C Journet, P Bernier, P Poulin. Science 290 (2000), pp. 1331−1334.

70 AA Mamedov, NA Kotov, M Prato, DM Guldi, JP Wicksted, A Hirsch. Nat Mater 1 (2002), pp. 190−194.

71 PD Calvert. Nature 399 (1999), pp. 210.

72 C Velasco-Santos, AL Martinez-Hernandez, VM Castano. Compos Interface 11 (2005), pp. 567

73 MJ O'Connell, P Boul, LM Ericson, C Huffman, Y Wang, E Haroz. Chem Phys Lett 342 (2001), pp. 265–271.

74 JL Bahr, ET Mickelson, MJ Bronikowski, RE Smalley, JM Tour. Chem Commun (2001), pp. 193–194.

75 A Star, JF Stoddart, D Steuerman, M Diehl, A Boukai, EW Wong. Angew Chem Int Ed 40 (2001), pp. 1721–1725.

76 DW Steuerman, A Star, R Narizzano, H Choi, RS Ries, C Nicolini. J Phys Chem B 106 (2002), pp. 3124–3130.

77 A Star, Y Liu, K Grant, L Ridvan, JF Stoddart, DW Steuerman. Macromolecules 36 (2003), pp. 553–560.

78 A Star, JF Stoddart. Macromolecules 35 (2002), pp. 7516–7520.

79 MJ O'Connell, P Boul, LM Ericson, C Huffman, Y Wang, E Haroz. Chem Phys Lett 342 (2001), pp. 265–271.

80 E Nativ-Roth, Y Levi-Kalisman, O Regev, R Yerushalmi-Rozen. J Polym Eng 22 (2002), pp. 353–368.

81 HS Xia, Q Wang, GH Qiu. Chem Mater 15 (2003), pp. 3879–3886.

82 YJ Kang, TA Taton. J Am Chem Soc 125 (2003), pp. 5650–5651.

83 M Shim, A Javey, NWS Kam, HJ Dai. J Am Chem Soc 123 (2001), pp. 11512–11513.

84 X Zhang, J Zhang, Z Liu. Appl Phys A 80 (2004), pp. 1813–1817.

85 P Petrov, F Stassin, C Pagnoulle, R Jerome. Chem Commun (2003), pp. 2904–2905.

86 N Jonathan, JN Coleman, U Khan, J Werner. WJ Blau, K Yurii. YG Gun'ko. Carbon, 44 (2006), pp. 1624-1652.

87 Z Spitalsky, D Tasis, K Papagelis, C Galiotis. Prog Polym Sci 35 (2010), pp. 357-401.

88 G Viswanathan, N Chakrapani, H Yang, B Wei, H Chung, K Cho. J Am Chem Soc 125 (2003), pp. 9258–9259.

89 F Liang, JM Beach, K Kobashi, AK Sadana, YI Vega-Cantu, JM Tour. Chem Mater 18 (2006), pp. 4764–4767.

90 Y Liu, DC Wu, WD Zhang, X Jiang, CB He, TS Chung. Angew Chem Int Ed 44 (2005), pp. 4782–4785.

91 X Wang, H Liu, L Qiu. Mater Lett 61 (2007), pp. 2350–2353.

92 X Tong, C Liu, HM Cheng, H Zhao, F Yang, X Zhang. J Appl Polym Sci 92 (2004), pp. 3697–3700.

93 D Bonduel, M Mainil, M Alexandre, F Monteverde, P. Dubois. Chem Commun (2005), pp. 781–783.

94 S Park, SW Yoon, KB Lee, DJ Kim, YH Jung, Y Do. Macromol Rapid Commun 27 (2006), pp. 47–50.

95 X Dong, L Wang, L Deng, J Li, J Huo. Mater Lett 61 (2007), pp. 3111–3115.

96 S Li, H Chen, W Bi, J Zhou, Y Wang, J Li. J Polym Sci A Polym Chem 45 (2007), pp. 5459–5469.

97 A Funck, W Kaminsky. Compos Sci Technol 67 (2007), pp. 906–915.

98 D Blond, V Barron, M Ruether, KP Ryan, V Nicolosi, W.J. Blau . Adv Funct Mater 16 (2006), pp. 1608–1614.

99 SJ Park, MS Cho, ST Lim, HJ Choi, MS Jhon. Macromol Rapid Commun 24 (2003), pp. 1070–1073.

100 Y Liu, J Tang, JH Xin. Chem Commun (2004), pp. 2828–2829.

101 G Guo, D Yang, C Wang, S Yang. Macromolecules 39 (2006), pp. 9035–9040.

102 B Yue, Y Wang, CY Huang, R Pfeffer, Z Iqbal. J Nanosci Nanotechnol 7 (2007), pp. 994–1000.

103 MSP Shaffer, K Koziol. Chem Commun (2002), pp. 2074–2075.

104 JJ Park, DM Park, JH Youk, WR Yu, J Lee. Carbon, 48 (2010), pp. 2899-2905.

105 Y Yang, X Xie, J Wu, YW Mai. J Polym Sci A Polym Chem 44 (2006), pp. 3869–3881.

106 M Kim, CK Hong, S Choe, SE Shim. J Polym Sci A Polym Chem 45 (2007), pp. 4413–4420.

107 X Li, W Guan, H Yan, L Huang. Mater Chem Phys 88 (2004), pp. 53–58.

108 S Qin, D Qin, WT Ford, JE Herrera, DE Resasco. Macromolecules 37 (2004), pp. 9963–9967.

109 S Qin, D Qin, WT Ford, JE Herrera, DE Resasco, SM Bachilo. Macromolecules 37 (2004), pp. 3965–3967.

110 NA Kumar, HS Ganapathy, JS Kim, YS Jeong. Eur Polym J 44 (2008), pp. 579–586.

111 S Chen, G Wu, Y Liu, D Long. Macromolecules 39 (2006), pp. 330–334.

112 HL Wu, YT Yang, CCM Ma, HC Kuan. J Polym Sci Part A Polym Chem 43 (2005), pp. 6084–6094.

113 A Maity, SS Ray, MJ Hato. Polymer 49 (2008), pp. 2857–2865.

114 Z Yao, N Braidy, GA Botton, A Adronov. J Am Chem Soc 125 (2003), pp. 16015–16024.

115 H Kong, C Gao, D Yan. J Am Chem Soc 126 (2004), pp. 412–413.

116 M Wang, KP Pramoda, SH Goh. Polymer 46 (2005), pp. 11510–11516.

117 H Kong, C Gao, D Yan. J Am Chem Soc 126 (2004), pp. 412–413.

118 T Matrab, J Chancolon, MM L'hermite, JN. Rouzaud, G Deniau, JP Boudou. Colloids Surf Physicochem Eng Asp 287 (2006), pp. 217–221.

119 D Baskaran, JW Mays, MS Bratcher. Angew Chem Int Ed43 (2004), pp. 2138–2142.

120 M Liu, Y Yang, T Zhu, Z Liu. J Phys Chem C 111 (2007), pp. 2379–2385.

121 AM Shanmugharah, JH Bae, RR Nayak, SH Ryu. J Polym Sci A Polym Chem 45 (2007), pp. 460–470.

122 J Cui, WP Wang, YZ You, C Liu, P Wang. Polymer 45 (2004), pp. 8717–8721.

123 CY Hong, YZ You, CY Pan. Chem Mater 17 (2005), pp. 2247–2254.

124 G Xu, WT Wu, Y Wang, W Pang, P Wang, Q Zhu. Nanotechnology 17 (2006), pp. 2458–2465.

125 GJ Wang, SZ. Huang, Y Wang, L Liu, J Qiu, Y Li. Polymer48 (2007), pp. 728–733.

126 G Xu, WT Wu, Y Wang, W Pang, Q Zhu, P Wang. Nanotechnology 18 (2007), pp. 145606 [7 pages].

127 G Xu, WT Wu, Y Wang, W Pang, Q Zhu, P Wang. Polymer 47 (2006), pp. 5909–5918.

128 G Xu, Y Wang, W Pang, WT Wu, Q Zhu, P Wang. Polym Int 56 (2007), pp. 847–852.

129 YZ You, CY Hong, CY Pan. Nanotechnology 17 (2006), pp. 2350–2354.

130 C Gao, W Li, H Morimoto, Y Nagaoka, T Maekawa. J Phys Chem B 110 (2006), pp. 7213–7220.

131 V Datsyuk, C Guerret-Piecourt, S Dagreou, L Billon, JC Dupin, E Flahaut. Carbon 43 (2005), pp. 873–876.

132 V Datsyuk, L Billon, C Guerret-Piecourt, S Dagreou, N Passade-Boupatt, S Bourrigaud. J Nanomater (2007), pp. 74769– 781.

133 XD Zhao, XH Fan, XF Chen, CP Chai, QF Zhou. J Polym Sci A Polym Chem 44 (2006), pp. 4656–4667.

134 M Dehonor, K Masenelli-Varlot, A Gonzalez-Montiel, C Gauthier, JY Cavaille, H Terrones . Chem Commun (2005), pp. 5349–5351.

135 DQ Fan, JP He, W Tang, JT Xu, YL Yang. Eur Polym J 43 (2007), pp. 26–34.

136 W Wu, S Zhang, Y Li, J Li, L Liu, Y Qin . Macromolecules 36 (2003), pp. 6286–6288.

137 HM Huang, IC Liu, CY Chang, HC Tsai, CH Hsu, RCC Tsiang. J Polym Sci A Polym Chem 42 (2004), pp. 5802–5810.

138 Baskaran, G Sakellariou, JW Mays, MS Bratcher. J Nanosci Nanotechnol 7 (2007), pp. 1560–1567.

139 R Blake, YK Gun'ko, J Coleman, M Cadek, A Fonseca, JB Nagy. J Am Chem Soc 126 (2004), pp. 10226–10227.

140 L Xie, F Xu, F Qiu, H Lu, Y Yang. Macromolecules 40 (2007), pp. 3296–3305.

141 JL Bahr, JM Tour. Chem Mater 13 (2001), pp. 3823–3824.

142 YZ You, CY Hong, CY Pan. Macromol Rapid Commun 27 (2006), pp. 2001–2006.

143 IC Liu, HM Huang, CY Chang, HC Tsai, CH Hsu, RCC Tsiang. Macromolecules 37 (2004), pp. 283–287.

144 HL Wu, YT Yang, CCM. Ma, HC Kuan. J Polym Sci Part A Polym Chem 43 (2005), pp. 6084–6094.

145 CF Kuan, HC Kuan, CCM Ma, CH Chen, HL Wu. Mater Lett 61 (2007), pp. 2744–2748.

146 SM Yuen, CCM Ma, CL Chiang, JA Chang, SW Huang, SC Chen. Composites A 38 (2007), pp. 2527–2535.

147 YC Jung, NG Sahoo, JW Cho. Macromol Rapid Commun 27 (2006), pp. 126–131.

148 HC Kuan, CCM Ma, WP Chang, SM Yuen, HH Wu, TM Lee. Compos Sci Technol 65 (2005), pp. 1703–1710.

149 K Kobashi, Z Chen, J Lomeda, U Rauwald, WF Hwang, JM Tour. Chem Mater 19 (2007), pp. 291–300.

150 S Qin, D Qin, WT Ford, DE Resasco, JE Herrera. Macromolecules 37 (2004), pp. 752–757.

151 G Wang, Y Dong, L Liu, C Zhao. J Appl Polym Sci 105 (2007), pp. 1385–1390.

152 H Li, F Cheng, AM Duft, A Adronov. J Am Chem Soc 127 (2005), pp. 14518–14524.

153 H Li, A Adronov. Carbon 45 (2007), pp. 984–990.

154 JE Riggs, DB Walker, DL Carroll, YP Sun. J Phys Chem B 104 (2000), pp. 7071–7076.

155 W Huang, Y Lin, S Taylor, J Gaillard, AM Rao, YP Sun. Nano Lett 2 (2002), pp. 231–234.

156 Y Lin, AM. Rao, B Sadanadan, EA Kenik, YP Sun. J Phys Chem B 106 (2002), pp. 1294–1298.

157 JE Riggs, Z Guo, DL Carroll, YP Sun. J Am Chem Soc 122 (2000), pp. 5879–5880.

158 R Czerw, Z Guo, PM Ajayan, YP Sun, DL Carroll. Nano Lett 1 (2001), pp. 423–427.

159 Y Lin, AM Rao, B Sadanadan, EA Kenik, YP Sun. J Phys Chem B 106 (2002), pp. 1294–1298.

160 H Hu, N Ni, SK Mandal, V Montana, B. Zhao, R.C. Haddon . J Phys Chem B 109 (2005), pp. 4285–4289.

161 JJ Ge, D Zhang, Q Li, H Hou, MJ Graham, L Dai. J Am Chem Soc127 (2005), pp. 9984–9985.

162 M Sano, A Kamino, J Okamura, S Shinkai. Langmuir 17 (2001), pp. 5125–5128.

163 FD Negra, M Meneghetti, E Menna. Fuller Nanotub Carbon Nanostruct 11 (2003), pp. 25–34.

164 J Chattopadhyay, FJ Cortez, S Chakraborty, NKH Slater, WE Billups. Chem Mater 18 (2006), pp. 5864–5868.

165 JJ Stephenson, JL Hudson, AD Leonard, BK Price, JM Tour. Addition of acid-sensitive addends, J Phys Condens Matter 19 (2007), pp. 3491–3498.

166 M Sano, A Kamino, S Shinkai. Angew Chem Int Ed 40 (2001), pp. 4661–4663.

167 H Kitano, K Tachimoto, Y Anraku. J Colloid Interface Sci 306 (2007), pp. 28–33.

168 SJ Han, B Kim, KD Suh. Macromol Chem Phys 208 (2007), pp. 377–383.

169 C Zhou, S Wang, Y Zhang, Q Zhuang, Z Han. Polymer 49 (2008), pp. 2520–2530.

170 DE Hill, Y Lin, AM Rao, LF Allard, YP Sun. Macromolecules 35 (2002), pp. 9466–9471.

171 W Guojian, Q Zehua, L Lin, S Quan, G Jianlong. Mater Sci Eng A 472 (2008), pp. 136–139.

172 D Baskaran, JW Mays, MS Bratcher. Polymer 46 (2005), pp. 5050–5057.

173 Y Lin, B Zhou, KAS Fernando, P Liu, LF Allard, YP Sun. Macromolecules 36 (2003), pp. 7199–7204.

174 JE Riggs, Z Guo, DL Carroll, YP Sun. J Am Chem Soc 122 (2000), pp. 5879–5880.

175 KAS Fernando, Y Lin, B Zhou, M Grah, R Joseph, LF Allard. J Nanosci Nanotechnol 5 (2005), pp. 1050–1055.

176 N Zhang, J Xie, M Guers, VK Varadan. Smart Mater Struct 13 (2004), pp. N1–N4.

177 B Zhao, H Hu, A Yu, D Perea, RC Haddon. J Am Chem Soc 127 (2005), pp. 8197–8203.

178 Y Ni, H Hu, EB Malarkey, B Zhao, V Montana, RC Haddon. J Nanosci Nanotechnol 5 (2005), pp. 1707–1712.

179 D Baskaran, JW Mays, MS Bratcher. Polymer 46 (2005), pp. 5050–5057.

JG Smith, JW Connell, DM Delozier, PT Lillehei, KA Watson, Y Lin. Polymer 45 (2004), pp. 825–836.

181 JG Smith, DM Delozier, JW Connell, KA Watson. Polymer 45 (2004), pp. 6133–6142.

182 D Hill, Y Lin, L Qu, A Kitaygorodskiy, JW Connell, LF Allard . Macromolecules 38 (2005), pp. 7670–7675.

183 D Baskaran, JR Dunlap, JW Mays, MS Bratcher. Macromol Rapid Commun 26 (2005), pp. 481–486.

184 BX Yang, JH Shi, KP Pramoda, SH Goh. Nanotechnology 18 (2007), pp. 125606–125607.

185 X Wang, H Liu, Y Jin, C Chen. J Phys Chem B 110 (2006), pp. 10236–10240.

186 X Lou, C Detrembleur, C Pagnoulle, R Jerome, V Bacharova, A Kiriy. Adv Mater 16 (2004), pp. 2123–2127.

187 X Lou, C Detrembleur, V Sciannamea, C Pagnoulle, R Jerome. Polymer 45 (2004), pp. 6097–6102.

188 Y Liu, Z Yao, A Adronov. Macromolecules 38 (2005), pp. 1172–1179.

189 HC. Wang, Y Li, MJ Yang. Sens Actuators B 124 (2007), pp. 360–367.

190 H Kitano, K Tachimoto, M Gemmei-Ide, N Tsubaki. Macromol Chem Phys 207 (2006), pp. 812–819.

191 WT Wu, L Shi, Y Wang, W Pang, Q Zhu. Nanotechnology 19 (2008), pp. 125607 [7pages].

192 VK Gupta, NB Pangannaya. Carbon nanotubes: bibliometric analysis of patents, World Patent Information, 22 (2000), pp. 185-189.

193 PR G Thomas, Ryne, JL Brian, JH Michael. US7361430 (2008).

194 G Nadia, L Joachim, ECK Cornelis, JH Anastasios. EP2062931 (2009).

195 AB Richard. US7411019 (2008).

196 SS Michael. U Monica, B Paul, AD Christopher, TM Tour. WK Carter , HH Robert, ES Richard. US7572426 (2009).

197 MF Valerie, QI Yu, JG Paul. US20100124713 (2010).

198 AA Mamedov, N Kotov, M Prato, DM Guldi, JP Wicksted, A Hirsch. Nat Mater 1 (2002), pp. 190–194.

199 M Olek, J Ostrander, S Jurga, H Mohvald, N Kotov, K Kempa. Nano Lett 4 (2004), pp. 1889–1895.

200 R Blake, YK Gun'ko, J Coleman, M Cadek, A Fonseca, JB Nagy. J Am Chem Soc 126 (2004), pp. 10226–10227.

201 R Blake, JN Coleman, MT Byrne, JE McCarthy, TS Perova, WJ Blau. J Mater Chem 16 (2006), pp. 4206–4213.

202 L Xie, F Xu, F Qiu, H Lu, Y Yang. Macromolecules 40 (2007), pp. 3296–3305.

203 GL Huang, YT Shieh, KC Hwang. Adv Funct Mater 14 (2004), pp. 487–491.

204 JN Coleman, M Cadek, R Blake, V Nicolosi, KP Ryan, C Belton. Adv Funct Mater 14 (2004), pp. 791–798.

205 KP Ryan, M Cadek, V Nicolosi, D Blond, M Ruether, G Armstrong. Compos Sci Technol 67 (2007), pp. 1640–1649.

206 C Velasco-Santos, AL Martinez-Hernandez, FT Fisher, R Ruoff, VM Castano. Chem Mater 15 (2003), pp. 4470–4475.

207 KW Putz, CA Mitchell, R. Krishnamoorti, PF Green. J Polym Sci B 42 (2004), pp. 2286–2293.

208 M Kang, SJ Myung, HJ Jin. Polymer 47 (2006), pp. 3961–3966.

209 WE Dondero, RE Gorga. J Polym Sci Part B Polym Phys 44 (2006), pp. 864–878.

210 MV Jose, D Dean, J Tyner, G Price, E Nyairo. J Appl Polym Sci 103 (2007), pp. 3844–3850.

211 Z Spitalsky, D Tasis, K Papagelis, C Galiotis. Prog Polym Sci 35 (2010), pp. 357-401.

212 HM Kim, K Kim, SJ Lee, J Joo, HS Yoon, SJ Cho. Curr Appl Phys 4 (2004), pp. 577–580.

213 P Pötschke, AR Bhattacharyya, A Janke. Carbon 42 (2004), pp. 965–969.

214 H Koerner, W Liu, M Alexander, P Mirau, H Dowty, RH Vaia. Polymer 46 (2005), pp. 4405–4420.

215 Y Mamunya, A Boudenne, N Lebovka, L Ibos, Y Candau, M Lisunova. Compos Sci Technol 68 (2008), pp. 1981–1988.

216 CA Mitchell, JL Bahr, S Arepalli, JM Tour, R Krishnamoorti. Macromolecules 35 (2002), pp. 8825−8830.

217 R Krishnamoorti, K Yurekli. Curr Opin Colloid Interface Sci 6 (2001), pp. 464−470.

218 ES Choi, JS Brooks, DL Eaton, MS Al-Haik, MY Hussaini, H Garmestani, D Li, K Dahmen. J Appl Phys 94 (2003), pp. 6034−603.

219 Z Jin, X Sun, G Xu, SH Goh, W Ji. Chem Phys Lett 318 (2000), pp. 505-510.

220 YC Chen, NR Raravikar, LS Schadler, PM Ajayan, YP Zhao. Appl Phys Lett 81 (2002), pp. 975.

221 'PolyOlefins Planning Service: Executive Report, Global Commercial Analysis' published by Nexant available on www.chemsystems.com (consulted on 01.04.2010).

222 F Ciardelli, S Coiai, E Passaglia, R Pucci, G Ruggeri. Polym Int 57 (2008), pp. 805-836.

223 Q Ling, J Sun, Q Zhao, Q Zhou. Polym Plast Tech Eng 49 (2010), pp. 481-486.

224 S Isaji, Y Bin, M Matsuo. Polymer 50 (2009), pp. 1046-1053.

225 K Prashantha, J Soulestin, MF Lacrampe, P Krawczak. Compos Sci Technol 69 (2009), pp. 1756-1763.

226 CA Mitchell, JL Bahr, S Arepalli, JM Tour, R Krishnamoorti. Macromolecules 35 (2002), pp. 8825–8830.

227 L Moreira, R Fulchiron, G Seytre, P Dubois, P Cassagnau. Macromolecules 43 (2010), pp. 1467–1472.

228 W Bauhofer, JZ Kovacsa. Compos Sci Technol 69 (2009), pp. 1486-1498.

229 C Perrot, PM Piccione, C Zakri, P Gaillard, P Poulin. J Appl Polym Sci 114 (2009), pp. 3515-3523.

230 J Honel, V Vikram. Deshpande. Science 325 (2009), pp. 1084-108

231 F Caka, MR Moroglu, H Cankurtaran, F Karaman. Sens Actu B Chem 145 (2010), pp. 126-132.

232 Y Ivanov, I Marinov, K Gabrovska, N Dimcheva, T Godjevargova. J Molecular Catalysis B: Enzymatic 63 (2010), pp. 141-148.

233 KU Jeong, JY Lim, JJ Lee, SL Kang, C Nah. PolymInt 59 (2010), pp. 100–106.

234 PR Thakre, DC Lagoudas. J App Polym Sci 116 (2010), pp. 1919-202.

235 JM Thomassin, I Huynen, R Jerome, C Detrembleur. Polymer 51 (2010), pp. 115-121.

236 SA Curran, D Zhang, WT Wondmagegn, AV Ellis, J Cech, S Roth, DL Carroll, J Mater Res 21 (2006), pp. 1071.

237 KS Liao, J Wang, D Fruchtl, NJ Alley, EP Dillon, R Barron, H Kim, HJ Byrne, WJ Blau, A Seamus. Chem Phys Lett 489 (2010), pp. 207-211.

238 P Pieta, GZ Zukowska, SK Das, F D'Souza. J Phys Chem C 114 (2010), pp. 8150–8160.

239 F Gao, L Viry, M Maugey, P Poulin, N Mano. Nature communications 1, Article 2, (doi:10.1038/ncomms1000).

240 K Saint-Aubin, P Poulin, H Saadaoui, M Maugey, C Zakri. Langmuir, 25 (2009), pp. 13206–13211.

241 M Panhuis, A Maiti, AB Dalton, A Noort, JN Coleman, B McCarthy, WJ lau. J Phys Chem B 107 (2003), pp. 478-482.

242 S Cranford, H Yao, C Ortiz, MJ Buehler. J Mechan Phys Solid 58 (2010), pp. 409-427.

243 X Chen, IJ Beyerlein, L C Brinson. Mechan Mater 41 (2009), pp. pp 279-292.

244 RG Lopez, C Boisson, F D'Agosto, R Spitz, F Boisson, D Gigmes, D Bertin. Macromol Rapid Comun 27 (2006), pp. 173-181.

Chapter 2

Pentadecane grafting onto nanotubes

2.1 Model compound approach for PE grafting onto nanotubes

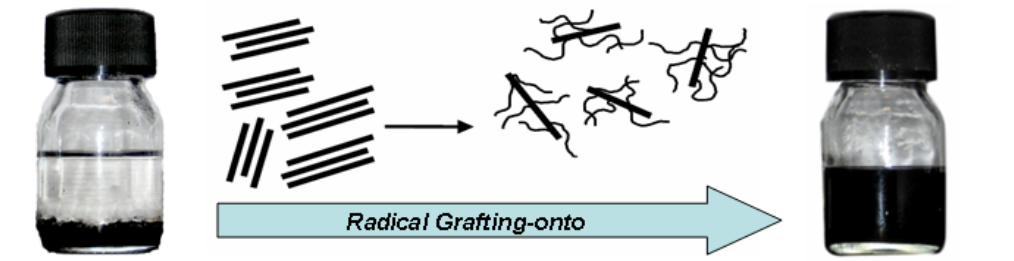

Pristine MWCNTs settled down in Dichlorobenzene

Pentadecance grafted MWCNTs dispersed in Dichlorobenzene

2.1.1 Overview

PE is by far the most common commercial polymers that we encounter in day-to-day life. A number of disadvantages prevent their even wider use. These include the lack of functional groups and polarity, which results in poor adhesion and incompatibility between polyolefins and other materials such as glass fibres, clays, metals, pigments, fillers, and most polymers. The properties of polyolefins are modified through the introduction of the fillers, but the components are not compatible as such. To reduce the interfacial tension between the matrix and the filler, fillers are often functionalised, coated by different techniques as detailed in literature review.

In order to prepare PE/nanotubes composite with enhanced properties of interest e.g. reinforcement, there must be a good dispersion of CNTs and some chemical linkage between the two phases of the composite. To overcome incompatibility of nanotubes and PE we envisaged a scheme to graft PE during extrusion through radical grafting onto nanotubes. But before using this procedure a model compound study was adopted to obtain optimised reaction conditions. Pentadecane was selected as a model since it represents the chemical structure of PE. Moreover use of pentadecane makes the extensive characterisation easier which might be difficult in case of PE since pentadecane is in liquid form at ambient temperature.

In this model compound study we observed that there is a tough competition between two reactions: combination of radicals and addition of radicals to unsaturated carbon bonds available on the surface of the nanotubes. We optimised our reaction conditions (e.g. temperature, concentration of reactants) to obtain high grafting density.

One of the most challenging tasks of this study was to identify the reaction pathways as there were many possible side reactions involving combination of radicals. We used gas chromatography mass spectroscopy (GC-MS) technique to follow the reaction trail. Grafting of pentadecane onto nanotubes was confirmed qualitatively (by Raman spectroscopy and transmission electron microscopy) and quantitatively (by thermogravimetric and elemental analysis).

The results of this model compound study provided a base for further exploitation of this strategy of 'grafting onto'.

2.1.2 Article Details

This work was published in Polymer,volume 50, issue 12, pages 2535-2543 on 5 June 2009, entitled 'Radical grafting of polyethylene onto MWCNTs: A model compound approach'. Parts of the contents of this paper were presented in '7th Eurofillers International conference − From macro to nanofillers for structural and functional polymer materials' held in the Alessandria site of the Polytechnic of Turin, Italy from 21 to 25 June, 2009; and in '5th International ECNP conference − Nanostructured Polymer and Nanocomposites' convened by The European Centre for Nanostructured Polymer at Ecole Nationale Supérieure d' Arts et Métiers ParisTech (ENSAM), Paris, France, from 15 to 17 April 2009.

2.2 Radical grafting of polyethylene onto MWCNTs: A model compound approach

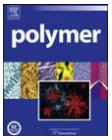

Sohaib Akbar [a,b,c], Emmanuel Beyou [a,b,c], Philippe Cassagnau [a,b,c], Philippe Chaumont [a,b,c], Gholamali Farzi [a,b,c]

[a] Université de Lyon, Lyon F-69003, France

[b] Université de Lyon 1, F-69003 Villeurbanne, France

[c] CNRS UMR5223, Ingénierie des Matériaux Polyméres, Laboratoire des Matériaux Polyméres et Biomatériaux, F-69622 Villeurbanne, France

2.2.1 Abstract

Covalent functionalisation of pentadecane-decorated multiwalled carbon nanotubes (MWCNTs) has been studied as a model compound approach for the grafting of poly(ethylene-co-1-octene) onto MWCNTs by reactive extrusion. It was accomplished through radical addition onto unsaturated bonds located on the MWCNTs' surface using dicumyl peroxide as hydrogen abstractor. It was found that this surface treatment results into the break-up of the native nanotube bundles and increases solubility in various solvents. Raman spectroscopy was utilized to follow the introduction of pentadecane on the MWCNTs'surface; while thermogravimetric analysis and elemental analysis indicated the extent of this grafting. Pentadecane functionalized MWCNTs were imaged by transmission electronic microscopy showing single long functionalized MWCNTs distinct from the starting pristine bundles.

2.2.2 Introduction

Carbon nanotubes (CNTs) are extremely promising for applications in materials science and engineering. Much attention has been paid to CNT-based nanocomposites for the preparation of high-performance materials exhibiting

improved or unusual mechanical and physical properties. The combination of a soft polymer matrix with nanosized rigid filler particles can provide new nanocomposite materials with largely improved modulus and strength. However, the homogeneous dispersion of raw CNTs within a polymeric matrix is relatively difficult to achieve, especially in apolar matrixes such as polyolefins. Indeed, carbon nanotubes tend to aggregate as very long bundles due to the high surface energy and the stabilization by numerous of π–π electron interactions among the tubes. Several methods for preparing polymer/CNTs nanocomposites have been explored to achieve good dispersion and load transfer, such as noncovalent [1,2,3] and covalent [4,5] approaches. The noncovalent methods, including solution mixing [6], melt mixing [7] and in situ polymerization [8] are simple and convenient; however, the dispersion of CNTs and the interfacial interaction between CNTs and polymer matrix are poor, especially in the case of melt mixing. In contrast, the covalent approaches, including "grafting to" [4,9] and "grafting from" [9,10], leading to chemical linkage between polymer and the surface of CNTs, improve the dispersion of CNTs in polymer matrices. However, the synthesis of end-functionalized polyethylene (PE), which is necessary in the "grafting to" approach, is difficult [11]. Otherwise, the grafting procedure can be achieved by *in situ* polymerization of ethylene as catalyzed directly from the nanotubes surface treated by a highly active metallocene-based complex [8,12].

Another promising route for a chemical modification of MWCNTs by PE is to use free radical initiators such as peroxides. The general mechanism of free radical grafting of vinyl compound from hydrocarbon chains detailed by Russell [13], Chung [14] and Moad [15] seems to express a widespread view. The grafting reaction starts with hydrogen abstraction by alkoxyl radicals generated from thermal decomposition of the peroxide. Then, the active species generated onto the hydrocarbon backbone react with unsaturated bonds located on the MWCNTs surface. This chemical modification is thus conceivable during reactive extrusion because the radicals' lifetimes (in the range of few milliseconds) are compatible with typical residence time in an extruder (around 1 min). Nevertheless, the main drawback of the free radical grafting is the low selectivity of the radical center, specially at high

temperatures (in the range of 150–200 °C, required for extrusion of polyethylene), leading to side reactions such as coupling and chain scission [13,[16]]. Moreover, performing this chemical modification by reactive processing brings in many constraints inherent to the processing (e.g. short reaction time, viscous dissipation and high temperature). For instance, the difference of viscosity between the monomer and the molten polymer could enhance these side reactions. So, to separate these physical influences from the chemical modification, the grafting reaction is, in this work, predicted with a model compound approach based on a radical grafting reaction between peroxide-derived alkoxyl radicals, and a low molar mass alkane representing characteristics moieties of PE. We resorted to pentadecane ($C_{15}H_{32}$) as model for polyethylene.

Indeed, high boiling points of long chain alkanes permit study under high temperature conditions, typically over 150 °C. It also gives clues about low viscosity at 150 °C, on top of that the formed products in the grafting experiment can hence be analysed more easily than in the polymer melt.

Scanning the factors influencing the selectivity toward hydrogen abstraction and radical grafting reaction is of particular interest and dicumyl peroxide (DCP) has been selected to generate alkoxyl radicals in presence of the alkane model. Experiments reported here involve decomposition of DCP. Its thermal decomposition is carried out in a range of temperatures close to the ones expected during reactive extrusion of poly(ethylene-co-1-octene) typically few minutes at 150–200 °C.

This manuscript aims at describing the course of the generated radical species and the extent of the grafting reaction in regards to the DCP concentration and temperature. This chemical functionalization approach leads to high degree of functionalization which influences solubility behaviour of the formed pentadecane-grafted MWCNTs in various solvents. In addition, pentadecane-grafted MWCNTs were analysed by Raman spectroscopy, transmission electronic microscopy, thermogravimetric analysis and elemental analysis.

2.2.3 Experimental

2.2.3.1 Materials

MWCNTs (Graphistrength™ C100: see salient characteristics in Table 2-1) were kindly supplied by ARKEMA.

Table 2-1: Characteristics of Graphistrength™ C100.

Manufacturing	CCVD
Apparent density	50–150 kg/m^3
Mean agglomerate size	200–500 µm
C contents	~90 wt%
Mean number of walls	5–15
Outer mean diameter	10–15 nm
Length	0.1–10 µm

The low molecular weight hydrocarbon substrate, used as model for poly(ethylene-co-octene), was pentadecane (99%, Sigma–Aldrich – France). Initiator was dicumyl peroxide (99%, Sigma–Aldrich – France) and all other solvents were used without any further purification so as to fit with the industrial conditions required in the melt processing.

2.2.3.2 Surface activation of MWCNTs

In this study, MWCNTs were oxidized in air at 450 °C for 1 h. Air oxidized MWCNTs are used throughout this study and referred as pristine (p-MWCNTs).

2.2.3.3 Decomposition of DCP in the presence of p-MWCNTs and alkanes

The thermolysis of dicumyl peroxide (DCP) in pentadecane was performed in a glass reactor. In a typical grafting experiment, DCP (0.23 g/0.85 mmol), as a radical initiator, was first mixed in with p-MWCNTs (50 mg) and pentadecane (7.69 g/36.26 mmol) and then sonicated for 15 min. After that, the suspension was degassed by 4 freeze-pump-thaws, and then it was heated to 150 °C under stirring. After 6 h, the reaction mixture was cooled down quickly and diluted in DMF for

characterization through gas chromatography analysis. The grafted MWCNTs were collected by centrifugation (11K rpm, 20 min) and subsequent filtration.

2.2.3.4 Recovery of free and tethered pentadecane molecules

The free pentadecane molecules were isolated from the grafted MWCNTs by exhaustive cleaning of the suspension by dialysis. In a typical process, 30 mL of the MWCNTs' suspension was introduced into a cellulose membrane (Spectra/Por, MW cut-off, 1000 by Spectrum Medical Industries, Inc.) and repeatedly dialyzed against DMF until no residual pentadecane could be detected in the recovered solution (determined gravimetrically). Then, the pentadecane-grafted MWCNTs suspension was dried at 80 °C to evaporate the solvent prior to characterization. Details of the specimens prepared and tested are given in Table 2-2.

Table 2-2: List of samples according to the experimental conditions.

Sample	Constituents	Reaction conditions	Principal product
A	MWCNTs (50 mg) + DCP (0.23 g) + pentadecane (7.69 g)	150 °C for 6 h	Penta-g-MWCNTs
B-1	Blank experiment: DCP (0.23 g) + pentadecane (7.69 g)	150 °C for 6 h	Interlinked pentadecane
B-2	Blank experiment: MWCNTs (50 mg) + DCP (0.23 g) + DMF (5 mL)	150 °C for 6 h	Cumyloxyl-g-MWCNTs
C	MWCNTs (50 mg) + DCP (0.23 g) + pentadecane (7.69 g)	At different temperatures for 6 h	Penta-g-MWCNTs
D	MWCNTs (50 mg) + DCP (different ratios		

2.2.4 Characterisation

Gas chromatography–mass spectrometry (GC–MS) was performed with an Agilent 6890 series GC system equipped with an HP-5ms (5%-phenyl)-methylpolysiloxane, ref. 19091S-433. The injector was at 250 °C and the temperature programme followed was: 50–310 °C at 20 °C/min. Injection and detection by MS were carried out at 280 °C.

Raman spectra were obtained by using a Raman spectrometer (RM1000, Renishaw, Wotton under Edge, U.K.). The sample was excited with Argon Laser at 514.5 nm. Thermogravimetric analysis (TGA) was carried out with a DuPont Instruments TGA 2950 thermobalance, controlled by a TC10A microprocessor. Samples were heated at 20 °C/min under a nitrogen flow (100 mL/min).

Elemental analysis (EA) was carried out (Analyzer: LECO SC144, Service central d'analyse du CNRS, Vernaison, France) to determine the contents of C and H.

Transmission electron microscopy (TEM) was carried out with a Philips CM-120 microscope (Philips Consumer Electronics BV, Eindhoven, The Netherlands) operated at 80 keV.

Solubility was determined gravimetrically. In a typical experiment, saturated solutions of penta-g-MWCNTs were prepared by sonication in vials. Sonication was done using S 40 H Elmasonic by Elma (Singem, Germany) for 15 min. Water bath temperature therein raised maximum to 35 °C. Vials were kept free standing over one month at room temperature and then the upper half aliquot part was carefully taken out with a syringe and heated to remove solvent under vacuum. All the weighting was carried out using an analytical balance with a sensitivity of 0.1 mg.

2.2.5 Results and discussion

2.2.5.1 Free radical grafting of pentadecane onto MWCNTs

Fig. 2-1 sums up main reactive pathways of free radical grafting of pentadecane onto MWCNTs with dicumyl peroxide as initiator.

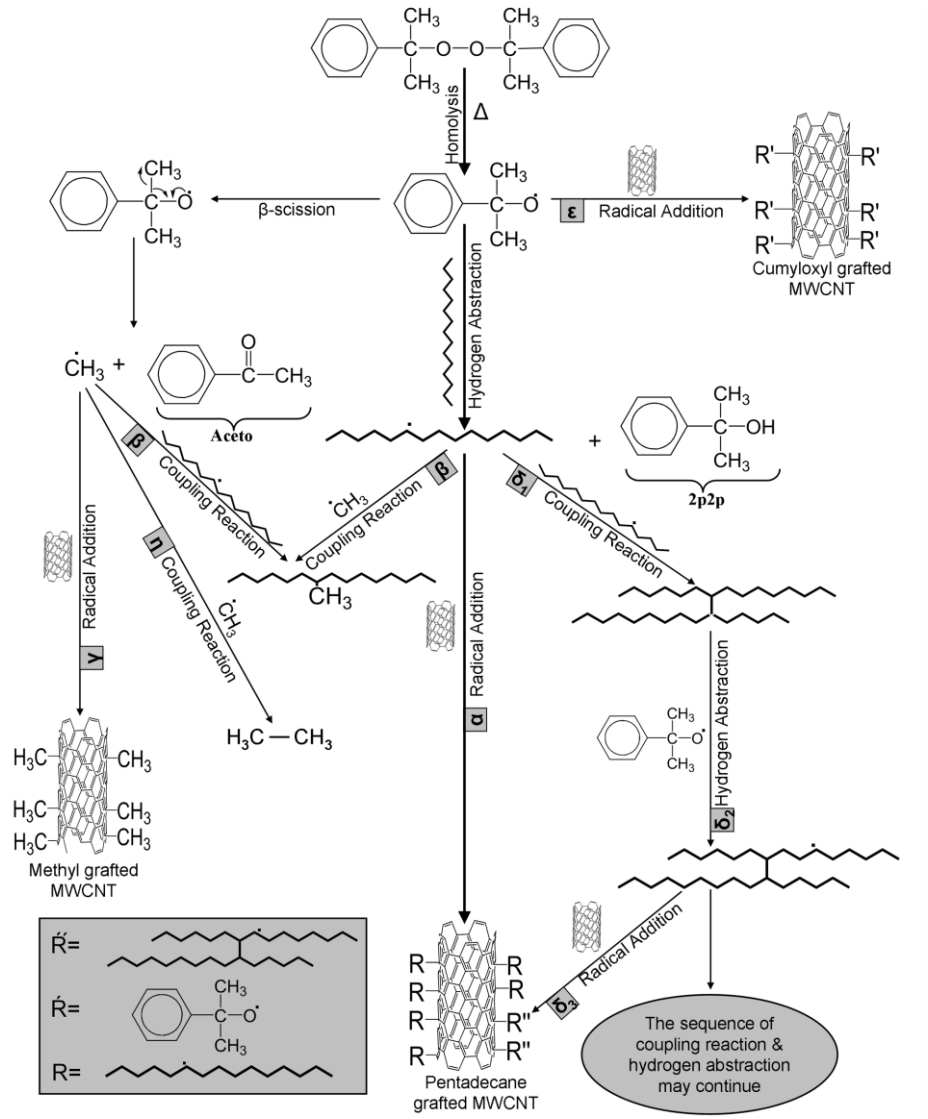

Figure 2-1: General reactive pathways of free radical grafting of pentadecane onto MWCNTs.

The hydrogen abstraction reaction from alkyl hydrocarbon bonds was studied starting from the reaction of DCP-derived radicals with pentadecane. However, the alkoxy radicals can undergo additional reactions including β-scission leading to the formation of methyl radicals [17]. These latter preferentially induce coupling reaction (Fig. 2-1, route β and η) or attack onto the sp^2 carbon of the MWCNTs (Fig. 2-1, route γ) whereas cumyloxyl radicals are more prone to hydrogen abstraction from pentadecane [15]. The formed pentadecyl radicals through hydrogen abstraction are able to react with MWCNTs by radical addition onto sp^2 carbon of the MWCNTs (Fig. 2-1, main route α) and with other radical species via the common radical coupling reactions (Fig. 2-1, routes δ_1 and β). According to the results of Johnston [18,19], based on a study of the crosslinking reaction of poly(ethylene-co-1-

octene) in the presence of DCP at 160 °C, coupling reactions are four times more prone to happen than scission reactions so we assume that pentadecyl radicals do not undergo scission reactions. First, we investigated the selectivity of cumyloxyl radicals, coming from the thermal decomposition of DCP, to find out the chemical structure of the formed species. As described in Fig. 2-1, the cumyloxyl radical, can undergo two main reactions leading to the formation of 2-phenyl-2-propanol (2p2p) through H-abstraction from the hydrocarbon substrate, or acetophenone (aceto) by intramolecular β-scission. We found it interesting to see whether the presence of the MWCNTs could modify the radical species course.

First, products arising from the reaction involving a solution of DCP in pentadecane (blank, sample B-1, Table 2-2) were analysed by GC–MS (Fig. 2-2). Three main peaks corresponding to 2p2p, aceto and pentadecane are observed in Fig. 2-2 confirming H-abstraction from pentadecane and β-scission reaction from cumyloxyl radicals respectively. The small peaks observed from 6 min to 14 min are attributed to interlinked pentadecane molecules and are believed to be synthesized by combination of the formed pentadecane radicals.

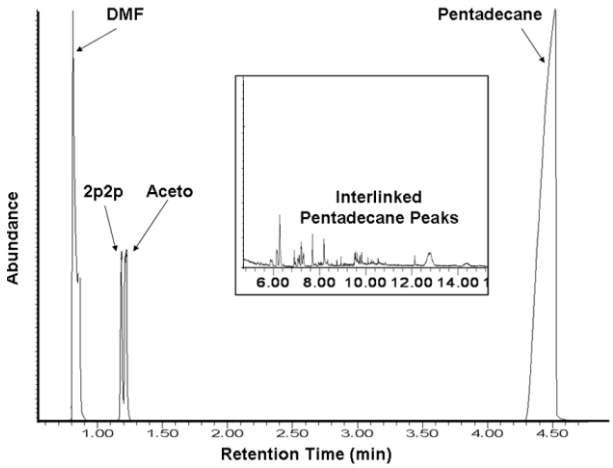

Figure 2-2: GC–MS chromatogram of the liquid phase of the blank sample B-1 (diluted with DMF after reaction); inset: a myriad of small pentadecane peaks observed after ca. 6 min.

For the reaction procedure where MWCNTs are included in the solution of DCP in pentadecane (sample A, Table 2-2), GC–MS analysis of the formed products (Fig. 2-3)

mainly displays a big peak corresponding to 2p2p and a smaller one attributed to aceto.

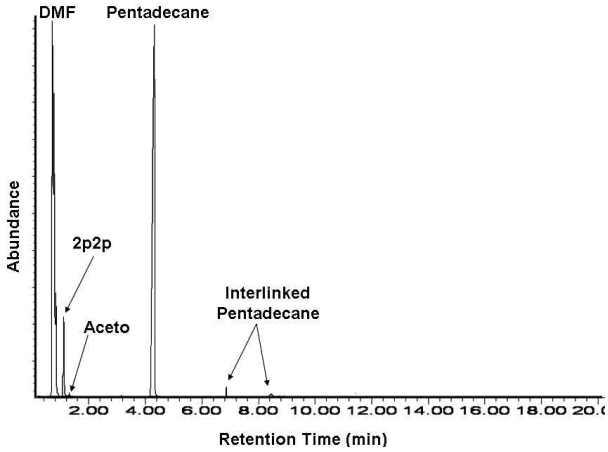

Figure 2-3: GC–MS chromatogram of the liquid phase of the sample A (diluted with DMF after reaction).

Assuming that the A_{2p2p}/A_{Aceto} area ratio of the corresponding peaks is directly linked to the [2p2p]/[aceto] concentration ratio [17], we investigated the course of pentadecane radicals through the calculations of A_{2p2p}/A_{Aceto}, A_{Penta}/A_{aceto}, A_{Penta}/A_{2p2p} area ratios (Table 2-3). The A_{2p2p}/A_{Aceto} area ratio is ten times higher in the case of sample A than in the case of sample B-1, suggesting that presence of MWCNTs favorably changes the course of reaction by limiting β-scission reaction and attracting cumyloxyl radicals. In a similar way, the area ratio A_{Penta}/A_{aceto} is higher for sample A and no significant change is observed for the A_{Penta}/A_{2p2p} ratio in any of the samples (Table 2-3).

Table 2-3: Area ratios of different constituents in GC analysis.

Ratio	Fig. 2-1, sample B-1	Fig. 2-2, sample A
A_{2p2p}/A_{Aceto}	∾0.9	∾10
A_{Penta}/A_{Aceto}	∾4	∾30
A_{Penta}/A_{2p2p}	∾5	∾4

Moreover, GC-MS chromatogram of sample A (Fig. 2-3) only displays two other peaks assigned to interlinked pentadecane molecules. On contrary, chromatogram of sample B-1 displays a large number of such peaks (Fig. 2-2) giving an evidence that

most radical pentadecane chains are grafted onto MWCNTs surface in case of sample A. Besides, no DCP traces were detected in any of the samples (A and B-1).

Direct evidence for covalent sidewall functionalization can be also found by Raman spectroscopy [20,21,22]. G band is a characteristic feature of the graphitic layers and corresponds to the tangential vibration of the carbon atoms. The second characteristic mode is a typical sign for defective graphitic structures (D band). The ratio between the G band and D band is a good indicator of the changes in chemistry of CNTs. Interestingly, Raman spectra of p-MWCNTs (Fig. 2-4a) and penta-g-MWCNTs (Fig. 2-4b) show two main peaks around 1350 cm^{-1} (D band) and 1586 cm^{-1} (G band). The relatively high intensity of the G band relative to D band ($A_D/G_D = 1.55$) for penta-g-MWCNT sample in comparison with that of p-MWCNT (i.e. $A_D/A_G = 1.2$) could be designated as an indicator of grafting species.

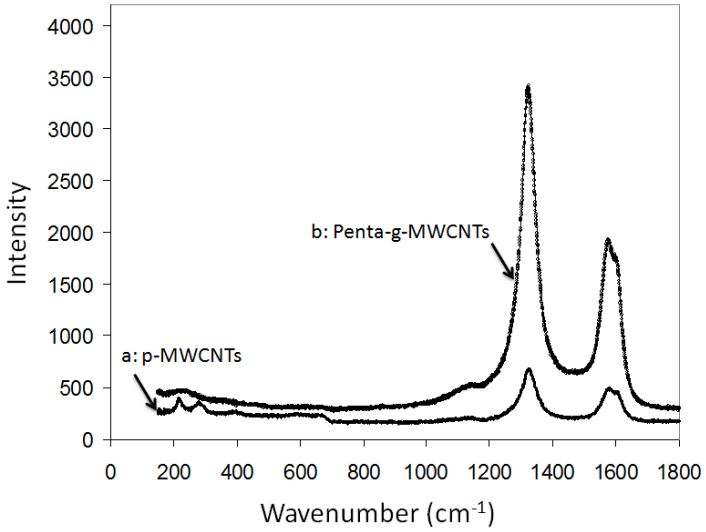

Figure 2-4: Raman spectra of: p-MWCNTs (a) and penta-g-MWCNTs (b).

To gain a more quantitative picture of the extent of nanotube functionalization, thermogravimetric analysis was performed on the reaction products. Indeed, it is well known that heating functionalized nanotubes in an inert atmosphere removes the organic moieties and restores the pristine nanotubes structure [23,24,25].It is noteworthy that the adsorbed molecules can be removed from the grafted ones by dialysis as mentioned in the experimental part. As shown in Fig. 2-5, the amount of

organic functionalities physically and/or covalently attached to the initial MWCNTs can be neglected (weight loss < 1.5%).

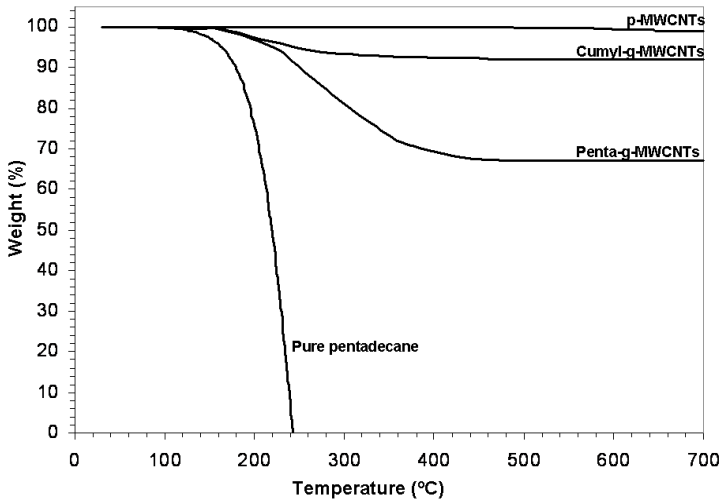

Figure 2-5: TGA data (under N2) for cumyl-g-MWCNTs and penta-g-MWCNTs with that of p-MWCNTs and pure pentadecane for corresponding reference.

After treatment with DCP (blank experiment B-2), the weight loss increases to 8% (Fig. 2-5) as expected for MWCNTs with more organic moieties on the surface. In addition, TGA results show that pure pentadecane can be completely decomposed at a temperature of 450 °C; therefore, the amount ofpentadecane that covalently attached to the p-MWCNTs is estimated by the weight loss of pentadecane-grafted MWCNTs sample between 180 °C and 450 °C. In Fig. 2-5, we estimate the weight of grafted pentadecane to be around 30%. It is notable here that this degree of functionalization is higher than those reported earlier for MWCNTs derivatized through the billups reaction (10–20%) [26]. The weight losses of blank sample B-2 and sample A, which are 8% for cumyloxyl groups and 30% for pentadecyl groups correspond to a surface coverage of approximately 31,600 cumyloxy groups per nanotube and 75,400 pentadecyl groups per nanotube (the calculations are based on a 5 mm long and 13 nm wide nanotube with a surface of 2.04×10^5 nm^2 and a volume of 8.8×10^5 nm^3). The average density of the nanotubes is 100 kg/m^3 so there are around 1.13×10^{13} nanotubes present per mg). Therefore, adsorptions of 0.08 mg cumyloxy group/mg CNTs (0.59 mmol/g) and 0.3 mg pentadecyl group/mg CNTs (1.42 mmol/g) suggest a grafting density of 0.034 mg/m^2 and

0.13 mg/m^2 respectively. Comparable grafting densities have been recently reported for pyrene polymer functionalized MWCNTs [27].

We can conclude that the grafting efficiency is higher for the pentadecyl radicals than for other radical species. These consequences might have originated because of two factors: (1) the increase of grafting efficiency suggests poor attack onto the sp^2 carbon of the MWCNTs by the cumyloxyl radicals; (2) the high molecular weight of the grafted molecules, i.e. pentadecane. Elemental analysis (Table 2-4) is also an indicator of degree of grafting.

Table 2-4: Carbon and hydrogen contents determined by elemental analysis.

Sample	Element	%
p-MWCNTs	C	87–90
	H	0.3–0.66
Penta-g-MWCNTs (A)	C	87–90
	H	5–6

We can observe that carbon content does not increase after the grafting procedure and hydrogen content increases from the range of 0.3–0.6 wt% for neat MWCNTs to the range of 5–6 wt% for the pentadecane-grafted MWCNTs. The hydrogen content of the grafted species, calculated from TGA, gives a value close to the one found from elemental analysis: a weight loss of 30% for the pentadecane-grafted MWCNTs (sample A) corresponds to 4.7 wt% H contents.

2.2.5.2 Influence of temperature

As discussed earlier, DCP generates methyl radicals through β-scission reaction (Fig. 2-1). This reaction is characteristic to tertiary peroxides, which undergo a unimolecular reorganisation of the primary alcoxyl radical into an alkyl radical (usually a methyl radical). It is also strongly sensitive to temperature as its driving force is entropic [28]. In order to increase the understanding of the cumyloxyl radicals' behaviour, the experiments C1 to C5 (Table 2-5) correspond to the ones performed with 3 wt% DCP, as hydrogen abstractor, at temperatures varying from 140 °C to 180 °C. For temperatures lower than 170 °C (samples C1–C3), the number

of pentadecyl groups per CNT, calculated through thermogravimetric analysis, varies from 62,800 to 77,900. The highest grafting density is obtained for sample C2 (i.e. 1.464 mmol/g).

Table 2-5: Effect of reaction temperature on the degree of grafting with 3% DCP.

Experiment	Reaction temperature (°C)	A_{2p2p}/A_{Aceto}	A_{Penta}/A_{2p2p}	Percent grafting[a] (weight loss in TGA)	Chains per CNT[b]	Grafting density[b]	
						mg m^{-2}	mmol g^{-1}
C1	140	~9	~4	25	62,800	0.108	1.180
C2	150	~10	~4	31	77,900	0.134	1.464
C3	160	~9	~5	27	67,800	0.117	1.278
C4	170	~4	~9	16	40,200	0.069	0.754
C5	180	~3	~15	10	25,100	0.043	0.470

[a] Based on TGA results.

[b] Based on calculations assuming avg. CNT length of 5 µm and OD of 13 nm. Number of chains includes interlinked chains as well.

For temperatures greater than 160 °C (i.e. 170 °C and 180 °C), the grafting density dramatically decreases from 1.278 mmol/g (weight loss = 27%) to 0.470 mmol/g (weight loss = 10%) and a fraction of insoluble product is detected. Moreover, the A_{2p2p}/A_{Aceto} area ratio (calculations are based on GC analysis of the resulting mixture) decreases by increasing temperature, while A_{Penta}/A_{2p2p} area ratio increases (Table 2-5). These results confirm that the β-scission reaction of cumyloxyl radical also increases as the temperature increases, leading to the formation of methyl radicals. These latter preferentially react by combination whereas cumyloxyl radicals are more prone to hydrogen abstraction from pentadecane [15].

2.2.5.3 Influence of DCP concentration

Maximum pentadecane grafting density was observed at 150 °C while on higher temperatures the amount of insoluble product was increased so experiments were conducted at 150 °C with various concentrations of DCP.

Experiments from D1 to D4 (Table 2-6) show that, for initiator concentration up to 3%, the more the DCP concentration is used the higher the grafting density is achieved (from 0.229 mmol/g to 1.464 mmol/g).

Table 2-6: Effect of amount of peroxide on degree of grafting at 150 °C.

Experiment	DCP (wt% of pentadecane)	Percent grafting[a] (weight loss in TGA)	Chains per CNT[b]	Grafting density[b]	
				mg m^{-2}	mmol g^{-1}
D1	0.5	5	12,600	0.021	0.229
D2	1	9	22,600	0.039	0.426
D3	2	15	37,700	0.065	0.710
A/D4[c]	3	31	77,900	0.134	1.464
D5	4	12	30,200	0.052	0.568
D6	5	8	20,100	0.034	0.371

[a] Based on TGA results.

[b] Based on calculations assuming avg. CNT length of 5 µm and OD of 13 nm. Number of chains includes interlinked chains as well.

[c] Samples A and D4 are basically same; here 'A' is named as 'D4' to keep the sequence.

For initiator concentration higher than 3 wt%, the grafting density decreases from 1.464 mmol/g to 0.371 mmol/g upon increasing DCP concentration up to 5%. Thus, to get high grafting efficiency, one should opt for optimal initiator concentration, i.e. 3 wt%, and choose the most favourable reaction temperature, i.e. 150 °C. Upon using higher amount of DCP yields a major part of MWCNTs that are not soluble in various solvents. This result is due to the fact that the presence of higher concentration of radicals changes the reaction kinetics, possibly leading to combination reactions (Fig. 2-1). This particular aspect needs further investigation in future studies to find out how concentration of different radicals changes the course of radical combination and addition.

2.2.5.4 Solubility behaviours of cumyl-g-MWCNTs and penta-g-MWCNTs

To investigate the stability of the p-MWCNTs and the functionalized MWCNTs in organic solutions, we prepared solutions by adding 200 mg of the samples into the same amount of various solvents followed by sonication for 15 min at 20 W and then

leaving them free standing for 5 min to 2 months. As illustrated in Fig. 2-6, for p-MWCNTs (unfunctionalized), we found unstable dispersions in both polar and nonpolar solvents meaning that it is not possible to well disperse p-MWCNTs in these solvents even after sonication.

Figure 2-6: Solubility behaviour of pristine carbon nanotubes (p-MWCNTs) after 5 min, cumyloxy grafted CNTs (cumyloxy-g-MWCNTs) after 30 min andpentadecane-grafted MWCNTs (penta-g-MWCNTs) after 2 months in DMF (A); acetone (B); chloroform (C); THF (D); toluene (E); DCB (F); xylene (G).

Two phenomena affect p-MWCNTs dispersion: nanotube morphology and attractive forces between the tubes. Not only the tube surfaces are attracted to each other by molecular forces, but the extremely high aspect ratios coupled with the flexibility also dramatically increase the possibilities for entanglements. For the cumyloxyl grafted MWCNTs (grafting density = 0.371 mmol/g), similar behaviour is observed suggesting that the grafting density is not high enough to ensure a good dispersion. In contrast, for pentadecane-grafted MWCNT, we found stable dispersions in DMF, toluene, DCB and xylene where the CNTs could not be centrifuged down easily (Fig. 2-6).

The obvious improvement in the suspension stability of the penta-g-MWCNTs confirms that the long alkane organic groups are covalently linked onto the sidewalls of MWCNTs that ensure fine dispersion. Three states of dispersion could be found in Fig. 2-6: sedimented—as in case of p-MWCNTs in all solvents despite sonication; swollen—as in case of cumyloxyl-g-MWCNTs and penta-g-MWCNTs in chloroform

and THF; and dispersed—as in case of penta-g-MWCNTs in DMF, toluene, DCB and xylene. The stability of pentadecane-grafted MWCNTs is disturbed in polar solvents such as acetone, chloroform and THF, however, pretty good solubility in DMF, toluene, DCB and xylene. The usual methods to separate the solubilized CNTs from those that are insoluble are vacuum filtration and Soxhlet extraction [29]. The solubility of these pentadecane stabilized dispersions was achieved according to the following procedure. At first, 200 mg of accurately weighed functionalized MWCNTs was added in 5 mL of the selected solvent under study in order to obtain a saturated solution. Then, the solution was sonicated, separated into three portions and left free standing for one month at room temperature. Then their upper half aliquot parts were carefully taken out with a syringe and solubility of pentadecane-grafted MWCNTs was finally calculated by an average weighing of the three samples after removing the solvent under vacuum at 100 °C for 12 h. The solubility values of pentadecane-grafted MWCNTs in typical organic solvents are given in Table 2-7.

The reported solubilities highly depend on degree of functionalization and values reported in Table 2-7 correspond to solutions of penta-g-MWCNTs with a grafting density of 1.464 mmol/g (sample A). Depending on the solvent, solubilities vary from 1.1 mg/mL to 19.2 mg/mL.

As shown in Table 2-7, penta-g-MWCNTs show the best solubility in dichlorobenzene (i.e. 19.2 mg/mL). These solubility values are close to those of octadecylamine modified MWCNTs reported by Guo [29] with solubilities varying from 9 mg/mL to 14.3 mg/mL in aromatic solvents and determined through UV/Vis absorption spectroscopy. As discussed by Guo [29], the relatively high solubilities of pentadecane-grafted MWCNT in various solvents provide the possibility to easily disperse MWCNTs which allows preparing MWCNTs/polymer composites.

Table 2-7: Room temperature stability and solubility of 'penta-g-MWCNTs' (sample A/D4) in various solvents.

Solvent	Solubility (mg mL^{-1})	Stability	Dielectric constant	Surface tension (20 °C in mN m^{-1})
n-Hexane	–	Suspension; complete precipitation with time	2	18.43
n-Heptane	–	Suspension; complete precipitation with time	1.9	20.14
n-Octane	–	Suspension; complete precipitation with time	1	21.62
Acetone	1.1	Metastable; high precipitation with time	20.7	25.2
THF	–	Suspension; complete precipitation with time	7.5	26.4
n-Pentadecane	–	Suspension; complete precipitation with time	2.2	26.9
Chloroform	–	Suspension; complete precipitation with time	4.8	27
Toluene	14.6	Stable over months; negligible precipitation with time	2.4	28.4
Xylene	16.3	Stable over months; negligible precipitation with time	2.6	30
DCB	19.2	Stable over months; negligible precipitation with time	2.8	33.6
DMF	13.9	Metastable; little precipitation with time	38	37.1

N.B. MWCNTs are reported in literature to have surface tension in the range of 40–80 mN m^{-1}.

It is evident from Table 2-7 that the classic principle of "like dissolves like" is no longer applicable here and does not explain well the solubility of functionalized nanotubes. Amazingly, even being nonpolar, penta-g-MWCNTs are not soluble in some nonpolar solvents like hexane, heptane, octane, and even in pentadecane; however soluble in toluene and xylene that are nonpolar as well. On the other hand these functionalized CNTs are soluble in one polar-aprotic solvent, i.e. DMF, but not

soluble in the others like THF and acetone. Various accounts suggest surface tension [27,30] and dielectric constant [31,32] are better indexes of polarity; hence might be used to investigate this strange solubility behaviour. Table 2-7 shows an interesting correlation of solubility of penta-g-MWCNTs with surface tension and dielectric constant of the solvents. As a rule of thumb, penta-g-MWCNTs make stable suspensions in all those solvents having surface tension and dielectric constant greater than those of pentadecane (i.e. grafted species).

When it comes to chloroform, its surface tension is almost equal to that of pentadecane and dielectric constant, too, not higher enough making it insoluble. Stephenson et al. [26] have also reported a meagre value of solubility (0.12 mg mL^{-1}) for alkyl chains grafted MWCNTs in chloroform.

In addition, a transmission electronic microscope was used to evaluate the local state of debundling of functionalized MWCNTs. TEM pictures of the sonicated p-MWCNTs, cumyl-g-MWCNTs and penta-g-MWCNTs are shown in Fig. 2-7, Fig. 2-8 and Fig. 2-9, respectively. Fig. 2-7 and Fig. 2-8 are shown at 1 µm scale, since it is hard to take close up photos by TEM in the presence of large accumulated mass that do not let the light to pass through.

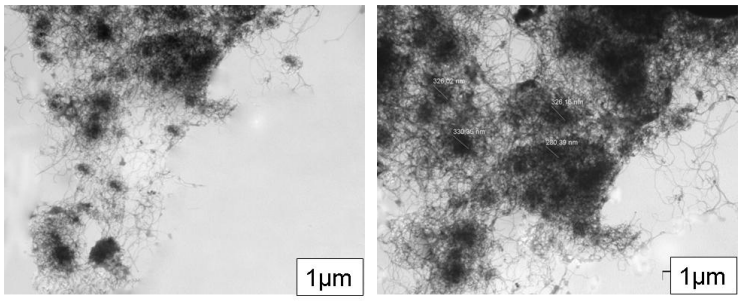

Figure 2-7: TEM images of p-MWCNTs.

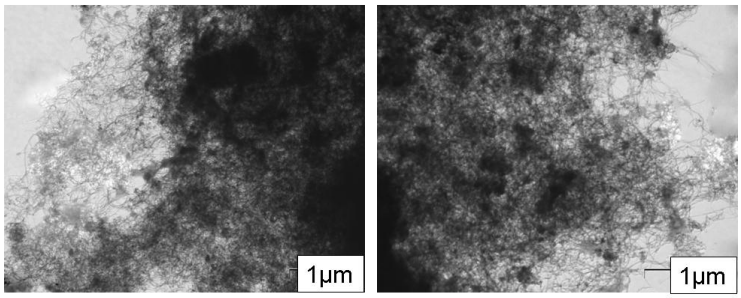

Figure 2-8: TEM micrographs of MWCNTs coated with cumyloxy groups.

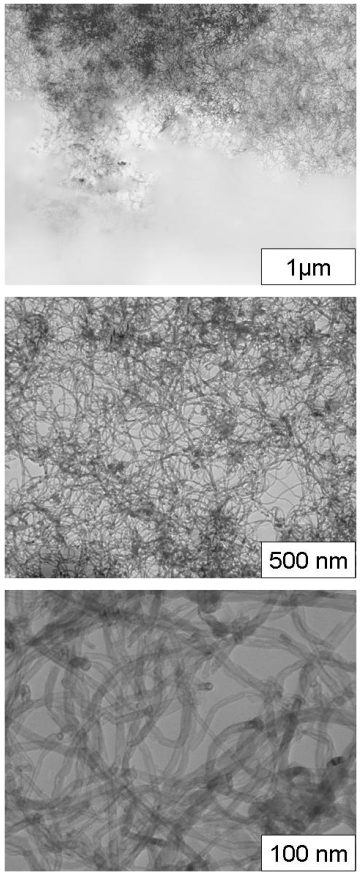

Figure 2-9: TEM micrographs of pentadecane-grafted MWCNTs.

Apparently, TEM observations demonstrate that the functionalization leads to better debundling of MWCNTs. Fig. 2-7 shows the morphologies of p-MWCNTs and illustrates the heavily entangled nature of CNTs within these agglomerates leading to the presence of large bundles and ropes scattered around. However, it is not easy to distinguish the differences between the number and the size of agglomerates in p-MWCNTs and cumyl-g-MWCNTs from the TEM micrographs (Fig. 2-7 and Fig. 2-8 respectively). TEM micrographs of cumyl-g-MWCNTs (Fig. 2-8) seem not to show

agglomerates as big as visible in Fig. 2-7 for p-MWCNTs. Here loosely entangled swelled mass shows that the functionalization has untied the otherwise tightly held bundles of p-MWCNTs. This morphology might better be understood considering the behaviour of cumyl-g-MWCNTs in various solvents (Fig. 2-6). Contrary to p-MWCNTs, cumyl-g-MWCNTs are precipitated as a swollen mass at the bottom of the vials, especially in toluene (Fig. 2-6) suggesting that functionalization has succeeded in unfastening the p-MWCNTs bundles, despite the low grafting density of cumyloxy groups.

In contrast, for the penta-g-MWCNTs sample, with a high grafting density, TEM micrographs at nanoscale show CNTs mostly debundled into individual tubes (Fig. 2-9) leading to a fine nanodispersion in various solvents (Fig. 2-6). Even at microscale, the image shows a large amount of light passing through TEM sample which gives an evidence of spacing between the individual nanotubes.

These results highlight that radical grafting of long alkane molecules onto the sidewalls of MWCNTs is a promising way to chemically graft polyethyleneonto MWCNTs.

2.2.6 Conclusion

Thermolysis of dicumyl peroxide initiator performed in pentadecane and in presence of MWCNTs (depending on the melt conditions set up to chemically modify polyethylene) appeared to induce alkane grafting onto MWCNTs. This method is a simple way to directly incorporate organic moieties onto the CNTs' surface leading to pentadecane-grafted MWCNTs with a grafting density as high as 1.46 mmol/g at 150 °C. At higher temperatures, the grafting density decreases because the β-scission reaction of cumyloxyl radical accelerates as the temperature increases, leading to the formation of methyl radicals. These latter preferentially react by combination whereas cumyloxyl radicals are more prone to hydrogen abstraction from pentadecane. Pentadecane-grafted MWCNTs have exhibited good dispersibility in various organic solvents and we showed that a grafting density of

1.464 mmol/g leads to a solubility of 19.2 mg/mL in dichlorobenzene. Moreover, TEM images clearly indicated that the pentadecane coating grafted on the sidewalls allows debundling of MWCNTs to a high exfoliation degree. We believe that this functionalization approach will provide convenience and versatility in building up polyolefin architectures on CNTs in future work.

2.2.7 References

1 S. Osswald, E. Flahaut and Y. Gogotsi, Chem Mater 18 (2006), pp. 1525–1533.

2 Y. Qiang, W. Li, X. Weidong, Z. Junfeng and L. Jianhua, Polymer 48 (2007), pp. 2866–2873.

3 X. Deng, G. Jia, H. Wang, H. Sun, X. Wang and S. Yang et al., Carbon 45 (2007), pp. 1419–1424.

4 S. Qin, D. Qin, W.T. Ford, D.E. Resasco and J.E. Herrera, Macromolecules 37 (2004), pp. 752–757.

5 V. Georgakilas, K. Kordatos, M. Prato, D.M. Guldi, M. Holzinger and A. Hirsch, J Am Chem Soc 124 (2002), pp. 760–761.

6 M.S.P. Shaffer and A.H. Windle, Adv Mater 11 (1999), pp. 937–941.

7 R. Haggenmuller, H.H. Gommans, A.G. Rinzler, J.E. Fischer and K.I. Winey, Chem Phys Lett 330 (2000), pp. 219–225.

8 D. Bonduel, M. Mainil, M. Alexandre, F. Monteverde and P. Dubois, Chem Commun (2005), pp. 781–783.

9 M.S.P. Shaffer and K. Koziol, Chem Commun (2002), pp. 2074–2075.

10 H. Kong, C. Gao and D.Y. Yan, J Am Chem Soc 126 (2004), pp. 412–413.

11 J.-Y. Dong and Y. Hu, Coord Chem Rev 250 (2006), pp. 47–65.

12 S. Park, S.W. Yoon, K.B. Lee, D.J. Kim, Y.H. Jung and Y. Do et al., Macromol Rapid Commun 27 (2006), pp. 47–50.

13 K.E. Russell, Prog Polym Sci 27 (2002), pp. 1007–1038.

14 T.C. Chung, Prog Polym Sci 27 (2002), pp. 39–85.

15 G. Moad, Prog Polym Sci 24 (1999), pp. 81–142.

16 R. Hettema, J. Van Tol and L.P.B.M. Janssen, Polym Eng Sci 39 (1999), pp. 1628–1641.

17 T. Badel, E. Beyou, V. Bounor-Legare, P. Chaumont, J.J. Flat and A. Michel, J Polym Sci Part A Polym Chem 45 (2007), pp. 5215–5226.

18 R.T. Johnston, Rubber Chem Technol 76 (2003), pp. 174–200.

19 R.T. Johnston, Sealing Technol 76 (2003), pp. 6–9.

20 S. Osswald, M. Havel and Y. Gogotsi, J Raman Spectrosc (2007), pp. 728–736.

21 S.J. Pastine, D. Okawa, B. Kessler, M. Rolandi, M. Llorente and A. Zettl et al., J Am Chem Soc 130 (2008), pp. 4238–4239.

22 Y. Ying, R.K. Saini, F. Liang, A.K. Sadana and W.E. Billups, Org Lett 5 (2003), pp. 1471–1473.

23 K. Hata, D.N. Futaba, K. Mizuno, T. Namai, M. Yumura and S. Iijima, Science 306 (2004), pp. 1362–1364.

24 Y. Chen, B. Wang, L.J. Li, Y. Yang, D. Ciuparu and S. Lim et al., Carbon 45 (2007), pp. 2217–2228.

25 R.B. Mathur, S. Seth, C. Lal, R. Rao, B.P. Singh and T.L. Dhami et al., Carbon 45 (2007), pp. 132–140.

26 J.J. Stephenson, A.K. Sadana, A.L. Higginbotham and J.M. Tour, Chem Mater 18 (2006), pp. 4658–4661.

27 S. Meuer, L. Braun, T. Schilling and R. Zentel, Polymer 50 (2009), pp. 154–160.

28 I.A. Opeida, A.F. Dmitruk and O.M. Zarechnaya, Russ Chem Bull Inter Ed 50 (2001), pp. 241–244.

29 Y. Qin, L. Liu, J. Shi, W. Wu, J. Zhang and Z.X. Guo et al., Chem Mater 15 (2003), pp. 3256–3260.

30 W. Shuhui and R.A. Shanks, J Appl Polym Sci 93 (2004), pp. 1493–1499.

31 H. Zia, J.K.H. Ma, J.P. O'Donnell and L.A. Luzzi, Pharm Res 8 (1991), pp. 502–504.

32 Y. Chernyak, J Chem Eng Data 51 (2006), pp. 416–418.

Chapter 3

Effect of TEMPO on grafting

3.1 Effect of a radical scavenger on pentadecane grafting density

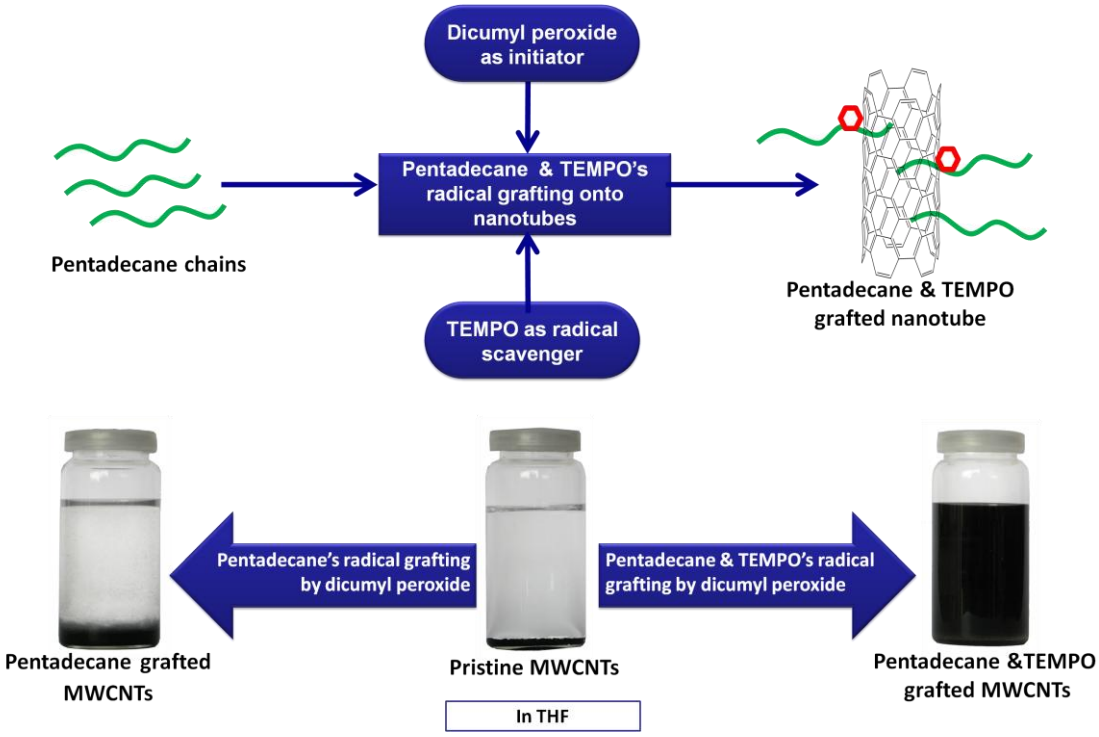

3.1.1 Overview

The study of pentadecane grafting onto nanotubes, in which pentadecane acted as a model compound for PE, shows that there is a tough competition between two reactions: combination of radicals and addition of radicals to unsaturated carbon bonds available on the surface of the nanotubes. In the first part of our model compound study we optimised our reaction conditions (e.g. temperature, concentration of reactants) to obtain higher grafting density. Here in this work, we used TEMPO as a radical scavenger. We envisaged that the radical scavenging ability of TEMPO would tilt the competition in favour of addition reaction by suppressing combination of radicals. One of the most difficult tasks of this study was to identify the reaction pathways as there were many possible side reactions involving combination of radicals. We used gas chromatography mass spectroscopy technique to determine various reaction products and by which we drew the reaction pathway. Grafting of pentadecane and TEMPO onto nanotubes was confirmed qualitatively (by Raman spectroscopy and transmission electron microscopy) and quantitatively (by

thermogravimetric and elemental analysis). The results of this model compound study showed an improvement in grafting density and helped in understanding the role of TEMPO in this reaction.

3.1.2 Article Details

This work is submitted for publication in 'Macromolecular Chemistry and Physics'. Parts of the contents of this paper were presented in '7th Eurofillers International conference – From macro to nanofillers for structural and functional polymer materials' held in the Alessandria site of the Polytechnic of Turin, Italy from 21 to 25 June, 2009.

3.2 A model compound study for Polyethylene grafting onto nanotubes: effect of a nitroxyl-based radical scavenger on functionalisation with pentadecane

Sohaib Akbar [a,b,c], Emmanuel Beyou [a,b,c], Philippe Chaumont [a,b,c], Flavien Melis [a,b,c]

[a] Université de Lyon, Lyon F-69003, France

[b] Université de Lyon 1, F-69003 Villeurbanne, France

[c] CNRS UMR5223, Ingénierie des Matériaux Polyméres, Laboratoire des Matériaux Polyméres et Biomatériaux, F-69622 Villeurbanne, France

3.2.1 Abstract

The radical grafting of pentadecane onto multiwalled carbon nanotubes (MWCNTs) has been investigated here which establishes a model for functionalisation of MWCNTs with molten polyethylene. In this model compound approach pentadecane radical grafting reaction has been studied in order to determine the reaction conditions necessary to enhance the degree of grafting while minimising side reactions such as radical combination reactions. The effect of a nitroxyle-based radical scavenger (i.e. TEMPO) on competition between pentadecane radicals' combination and addition to nanotubes has been explored. It was observed that the use of TEMPO resulted into a relatively higher grafting density without excessive pentadecane branching/crosslinking. We used qualitative and quantitative techniques such as gas chromatography–mass spectroscopy, thermogravimetry, Raman and elemental analysis to confirm reaction products and nanotubes functionalisation. It was also observed that the addition of TEMPO influences the solubility behaviour of functionalised carbon nanotubes.

3.2.2 Introduction

Incorporation of carbon nanotubes (CNTs) into a polymer matrix is a very attractive way to combine the mechanical and electrical properties of individual nanotubes with the advantages of plastics. The unique properties of individual CNTs make them the ideal reinforcing agents in a number of applications [1,2] but the low compatibility of CNTs set a strong limitation to disperse them in a polymer matrix. It is believed that incorporation of CNTs in polymer matrix may lead to ultimate fibre reinforcement nanocomposites with significantly enhanced mechanical properties. However, carbon nanotubes are strongly affected by Van der Waals' forces which give rise to the formation of aggregates and make their dispersion difficult in polymers. The non-covalent approaches to prepare polymer/CNTs composites via processes such as solution mixing [3], melt mixing [4], surfactant modification [5], polymer wrapping [6], polymer absorption [7] and in situ polymerisation [8,9] are simple and convenient but interaction between the two components remains weak. Functionalisation of the nanotubes' surface is a method to introduce reactive moieties, to disrupt the rope structure, and to improve dispersion in composites. Functional moieties are attached to open ends and sidewalls to improve the solubility of nanotubes [10-13] while the covalent polymer grafting approaches, including 'grafting to' [1,14,15] and 'grafting from' [1,16,17] that create chemical linkages between polymer and CNTs, can significantly improve dispersion. Polyethylene (PE) is one of the most widely used commercial polymer due to the excellent combination of low coefficient of friction, chemical stability and excellent moisture barrier properties [18]. To improve the stiffness and rigidity of PE, CNTs can be used to make CNT/PE composites [18-21]. A promising route for a chemical modification of MWCNTs by PE is to use free radical initiators such as peroxides [22-24]. The main approach exploited in this functionalisation strategy is polymer radical additions to the CNT double bonds. This grafting reaction has been recently predicted with a model compound approach based on a radical grafting reaction between peroxide-derived alkoxyl radicals, and low molar mass alkanes representing characteristics moieties of polyethylene and polypropylene [25,26]. Nevertheless, the main drawback of the free radical grafting is the low selectivity of the radical

centre, especially at high temperatures (in the range of 150-200°C, required for extrusion of polyethylene) leading to side reactions such as coupling and chain scission [22, 27]. Using pentadecane as a model for polyethylene and temperatures greater than 160°C, we showed that the grafting density dramatically decreased because the □-scission reaction of cumyloxyl radical lead to side reactions [25].

In this paper, we describe the effect of a nitroxyl-based radical scavenger (i.e. TEMPO) on the course of grafting reaction. TEMPO is usually used in nitroxide mediated polymerisations [28,29]; and in this case of pentadecane radical grafting onto nanotubes, it acts as a radical scavenger by suppressing the combination of pentadecane radicals and hence promoting their addition to unsaturated carbon bonds on the surface of nanotubes. Moreover, we also examine the effect of TEMPO inclusion on the solubility behaviour of functionalised carbon nanotubes. This study helps in understanding the possibility of grafting polyethylene onto nanotubes; moreover, optimisation achieved in this model will be used for polyethylene grafting in our future work.

3.2.3 Experimental

3.2.3.1 Materials

MWCNTs (Graphistrength™ C100; see characteristics in table 3-1) were kindly furnished by ARKEMA, France. Pentadecane (Sigma-Aldrich-France; 99% pure) was employed as a low molecular weight hydrocarbon substrate model for the poly(ethylene-co-octene).

Dicumyl peroxide (DCP, Sigma-Aldrich-France; 99% pure) was used as initiator for radical generation. 2,2,6,6-tetramethylpiperidinooxyl (TEMPO), supplied by Sigma-Aldrich-France, has been used as radical scavengers. Dimethylformamide (DMF, Sigma-Aldrich-France; 99% pure) and Dichlorobenzene (DCB, Sigma-Aldrich-France; 99% pure) were used as solvent in some experiments.

Table 3-1: Characteristics of Graphistrength™ C100.

Manufacturing	CCVD
Apparent density	50–150 kg/m^3
Mean agglomerate size	200–500 µm
C contents	~90 wt%
Mean number of walls	5–15
Outer mean diameter	10–15 nm
Length	0.1–10 µm
Elemental analysis of pristine MWCNTs shows: N, 0.78%; O, 0.89%; H, 0.30%; P, 1.81%.	
Raman spectrum of pristine MWCNTs is shown in figure 3-7.	
TGA shows < 1.5% weight loss over a temperature range of 30 to 700°C shown in figure 3-8.	

3.2.3.2 Thermolysis of DCP in the presence of pristine MWCNTs, petandecane and a radical scavenger (TEMPO)

The thermal decomposition of DCP in a solution of TEMPO in pentadecane was performed in a glass reactor. In a typical grafting experiment (see table 3-2), DCP (0.23g/0.85mmole) was first mixed in with p-MWCNTs (50mg), pentadecane (7.69g/36.26mmole) and TEMPO (0.13g/0.85mmole) and then sonicated for 15 min. After that, the suspension was degassed by 4 freeze-pump-thaws, and then it was heated to 160°C under stirring. After 6 hours, the reaction mixture was cooled down quickly. The grafted MWCNTs were collected by centrifugation (11000 rpm, 20 min) and subsequent filtration to remove all solid contents from reaction mixture. The liquid portion was passed through GC-MS while solid part was purified and characterised.

Table 3-2: List of samples according to the experimental conditions.

Sample	Description	Acronym	Composition of reactants
1	Crosslinked Pentadecane via DCP	-	Pentadecane: 7.69g/36.26mmole DCP: 0.23g/0.85mmole Solvent: pentadecane itself
2	MWCNTs functionalisation by cumyloxyl radicals	Cumyloxyl-g-MWCNTs	MWCNTs: 50mg DCP: 0.23g/0.85mmole Solvent: DMF
3	MWCNTs functionalised by pentadecane	Penta-g-MWCNTs	MWCNTs: 50mg Pentadecane: 7.69g/36.26mmole DCP: 0.23g/0.85mmole Solvent: pentadecane itself
4	MWCNTs functionalised by TEMPO and cumyloxyl radicals	Cumyloxyl.TEMPO-g-MWCNTs	MWCNTs: 50mg DCP: 0.23g/0.85mmole TEMPO: 0.04g/0.26mmole Solvent: DMF
5	MWCNTs functionalisation by TEMPO controlled radical grafting of pentadecane	Penta.TEMPO-g-MWCNTs	MWCNTs: 50mg Pentadecane: 7.69g/36.26mmole DCP: 0.23g/0.85mmole TEMPO: 0.1328 g/0.85mmole Solvent: pentadecane itself
B-1	DCP thermolysis in DMF	-	DCP: 0.23g/0.85mmole DMF: 10 ml
B-2	DCP thermolysis in DCB	-	DCP: 0.23g/0.85mmole DCB: 10 ml
B-3	DCP thermolysis in the presence of TEMPO in DCB	-	DCP: 0.23g/0.85mmole TEMPO: 0.04g/0.26mmole DCB: 10 ml

3.2.3.3 Purification of pentadecane grafted MWCNTs

Functionalised MWCNTs were purified from free moieties (i.e. pentadecane, TEMPO and various compounds produced via radical combinations) by exhaustive cleaning of the suspension by dialysis. In a typical example, 30mL of the MWCNTs suspension (after completion of the reaction) was introduced into a cellulose membrane (Spectra/Pro, MW cut-off, 1,000 by Spectrum Medical Industries, Inc.) and repeatedly dialysed against DMF until no residual mass could be detected in the recovered solution (determined gravimetrically). Then, the functionalised MWCNTs suspensions were vacuum dried at 80°C for 48 hours to evaporate the solvent prior to characterisation.

3.2.3.4 Methodology of experiments

As aforementioned, the effect of TEMPO has been studied here on pentadecane grafting onto nanotubes (sample 3 & 5). However during the course of study, functionalisation of MWCNTs by cumyloxyl and TEMPO radicals (sample 4 & 6) emerged as an interesting aspect of this work and therefore also investigated along with the main objective. Description of the samples is summarised in Table 3-2.

Details about samples 1-3 are available in our previous study [25] and only the relevant results are mentioned herein for comparison. Three blank specimens (B-1; B-2; B-3) were also prepared for reference and confirmation of some results. Solvent (DCB or DMF) was used only in those reactions in which pentadecane was not added. In the samples containing pentadecane, solvent was added after the reaction just to facilitate chromatography.

3.2.4 Characterisation

Gas chromatography-mass spectrometry (GC-MS) was performed with an Agilent 6890 series GC system equipped with a HP-5ms (5%-phenyl)-methylpolysiloxane. The injector was at 250ºC and the temperature program followed was: 50-310ºC at 20ºC/min. Injection and detection by MS was carried out at 280ºC. Samples in which DMF was not used as solvent in the first place, were diluted with DMF prior to GC-MS. Samples for GC-MS analysis were prepared by adding DMF (50 w/w %) in the filtrate after filtering out functionalised nanotubes.

The Raman analysis of pristine and functionalised MWCNTs was carried out on a Horiba Jobin-Yvon LabRAM ARAMIS Raman confocal microscope (632.8 nm, Aramis CRM, Horiba Jobin Yvon, Edison, NJ). A 50× objective was used to focus 18.5 mW of He−Ne laser light onto the sample surface with a spot size of about 1 µm.

Thermogravimetric analysis (TGA) was carried out with a DuPont Instruments TGA 2950 thermobalance, controlled by a TC10A microprocessor. Samples were heated at 20°C/min under a nitrogen flow (100mL/min).

Elemental analysis (EA) was carried out (Analyzer: LECO SC144, Service central d'analyse du CNRS, Vernaison, France) to determine the contents of H, O, N and P.

Solubility was determined gravimetrically. In a typical experiment, saturated solutions of Penta-g-MWCNTs were prepared by sonication in vials. Sonication was accomplished using Vibracell™ 75041 (Bioblock Scientific, Illkirch, France) apparatus equipped with 3mm probe set at 40% of 750 W for 30 sec. Vials were kept free standing over three weeks at room temperature and then the upper half aliquot part was carefully taken out with a syringe and heated to remove solvent under vacuum. All the weightings were carried out using an analytical balance with a sensitivity of 0.1 mg.

3.2.5 Results and discussion

3.2.5.1 Radical grafting of pentadecane onto MWCNTs controlled by a radical scavenger

Figure 3-1 sums up main reactive pathways of free radical grafting of pentadecane onto MWCNTs with dicumyl peroxide as initiator and TEMPO as radical scavenger. The main step is the formation of DCP-derived radicals and its hydrogen abstraction reaction from pentadecane bonds. However, the alkoxy radicals can undergo additional reactions including β-scission leading to the formation of methyl radicals [30]. These latter preferentially induce coupling reaction (Figure 3-1, route β and η) or attack onto the sp^2 carbon of the MWCNTs (Figure 3-1, route γ) whereas cumyloxyl radicals are more prone to hydrogen abstraction from pentadecane [24,25,30].

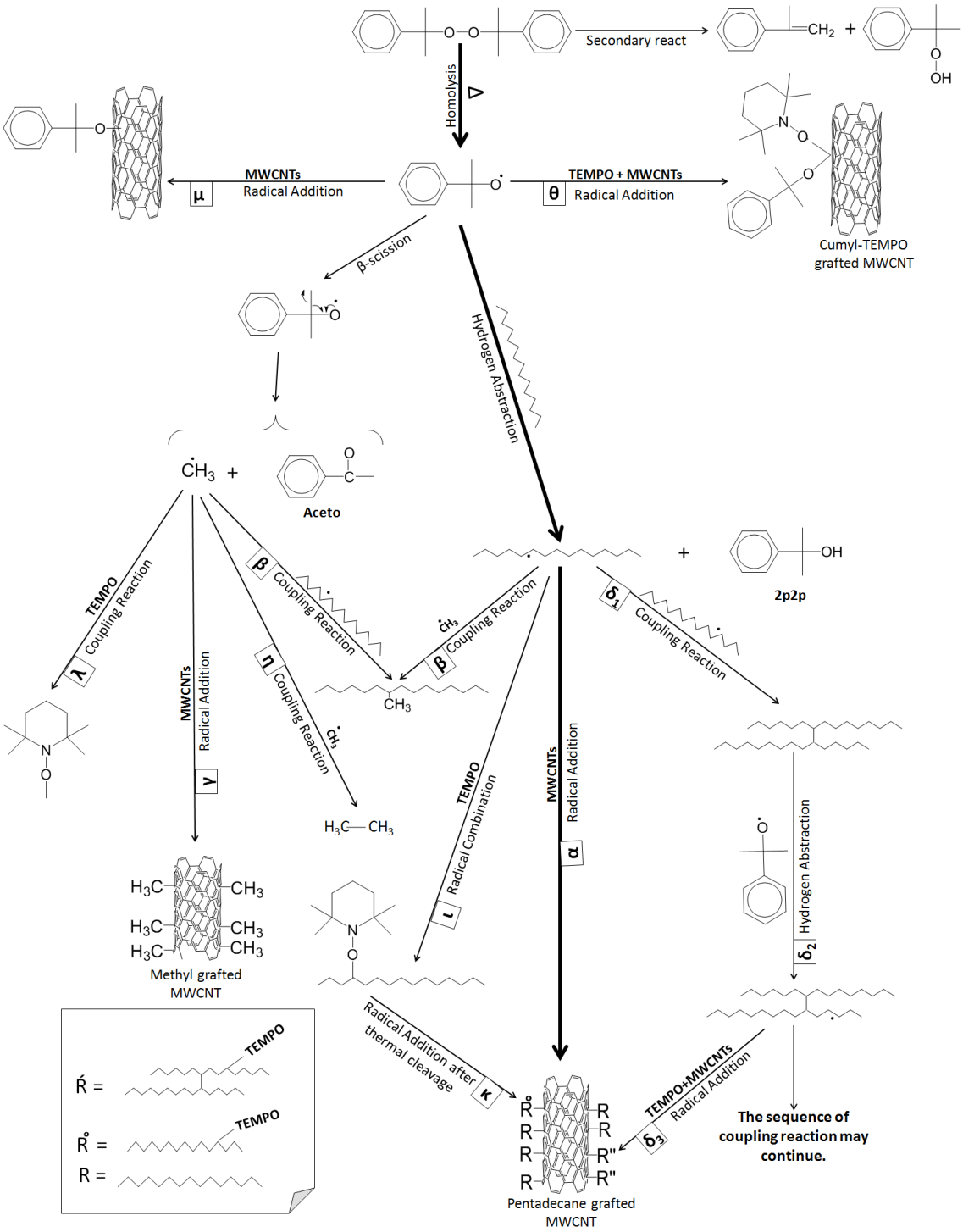

Figure 3-1: Reaction scheme for grafting pentadecane onto nanotubes with incorporation of TEMPO as a radical scavenger.

The formed pentadecyl radicals through hydrogen abstraction are able to react with MWCNTs by radical addition onto sp^2 carbon of the MWCNTs (Figure 3-1: main route α) and with other radical species via the common radical coupling reactions (Figure

3-1 : route δ_1 and β). According to Johnston [31,32] coupling reactions are four times more prone to happen than scission reactions, when using poly(ethylene-co-1-octene) in the presence of DCP at 160°C, so we assume that pentadecyl radicals do not undergo scission reactions. In competition to these coupling reactions (route β, η, δ_1 and δ_2) some other combinations reactions such as λ, L and δ_3 can also occur with the active participation of TEMPO radicals. The latter combination reactions actually are reversible reactions which may favour the addition of pentadecyl radicals to MWCNTs leading to a higher grafting density. In case of reaction λ there exists a possibility that after combination of methyl and TEMPO radicals a cleavage of bond happens between N and O creating further radicals. However we didn't show this in reaction scheme for brevity. First we present here the effect of TEMPO on the thermolysis of DCP in the presence of a solvent (sample 2 &4). This helps in understanding further discussion about our main task in which pentadecane was grafted onto nanotubes (sample 3 & 5).

3.2.5.2 Effect of TEMPO on the thermolysis of DCP in DMF and DCB as solvents

After treatment of MWCNTs with DCP in DMF at 150°C (sample 2), we have previously reported that the corresponding functionalised carbon nanotubes were not soluble because of low degree of grafting. Here we did this blank experiment again to carry out GC-MS analysis on the supernatant solution. Figure 3-2 shows GS-MS chromatograms of sample 2 at 150°C and 160°C.

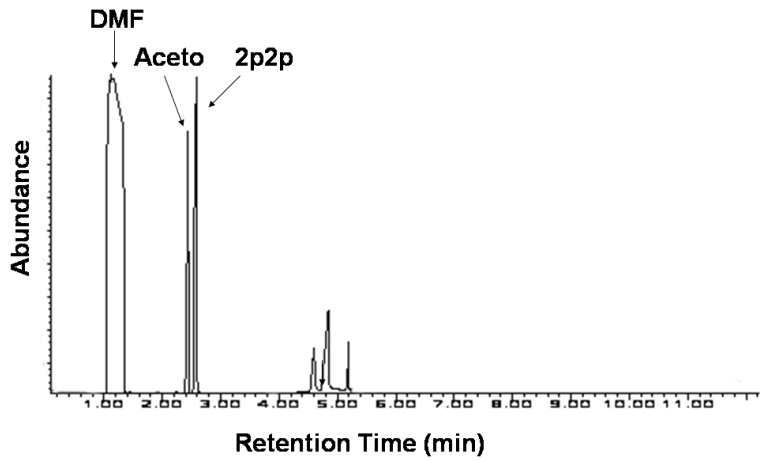

(a)

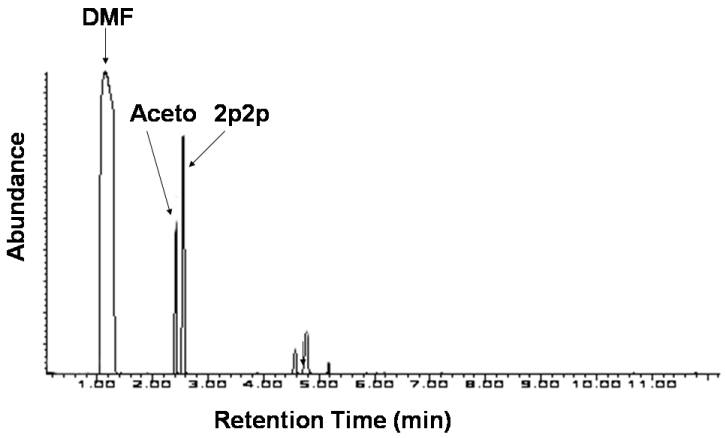

(b)

Figure 3-2: GC-MS chromatogram of the reaction filtrate of the sample 2: at 150ºC (a); at 160ºC (b).

Surprisingly, 2-phenyl-2-propanol (2p2p) peaks of considerable area are detectable in both chromatograms (Figures 3-2a and 3-2b). Moreover, some other unrecognised peaks around 4.7 minutes are observed (not labelled) in Figure 3-2 and no DCP traces are detected.

As mentioned before, 2p2p is expected to come from hydrogen abstraction from alkane chains (Figure 3-1); but in the absence of any alkane the production of 2p2p was a little astonishing. Two main ways may explain this outcome: first, cumyloxyl radicals abstract hydrogen from other cumyloxyl radicals; second, cumyloxyl radicals abstract hydrogen from DMF to produce 2p2p. In order to gain a better understanding of the cumyloxyl radicals behaviour, DCB was selected as reference solvent because of its high boiling point (≈180°C) and its chemical structure that doesn't offer any hydrogen abstraction reaction. Products arising from the reaction involving solutions of DCP in DMF (blank sample B-1, table 3-2) and in DCB (blank sample B-2, table 3-2) were analysed by GC-MS (Figure 3-3).

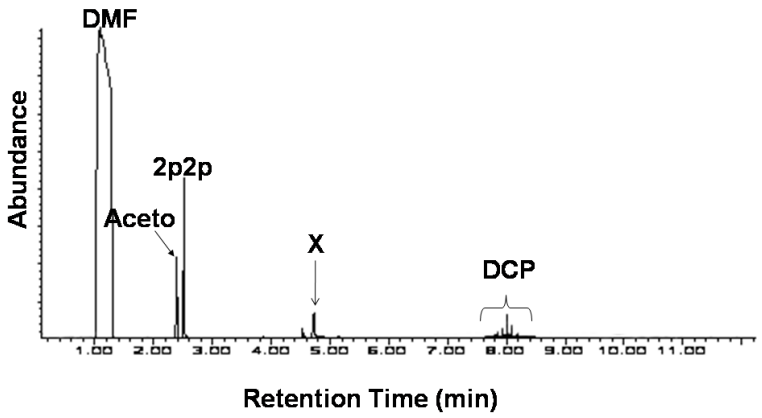

(a)

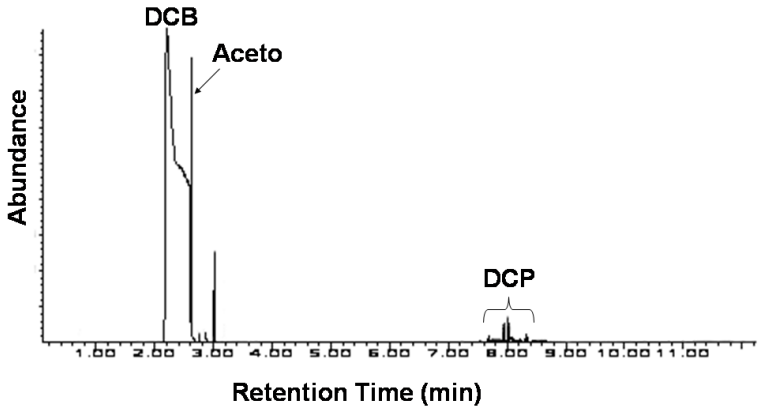

(b)

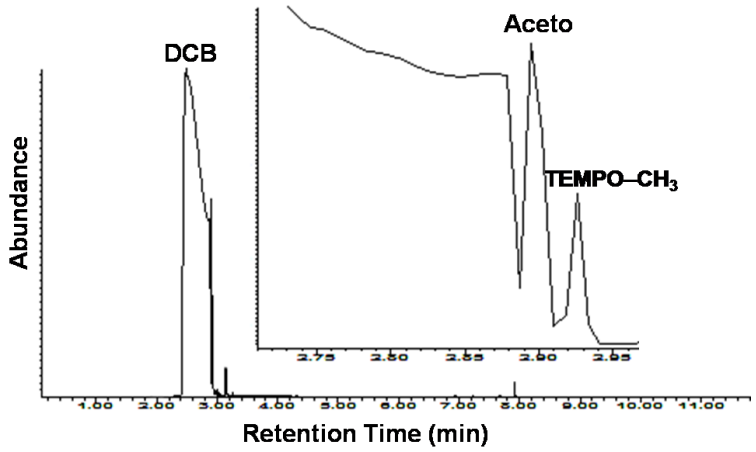

(c)

Figure 3-3: GC-MS chromatograms of blank sample A-1 (a); blank sample A-2 (b); and blank sample A-3 (c). [X = N,N'-(ethane-1,2-diyl)bis(N-methylformamide), see mass spectrum in figure 3-S1.]

The peak corresponding to 2p2p, related to a H-abstraction reaction, was observed only in the presence of DMF as solvent (Figure 3-3a). This result rules out the

hypothesis that cumyloxyl radicals could abstract hydrogen from other cumyloxyl radicals and suggests that cumyloxyl radicals abstract hydrogen from DMF. Indeed, N,N'-(ethane-1,2-diyl)bis(N-methylformamide) (named X in Figure 3-3a) was identified (see mass spectrum in Figure 3-S1) as one of the products arising from the reaction of DCP with DMF (Figure 3-4).

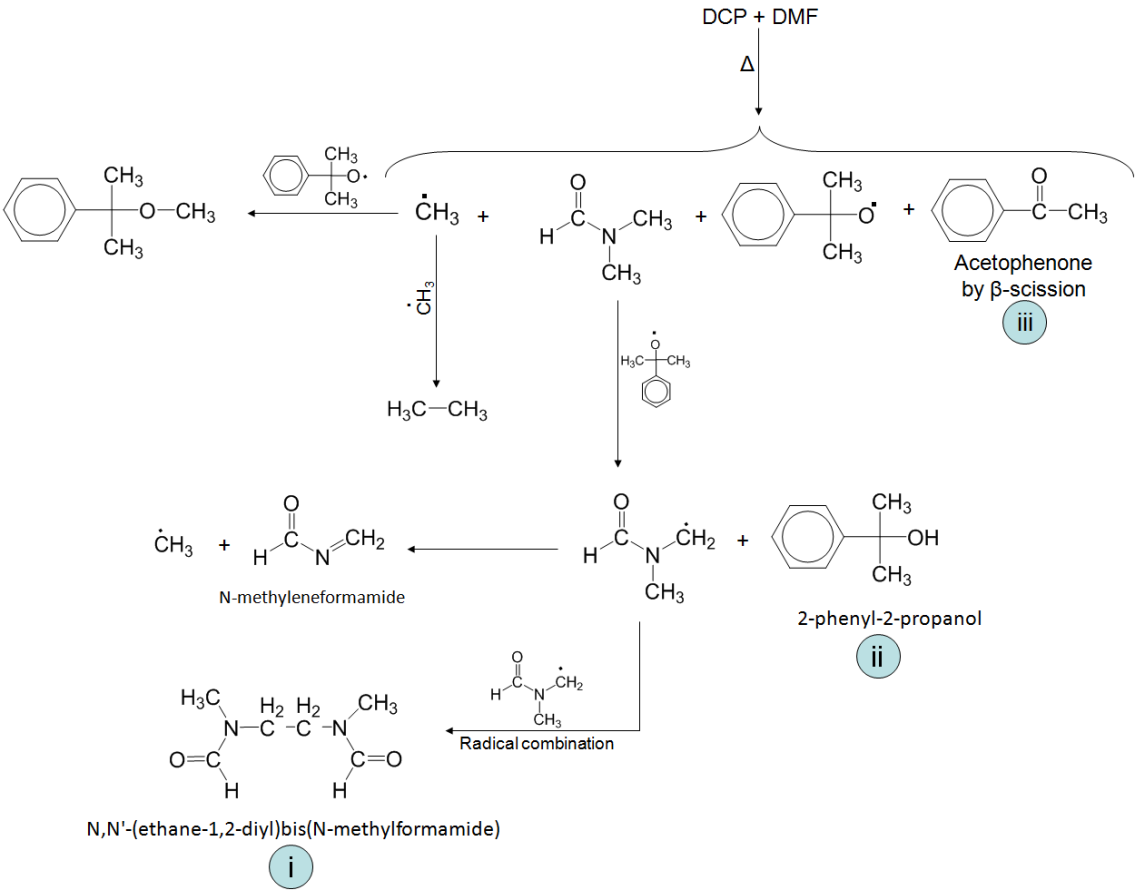

Figure 3- 4: Reaction scheme supposed for hydrogen abstraction reaction from DMF by cumyloxyl radicals. The products i, ii and iii were confirmed through GC-MS.

Some other peaks found in the GC-MS chromatogram could not be recognised and may be due to the hydrogen abstraction of radicals generated from DMF that led to the production of 2p2p. The peaks located at a time retention close to 8 minutes may be attributed to DCP as the mass spectra of these peaks are similar to that of DCP with some variations probably due to combination with some radicals. Such peaks associated with DCP are not visible in Figure 3-2, suggesting that cumyloxyl radicals' course of reaction changes in the presence of MWCNTs.

The reactions in which TEMPO radicals are added along with DCP in DCB solvent (sample B-3, table 3-2), have been carried out to check TEMPO's radical scavenging ability towards methyl radicals (Figure 3-1 and Figure 4). GC-MS analysis of the formed products (Figure 3-3c) mainly displays two peaks corresponding to acetophenone (aceto) and TEMPO-CH_3 (see Figure 3-S2 for mass spectrum of TEMPO-CH_3) with no trace of 2p2p, as expected. On contrary, adding TEMPO in a solution of MWCNTs and DCP in DMF (sample 4, table 3-2) results in the production of a mixture of aceto, TEMPO-CH_3, 2p2p and some unrecognised products (Figure 3-5).

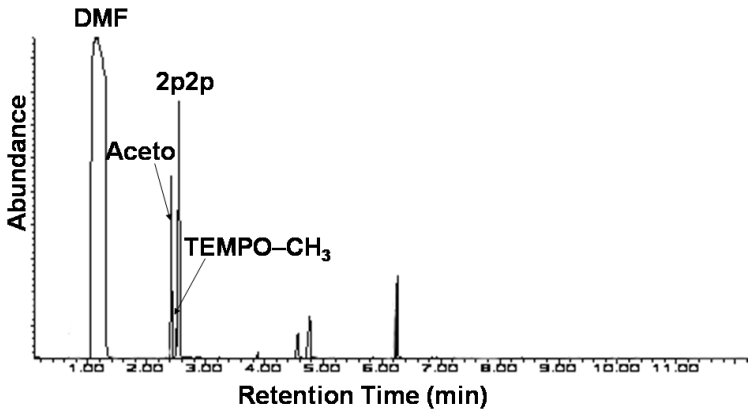

Figure 3-5: GC-MS chromatogram of the reaction filtrate of cumyloxyl.TEMPO-g-MWCNTs (sample 4).

In addition, a new peak is observed at a retention time of 6.4 minutes (Figure 3-5) in comparison with the GC-MS chromatogram of sample 2 (Figure 3-2) which may be attributed to a product formed by a radical combination between DMF radicals and TEMPO radicals as its mass spectrum resembles with TEMPO with some additions corresponding to combination with other radicals (mass spectrum in figure 3-S4).

In conclusion, our blanks experiments confirmed: (1) cumyloxyl radicals can abstract hydrogen from DMF (experiments B-1, B-2); (2) β-scission is much more likely to happen in the absence of MWCNTs and/or pentadecane; (3) TEMPO work efficiently to scavenge radicals in order to prevent unwanted combination reactions (experiment B-3).

According to these results, TEMPO radicals may be suitable to control and to improve the radical grafting of pentadecane onto MWCNTs by limiting the formation of interlinked pentadecane and methyl functionalised pentadecane. Moreover, the corresponding TEMPO-based alkoxyamines may also add to MWCNTs through the thermal cleavage of the alkoxyamine bond, which can also take part in enhancing the grafting density of pentadecane onto nanotubes.

3.2.5.3 Effect of TEMPO on the radical grafting of pentadecane onto MWCNTs

As discussed in our previous study [25], the products arising from the reaction involving a solution of DCP in pentadecane (blank, sample 1, table 3-2), were identified by GC-MS (Figure 3-S3). As expected, we obtained 2-phenyl-2-propanol (2p2p) through H-abstraction from the hydrocarbon substrate, acetophenone (aceto) by intramolecular β-scission and interlinked pentadecane molecules through combination of the formed pentadecane radicals. Moreover, it was verified that, contrary to sample 1, the presence of MWCNTs in sample 3 (at optimal reaction conditions) affects the radical course in three ways: (1) it lowers the interlinking of pentadecane chains (see GC-MS chromatogram, Figure 3-6a); (2) it causes radical grafting on sidewalls of nanotubes; (3) it restrains β-scission reaction. As discussed by Chaudhary [33,34], the reaction of TEMPO with an alkane and dicumyl peroxide is expected to yield a bimolecular combination of free radicals that is not susceptible to chain transfer.

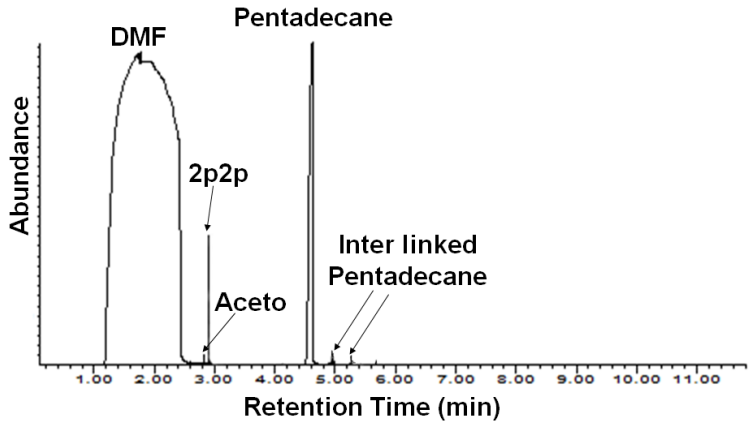

a)

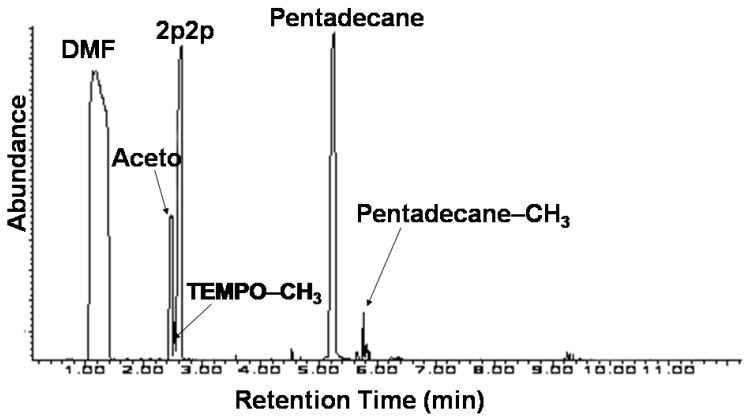

b)

Figure 3-6: GC-MS chromatograms of the reaction filtrate of: Penta-g-MWCNTs, sample 3, (a); Penta.TEMPO-g-MWCNTs, sample 5, (b). Diluted with DMF after reaction

The location of the grafted species is controlled by concentration, solubility and diffusion of the peroxide and the nitroxyl species within the reaction medium [33]. Here, in the presence of MWCNTs this reaction leads to the appearance of additional peaks in the GC-MS chromatogram of the reaction filtrate (Figure 3-6b). It displays new small peaks located at retention times of 2.5 minutes and 5.8 minutes corresponding to TEMPO-CH_3 and CH_3-pentadecane, respectively. Moreover, some peaks are observed at around 9.3 minutes suggesting the formation of a little ungrafted interlinked pentadecane despite the presence of TEMPO.

3.2.5.4 Qualitative evidence for covalent sidewall functionalisation: Raman analysis

Raman spectroscopy is a powerful technique to investigate the structure changes of carbon nanotubes after functionalisation [35, 36]. Raman spectra of p-MWCNTs (Figure 3-7) show two main peaks around 1330cm^{-1} and 1583cm^{-1}, corresponding to D-band (the disordered graphite structure) and G-band (sp2-hybridised carbon), respectively.

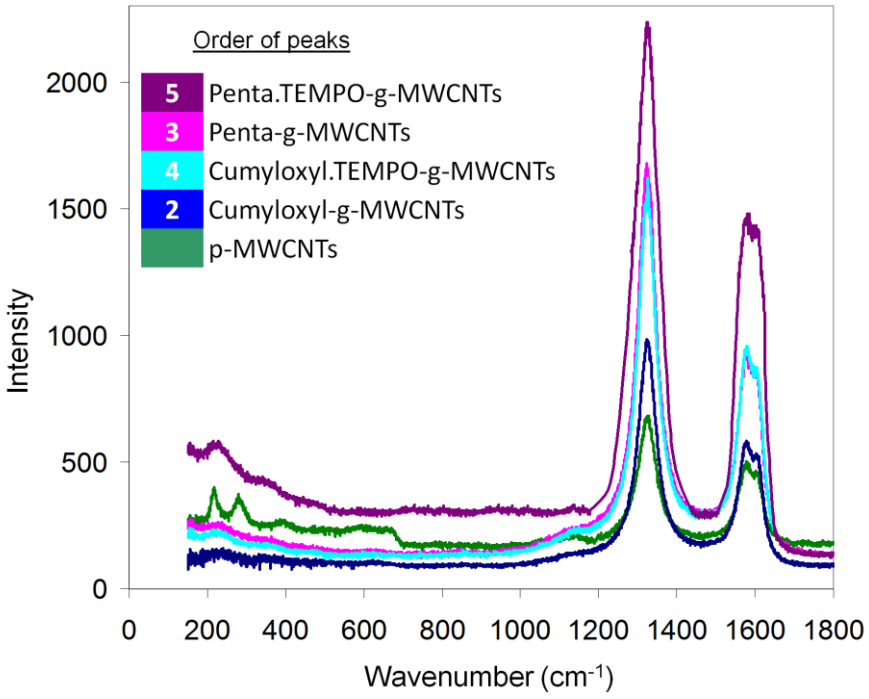

Figure 3-7: Raman spectra of pristine and various functionalised nanotubes.

The A_D/A_G ratio, which was defined as the intensity ratio of the D-band to G-band of CNTs, directly indicates the structural changes in nanotubes. Some authors used D to G area ratios (A_D/A_G) rather than intensity [37] which is a better indicator. The relatively high area ratio of the G band relative to D band for cumloxyl.-g-MWCNTs (A_D/A_G = 1.34), penta-g-MWCNT (A_D/A_G = 1.51, cumloxyl.TEMPO-g-MWCNTs (A_D/A_G =1.43), penta.TEMPO-g-MWCNTs (A_D/A_G =1.63), in comparison with that of p-MWCNT (i.e. A_D/A_G =1.20) could be designated as an indicator of grafting species.

3.2.5.5 Estimation of the extent of nanotubes' functionalisation by thermogravmetric analysis (TGA) and elemental analysis (EA)

It is well known that heating functionalised nanotubes in an inert atmosphere removes the organic moieties and restores the pristine nanotubes' structure [38]. Therefore, in order to gain a more quantitative picture of the extent of nanotubes' functionalisation, thermogravimetric analysis was performed on the reaction products and pure reactants for reference. Before carrying out TGA, the adsorbed (non-covalently attached) molecules were removed from the grafted one (covalently

attached) by dialysis as mentioned in the experimental part. As shown in Figure 3-8, the amount of organic functionalities physically and/or covalently attached to the initial MWCNTs can be neglected (weight loss < 1.5%).

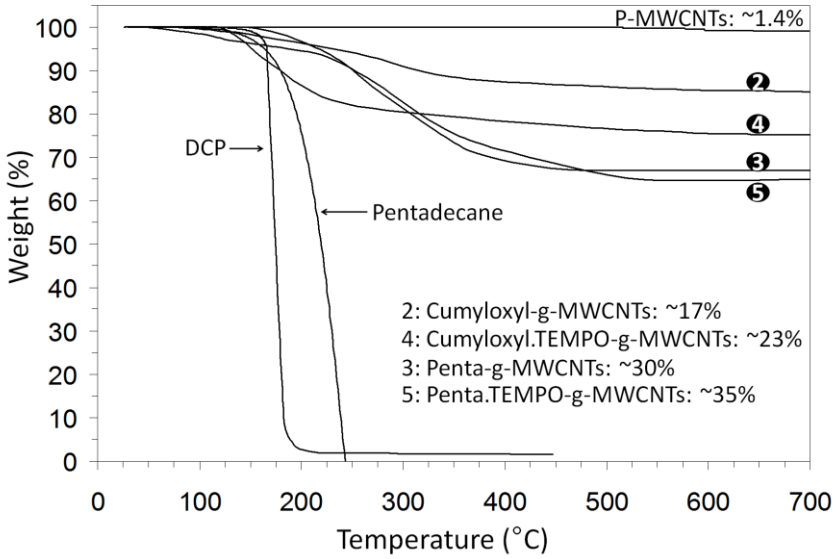

Figure 3-8: TGA weight loss data (under nitrogen) for various samples (see details in table 3-2). Pure products (i.e. DCP, pentadecane and pristine nanotubes) are shown for corresponding reference.

After treatment of MWCNTs with DCP, at 160°C (sample 2, Table 3-2), the weight loss increased to 17% between 100°C and 600°C as expected for MWCNTs with more organic moieties on the surface (Figure 3-8). We estimated the weight percentage of pentadecane to be around 17% because pure DCP is completely decomposed at a temperature of 200°C (Figure 3-8). The weight loss for cumyloxyl.TEMPO-g-MWCNTs (sample 4, Table 3-2) is around 23% that is around 6-7 percentage points more than that of cumyloxyl-g-MWCNTs. This increase in the weight loss suggests a higher degree of grafting for cumyloxy groups by using TEMPO in the reaction mixture and/or the grafting of TEMPO groups as well as cumyloxy groups onto MWCNTs. In the latter case, the polarity of the corresponding functionalised MWCNTs is expected to be higher than that of cumyloxyl-g-MWCNTs. Solubility behaviour of TEMPO grafted nanotubes is discussed ahead, which helps in understanding the polar nature of grafted TEMPO.

Similarly, the amount of pentadecane that covalently attached to the p-MWCNTs (sample 3, Table 3-2) is estimated by the weight loss of penta-g-MWCNTs between 100°C and 600°C. Indeed, TGA results show that pure pentadecane completely decomposes at a temperature of 240°C (Figure 3-8). We estimated the weight percentage of pentadecane to be around 30%. As described for cumyloxyl.TEMPO-g-MWCNTs sample, along the similar lines, TEMPO contributes to increase the weight loss of around 5 percentage points (i.e. 35%, Figure 3-8) for penta.TEMPO-g-MWCNTs (sample 5, Table 3-2). It confirms that TEMPO acts as a radical scavenger which contributes to increase the degree of grafting. A qualitative indication of grafting comes from the colour of the mixture starting from dark yellow with free TEMPO before heating and turning lighter at the end of the reaction showing consumption of TEMPO during reaction. An increase in TEMPO/DCP molar ratio from 1 to 2 did not change the degree of grafting. Reaction temperature is also a key parameter in a radical grafting reaction, therefore, some experiments were conducted at temperatures varying from 150°C to 180°C (Table 3-3).

Table 3-3: Effect of reaction temperature on the degree of grafting.

Sample	Reaction Temperature (°C)	Weight loss (TGA) wt%
4 Cumyloxyl.TEMPO-g- MWCNTs	150	11
	160	23
5 Penta.TEMPO-g- MWCNTs	150	26
	160	35
	170	27
	180	15

For both samples 4 and 5, the weight loss observed by TGA increases by increasing reaction temperature from 150°C to 160°C. However, for the temperatures greater than 160°C (i.e. 170°C and 180°C) the degree of grafting dramatically decreases from 35% to 15%. These results confirm that the β-scission reaction of cumyloxyl radical also increases as the temperature increases, leading to the formation of methyl radicals that preferentially react by combination (Figure 3-1). The optimal reaction temperature is 160°C. It's worth mentioning that behaviour of DCP radicals'

generation and hydrogen abstraction is reported complex and different at a temperature higher than 170°C [39,40].

Elemental analysis (EA) is also an indicator of degree of grafting. A good agreement between degrees of grafting calculated from EA and TGA analysis is observed whatever the sample (Table 3-3). It is worth mentioning that nitrogen content in samples 4 and 5 suggests grafting of TEMPO-based groups onto MWCNTs permitting the calculation of TEMPO's degree of grafting (Table 3-4). For instance, Penta.TEMPO-g-MWCNTs (sample 5, Table 3-2) contains 0.6% more N than pristine nanotubes, which correspond to 8% TEMPO by weight. The total amount of grafting species calculated from EA equals to the sum of TEMPO content and pentadecane contents. For sample 5, we obtained 32% and 35% from EA and TGA, respectively. In other words we can state that sample 5 contains 0.781 $mg.m^{-2}$ of pentadecane and 0.176 $mg.m^{-2}$ of TEMPO grafted onto its surface.

Table 3-4: Degree of grafting with 3% DCP, calculated by TGA and EA.

Sample	Degree of Grafting (TGA)*	Degree of Grafting (EA)*				
	wt%	Elemental wt%	wt%			Pentadecane $mg.m^{-2}$
			TEMPO	Cumyl.	Penta.	
2 Cumloxyl-g-MWCNTs	17	O: 1.8	-	15	-	-
3 Penta-g- MWCNTs	30	H: 4.0	-	-	26	0.823
4 Cumloxyl.TEMPO-g-MWCNTs	23	N: 0.7 H:2.5	8	15	-	-
5 Penta.TEMPO-g-MWCNTs	35	N: 0.6 H:5.1	7	Nil†	25	0.781

* The values reported here are averages of 2-3 test samples. Degree of grafting is calculated based on the indicated element weight percent.

† Supposed nil for calculations.

N.B. All percentages shown above are rounded off and calculated after deduction of pristine MWCNTs values mentioned in table 3-1. Grafting density in $mg.m^{-2}$ is based on calculations assuming avg. CNT length of 5µm and OD of 13nm

3.2.5.6 Solubility/dispersibility behaviour of functionalised MWCNTs

While raw MWCNTs form aggregates/bundles and settled down in most solvents, organic solubility can be achieved by appending alkyl groups onto the MWCNTs. The visual aspect of the dispersions is significantly different depending on the solvent and covalent functionalisation. In order to investigate the stability of functionalised nanotubes in different solvents, we prepared samples by adding 200 mg of the samples into the same amount of various solvents followed by sonication for 30 seconds and then leaving them free standing for 5 min. to 4 weeks. As illustrated in Figure 3-9 and Table 3-5, for p-MWCNTs (un functionalised), we found unstable dispersions in most solvents meaning that it is not possible to well disperse p-MWCNTs in these solvents even after sonication.

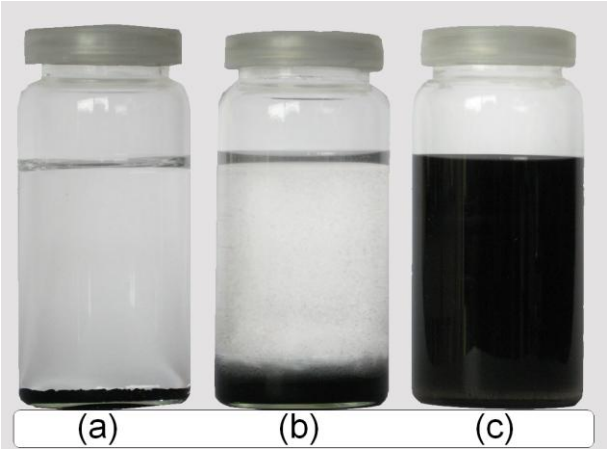

Figure 3-9: Solubility/dispersibility behaviour in THF: pristine carbon nanotubes after 5 min (a); pentadecane grafted MWCNTs, sample 3, after one week (b); and pentadecane and TEMPO grafted MWCNTs, sample 5, after one month (c).

The solubility values of samples 2-5 in different solvents are given in Table 3-5. These values are averages of three calculations made according to the procedure mentioned in experimental section.

Figure 3-9 shows the states of dispersion: sedimented —as evident in vial 'a' p-MWCNTs in THF; swollen —as obvious in vial 'b' for Penta-g-MWCNTs in THF (sample 3, Table 3-2); and dispersed—as apparent in vial 'c' for Penta.TEMPO-g-MWCNTs in THF (sample 5, Table 3-2). The behaviour of sample 5 in contrast to sample 3 shows

the polar behaviour of grafted TEMPO as it makes functionalised nanotubes soluble in polar solvents like THF and chloroform.

Table 3-5: Solubility of functionalised MWCNTs in various organic solvents.

Sample	Solubility (mg.ml^{-1})						
	Acetone	THF	Chloroform	Toluene	Xylene	DCB	DMF
2 Cumyloxyl-g-MWCNTs	7 [b]	7.2 [b]	5.3 [b]	2.9 [b]	×	×	7.1 [b]
3 Penta-g- MWCNTs	1.1 [a]	×	×	14.6 [b]	16.3 [b]	19.2 [c]	13.9 [c]
4 Cumyloxyl.TEMPO-g-MWCNTs	4.7 [b]	11.9 [c]	11.2 [c]	4.5 [a]	×	8.2 [c]	8.3 [b]
5 Penta.TEMPO-g- MWCNTs	6.4 [b]	13.1 [c]	13.6 [c]	2.5 [a]	×	1.2 [a]	12.1 [b]

[a] metastable; high aggregation/precipitation with time.
[b] metastable; some aggregation/precipitation with time.
[c] stable over weeks; negligible aggregation/precipitation with time.
× not soluble.
N.B. p-MWCNTs are not soluble in any of these solvents.

A qualitative but very strong argument indicating the presence of different kind of species on the surface of functionalised nanotubes is the dissimilar behaviour of the samples in different solvents. For instance, Penta-g-MWCNTs (sample 3, Table 3-2) is not soluble in THF and chloroform but incorporation of TEMPO make them soluble in these solvents (sample 5, Table 3-5). For example, using THF as solvent, the solubility of sample 3 is 0mg.ml^{-1} and the solubility of sample 5 is 13.1mg.ml^{-1}. On the contrary, the solubilities of sample 5 in aromatic solvents such as Toluene, Xylene and Dichlorobenzene decreases to values close to 0 mg.ml^{-1} in comparison with that of sample 3 (around 15 mg.ml^{-1}). This behaviour suggests the presence of alkyl groups with different polarities on the MWCNTs changing the affinity between solvent and functionalised nanotubes. Cumyloxy-TEMPO functionalised MWCNTs (sample 4) also display better solubilities in polar solvent than the corresponding sample without TEMPO moiety (sample 2, Table 3-5). However, no great change of solubilities is observed in aromatic solvents for samples 2 and 4.

3.2.6 Conclusion

This study provides a model base for polyethylene grafting onto nanotubes. We selected pentadecane as a model compound for polyethylene and investigated a simple radical grafting approach based on the use of dicumyl peroxide as an alkane hydrogen abstractor and in presence of TEMPO as radical scavengers. Incorporation of TEMPO as radical scavenger in the grafting reaction of pentadecane onto MWCNTs serves two purposes: Firstly, it actively suppresses radical combination reactions and hence promotes pentadecyl radicals' addition to nanotubes (~16% increase in grafting density); and secondly, it effectively changes the polarity balance of the grafted species, making pentadecane and TEMPO functionalised nanotubes soluble in solvents such as THF and chloroform. Various characterisation techniques such as GC-MS, Raman analysis, TGA, elemental analysis were used to confirm functionalisation of MWCNTs by pentadecane and TEMPO groups and to verify reaction pathways. We believe that this functionalisation model would provide convenience and versatility in building up polyolefin architectures on CNTs and serve as a base for future work.

3.2.7 References

1 Spitalsky Z, Tasis D, Papagelis K, Galiotis C. Prog Polym Sci 2010;35:357-401.

2 Bandaru PR. J Nanosci Nanotechnol 2007;7:1239–67.

3 Shaffer MSP, Windle, AH. Adv Mater 1999;11:937-41.

4 Haggenmuller R, Gommans, HH, Rinzler AG. Fischer JE, Winey KI. Chem Phys Lett 2000;330:219-25.

5 Kang YJ, Taton TA. J Am Chem Soc 2003;125:5650−51.

6 Star A, Stoddart JF. Macromolecules 2002;35:7516−20.

7 Barraza HJ, Pompeo F, O'Rear EA, Resasco DE. Nano Lett 2002;2:797−802.

8 Bonduel D, Mainil M, Alexandre M, Monteverde F, Dubois P. Chem Commun 2005;6:781-783.

9 Park S, Yoon SW, Lee KB, Kim DJ, Jung YH, Do Y, Paik HJ, Choi IS. Macromol Rapid Commun 2006;27:47-50.

10 Shofner ML, Khabashesku VN, Barrera EV. Chem Mater 2006;18:906–13.

11 Bahr JL, Tour JM. Chem Mater 2001;13:3823-24.

12 Georgakilas V, Kordatos K, Prato M, Guldi DM, Holzinger M, Hirsch, AJ. J Am Chem Soc 2002;124:760-761.

13 Peng H, Reverdy P, Khabashesku VN, Margrave JL. Chem Commun 2003; 362-363.

14 Qin S, Qin D, Ford WT, Resasco DE, Herrera JE. Macromolecules 2004;37:752-757.

15 Riggs JE, Guo Z, Carroll DL, Sun Y-P. J Am Chem Soc 2000;122:5879-80.

16 Shaffer MSP, Koziol K. Chem Commun 2002;18:2074-75.

17 Kong H, Gao C, Yan DY. J Am Chem Soc 2004;126:412-413.

18 Kaminsky W. Macromol Chem Phys 2008;209(5): 459-466.

19 Ruan S, Gao P, Yu TX. Polymer 2006;47:1604–11.

20 Tang W, Santare MH, Advani SG. Carbon 2003;41:2779–85.

21 Yang BX, Pramoda KP, Xu GQ, Goh SH. Adv Funct Mater 2007;17:2062–69.

22 Russell K.E. Prog Polym Sci 2002;27:1007-38.

23 Chung TC. Prog Polym Sci 2002;27:39-85.

24 Moad G. Prog Polym Sci 1999;24:81-142.

25 Akbar S, Beyou E, Cassagnau P, Chaumont P, Farzi G. Polymer 2009;50:2535-43.

26 Farzi G, Akbar S, Beyou E, Cassagnau P, Melis F. Polymer 2009;50:5901-08.

27 Hettema R, Van Tol J, Janssen LPBM. Polym Eng Sci 1999;39:1628-41.

28 Celle C, Ostaci R-V, Beyou E, Seytre G, Drockenmuller E, Chapel. J-P J Polym Sci : Part A Polym Chem 2008; 46:3367-74.

29 Bailly, B.; Donnenwirth, A-C.; Bartholome, C.; Beyou, E.; Bourgeat-Lami, E. J Nanomaterials 2006, 2006, article ID 76371, DOI: 10.1155/JNM/2006/76371.

30 Badel T, Beyou E, Bounor-Legare V, Chaumont P, Flat JJ, Michel A. J Polym Sci Part A Polym Chem 2007;45:5215-26.

31 Johnston RT. Rubber Chem Tech 2003;76:174-200.

32 Johnston RT. Sealing Technology 2003;76:6-9.

33 Weaver JD, Chowdhury AK, Mowery DM, Esseghir M, Cogen JM, Chaudhary BI. J Polym Sci Part A Polym Chem 2008;46:4542-55.

34 Chaudhary BI, Peterson TH, Wasserman E, Costeux S, Klier J, Pasztor AJ. Polymer 2010;51:153-163.

35 Ying Y, Saini RK, Liang F, Sadana AK, Billups WE. Org Lett 2003;5:1471-73.

36 Osswald S, Havel M, Gogotsi Y, Journal of Raman Spectroscopy, 2007:728-736.

37 Park MJ, Lee JK, Lee BS, Lee Y-W, Choi IS, Lee S-G. Chem Mater 2006;18:1546–51.

38 Mathur RB, Seth S, Lal C, Rao R, Singh BP, Dhami TL, Rao AM. Carbon 2007;45:132-140.

39 Msakni A, Cassagnau P, Chaumont P. Rehol Acta 2007;46: 933-943.

40 Akbar S, Beyou E, Cassagnau P, Chaumont P. Mater Chem Phys 2009;117: 482-488.

3.2.8 Supporting Information

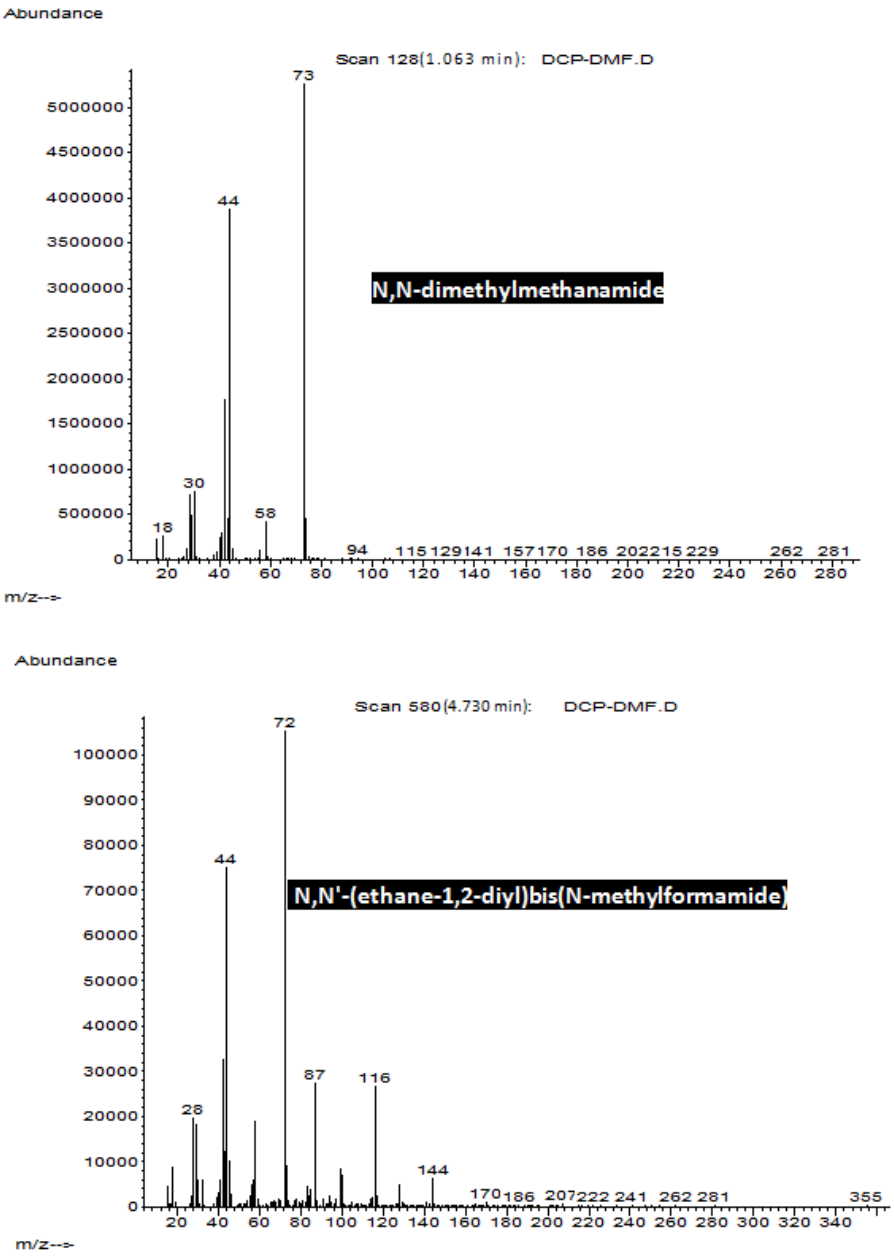

Figure 3-S1: Mass spectrum of DMF and N,N'-(ethane-1,2-diyl)bis(N-methylformamide) obtained in GC-MS analysis (sample B-1, Figure 3-3a). The comparison of these two spectra clearly indicates the coupling of radicals generated from DMF.

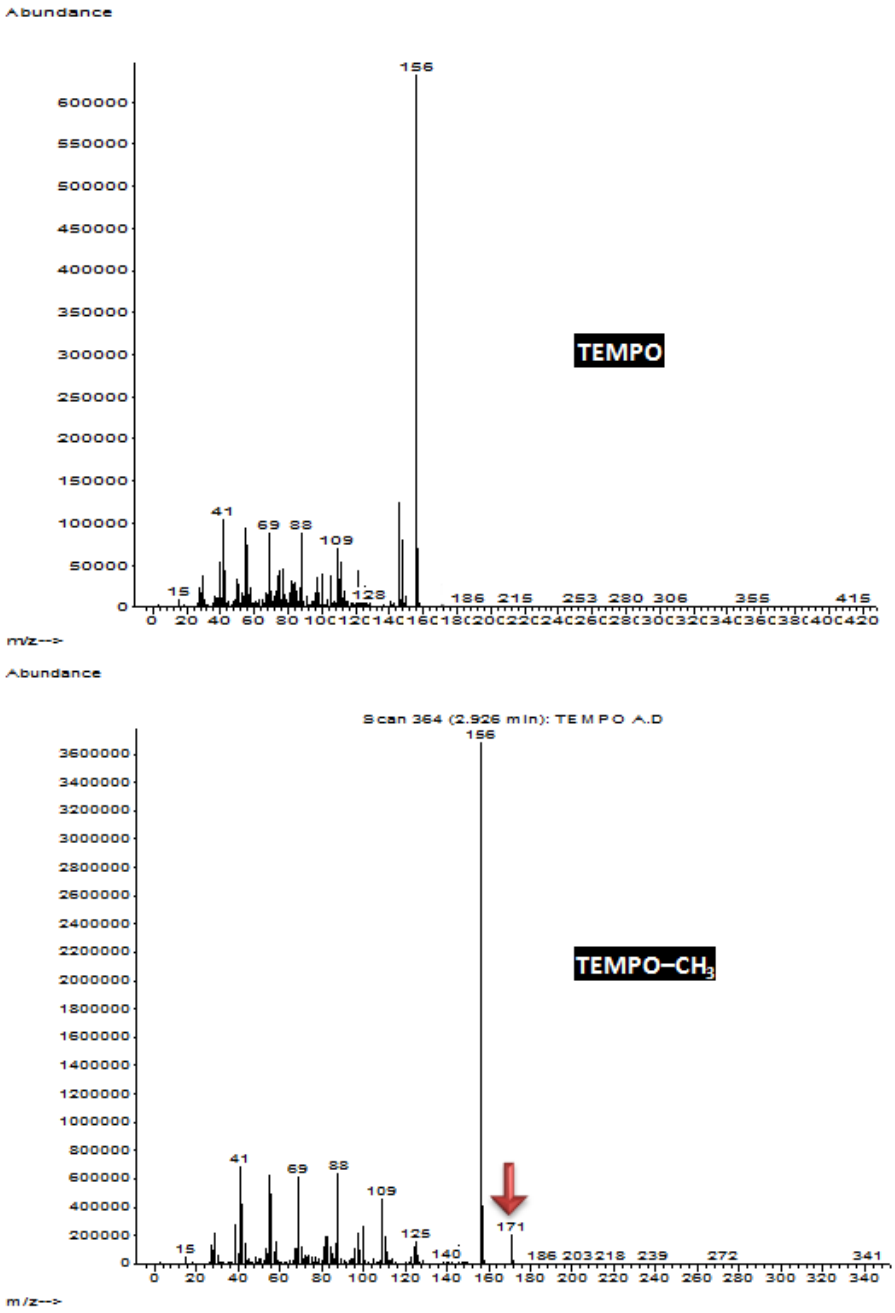

Figure 3-S2: Mass specta of TEMPO and TEMPO–CH3 obtained in GC-MS analysis (sample B-3, Figure 3-3c). The development of a new peak at m/z 171 corresponds to the addition of CH3 (m/z 15) to TEMPO (m/z 156).

.

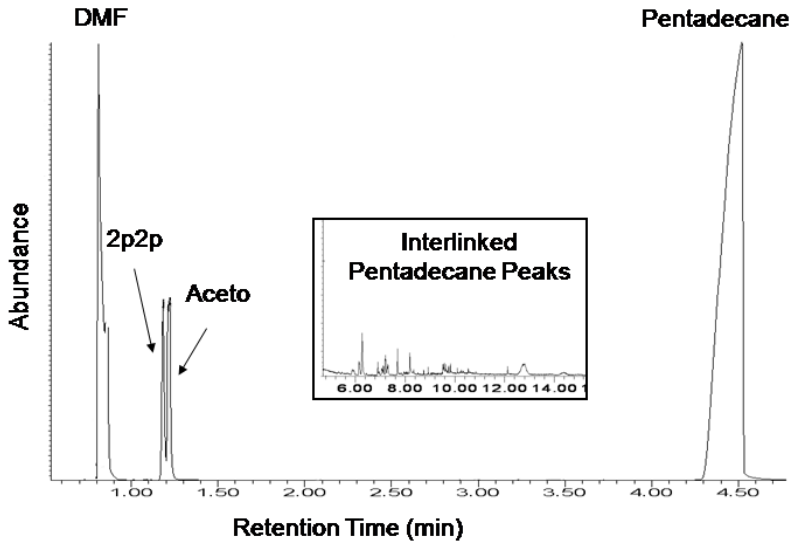

Figure 3-S3 : GC-MS chromatogram of the reaction filtrate of the blank sample (diluted with DMF after reaction); Inset: a myriad of small pentadecane peaks observed after ca. 6 min. Details about this sample are available in our previous study (Akbar S, Beyou E, Cassagnau P, Chaumont P, Farzi G. Polymer 2009;50:2535-43.).

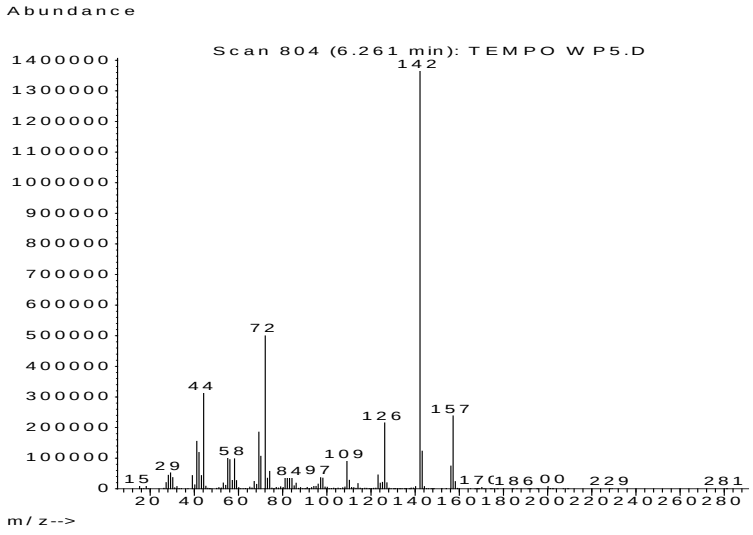

Figure 3-S4 : Mass spectrum of a radical combination product that seems to be the combination of TEMPO with another radical produced in reaction (sample 4, Figure 3-5).

Chapter 4

Polyethylene grafting onto nanotubes

4.1 Grafting of polyethylene onto nanotubes by different ways

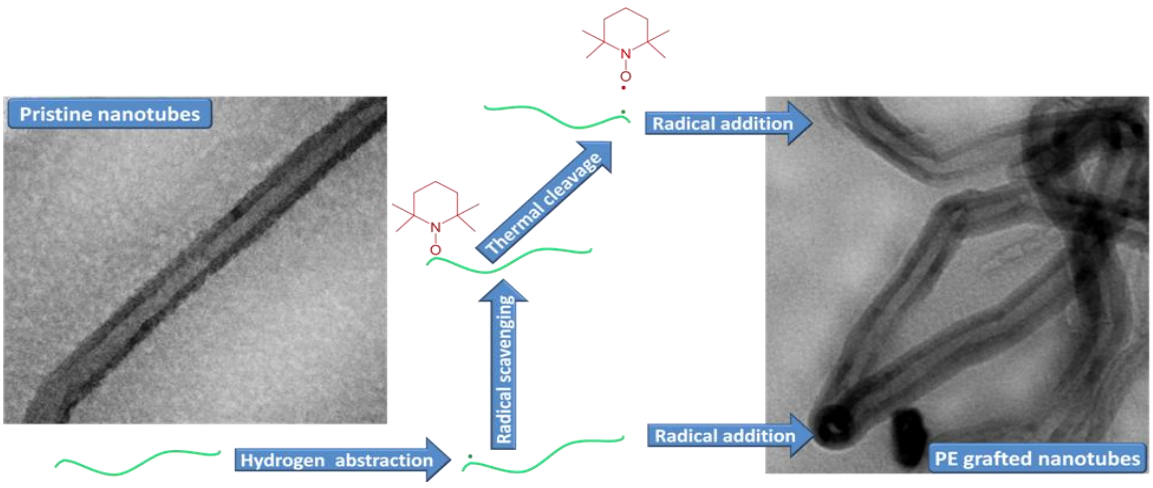

4.1.1 Overview

Polymer-based composites reinforced by carbon fibers have been widely used in advanced structures. Compared to the fibers, carbon nanoubes have many superior mechanical properties such as elastic moduli of 1–5 TPa and fracture strain of 10–100 times better. In addition, their aspect ratio is much greater, which is preferable in making a stronger composite. As such, carbon nanotubes are being considered in place of fibers for reinforcing polymers. Some experimental works have been reported on various polymer–nanotube composites.

PE is the one of the most common commercial polymers that we encounter in day-to-day life. A number of disadvantages prevent their even wider use. The properties of polyolefins are modified through the introduction of the fillers, but the components are not compatible as such. To reduce the interfacial tension between the matrix and the filler, fillers are often functionalised, coated by different techniques as detailed in literature review.

Since carbon nanotubes are fullerene-related structures, it may be possible to form chemical bonds between nanotube and polyethylene chains using free-radical generators such as peroxide. In principle, radicals can be generated on polyethylene

chains either by the abstraction of a hydrogen atom attached to the polymer backbone or by the cleavage of the backbone to yield terminal radicals. The former is frequently encountered as a result of chemical or radiation attack. For example, an oxy radical generated by homolysis of peroxide is capable of abstracting a hydrogen atom from a polyethylene chain and thereby generating a radical. Depending on the hydrogen that is removed, the radical site could be anywhere on the polymer chain. The backbone cleavage is generally caused by severe physical deformation in the molten state under conditions of extreme shear. For example, in the reported experimental works, the nanotube–polymer mixture is first stretched at or above the melting temperature of the polymer in order to have a uniform dispersion of the nanotubes. During this process, radicals can be generated by carbon–carbon bond cleavage. This work concentrates of grafting PE onto nanotubes based on our model compound studies. Moreover, the possibility of PE grafting through end-functionalised nanotubes is also explored. Grafting of PE onto nanotubes was confirmed qualitatively (by Raman spectroscopy and transmission electron microscopy) and quantitatively (by thermogravimetric and elemental analysis).

The results of study show the potential of radical chemistry for PE grafting on nanotubes to prepare reinforced composites.

4.1.2 Article Details

This work is in the process of submission for publication. This work was done in collaboration with another research group from 'Laboratoire de Chimie, Catalyse, Polymères et Procédés, Lyon 1'. Parts of the contents of this paper were presented in '3rd Young Scientist Conference - Nanostructured Polymer materials' held in the Madrid, Spain from 25 to 27 April, 2010; and in '6th International ECNP conference – Nanostructured Polymer and Nanocomposites' convened by The European Centre for Nanostructured Polymer in Madrid, Spain, from 28 to 30 April 2010.

4.2 Synthesis of Polyethyelene-Grafted Multiwalled Carbon Nanotubes by using TEMPO- and thiol-terminated polyethylenes

Sohaib Akbar[1], Emmanuel Beyou[1*], Philippe Chaumont[1], Jérôme Mazzolini, Edgar Espinosa, Franck D'Agosto[2], Christophe Boisson[2]

[1] Université de Lyon, Lyon, F-69003, France, Université Lyon 1, Lyon, F-69003, France, CNRS UMR5223, Ingénierie des Matériaux Polymères: Laboratoire des Matériaux Polymères et Biomatériaux, 15 boulevard Latarget, F-69622 Villeurbanne, France

[2] Université de Lyon, Université Lyon 1, CPE Lyon, CNRS, UMR 5265, Laboratoire de Chimie, Catalyse, Polymères et Procédés (C2P2), LCPP group, 43, Bd. du 11 Novembre 1918, F-69616 Villeurbanne, France

4.2.1 Abstract

Polyethylene, alkoxyamine- and thiol-terminated polyethylenes can be converted to macroradicals using a peroxide, a thermal cleavage of the alkoxyamine and a hydrogen transfer reaction of the thiol, respectively. The addition of these macroradicals to multiwalled carbon nanotubes (MWCNTs) were compared by performing grafting reactions at 160°C in 1,3-dichlorobenzene as solvent. Raman spectroscopy was utilised to follow the introduction of polyethylene on the MWCNTs' surface while thermogravimetric and elemental analysis indicated the extent of this grafting. The grafting ratio was found to be in the 19–36wt% range. Polyethylene functionalised MWCNTs was imaged by transmission electronic microscopy showing a PE layer with various thicknesses covering the surface of nanotubes. It was found that higher levels of grafting were obtained using PE-TEMPO and PE-SH rather than a radical grafting reaction in which dicumyl peroxide, polyethylene and MWCNTs were reacted.

4.2.2 Introduction

Polymer nanocomposites containing carbon nanotubes (CNT) have attracted much attention due to the excellent mechanical, electrical and thermal properties of CNTs [1-3]. Simple melt compounding is often difficult to achieve because CNT tend to form agglomerates during processing of composites. Indeed, carbon nanotubes form clusters as very long bundles due to the high surface energy and the stabilization by numerous of π–π electron interactions among the tubes. The mechanical properties of polyethylene (PE) reinforced by carbon nanotubes do not improve significantly since although the stiffness and strength increase, the ductility decreases [4-6]. The weak polymer-CNT interfacial adhesion prevents efficient stress transfer from the polymer matrix to CNT. A strategy for enhancing the compatibility between nanotubes and polyolefins consists in functionalising the sidewalls of CNT with polymers either by a 'grafting to' or a 'grafting from' approach. The "grafting from" approach involves the growth of polymers from CNT surfaces via in situ polymerisation of olefins initiated from chemical species immobilised on the CNT. As an example, Ziegler-Natta or metallocene catalysts for ethylene polymerisation can be immobilised on nanotubes to grow PE chains from their surface. However covalent linkages or strong interactions between PE chains and nanotubes cannot be created during polymerisation [7,8]. The "grafting to" approach is usually based on a radical process and requires the synthesis of a polymer with reactive groups9 or the use of a radical precursor [10,11]. In a subsequent reaction, the polymer chain is attached to the surface of nanotubes generally by addition reactions. Typically, peroxides are used as hydrogen abstractors to chemically react with polyolefins in the molten state. The radicals formed in the decomposition process must be able to abstract hydrogen atoms from the polyolefin to form macro radicals that can react with unsaturated systems [10,11] This grafting reaction has been previously described with a model compound approach involving a radical grafting reaction between a set of model alkyl radicals (formed by reaction of peroxide-derived alkoxy radicals with low molecular-weight alkanes) and multiwalled carbon nanotubes (MWCNTs) [12,13]. Recently, D'Agosto and Boisson [14-18] developed new strategies that rely on a one step *in situ* functionalisation reaction within an ethylene

polymerisation reactor to introduce a variety of functional groups including alkoxyamine [14-16] and thiol [16, 18] functions at the end of polyethylene chains. Di-polyethylenyl magnesium compound ($MgPE_2$) were prepared using a neodymium metallocene complex which catalysed polyethylene chain growth on magnesium compounds. $MgPE_2$ was in situ reacted with 2,2,6,6-tetramethylpiperidinyl-1-oxy (TEMPO) radical or elemental sulphur to provide a macroalcoxyamine (PE-TEMPO) and polysulphur based product (PE-S_n-PE) respectively. Polymers were recovered by simple precipitation. PE-SH was obtained by simple reduction of PE-S_n-PE. According to these results, we plan to investigate a strategy based on the use of those polyethylenes to generate radical-terminated chains formed either by thermal loss of a nitroxide (PE-TEMPO) or H-abstraction onto a thiol (PE-SH) and graft them onto CNTs. Indeed, Jerome [19] showed an efficient attachment of poly(2-vinylpyridine) (P2VP) of controlled molecular weight end-capped by TEMPO to CNT sidewalls by heating of TEMPO-terminated P2VP. Using the same strategy Liu [20] functionalized shortened CNT with PS and poly[(*tert*-butyl acrylate)-*b*-styrene] and Wang [21] grafted poly(4-vinylpyridine-*b*-styrene) onto CNT.

Experiments reported here assess the thermal decomposition of TEMPO-terminated polyethylene at temperatures above 140°C to generate radical-terminated chains and graft them to MWCNTs. A second method to graft polyethylene onto CNT involving the use of dicumyl peroxide (DCP) in the presence of thiol-terminated polyethylene is also described. These functionalisation approaches have been compared with the reaction in which unfunctionalized PE is grafted onto CNT in the presence of DCP and TEMPO. In addition, the grafting of PE chains is discussed with the help of transmission electronic microscopy images.

4.2.3 Experimental

4.2.3.1 Materials

A commercial LDPE brand Finathene^{TM} (Fina Chemicals, Belgium, MW=90000g/mole; density = 0.92 g.cm^{-3}) was used in this study. End functionalised PE (PE-TEMPO, 60% TEMPO functionalised, Mn=1400g/mol and PE-SH, 78% SH functionalised,

Mn=820g/mol) used in this study was prepared according to previously reported procedure [14-16].

MWCNTs (Graphistrength™ C100) were kindly furnished by ARKEMA, France. Pentadecane (Sigma-Aldrich-France; 99% pure) was employed as a low molecular weight hydrocarbon substrate model for the poly(ethylene-co-octene). Dicumyl peroxide (DCP, Sigma-Aldrich-France; 99% pure) was used as initiator for radical generation. 2,2,6,6-tetramethylpiperidinooxyl (TEMPO), supplied by Sigma-Aldrich-France, has been used as radical scavengers. Dimethylformamide (DMF, Sigma-Aldrich-France; 99% pure) and Dichlorobenzene (DCB, Sigma-Aldrich-France; 99% pure) were used as solvent.

4.2.3.2 PE Grafting onto MWCNTs via peroxide

Description of samples and composition of reactants is given in table 4-1.

Table 4-1: List of samples according to the experimental conditions

Sample	Description	Acronym	Composition of reactants
1	Crosslinked LDPE	PE_c	LDPE: 1g DCP: 0.03g Solvent: DCB 50ml
2	MWCNTs functionalisation by LDPE using DCP	PE-g-MWCNTs	MWCNTs: 50mg LDPE: 1g DCP: 0.03g Solvent: DCB 50ml
	Samples 2-A and 2-B were prepared with PE having mol. wt. ~1400 and 700 $g.gmol^{-1}$ respectively instead of LDPE.		
3	MWCNTs functionalisation by LDPE using DCP and TEMPO	PE.TEMPO-g-MWCNTs	MWCNTs: 50mg LDPE: 1g DCP: 0.03g TEMPO: 0.25g Solvent: DCB 50ml
4	MWCNTs grafted via TEMPO functionalised PE	$PE_{f\text{-}TEMPO}$-g-MWCNTs	MWCNTs: 50mg $PE_{f\text{-}TEMPO}$: 1g Solvent: DCB 50ml
5	MWCNTs grafted via SH functionalised PE	$PE_{f\text{-}SH}$-g-MWCNTs	MWCNTs: 50mg DCP: 0.03g $PE_{f\text{-}SH}$: 1g Solvent: DCB 50ml

Grafting reactions were carried out in glass reactors. In order to prepare PE-g-MWCNTs, DCP (0.03 g / 0.11 mmole) and LDPE (1g / 0.011 mmole) were mixed in 50 mL of DCB along with 50 mg of MWCNTs. The mixture was then sonicated for one minute and degassed by four freeze-pump-thaw cycles. Grafting reactions were carried out under constant stirring and heating at 160°C for 6 hours. At the end of the reaction PE grafted MWCNTs were collected by centrifugation (11K rpm, 10 min) and subsequent filtrations. PE.TEMPO-g-MWCNTs prepared along the similar lines with the additional presence of TEMPO, i.e. 0.25 g / 1.6 mmole. Purification of grafted nanotubes was performed by Soxhlet extraction with DCB as solvent for 24 hr. Solid materials and filtrates were collected and characterised.

4.2.3.3 PE Grafting onto MWCNTs via end-functionalised PE

For the preparation of PE grafted nanotubes by means of TEMPO functionalised polyethylene, 50 mg of MWCNTs and 1 g (1 mmole) of PE-TEMPO were mixed in 50 ml of DCB in a Schlenk-type reactor. Similarly, in order to perform PE grafting through thiol functionalised polyethylene, 0.03 g/0.11 mmole of DCP and 1 g (1.02 mmole) of PE-SH were dissolved in 50 ml of DCB together with 50 mg of MWCNTs. After sonication for one minute the mixtures were degassed at least three times. The reactors were then placed in an oil bath at a temperature of 160°C for 8 hours. At the end of the reaction the contents were filtered out and dried in vacuum at 80°C for 48 hours. The products were thoroughly washed for purification prior to characterisation.

4.2.4 Characterisation

Purification of PE grafted nanotubes was carried out by washing with DCB in a Soxhlet apparatus for 24 hr to extract non-grafted material. These purified nanotubes were passed through various characterisations.

Thermogravimetric analysis (TGA) was carried out with a DuPont Instruments TGA 2950 thermobalance, controlled by a TC10A microprocessor. Samples were heated at 20°C/min under a nitrogen flow (100mL/min).

Pyrolysis-Gas chromatography-mass spectrometry (Py-GC-MS). Samples were pyrolysed by gradual heating up to 700°C and the resulting fragmented products were analysed by GC-MS. Gas chromatography-mass spectrometry (GC-MS) was performed with an Agilent 6890 series GC system equipped with a HP-5ms (5%-phenyl)-methylpolysiloxane, ref. 19091S-433. The injector was at 250ºC and the temperature programme followed was: 50-310ºC at 20ºC/min. Injection and detection by MS was carried out at 280ºC.

The Raman spectra of pristine and PE grafted nanotubes were obtained by a Horiba Jobin-Yvon LabRAM ARAMIS Raman confocal microscope (632.8 nm, Aramis CRM, Horiba Jobin Yvon, Edison, NJ). A 50× objective was used to focus 18.5 mW of He−Ne laser light onto the sample surface with a spot size of about 1 µm.

Elemental analysis (EA) was carried out (Analyzer: LECO SC144, Service central d'analyse du CNRS, Vernaison, France) to determine the contents of H and N.
Sonication was accomplished using Vibracell™ 75041 (Bioblock Scientific, Illkirch, France) apparatus set at 40% of 750 W for 30 sec.

Transmission electron microscopy (TEM) was carried out with a Philips CM-120 microscope (Philips Consumer Electronics BV, Eindhoven, The Netherlands) operated at 80 keV.

4.2.5 Results and discussion

4.2.5.1 Synthesis of PE grafted nanotubes via peroxide (with and without TEMPO)

Mylvaganam et al [22] have predicted with the aid of a quantum mechanics analysis that covalent bond formation between alkyl radicals and carbon nanotubes is energetically favourable; and that this reaction may take place at multiple sites of nanotubes. Hence one way to improve the load transfer of carbon nanotubes/PE composite via chemical bonds at the interface is to use free-radical generators such as peroxide in conjunction with preformed PE or to perform in situ polymerisation in the presence of nanotubes. Recently, we have described the 'grafting to' method with a model compound approach involving a radical grafting reaction induced by mixing peroxide-derived alkoxyl radicals, pentadecane and multiwalled carbon nanotubes (MWCNTs) [12]. Alkyl radicals produced from pentadecane are good representatives of linear polyethylene chain radicals. This strategy is based on the formation of multiple covalent bonds between polyethylene chain radicals and

nanotubes. Figure 4-1 sums up the main reactive pathways for free radical grafting of PE onto MWCNTs with dicumyl peroxide as initiator and TEMPO as radical scavenger.

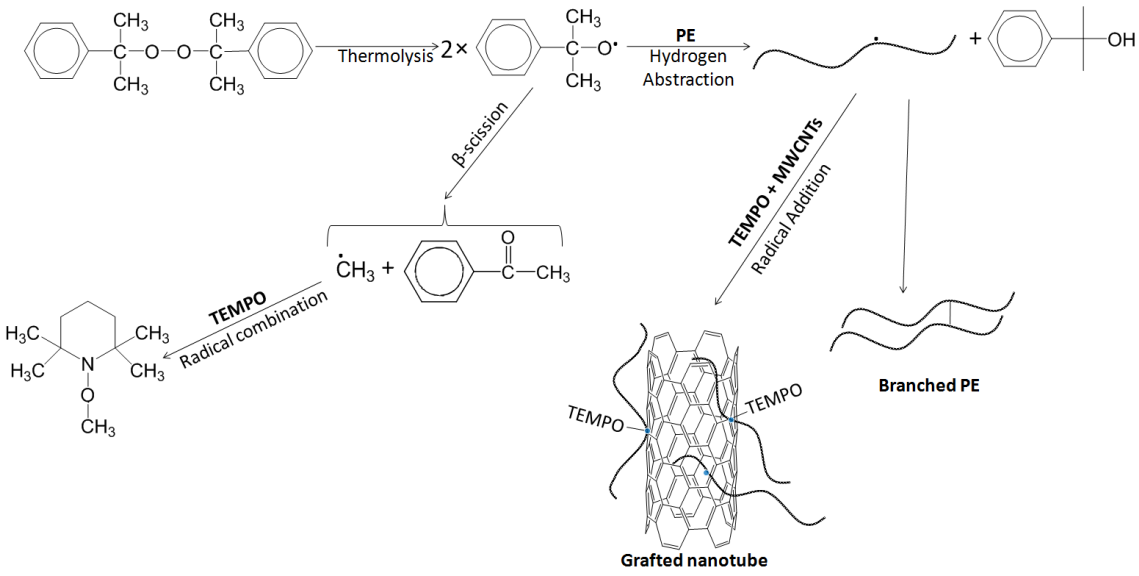

Figure 4-1: Reaction scheme for PE grafting onto MWCNTs with TEMPO as a radical scavenger.

The main step is the formation of DCP-derived alkoxy radicals that abstract hydrogen from the polyethylene backbone. However, the alkoxy radicals can undergo additional reactions including β-scission leading to the formation of methyl radicals [23,24]. These latter preferentially induce coupling reaction or attack onto the sp^2 carbon of the MWCNTs whereas cumyloxyl radicals are more prone to hydrogen abstraction from polyethylene [25]. The formed PE-based radicals are able to react with MWCNTs by radical addition onto sp^2 carbons of the MWCNTs (Figure 4-1) and with other radical species via the common radical-radical coupling reactions. According to Johnston [26,27] coupling reactions are four times more prone to happen than scission reactions, when using poly(ethylene-*co*-1-octene) in the presence of DCP at 160°C. Thus, we assume that for PE-based radicals scission reactions may be disfavoured. As discussed recently using a model compound approach [28], the presence of TEMPO radicals creates competitive combinations reactions that are actually reversible reactions which may favour the addition of PE-based radicals to MWCNTs (Figure 4-1).

4.2.5.2 Synthesis of PE grafted nanotubes via end functionalised PE

In recent studies, the production of polyethylene chains carrying alkoxyamine [14-17] and thiol [18] end-groups has been described. The homolytic cleavage of alkoxyamine-terminated PE leads to the formation of stable nitroxyl radicals and PE radicals. We investigate a strategy based on the use of polyethylene radical-terminated chains that could be formed by thermal activation (Figure 4-2a).

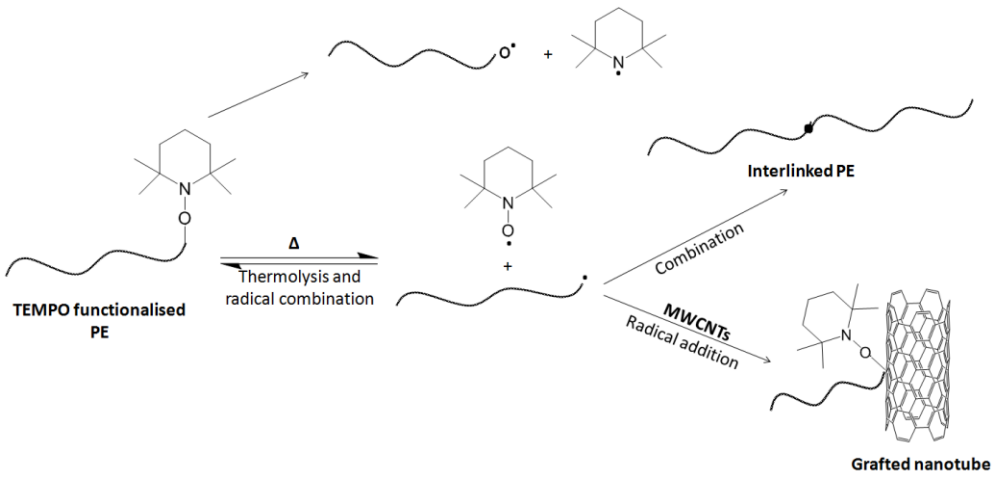

(a)

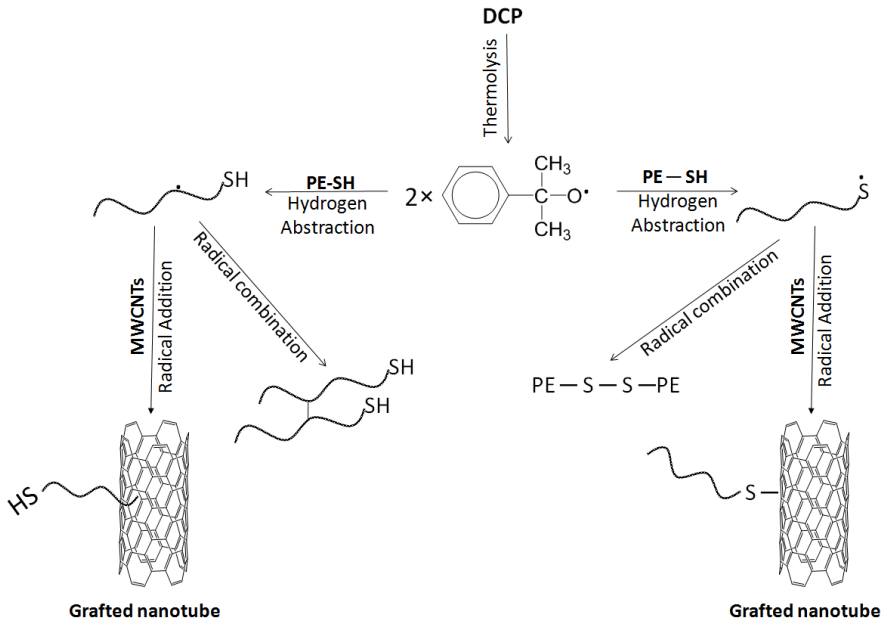

(b)

Figure 4-2: Reaction scheme for end functionalised PE grafting onto MWCNTs: (a) via PE-TEMPO; (b) via PE-SH

The reversible termination of the polyethylene chain is the key step for reducing the overall concentration of the radical chain end. The extremely low concentration of reactive chain ends is expected to minimize irreversible termination reactions, such as combination or disproportionation [29] (Figure 4-2a). The NO-C bond in N-alkoxyamines is usually considered as the most labile. However, it is worth mentioning here that the competitive N-OC bond cleavage must be also considered at high temperatures [30,31] (Figure 4-2a). Thiol-terminated polyethylene has been also grafted onto CNTs using a similar procedure. In the presence of DCP-derived radicals and MWCNTs, thiyl radicals are formed and are expected to react by radical addition onto sp^2 carbon of the MWCNTs (Figure 4-2b).

4.2.5.3 Qualitative evidence for covalent sidewall functionalisation: Raman analysis

Raman spectroscopy can give direct evidence for covalent sidewall functionalisation.[32-34] Gao et al [35] reported the analyses by Raman spectroscopy of polymer coating on MWCNTs may lead to the observation of three different signals: (1) only CNT signals are detectable if the polymer layer is transparent, (2) only polymer signals are present if the polymer layer can absorb and reflect the whole excitation energy, and (3) no signals or a strong photoluminescence can be observed if there is energy transfer between nanotubes and polymer chains or if the coated polymer changes the electronic property of CNTs. The Raman spectra of CNTs usually exhibit three characteristic bands: the tangential stretching G mode (1500–1600 cm^{-1}), the D mode (~1350 cm^{-1}) and the radial breathing modes (RBMs) (100–400 cm^{-1}) [36]. Raman spectra of p-MWCNTs (Figure 4-3) shows two main peaks around 1330 cm^{-1} and 1583 cm^{-1}, corresponding to D-band (the disordered graphite structure) and G-band (sp2-hybridised carbon), respectively.

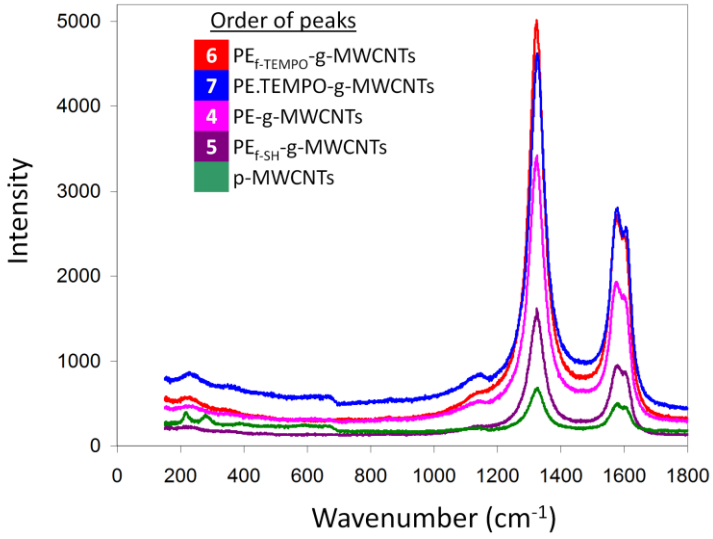

Figure 4-3: Raman spectra of pristine and various functionalised nanotubes. Variations in D band — 1330 cm-1; G band — 1583 cm-1; and D´ — 1608 cm-1 are visible. The legend follows the order of the peaks.

A typical additional Raman band, D', just after G band is only observed for MWCNTs. Similar to the D band, D' is a double-resonance Raman feature induced by disorder, defects or ion intercalation between the graphitic walls. Some authors used G to D area ratios rather than intensity which is a better indicator as it covers both height and width of the Raman peaks [37]. Table 4- 2 shows the area ratios of D to G band, and D' to G band.

Table 4- 2: Area ratios of D and G bands in Raman spectra for pristine and various PE grafted nanotubes.

Sample	A_D/A_G	$A_{D'}/A_G$
2 PE-g- MWCNTs	1.53	0.84
3 PE.TEMPO-g- MWCNTs	1.59	0.92
4 $PE_{f\text{-}TEMPO}$-g- MWCNTs	1.67	0.89
5 $PE_{f\text{-}SH}$-g- MWCNTs	1.44	0.90

For samples 2-5, the corresponding area ratios are larger than that of as-received pristine carbon nanotubes. Increases in these ratios are indicative of structural defects in MWCNTs' surface due to covalent bonding with PE. Another interesting feature is the disappearance of RBM bands which were obvious in case of pristine MWCNTs (ca. 220 cm^{-1} and 282 cm^{-1}, Figure 4-3). This fading of diameter sensitive bands is believed to be caused by an increase in thickness of the tubes due to polymer grafting [38,39].

4.2.5.4 PE grafting density

Heating functionalised nanotubes in an inert atmosphere removes the organic moieties and restores the pristine nanotubes' structure. Therefore, thermogravimetric analysis was performed on the reaction products in order to gain a more quantitative picture of the extent of nanotubes' functionalisation. Before carrying out TGA, the adsorbed (non-covalently attached) molecules were discussed from the grafted ones by extensive washings with DCB as mentioned in the experimental part.

The TGA traces for both the starting pure reactants and the PE-grafted nanotubes are shown in Figure 4-4.

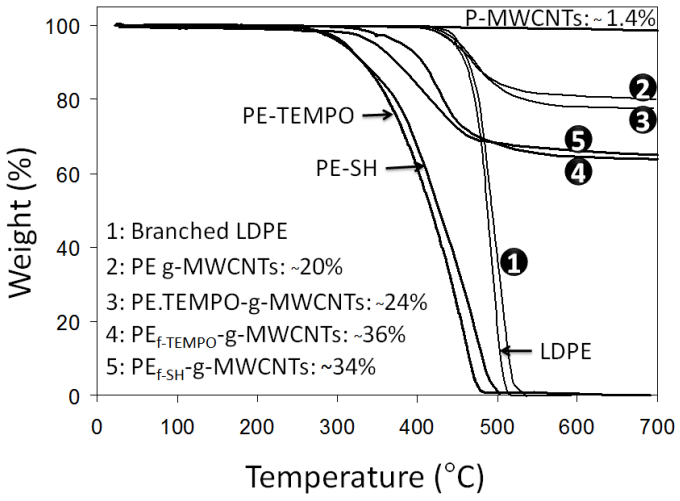

Figure 4-4: TGA weight loss data (under nitrogen) for various samples (see details in table 4-1). Pure products (i.e. PE-SH, PE-TEMPO, LDPE and pristine nanotubes) are shown for corresponding reference.

Pure reactants completely decompose in the temperature range between 300 and 510°C. As shown in Figure 4-4, the amount of organic functionalities physically and/or covalently attached to the initial p-MWCNTs can be neglected (weight loss < 1.5%). PE-grafted onto MWCNTs are degraded at 300-540°C, which are nearly the same temperatures as pure PE reactants. In figure 4-4, the weight of grafted PE is estimated to be in the range 19-36% depending on the experimental procedure (Table 4-3). The corresponding grafting densities can be calculated using a specific surface area (SSA) of 225m^2/g for MWCNTs [13, 40]. The calculated grafting densities are varying from 1.1$mg.m^{-2}$ (0.012$\mu mol.m^{-2}$) for high molar mass LDPE (sample 2, Table 4-3) to 2.3$mg.m^{-2}$ (2.8 $\mu mol.m^{-2}$) for low molar mass thiol end-functionalised PE (sample 5, Table 4-3). LDPE grafting density on nanotubes is 1.1$mg.m^{-2}$ while incorporation of TEMPO raises the grafting density to 1.4$mg.m^{-2}$ (sample 3, Table 4-3). This increase in the weight loss suggests a higher degree of grafting for PE chains by using TEMPO in the reaction mixture and/or the grafting of TEMPO groups as well as PE chains onto MWCNTs. A qualitative indication of TEMPO consumption comes from the colour of the mixture starting from dark yellow with free TEMPO before heating and turning lighter at the end of the reaction. In order to improve the understanding of the polyethylene radicals behaviour towards carbon nanotubes, the samples 2-A and 2-B (table 4-3) correspond to the ones performed with low molar masses linear PE (1490g/mol and 770g/mol, respectively). For both samples 2-A and 2-B, the weight loss observed by TGA increases to 28% and 29%, respectively (Table 4-3) despite their low molar masses (e.g. 1490g/mol and 770g/mol) in comparison with that of LDPE (e.g. 90000g/mol). These results indicate that the use of short PE chains permit a significant increase of the grafting density (e.g. 1.2$\mu mol.m^{-2}$ (1.7$mg.m^{-2}$) and 2.5$\mu mol.m^{-2}$ (1.8$mg.m^{-2}$)) in comparison with the grafting density obtained with LDPE (e.g. 0.012$\mu mol.m^{-2}$ (1.3$mg.m^{-2}$), Table 4-3). It suggests that longer polymer chains cover a larger surface decreasing the grafting density, as previously described by Jerome et al [19, 41] for the attachment of poly(2-vinylpyridine) (P2VP) and polystyrene (PS) onto MWCNTs. Indeed, they observed that PS grafting density decreases from 0.045$\mu mol.m^{-2}$ to 0.01$\mu mol.m^{-2}$ by increasing the molecular weight of PS-TEMPO from 3000g/mol to 30000g/mol [41].

By using TEMPO-terminated PE (sample 4, Table 4-3), the PE radical grafting reaction onto MWCNTs is improved although the functionalisation of PE was only 60%. Indeed, we obtained a PE grafting density of 2.5mg.m^{-2} (1.78µmol.m^{-2}) (Table 4-3) in comparison with the corresponding non functional PE with the same molar mass (i.e. 1.7mg.m^{-2} (1.2µmol.m^{-2})) (sample 2-A, Table 4-3). In the presence of a thiol-terminated polyethylene (i.e. PE-SH, sample 5, Table 4-3), a hydrogen transfer process is required between cumyloxyl radicals and/or radicals located onto the MWCNTs and the thiol derivative. Then, the generated thiyl radicals can react with unsaturations of MWCNTs, leading to PE-*g*-MWCNTs. The grafting density of sample 5 (e.g. 2.8µmol.m^{-2} (2.3mg.m-2), Table 4-3) is similar to that of TEMPO end-functionalised PE (1.78µmol.m-2 (2.5 mg.m-2), sample 4, Table 4-3). A greater efficiency of addition of carbon centered radicals to MWCNTs than that of sulfur radicals is usually observed (well known for C_{60} [42]), but is not observed here. This may be attributed to both the lower molar mass of thiol end-funtionalised PE and the higher SH degree of functionalisation (e.g. 78% and 60% for TEMPO end-functionalised PE).

Elemental analysis (EA) is also an indicator of degree of grafting and a good agreement between grafting densities calculated from EA and TGA analysis was obtained (e.g. 2 mg.m^{-2} and 2.3mg.m^{-2}, sample 5, Table 4-3).

Pyrolysis-GC-MS analyses were also performed on samples 3-5 (Table 4-1) in order to characterise TEMPO- and sulfur-based molecules. Indeed, the main role of thermal cracking is to decompose of long hydrocarbon molecules into smaller ones. Cracking of LDPE occurs by random chain scission and therefore a broad hydrocarbon spectrum is produced [43, 44]. Herein, pyrolysis of PE-grafted MWCNTs (samples 3-5, Table 4-1) is expected to produce N- or S-containing molecules and small segments such as C_4H_8, C_5H_{10}, C_6H_{12}, and so on. Figure 4-5 shows the pyrogram obtained for sample 3 which is mainly characterised by aliphatic compounds like C_6H_{12} (m/z 84) and C_8H_{16} (m/z 112).

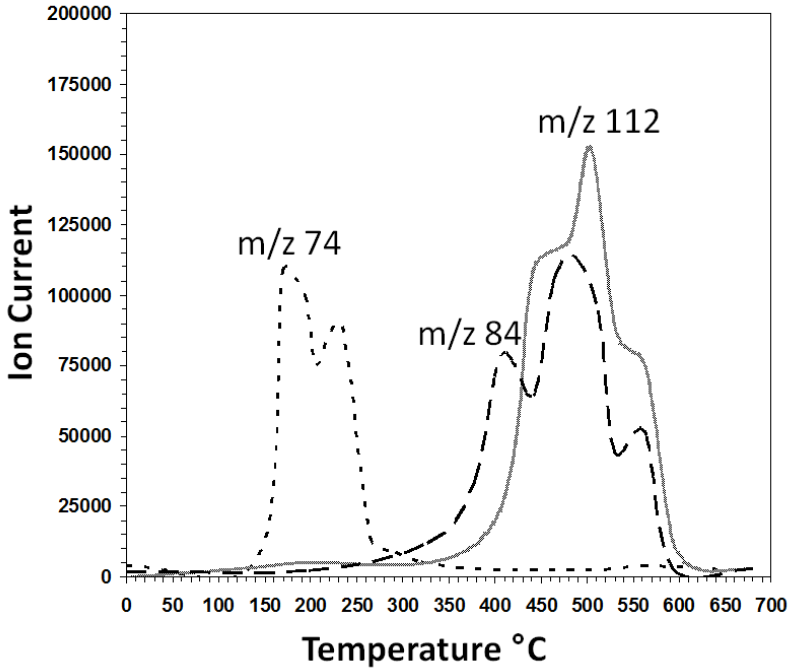

Figure 4-5: Pyrogram of PE.TEMPO-g-MWCNTs (sample 3) in the temperature range 100-600°C . Ion current vs time for m/z 74, 84, and 112 corresponding to TEMPO, C4H8 and C5H10 respectively.

These fragments are obtained in the temperature range of 400 to 590°C, which is in agreement with weight loss data for sample 3 obtained by TGA (figure 4-4). Another huge ion current (m/z 74) is observed in Figure 4-5 which is believed to originate from the fragmentation of TEMPO groups and probably corresponding to $(CH_3)_2CH_2NO$ (m/z 74). Figure S1 (in supporting information) shows the pyrogram of sample 5. Although we could not detect any traces of sulphur by this technique, small polyolefin segments obviously coming from PE disintegration were observed. Nonetheless, elemental analysis have already shown the presence of S and N (table 4-3).

Table 4-3: Effect of the grafting procedure on the degree of PE grafting.

Sample	Elemental wt%	Calculation from	Degree of PE Grafting		
			wt%	mg.m^{-2}	µmol.m^{-2}
2	H: 3.1	EA	22	1.2	0.013
PE-g-MWCNTs		TGA	20	1.1	0.012
2-A	-	TGA	28	1.7	1.2
2-B	-	TGA	29	1.8	2.5
3	N: 0.5	EA	26	1.5	0.016
PE.TEMPO-g-MWCNTs	H: 3.7	TGA	24	1.4	0.015
4	N: 0.3	EA	34	1.9	1.36
$PE_{f\text{-}TEMPO}$ -g- MWCNTs	H: 4.8	TGA	36	2.5	1.78
5	S: 0.8	EA	30	2	2.4
$PE_{f\text{-}SH}$-g-MWCNTs	H: 4.2	TGA	34	2.3	2.8

N.B**:** Elemental analysis of pristine MWCNTs shows: N, 0.78%; O, 0.89%; H, 0.30%; P, 1.81%.; S, <0.2%. All values shown above are rounded off. Elemental wt% values are shown after deducting corresponding pristine nanotubes values. Grafting density in mg.m^{-2} is based on calculations assuming a specific surface area of 225 m^2.g^{-1} for MWCNTs.

4.2.5.5 Morphological characterisation of PE-grafted MWCNTs

To go one step forward, the morphological structures of p-MWCNTs and PE-grafted MWCNTs (samples 2-5) were examined by transmission electron microscopy (TEM). In these experiments, a few drops of dilute solutions of PE-grafted nanotubes in hot DCB were initially deposited onto a carbon-coated copper grid and further observed in a dried state after evaporation of the solvent. Functionalisation of MWCNTs by PE can be clearly seen in the TEM images of Figure 4-6.

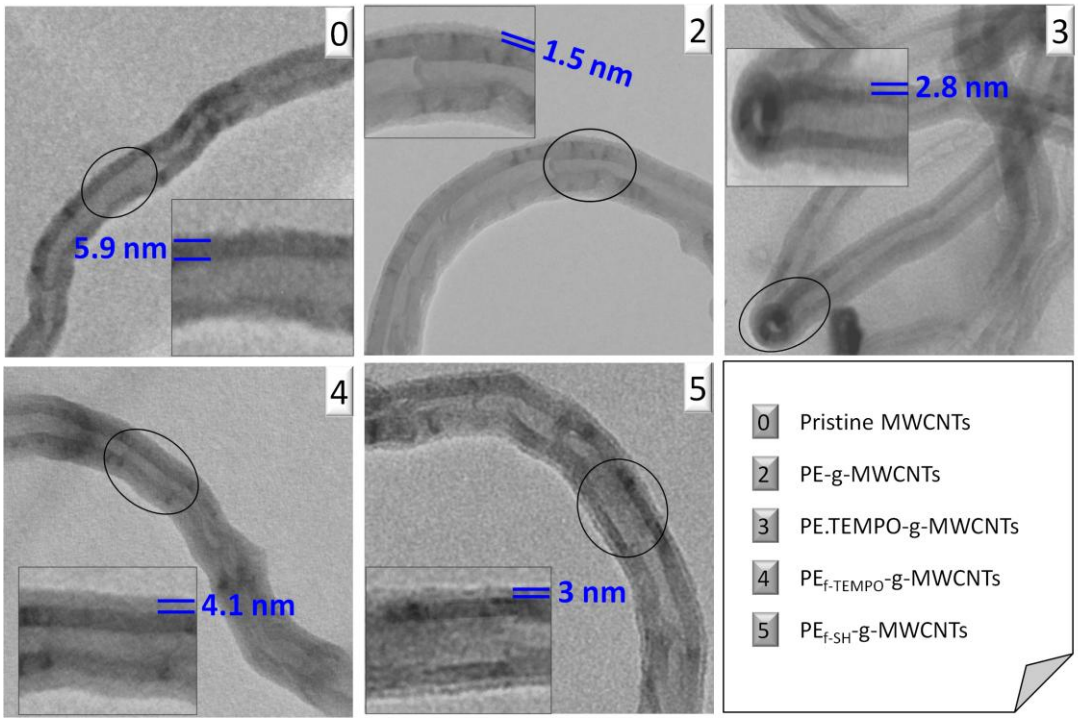

Figure 4-6: TEM pictures of p-MWCNTs (0); PE-g-MWCNTs (2); PE.TEMPO-g-MWCNTs (3) ; PEf-TEMPO-g-MWCNTs (4); PEf-SH-g-MWCNTs (5).

As emphasised by the enlargment of TEM images in Figure 4-6, a contrast difference gives the indication that the MWCNTs are uniformly coated with the polymer layer, forming PE-grafted MWCNTs core-shell nanostructures. This result tends to support that the grafting onto process occurred over the entire surface of the initial MWCNT. The shell thickness of the PE coating is varying from 1.5nm (LDPE-gMWCNTs, sample 2, 4-6) to 4.1nm ($PE_{f\text{-}TEMPO}$-g-MWCNTs, sample 4, figure 4-6). The TEM observations are consistent with the TGA results : the grafted polymer contents can be highered by using end-functionalized PE (samples 4-5). In addition, as pointed out by Gao et al [45], the electron beam may destroy polymer chains especially at high resolution so the amount of polymer observed in the presented TEM images may represent a lower limit.

4.2.6 Conclusion

We investigated various ways to convalently functionalise multiwalled carbon nanotubes (MWCNTs) with polyethylene (PE). First, MWCNTs were successfully functionalised through a simple radical grafting approach based on the thermolysis

of dicumyl peroxide initiator performed in dichlorobenzene and in presence of PE and MWCNTs at 160°C. Raman, TGA data and EA attested for successful functionalisation of MWCNTs by polyethylene. Incorporation of TEMPO radicals as radical scavengers in the grafting reaction of polyethylene onto MWCNTs slightly increased the extent of polyethylene grafting 1.1mg.m^{-2} (0.012µmol.m^{-2}) to 1.4mg.m^{-2} (0.015µmol.m^{-2}). However, PE grafting density was significantly increased to 2.3 - 2.5mg.m^{-2} (~2.5µmol.m^{-2}) by using TEMPO- and thiol-terminated polyethylenes which was attributed to their low molar masses together with their specific chain-end reactivity. Moreover, TEM images clearly indicated that the MWCNTs were uniformly coated with the polymer layer, forming PE-grafted MWCNTs core-shell nanostructures with a PE shell thickness varying from 1.5nm to 4.1nm.

Future work will consist in performing this procedure in an extruder and investigating the effects of this grafting on mechanical, rheological, and electrical properties of PE/CNTs composites.

4.2.7 References

1. Connell, M.O.; Carbon Nanotubes : Properties and Applications : CRC Press, 2006.
2. Gogotsi Y. ; Carbon Nanomaterials : CRC Press, 2006.
3. Zdenko Spitalsky Z.; Tasis D.; Papagelis K.; Galiotis C. Prog Polym Sci 2010,35,357.
4. Shofner M.L.; Khabashesku V.N.; Barrera E.V. Chem Mater 2006,18,906.
5. Mahfuz H. ;Adnan A. ; Rangari V.K.; Jeelani S. Int J Nanosci 2005, 4,55.
6. Ruan S.; Gao P.; Yu T.X. Polymer 2006,47,1604.
7. Tong X.; Liu C.; Cheng H.M.; Zhao H.; Yang F.; Zhang X. J Appl Polym Sci 2004,92,3697.
8. Funk A. ; Kaminsky W. Compos Sci Technol 2007,67,906.
9. Yang B.X.; Pramoda K.P.; Xu G.Q.; Goh S.H. Adv Funct Mater 2007,17,2062.
10. Robin J.J.; Boyer C.; Boutevin B.; Loubat C. Polymer 2008,49,4519.
11. Hoight A.H.; Meijer J.; Jelenic J. Reactive modifiers for polymers, London : Al-Malaïka S. Eds. 1997, 84 and references therein.
12. Akbar S.; Beyou E.; Cassagnau P. ; Chaumont P. ; Farzi G. Polymer 2009,50,2535.
13. Farzi G.; Akbar S. ; Beyou E. ; Cassagnau P. ; Melis F. Polymer 2009,50,5901.
14. Lopez R.G. ; Boisson C. ; D'Agosto F. ; Spitz R. ; Boisson F. ; Bertin D. ; Tordo P. Macromolecules 2004 ,37,3540.
15. Lopez R.G. ; Boisson C. ; D'Agosto F. ; Spitz R. ; Boisson F. ; Gigmes D. ; Bertin D. J Polym Sci Polym Chem 2007,45,2705.
16. Mazzolini J. ; Espinosa E. ; D'Agosto F. ; Boisson C. Polymer Chem, 2010,1 ,793.
17. D'Agosto F. ; Boisson C. Aust. J. Chem. 2010, 63, 1155.
18. Mazzolini J. ; Boyron O. ; Delolme F. ; Gigmes D. ; Bertin D. ; D'Agosto F. ; Boisson C. Macromolecules 2010, DOI: 10.1021/ma101265t
19. Lou X. ; Detrembleur C. ; Pagnoulle C. ; Jerome R. ; Bacharova V. ; KiriyA. ; Stamm M. Adv Mater 2004,16,2123.
20. Liu Y. ; Yao Z. ; Adronov A. Macromolecules 2005,38,1172.
21. Wang H.C. ; Li Y. ; Yang M.J. Sens Actuators B 2007,124,360.
22. Mylvaganam K.; Zhang L.C. J Phys Chem B 2004,108,5217.
23. Badel T. ; Beyou E. ; Bounor-Legare V. ; Chaumont P. ; Flat J.J. ; Michel A. J Polym Sci Part A : Polym Chem 2007,45,5215.
24. Badel T.; Beyou E.; Bounor-Legare V.; Chaumont P.; Flat J.J.; Michel A. Macromol Chem Phys 2009,210,1087.

25. Moad G. Prog Polym Sci 1999,24,81.
26. Johnston R.T. Rubber Chem Tech 2003,76,174.
27. Johnston R.T. Sealing Technology 2003,76,6.
28. Akbar S.; Beyou E.; Chaumont P.; Melis F. Macromol Chem Phys 2010, accepted
29. Hawker C.J.; Bosman A.W.; Harth E. Chem Rev 2001,101,3661.
30. Gaudel-Siri A.; Siri D.; Tordo P. ChemPhysChem 2006,7,430.
31. Gigmes D.; Gaudel-Siri A.; Marques S.R.A.; Bertin D.; Tordo P.; Astoffi P.; Greci L.; Rizzoli C. Helv chim Acta 2006,89,2312.
32. Osswald S.; Havel M.; Gogotsi Y. Journal of Raman Spectroscopy, 2007,728.
33. Pastine S.J.; Okawa D.; Kessler B.; Rolandi M.; Llorente M.; Zettl A.; Fréchet J.M.J. J Am Chem. Soc 2008,130,4238.
34. Ying Y.; Saini R.K.; Liang F.; Sadana A.K.; Billups W.E. Org Lett 2003,5,1471.
35. Gao C.; Jin Y.Z.; Kong H.; Whitby R.L.D.; Acquah S.F.A.; Chen G.Y.; Qian H.; Hartschuh A.; Silva S.R.P.; Henley S.; Fearon P.; Kroto H.W.; Walton D.R.M. J Phys Chem B 2005,109,11925.
36. Rao A.M.; Richter E.; Bandow S.; Chase B.; Eklund P.C.; Williams K.A.; Fang S.; Subbaswamy K.R.; Menon M.; Thess A.; Smalley R.E.; Dresselhaus G.; Dresselhaus M.S. Science 1997,275,187.
37. Park M.J.; Lee J.K.; Lee B.S.; Lee Y-W.; Choi I.S.; Lee S-G. Chem Mater 2006,18,1546.
38. Menard-Moyon C.; Izard N.; Doris E.; Mioskowski C. J Am Chem Soc 2006,128,6552.
39. Sadowska K.; Roberts K.P.; Wiser R.; Biernat J.F.; Jablonowska E.; Bilewicz R. Carbon 2009,47,1501.
40. Peigney A. ; Laurent C.. Flahaut E.; Bacsa R. ; Rousset A. Carbon 2001,39,507.
41. Lou X. ; Detrembleur C. ; Sciannamea V. ; Pagnoulle C. ; Jerome R. Polymer 2004,45,6097.
42. Krusic P.J.; Wasserman E.; Parkinson B.A.; Malone B.; Holler E.R. J Am Chem Soc 1991,113,6274.
43. Scheirs J.; Kaminsky W. Thermal and catalytic conversion of polyolefins. 2006, Wiley.
44. Cit I.; Sinag A.; Yumak T.; Ucar S.; Misirlioglu Z.; Canel M. Polym Bull 2010,64,817.
45. Gao C.; Vo C.D.; Jin Y.Z.; Li W.; Armes S.P. Macromolecules 2005, 38, 8634.

Chapter 5

Polypropylene grafting onto nanotubes

5.1 Tetramethylpentadecane and PP grafting onto nanotubes

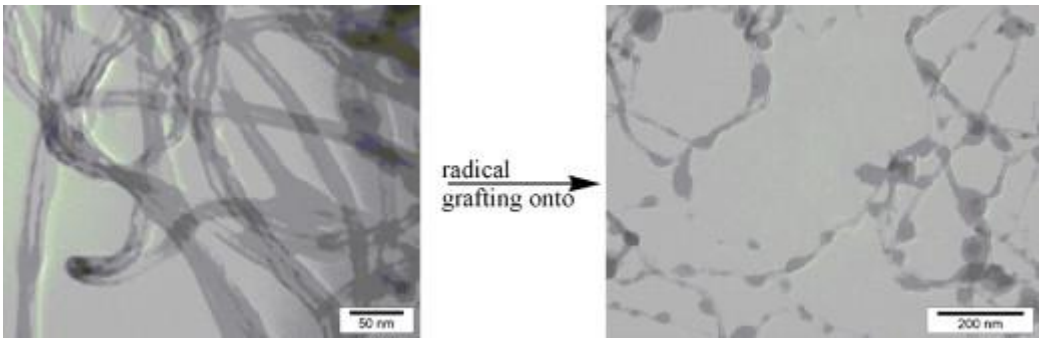

5.1.1 Overview

PP is a convenient thermoplastic with a balance between processing and performance. The melting temperature (Tm = 162 — 165°C) is high enough to resist boiling water yet low enough to permit ease of thermoforming composite sheets. PP is available in grades intended for extrusion into film, sheet and profiles, injection, moulding, and thermoforming.

The extraordinary versatility of reinforced PP suits a wide spectrum of end-us applications for fibers, films, moulded pats. However, there always exist certain shortcomings in physical and chemical properties that can limit its use for certain applications. Currently automotive and appliance applications employ glass or mineral filled systems with loading levels ranging from 15 to 50 percent. However this leads to greater moulded part weight. PP is non polar and therefore lacks interaction with other materials such as glass fibres, clays, metals, pigments, fillers etc. Therefore, when PP nanocomposites are manufactured they exhibit less significant improvement in physical, chemical and mechanical properties if PP does not have a good interaction with nanofiller. Although physical blending with CNTs is an economic way to modify polypropylene performance, compatibilizing agents are necessary for creating strong interface between filler particles and the polymer phase. In both academic and industrial locations, the study of PP nanocomposites is an intense area of current interest and investigation. The driving force for such efforts is attributed to huge commercial opportunities in both automotive and

packaging applications. Material design at relatively low nanofiller loading can address the inherent shortcomings of polypropylene resin by itself and can do so with favourable cost, processing and reduced moulded-part weight profiles. In order to prepare PE/nanotubes composite with enhanced properties of interest e.g. reinforcement, there must be a good dispersion of CNTs and some chemical linkage between the two phases of the composite. To overcome incompatibility of nanotubes and PE we envisaged a scheme to graft PE during extrusion through radical grafting onto nanotubes. But before using this procedure a model compound study was adopted to obtain optimised reaction conditions. Pentadecane was selected as a model since it represents the characteristics of PE. Moreover use of pentadecane makes the extensive characterisation easier which might be difficult in case of PE since pentadecane is in liquid form at ambient temperature.

In this study we functionalised MWCNTs by tetramethylpentadecane (TMP), 1-dodecanethiol (DT) and polypropylene (PP) through radical addition onto MWCNTs' surface using dicumyl peroxide as hydrogen abstractor. TMP acts as a model for PP in the model compound approach. We also optimised our reaction conditions (e.g. temperature, concentration of reactants) to obtain high grafting density. Functionalisation of nanotubes was confirmed qualitatively (by Raman spectroscopy and transmission electron microscopy) and quantitatively (by thermogravimetric and elemental analysis).

5.1.2 Article Details

This study was published in Polymer, volume 50, issue 25, pages 5901-5908 on 27 November 2009, entitled ‘Effect of radical grafting of tetramethylpentadecane and polypropylene on carbon nanotubes' dispersibility in various solvents and polypropylene matrix’. This piece of work was carried out in association with a post-doctorate researcher (Gholamali Farzi) based on the idea and strategy we established on in chapter 2.

5.2 Effect of radical grafting of tetramethylpentadecane and polypropylene on carbon nanotubes' dispersibility in various solvents and polypropylene matrix

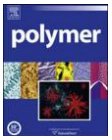

Gholamali Farzi [a,b,c], Sohaib Akbar [a,b,c], Emmanuel Beyou [a,b,c], Philippe Cassagnau [a,b,c]

[a] Université de Lyon, Lyon F-69003, France

[b] Université de Lyon 1, F-69003 Villeurbanne, France

[c] CNRS UMR5223, Ingénierie des Matériaux Polyméres, Laboratoire des Matériaux Polyméres et Biomatériaux, F-69622 Villeurbanne, France

5.2.1 Abstract

Multiwalled carbon nanotubes (MWCNTs) have been functionalized by tetramethylpentadecane (TMP), 1-dodecanethiol (DT) and polypropylene (PP) through radical addition onto MWCNTs' surface using dicumyl peroxide as hydrogen abstractor. Surface functionalized MWCNTs were characterized by Raman, IR spectroscopy, elementary analysis (EA) and thermogravimetric analysis (TGA). We studied the effect of temperature, peroxide concentration and solvent on TMP grafting densities and it was found that this surface treatment lead to a fair solubility in various solvents. TMP-functionalized MWCNTs were also imaged by transmission electronic microscopy showing single long functionalized MWCNTs distinct from the starting pristine bundles. For the first time, PP was then grafted onto MWCNTs through a radical grafting reaction. However, scanning electronic microscopy images of PP-functionalized MWCNTs/PP composites did not show a significant improvement in MWCNTs dispersion within the PP matrix.

5.2.2 Introduction

Polymer nanocomposites containing carbon nanotubes (CNTs) have attracted much attention due to the excellent mechanical, electrical and thermal properties of CNTs

[1,2,3]. Simple melt compounding is often difficult to achieve because CNTs tend to form agglomerates during processing of composites. Indeed, carbon nanotubes form clusters as very long bundles due to the high surface energy and the stabilization by numerous of π–π electron interactions among the tubes. Chemical modification of the CNTs' surface [4,5,6] and in situ polymerisation [7,8] have been used to achieve optimal enhancement in the properties of CNT/polymer composites. The use of "grafting to" [9,10,11,12] and "grafting from" [9,13,14,15,16] approaches, leading to chemical linkage between polymer and the surface of CNTs, have been also explored to improve the interfacial interaction between CNTs and polymer matrix. Polypropylene (PP) is one of the most widely used commercial polymer due to the excellent combination of mechanical resistance, chemical stability and excellent moisture barrier properties [17]. Although physical blending with CNTs is an economic way to modify polypropylene performance, compatibilizing agents are necessary for creating strong interface between filler particles and the polymer phase. Maleic anhydride grafted polypropylene (MA-*g*-PP) is often used as a compatibilizer which can improve the PP/CNTs composite properties by strong hydrogen bonding between hydroxyl groups located on the acidic-treated CNTs surface and anhydride groups of MA-g-PP [18,19].

A more promising way to disperse CNTs in polyolefins is the in situ polymerisation approach because homogenous metallocene catalysts are soluble in hydrocarbons. First, the co-catalyst methylaluminoxane (MAO) is anchored on the CNT surface through covalent bonding to –COOH or –OH groups which are inherent to partially oxidized CNTs. Then, the metallocene catalyst and the monomer are added yielding polyolefin chains attached directly to CNTs [17,20,21,22]. Another strategy for enhancing compatibility between nanotubes and polyolefins consists in the sidewall CNT functionalization with short alkyl chains [23,24]. This method involves thermal decomposition of an alkyl peroxide (radical initiator) at 100 °C in toluene providing alkyl radicals which can react with unsaturated bonds located on the CNT surface. Peroxides are also used as hydrogen abstractors to chemically modify polyolefins in the molten state [25,26]. In this latter case, the radicals formed in the decomposition process must be able to abstract hydrogen atoms from polyolefin and to form radical

centres that can react with unsaturated systems. This grafting reaction has been previously described [27,28,29] with a model compound approach involving a radical grafting reaction between peroxide-derived alkoxyl radicals, a set of low molecular weight alkanes and a monomer [27,28] or multiwall carbon nanotubes (MWCNTs) [29]. Herein, we use the radical mechanism for attaching tetramethylpentadecane (TMP) as model for PP, dodecanethiol (DT) and PP to multiwall carbon nanotubes (MWCNTs). Experiments reported here involve thermal decomposition of dicumyl peroxide (DCP), used as hydrogen abstractor, at temperatures above 130 °C.

The extent of grafting has been evaluated by thermogravimetric analysis, elemental analysis and scanning electronic microscopy (SEM) observations. We studied solubility behaviour of the formed TMP- and DT-grafted-MWCNTs in various solvents according to their grafting densities. In addition, PP coated MWCNTs were dispersed in a molten PP matrix before imaging by SEM.

5.2.3 Experimental

5.2.3.1 Materials

MWCNTs (Graphistrength™ C100, manufacturing: catalytic chemical vapour deposition (CCVD), average outer diameter: 10–15 nm, length: 0.1–10 µm, average number of walls: 5–15, C contents: 91%.) were kindly supplied by ARKEMA.
The low molecular weight hydrocarbon substrate, used as model for polypropylene, was 2,6,10,14-tetramethylpentadecane (TMP, 99%, Sigma–Aldrich-France). Dodecanethiol (DT, 99%, Acros) was used as received. A commercial grade of polypropylene (PPH7060) supplied by Atofina was used as the polymer matrix. Dicumyl peroxide (99%, Sigma–Aldrich-France) and all other solvents (dimethylformamide (DMF), dichlorobenzene (DCB)) were used without any further purification so as to fit the industrial conditions required in the melt processing.

5.2.3.2 Surface activation of MWCNTs

In this study, MWCNTs were oxidized in air at 450 °C for 1 h. Air oxidized MWCNTs are used throughout this study and referred as pristine (p-MWCNTs).

5.2.3.3 Decomposition of DCP in the presence of p-MWCNTs and hydrocarbon substrates

The thermolysis of dicumyl peroxide (DCP) in hydrocarbon substrates was performed in a glass reactor. For experiments conducted in solution, DCP (0.12 g/0.44 mmol) was first mixed in a mixture of p-MWCNTs (50 mg), TMP (1 g/3.73 mmol) and DMF (or DCB; 10 mL) and then sonicated for 15 min. Afterwards, the suspension was degassed by 3 freeze–pump–thaws, and then it was heated up to 160 °C for 6 h under stirring. The grafted MWCNTs were collected by centrifugation (11 K rpm, 20 min) and subsequent filtration. A similar procedure was employed to graft dodecanethiol and PP while maintaining the same molar ratio and using DCB as solvent for PP grafting reaction.

5.2.3.4 Recovery of free and tethered molecules/PP chains

The free molecules (TMP and DT) and PP chains were isolated from the grafted ones by exhaustive cleaning of the suspension by dialysis and Soxhlet extraction, respectively. In a typical process for the extraction of TMP (or DT), 30 mL of the MWCNTs' suspension was introduced into a cellulose membrane (Spectra/Por, MW cut-off, 1000 by Spectrum Medical Industries, Inc.) and repeatedly dialyzed against DCB (or DMF for DT) until no residual TMP (or DT) could be detected in the recovered solution (determined gravimetrically). Then, the alkane-grafted MWCNTs suspension was dried at 80 °C to evaporate the solvent prior to characterization.

PP is not soluble in any solvent at ambient temperature so it was necessary to use soxhlet extractor to recover free PP and tethered PP in DCB at elevated temperatures. In a typical procedure, 1 g of the solid fraction filtered from MWCNTs' suspension in DCB (after reaction) was put in a cellulose thimble (Macherey–Nagel

GMBH & Co) and placed into the Soxhlet extractor refluxed with DCB at 140 °C for 4 days. The non-soluble PP-*g*-MWCNTs were collected from thimble and dried at 90 °C under vacuum.

5.2.3.5 PP/PP-g-MWCNTs nanocomposites processing

For processing, Haake Polylab Rheomixer fitted with "Rheomix 600" internal mixer with two rotors running in a contra-rotating way was used. Each batch was of ~ 50 cm^3 (44 ± 1 g) to fill the mixing chamber so as to receive the excellent shearing action to ensure the proven finest mixing. The amount of nanofiller in the final composites has been fixed to 3 wt%. Processing temperature was 200 °C and rotors rpm were 50.

5.2.4 Characterisation

Gas chromatography–mass spectrometry (GC–MS) was performed with an Agilent 6890 series GC system equipped with a HP-5 ms (5%-phenyl)-methylpolysiloxane, ref. 19091S-433. The injector was at 250 °C and the temperature programme followed was: 50–310 °C at 20 °C/min. Injection and detection by MS was carried out at 280 °C.

Raman spectra were obtained by using a Raman spectrometer (RM1000, Renishaw, Wotton under Edge, U.K.). The sample was excited with Argon Laser at 514.5 nm.
FTIR spectra were recorded on a Perkin–Elmer spectrometer 2000 using powder-pressed KBr pellets. Specimens for the measurements were prepared by mixing 2 mg of the sample powder with 100 mg of KBr and pressing the mixture into pellets. FTIR spectra were obtained at a resolution of 2.0 cm^{-1} at room temperature in the range of 4000 to 400 cm^{-1} wavenumber and averaged over 16 scans.

Thermogravimetric analysis (TGA) were performed with a DuPont Instruments TGA 2950 thermobalance, controlled by a TC10A microprocessor. Samples were heated at 20 °C/min under a nitrogen flow (100 mL/min).

Elemental analysis (EA) was carried out (Analyzer: LECO SC144, Service central d'analyse du CNRS, Vernaison, France) to determine carbon and hydrogen contents. Transmission electron microscopy (TEM) was carried out with a Philips CM-120 microscope (Philips Consumer Electronics BV, Eindhoven, The Netherlands) operated at 80 keV. Scanning electron microscopy (SEM) was performed with a Hitachi S800 microscope operated at 15 KV.

Solubility was determined gravimetrically. In a typical experiment, saturated solutions of alkane-*g*-MWCNTs were prepared by sonication in vials. Sonication was done using S 40 H Elmasonic by Elma (Singem, Germany) for 30 min. Water bath temperature therein raised maximum to 35 °C. Vials were kept free standing over one month at room temperature and then the upper half aliquot part was carefully taken out with a syringe and heated to remove solvent under vacuum. All the weighting was carried out using an analytical balance with a sensitivity of 0.1 mg.

5.2.5 Results and discussion

5.2.5.1 Free radical grafting of TMP, DT and PP onto MWCNTs

We resorted to 2,6,10,14-tetramethylpentadecane (TMP, $C_{19}H_{40}$) as model for polypropylene. Indeed, high boiling points of long chain alkanes permit study under high temperature conditions, typically over 150 °C. It also gives clues about low viscosity at 150 °C; on top of that the formed products in the grafting experiment can hence be analysed more easily than in the polymer melt. Thermolysis of dicumyl peroxide initiator performed in TMP and in presence of MWCNTs is depicted in Fig. 5-1.

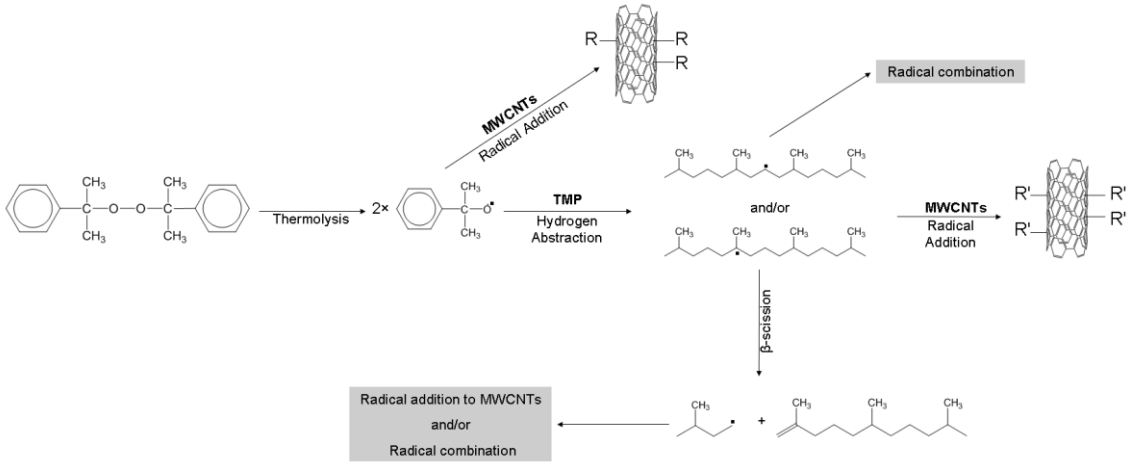

Figure 5-1: Reaction scheme for the addition of TMP onto CNT in the presence of DCP. (NB: Hydrogen abstraction from PP is also possible at other places where steric hindrance does not have a strong effect.)

Experiments as reported here involved decomposition of dicumyl peroxide (DCP) whose thermal decomposition is carried out in a range of temperatures close to the ones expected during reactive extrusion of polypropylene typically few minutes at 150–200 °C. As shown in Fig. 5-1, the formed peroxide radicals have a high tendency to react readily with unsaturated systems and are also prone to hydrogen abstraction from hydrocarbon substrates [30]. In this latter case, it is expected that the active species generated onto the hydrocarbon backbone react with unsaturated bonds located on the MWCNTs surface. The main drawback of free radical grafting is low selectivity of radical centres, especially at high temperature (150–200 °C for the extrusion of PP) causing side reactions such as chain scission for PP derivatives (Fig. 5-1) [30,31]. However, this method is a simple way to directly incorporate organic moieties onto the CNTs' surface leading to TMP and PP grafted MWCNTs. Dodecanethiol has been also grafted onto CNTs using the same procedure. The thiol family of compounds is widely used for controlling molar mass in free radical polymerizations via a chain transfer process. The chain transfer process displays two contiguous steps: transfer of the thiyl hydrogen to the growing polymer chain followed by re-initiation, whereby a thiyl radical adds to a monomeric double bond. In the presence of MWCNTs, thiyl radicals are expected to react by radical addition onto sp^2 carbon of the MWCNTs. First, according to our previous results [29] based on a study of the radical grafting of polyethylene derivatives onto MWCNTs, we

investigated MWCNTs' sidewall functionalization by TMP, DT and PP in the presence of 1 wt% DCP at 160 °C. DMF and DCB were used as solvents. For PP-based experiments, only DCB was used, as suitable hot solvent for PP. It is noteworthy that the unreacted molecules/polymer chains are removed from the grafted ones by dialysis/soxhlet extraction as mentioned in the experimental part. The efficient MWCNTs' sidewall functionalization by TMP, DT and PP has been confirmed with the aid of Raman and FTIR vibrational spectra.

Raman spectra of p-MWCNTs and alkane-based derivatives-*g*-MWCNTs (Fig. 5-2) show two strong bands around 1340 cm^{-1} (D band) and 1590 cm^{-1} (G band). D-band is attributed to disorder or sp^3-hydridized carbons in the hexagonal framework of the nanotubes walls (typical sign for defective graphitic structures) and G-band is a characteristic feature of the graphitic layers and corresponds to the tangential vibration of the carbon atoms [29,32,33].

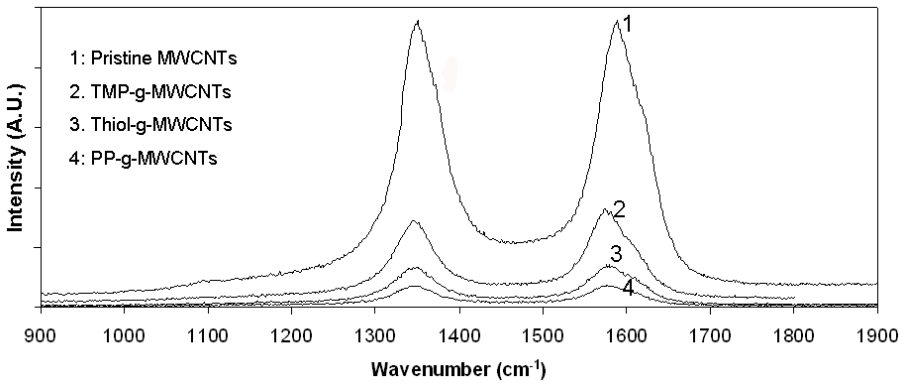

Figure 5-2: Raman spectra of pristine and TMP-, DT- and PP-*g*-MWCNTs.

The ratio in intensities between the D band and G band is a good indicator of the changes in chemistry of CNTs. We can observe a relatively low intensity of the D band relative to G band ($I_D/I_G < 1$) for all the alkane-based derivatives-*g*-MWCNT samples (Fig. 5-2, Table 5-1) in comparison with that of p-MWCNT (i.e. $I_D/I_G \approx 1$, Fig. 5-2, Table 5-1) whatever are the grafting experimental conditions. This behaviour

could be interpreted as an indication of the increase in the number of sp^3 hybridized carbon atoms after polymer functionalization.

Table 5-1: Band intensity ratios (I_D/I_G) of different samples in Raman spectra.

Sample	I_D/I_G
Pristine MWCNTs	0.99
TMP-*g*-MWCNTs	0.93
DT-*g*-MWCNTs	0.95
PP-*g*-MWCNTs	0.86

TMP-*g*-MWCNTs and PP-*g*-MWCNTs were additionally analysed by FTIR spectroscopy (Fig. 5-3). The emergence of nearly identical series of vibrational bands for both grafted and non-grafted species suggest the successful grafting of TMP and PP onto MWCNTs. Then, we found it interesting to see whether the temperature, the peroxide concentration and the solvent could modify the TMP grafting density and the solubility of the resulting products.

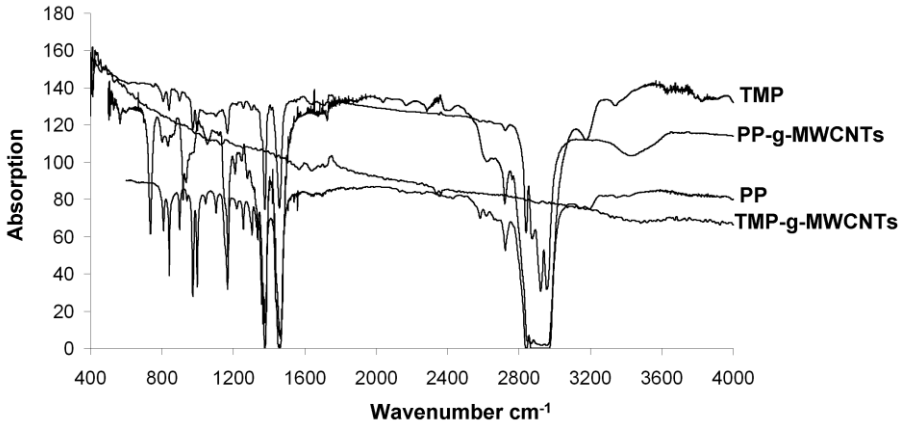

Figure 5-3: FTIR spectra of TMP- and PP-*g*-MWCNTs, along with pure TMP and PP spectra for reference.

5.2.5.2 Effect of temperature, DCP concentration and solvent on TMP grafting density

In order to increase the understanding of the cumyloxyl radicals behaviour, experiments from 1 to 6 (Table 5-2) correspond to the ones performed with TMP and 1 wt% DCP relative to TMP in DMF as solvent at temperatures varying from 130 °C to

180 °C. The TGA traces for both the starting pure TMP and the TMP-grafted nanotubes are shown in Fig. 5-4. Pure TMP sample completely decomposes in the temperature range between 180 and 250 °C. For TMP-grafted nanotubes, one decomposition event is clearly visible at ca. 450 °C attributed to the loss of TMP (Fig. 5-4). In Fig. 5-4, we estimate the weight of grafted TMP to be around 8%. The TMP weight loss increases from 3.2% to 8.9% by increasing the reaction temperature from 130 °C to 160 °C (experiments 1–6, Table 5-2). The corresponding grafting densities can be calculated using the theoretical specific surface area (SSA) of MWCNTs defined as the following equation [34]:

$$\mathrm{SSA}\left(\mathrm{m}^2\cdot\mathrm{g}^{-1}\right) = \frac{1315 * d_e}{n d_e - 0.68\left[\sum_{i=1}^{n-1} i\right]}$$

where d_e is the external diameter in nm and n is the number of shells.

Table 5-2: Effect of temperature on grafting density for the preparation of TMP-*g*-MWCNTs (DCP conc.:1 wt%; DMF as solvent).

Experiment	Temperature (°C)	TGA (wt loss %)	Grafting density[a] (mg m^{-2})
1	130	3.2	0.15
2	140	3.0	0.14
3	150	7.8	0.38
4	160	8.9	0.43
5	170	6.3	0.30
6	180	5.5	0.26

[a] Based on calculations assuming a specific surface area of 225 $m^2\ g^{-1}$ for MWCNTs.

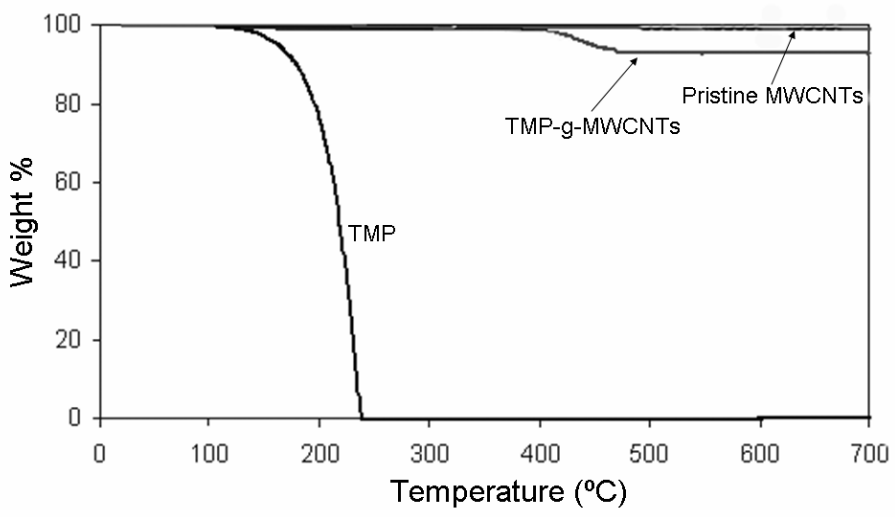

Figure 5-4: TGA data (under N_2) for TMP-*g*-MWCNTs (experiment 3, Table 5-2) and the corresponding references of p-MWCNTs and pure TMP.

For our Graphistrength™ C100 MWCNTs, we obtain an average SSA of 225 $m^2 g^{-1}$. The calculated grafting densities are varying from 0.15 mg m^{-2} to 0.43 mg m^{-2} (Table 5-2). The grafting density decreases from 0.43 mg m^{-2} to 0.26 mg m^{-2} for reaction temperatures above 160 °C (i.e. 170 °C and 180 °C, Table 5-2), suggesting that shorter half time life of DCP initiator favours competitive reactions which might lead to combination reactions.

Peroxide concentration is also a key parameter in a radical grafting reaction so experiments with various DCP content (1 wt%–18 wt%, Table 5-3) were conducted at 160 °C (optimal temperature for TMP grafting density). Experiments from 1 to 9 (Table 5-3) show that the TMP weight loss determined by TGA slightly increases from 8% to 15% by increasing initiator concentration from 1 wt% to 12 wt%. Comparable weight losses have been recently reported by Koval'chuck [23] for undecanyl-*g*-MWCNTs but the current functionalization is feasible for a wider compound range. The corresponding grafting densities increase from 0.39 mg m^{-2} to 0.78 mg m^{-2} respectively (Table 5-3).

Table 5-3: Effect of DCP concentration on grafting density for the preparation of TMP-*g*-MWCNTs (160 °C, with DMF as solvent).

Experiment	DCP (wt% of TMP)	EA (H content, %)	EA (C content, %)	Percent grafting (TGA weight loss)	Grafting density[a] (mg m^{-2})	
					EA	TGA
1	1	–	–	8	–	0.39
2	1.5	3.25	88.75	8.9	0.52	0.43
3	3	3.55	88.44	12	0.62	0.61
4	4.5	3.71	88.3	13	0.67	0.66
5	6	3.75	88.26	13	0.69	0.66
6	9	3.78	88.21	13.5	0.70	0.69
7	12	3.84	88.16	15	0.72	0.78
8	15	3.79	88.20	13	0.70	0.66
9	18	3.31	88.70	11	0.54	0.55

EA of pristine MWCNTs shows: carbon 90%, hydrogen 1.4%.
a Based on calculations assuming a specific surface area of 225 m2 g–1 for MWCNTs.

Elemental analysis (EA) is also an indicator of degree of grafting and a good agreement between grafting densities calculated from EA and TGA analysis was obtained (e.g. 0.72 mg m^{-2} and 0.78 mg m^{-2} respectively, experiment 7, Table 5-3). For peroxide concentration higher than 12 wt%, the grafting density decreases from 0.78 mg m^{-2} to 0.55 mg m^{-2} upon increasing DCP concentration up to 18 wt% (Table

5-3). It suggests that the presence of higher concentration of radicals changes the reaction kinetics, possibly leading to combination reactions (Fig. 5-1). We can also speculate on the various radicals that can add to MWCNTs. However, according to the literature [19,35], the efficiency of addition of carbon radicals to MWCNTs is expected to be greater than that of oxygen radicals.

The optimal DCP concentration for the TMP radical grafting reaction is 12 wt% at 160 °C. However, the following experiments involve a usual low concentration of DCP (1.5 wt%) in order to prevent PP from degradation [36,37]. In order to check the influence of solvent onto TMP grafting density, experiments were therefore conducted at 160 °C with 1.5 wt% DCP in two kinds of solvents: DMF and DCB, which is a good solvent for PP at high temperatures. The initial visual aspect of the MWCNTs dispersions in DMF and in DCB is somewhat different. The dispersion of MWCNTs is totally unstable in DMF due to poor hydrogen bonding ability whereas MWCNTs take some time before settling down in DCB solution showing an affinity (though very low) with this solvent. After the radical grafting reaction in these solvent, it is observed that DCB ensures better TMP grafting density than DMF (0.75 mg m^{-2} and 0.43 mg m^{-2} from TGA respectively, Table 5-4) which may be attributed to the better miscibility of TMP with DCB. Using TMP as solvent, the grafting density increases to 0.92 mg m^{-2} suggesting a poorer TMP-based radical attack onto the sp^2 carbon of the MWCNTs in dilute media.

Table 5-4: Influence of solvent on TMP grafting density onto MWCNTs (DCP conc.:1.5 wt%).

Solvent	EA (H content, %)	TGA (wt loss %)	Grafting density (mg m^{-2})	
			EA	TGA
DMF	3.25	8.9	0.52	0.43
DCB	3.81	14.4	0.71	0.75
TMP (“bulk” = “Master-batch”)	4.15	17.2	0.83	0.92

In the presence of a thiol (i.e. DT), a hydrogen transfer process is required between cumyloxyl radicals and/or radicals located onto the MWCNTs and the thiol derivative. Then, the generated thiyl radicals can react with unsaturated compounds, such as MWCNTs, leading to DT-*g*-MWCNTs. The experiment was conducted at 160 °C in DMF with 1.5 wt% DCP and a grafting density of 0.20 mg m^{-2} was calculated

from TGA. This value is approximately lowered by a factor 2 in comparison with the TMP grafting density (e.g. 0.43 mg m^{-2}, Table 5-4) suggesting that the efficiency of addition of carbon radicals to MWCNTs is greater than that of sulfur radicals, which is well-known for C_{60} [19,35] and a low occurrence of hydrogen transfer reactions between DT and radical species.

It is expected that this functionalization approach will provide convenience and versatility in building up PP architecture on CNTs. For the first time, PP has been grafted onto MWCNTs through this radical grafting reaction, carried out under similar experimental conditions (1.5 wt% DCP, 160 °C) and using 1,2-dichlorobenzene (DCB) as solvent able to solubilize PP partially at elevated temperature. The corresponding PP-grafted nanotubes were analysed by TGA after a purification by soxhlet extraction in DCB. However, it was not possible to obtain reproductible results with weight losses varying from 50% to 80% for the above-mentioned experiment. This behaviour may be attributed to the purification procedure which does not permit to remove all the free PP chains. One may also speculate on the degradation behaviour of PP through the well-known β-scission reaction occurring in the presence of radical species therefore we were not able to give a PP grafting density. Nevertheless, the microstructure of the corresponding nanocomposites in PP matrix is discussed ahead in Section 6.2.5.4.

5.2.5.3 Morphology and solubility

As an additional evidence for the functionalization of TMP and PP onto MWCNTs, TEM pictures of the sonicated p-MWCNTs, TMP-*g*-MWCNTs and PP-*g*-MWCNTs are shown in Fig. 5-6.

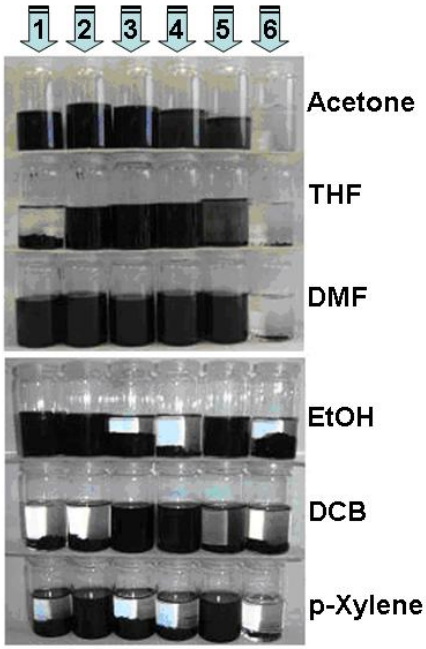

Figure 5-5: Solubility behaviour of (1) DT-*g*-MWCNTs, (2) DCP-*g*-MWCNTs, (3) TMP-*g*-MWCNTs (0.92 mg m^{-2}), (4) TMP-*g*-MWCNTs (0.75 mg m^{-2}), (5) TMP-*g*-MWCNTs (0.43 mg m^{-2}), (6) MWCNTs in various solvents.

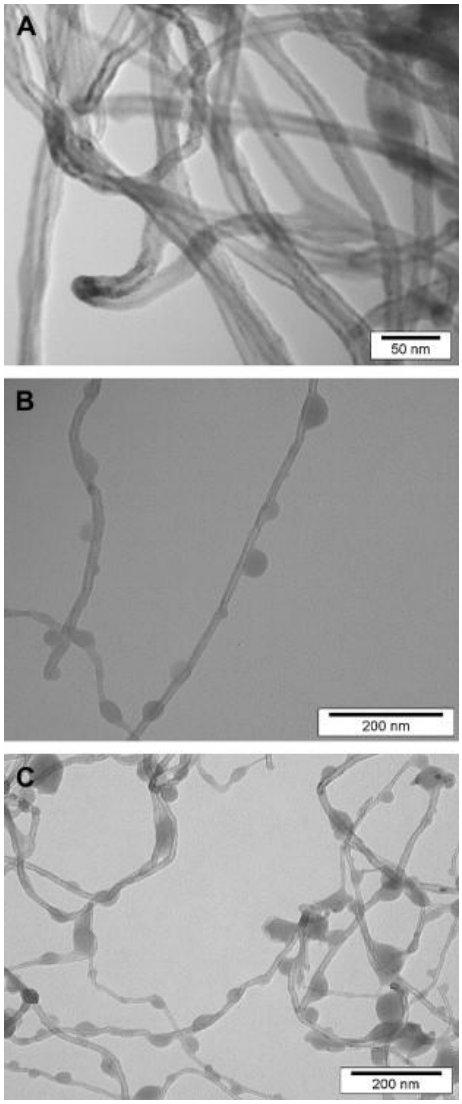

Figure 5-6: TEM micrographs of (A) bare MWCNTs, (B) TMP-*g*-MWCNTs, (C) PP-*g*-MWCNTs.

TEM analysis of TMP- and PP-*g*-MWCNTs exhibit predominant individual CNTs completely separated from the starting bundle. It demonstrates that the functionalization leads to better debundling of MWCNTs. Moreover, the surface of the p-MWCNTs seems to be smooth without any extra phase adhering to them (Fig. 5-6a) whereas the surface of TMP- and PP-*g*-MWCNTs is rough (Fig. 5-6b and c). Images reveal the presence of bumps on the sidewalls of the tubes. According to the literature [29,32,38,39,40], this morphology can be attributed to alkyl moieties attached to the tube wall.

Organic solubility can be achieved by appending DT and TMP alkyl chains onto the MWCNTs and the morphology might better be understood considering the behaviour of raw- and functionalized MWCNTs in various solvents. The visual aspect of the dispersions is significantly different depending on the solvent and covalent functionalization.

Solutions were prepared by adding 20 mg of the samples into the same amount of various solvent followed by sonication for 15 min at 20 W and then leaving them free standing for one month. Room temperature solubility in various solvent were determined for TMP-*g*-MWCNTs with grafting densities varying from 0.43 mg m^{-2} to 0.92 mg m^{-2} and DT-*g*-MWCNTs with a grafting density of 0.20 mg m^{-2} (Table 5-5). While raw MWCNTs form aggregates/bundles and settled down in most solvents, MWCNTs covered with TMP chains form stable colloidal suspensions in Acetone, THF, DMF and DCB (Fig. 5-5).

Table 5-5: Room temperature solubilities (in mg. mL^{-1}) of TMP- and DT-*g*-MWCNTs in various solvents at given grafting densities.

Solvent	DT-*g*-MWCNTs 0.20 mg m^{-2}	TMP-*g*-MWCNTs 0.92 mg m^{-2}	TMP-*g*-MWCNTs 0.75 mg m^{-2}	TMP-*g*-MWCNTs 0.43 mg m^{-2}
Acetone	5.4	23.2	13.1	9.2
THF	N/D	20.9	13.1	8.3
DMF	5.1	8.7	6.6	6.3
ETOH	26.5	N/D	N/D	4.8
DCB	N/D	18.2	12.2	5.8
Xylene	N/D	N/D	N/D	18.8

N/D: not determinable.

N.B. Pristine MWCNTS are not soluble in any of these solvents.

These suspensions are very little disturbed with time indicating that the long alkane organic groups covalently linked onto the sidewalls of MWCNTs ensure fine dispersion. In addition, contrary to TMP-*g*-MWCNTs, DT-*g*-MWCNTs give stable suspensions in EtOH suggesting that DT-*g*-MWCNTs suspension contains less remaining nanotubes aggregates in hydrophilic solvent. In this latter case, the thiyl grafting groups may slightly increase the polarity of the MWCNTs. The unstable DT-*g*-MWCNTs suspension in both THF and DCB solvents may be attributed to the lower DT grafting density in comparison with the TMP one (e.g. 0.20 mg m^{-2} and

0.43 mg m^{-2}, respectively) while various accounts suggest that surface tension [29,41,42] and dielectric constant [29,43] of the solvent are key parameters to make stable suspensions. The reported solubilities in Table 5-5 highly depend on degree of functionalization and solvent. For TMP grafted MWCNTs, the best solubilities are obtained for samples prepared from a radical grafting reaction in bulk. In the latter case, we assume that the higher TMP grafting density (e.g. 0.92 mg m^{-2}, Table 5-5) explains this result. As a general rule, in most solvent the solubility of TMP-*g*-MWCNTs increases with increasing the TMP grafting density. These solubility values are higher than those of pentadecane-*g*-MWCNTs [29] and octadecylamine modified MWCNTs [43] in polar solvent (e.g. Acetone, DMF and THF). For example, the high grafting density of TMP onto MWCNTs (e.g. 0.92 mg m^{-2}) permit to obtain solubilities of 8.7, 23.2 and 20.9 mg mL^{-1} in DMF, Acetone and THF, respectively while pentadecane-*g*-MWCNTs display a solubility of 1.1 mg mL^{-1} in Acetone and are not soluble in THF [29]. Surprisingly, we found unstable TMP-*g*-MWCNTs dispersions in xylene when the TMP grafting density is higher than 0.43 mg m^{-2}. In addition, the solubility of the DT-*g*-MWCNTs is lower than that of TMP-*g*-MWCNTs in all solvent except in ethanol, as described above.

5.2.5.4 PP/PP-*g*-MWCNTs nanocomposites

PP coated MWCNTs have been dispersed within a commercially available PP matrix using a contra-rotating Haake Rheomixer. The amount of nanofiller in the final composites has been fixed to 3 wt%. Morphological analysis is very important for the evaluation of dispersion and it was examined by using scanning electron microscopy (SEM). For a simple melt blend of PP with untreated MWCNTs, SEM images of the resulting material only show clusters of a few tens micrometers of diameter (Fig. 5-7) evidencing a poor interfacial adhesion in the material, as reported by Lee [19] for untreated MWCNT/PP composites MWCNTs containing of 2 wt%.

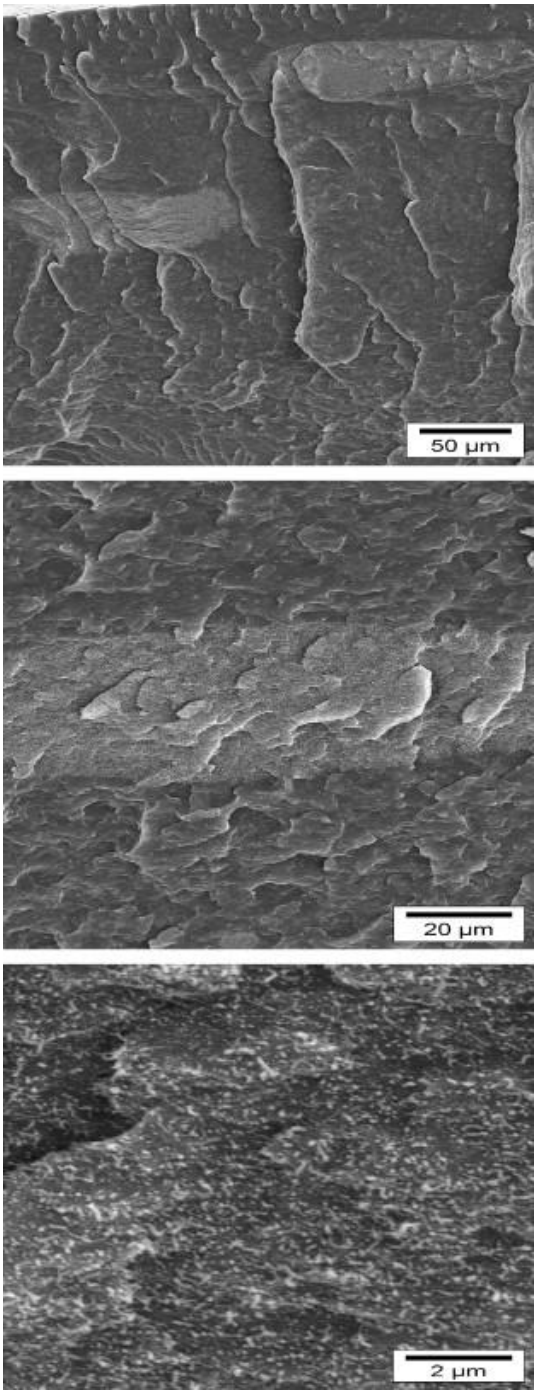

Figure 5-7: SEM micrographs of PP/MWCNTs composites with MWCNTs loading of 3 wt%.

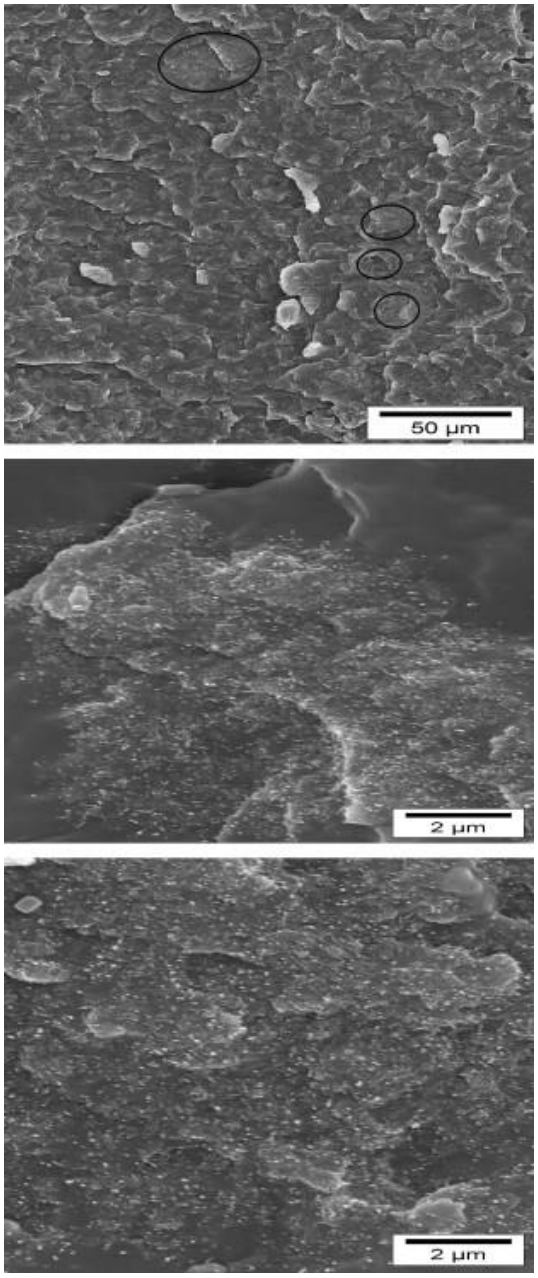

Figure 5-8: SEM micrographs of PP/PP-g-MWCNT composites with MWCNTs loading of 3 wt%.

In some areas, the concentration of neat-MWCNTs is high and the nanotubes are entangled together whereas none of neat-MWCNTs can be found in other areas. The interfacial bonding at the interface PP/MWCNTs composite is expected to prevent

MWCNTs from agglomeration. SEM images of the PP/PP-*g*-MWCNTs composites MWCNTs containing of 3 wt% (Fig. 5-8) demonstrate that there are still some areas where PP-*g*-MWCNTs are not found which is obviously connected with improper filler distribution. Nevertheless, sizes of the aggregates are slightly reduced in comparison with those of untreated MWCNT/PP composites indicating that the agglomerates have been partly destroyed through the functionalization. It is then clear from these results that the grafting of PP onto MWCNTs provides a low steric barrier against the strong intermolecular Van der Waals interactions among nanotubes within the PP matrix.

5.2.6 Conclusion

MWCNTs were successfully functionalized through a simple radical grafting approach based on the use of dicumyl peroxide as an alkane hydrogen abstractor. Raman, FTIR and TGA data attested for successful functionalization of MWCNTs by TMP and DT. For experiments conducted in DMF at 160 °C with 1.5 wt% DCP, TMP and DT grafting densities were as high as 0.43 and 0.20 mg/m^2, respectively. The lower grafting density obtained for DT may be attributed to the lower efficiency of addition of sulfur radicals to MWCNTs. Moreover, TEM images showed the presence of individual MWCNTs with a characteristic rough surface. TMP grafted MWCNTs exhibited dispersibility in various organic solvents with solubilities varying from 4.8 mg/mL in ethanol to 23.2 mg/mL in acetone. SEM images of the PP-*g*-MWCNTs nanocomposites with filler loadings of 3 wt% in PP matrix did not show a significant improvement in MWCNTs dispersion within the PP matrix although sizes of the aggregates were slightly reduced. Future work will focus on the influence of melt processing conditions (shear/stress, mixing time…) on PP-*g*-MWCNTs dispersibility in order to obtain deep insight into the microstructural features.

5.2.7 References

1 C.P. Poole and F.J. Owens, Introduction to nanotechnology, Wiley-Interscience, Weinheim (2003).

2 M.O. Connell, Carbon nanotubes: properties and applications, CRC Press (2006).

3 Y. Gogotsi, Carbon nanomaterials, CRC Press (2006).

4 J. Liu, A.G. Rinzler, H. Dai, J.H. Hafner, R.K. Bradley and P.J. Boul et al., Science 280 (1998), pp. 1253–1256.

5 C. Wang, Z. Guo, S. Fu, W. Wu and D. Zhu, Prog Polym Sci 29 (11) (2004), pp. 1079–1141.

6 M. Moniruzzaman and K.I. Winey, Macromolecules 39 (16) (2006), pp. 5194–5205.

7 C.G. Zhao, G.J. Hu, R. Justice, D.W. Schaefer, S. Zhang and C.C. Han, Polymer 46 (14) (2005), pp. 5125–5132.

8 M. Trujillo, M.L. Arnal, A.J. Muller, E. Laredo, S. Bredeau and D. Bonduel et al., Macromolecules 40 (17) (2007), pp. 6268–6276.

9 S. Qin, D. Qin, W.T. Ford, D.E. Resasco and J.E. Herrera, Macromolecules 37 (3) (2004), pp. 752–757.

10 Y.P. Sun, W.J. Huang, Y. Lin, K.F. Fu, A. Kitaygorodskiy and L.A. Riddle et al., Chem Mater 13 (9) (2001), pp. 2864–2869.

11 W.J. Huang, Y. Lin, S. Taylor, J. Gaillard, A.M. Rao and Y.P. Sun, Nano Lett 2 (3) (2002), pp. 231–234.

12 Y. Lin, B. Zhou, K.A.S. Fernando, P. Liu, L.F. Allard and Y.P. Sun, Macromolecules 36 (19) (2003), pp. 7199–7204.

13 M.S.P. Shaffer and K. Koziol, Chem Commun (2002), pp. 2074–2075.

14 H. Kong, C. Gao and D.Y. Yan, J Mater Chem 14 (9) (2004), pp. 1401–1405.

15 C. Gao, S. Muthukrishnan, W.W. Li, J.Y. Yuan, Y.Y. Xu and A.H.E. Muller, Macromolecules 40 (6) (2007), pp. 1803–1815.

16 H. Kong, C. Gao and D.Y. Yan, J Am Chem Soc 126 (2) (2004), pp. 412–413.

17 W. Kaminsky, Macromol Chem Phys 209 (5) (2008), pp. 459–466.

18 Y. Wang, J. Wu and F. Wei, Carbon 41 (2003), pp. 2939–2948.

19 S.H. Lee, E. Cho, S.H. Jeon and J.R. Youn, Carbon 45 (2007), pp. 2810–2822.

20 D. Bonduel, M. Mainil, M. Alexandre, F. Monteverde and P. Dubois, Chem Commun (2005), pp. 781–783.

21 S. Park, S.W. Yoon, K.B. Lee, D.J. Kim, Y.H. Jung and Y. Do et al., Macromol Rapid Commun 27 (1) (2006), pp. 47–50.

22 A.A. Koval'chuk, V.G. Shevchenko, A.N. Shchegolikhin, P.M. Nedorezova, A.N. Klyamkina and A.M. Aladyshev, Macromolecules 41 (9) (2008), pp. 3149–3156.

23 A.A. Koval'chuk, V.G. Shevchenko, A.N. Shchegolikhin, P.M. Nedorezova, A.N. Klyamkina and A.M. Aladyshev, Macromolecules 41 (20) (2008), pp. 7536–7542.

24 P. Umek, J.W. Seo, K. Hernadi, A. Mrzel, P. Pechy and D.D. Mihailovic et al., Chem Mat 15 (25) (2003), pp. 4751–4755.

25 J.J. Robin, C. Boyer, B. Boutevin and C. Loubat, Polymer 49 (21) (2008), pp. 4519–4528.

26 A.H. Hoight, J. Meijer and J. Jelenic, Reactive modifiers for polymers, Al-Malaïka S, London (1997) p. 84, and references therein.

27 T. Badel, E. Beyou, V. Bounor-Legare, P. Chaumont, J.J. Flat and A. Michel, J Polym Sci Part A Polym Chem 45 (22) (2007), pp. 5215–5226.

28 T. Badel, E. Beyou, V. Bounor-Legare, P. Chaumont, J.J. Flat and A. Michel, Macromol Chem Phys 210 (13–14) (2009), pp. 1087–1095.

29 S. Akbar, E. Beyou, P. Cassagnau, P. Chaumont and F. Gholamali, Polymer 50 (12) (2009), pp. 2535–2543.

30 K.E. Russell, Prog Polym Sci 27 (6) (2002), pp. 1007–1038.

31 R. Hettema, J. Van Tol and L.P.B.M. Janssen, Polym Eng Sci 39 (9) (1999), pp. 1628–1641.

32 J.L. Bahr, J. Yang, D.V. Kosnykin, M.J. Bronikowski, R.E. Smalley and J.M. Tour, J Am Chem Soc 123 (27) (2001), pp. 6536–6542.

33 S. Osswald, M. Havel and Y. Gogotsi, J Raman Spectrosc 16 (6) (2007), pp. 728–736

34 A. Peigney, C. Laurent, E. Flahaut, R. Bacsa and A. Rousset, Carbon 39 (4) (2001), pp. 507–514.

35 P.J. Krusic, E. Wasserman, B.A. Parkinson, B. Malone and E.R. Holler, J Am Chem Soc 113 (16) (1991), pp. 6274–6275.

36 M. Ratzsch, M. Arnold, E. Borsig, H. Bucka and N. Reichelt, Prog Polym Sci 27 (7) (2002), pp. 1195–1282.

37 R.R. Bahu, N.K. Singha and K. Nashar, J Appl Polym Sci 113 (3) (2009), pp. 1836–1852.

38 J.L. Hudson, H.H. Jian, A.D. Leonard, J.J. Stephenson and J.M. Tour, Chem Mat 18 (11) (2006), pp. 2766–2770.

39 J.J. Stephenson, A.K. Sadana, A.L. Higginbotham and J.M. Tour, Chem Mat 18 (19) (2006), pp. 4658–4661.

40 A.C. Dyke and J.M. Tour, Nano Lett 3 (9) (2003), pp. 1215–1218.

41 S. Meuer, L. Braun, T. Schilling and R. Zentel, Polymer 50 (1) (2009), pp. 154–160.

42 W. Shuhui and R.A. Shanks, J Appl Polym Sci 93 (3) (2004), pp. 1493–1499.

43 Y. Qin, L. Liu, J. Shi, W. Wu, J. Zhang and Z.-X. Guo et al., Chem Mater 15 (17) (2003), pp. 3256–3260.

Chapter 6

Conclusions & perspective

6.1 Conclusions

In the frame of this study, an original method of preparing polyolefin/nanotubes composites is developed. This convenient method can be employed to graft polyolefin on nanotubes during the process of extrusion.

The most frequent method for preparing polymer nanotubes composites has been mixing nanotubes and polymer in a suitable solvent and to evaporate the solvent to form composite film. But to increase the advantages at its best, one needs: (i) high interfacial area between nanotubes and polymer; and, (ii) strong interfacial interaction. Unfortunately this solvent technique does not help much in achieving these targets; and as a result a nanocomposite having properties much inferior to theoretical expectations are obtained.

In order to obtain higher contact area between nanotubes and polymer, the issue of dispersion needs to be addressed. Uniform dispersion of these nanotubes produces immense internal interfacial area, which is the key to enhancement of properties of interest. On the other hand modification of nanotubes surface through functionalisation is required for creating an effective interaction with the host matrix and to make nanotubes soluble and dispersible. The idea of grafting PE or PP with the help of peroxide during extrusion is exciting. We envisaged that cumlyoxly radical generated by thermolysis of DCP would abstract hydrogen from polyolefin chains, thus creating polyolefin macroradicals. These macroradicals could add to the unsaturated carbon bonds on the surface of the nanotubes. The upside of this strategy is that radicals have short lifetimes which make the procedure possible in an extruder where the residence time is generally low. On the contrary, the downside is the low selectivity of radicals. During the reacting there exist a competition between radical combination reactions and radical addition reactions.

In first part model compound study we selected pentadecane as our model compound as pentadecane represents the chemical structure of PE. We carried out the reaction in a glass reactor to graft PE onto nanotubes. Different possibilities of

radical combination and addition made the reaction complex. We used GC-MS to follow the reaction pathways and by adjusting temperature and concentration of reactants we acquired the maximum grafting of pentadecane (i.e. 30 wt %). Despite optimising the reaction conditions we observed that the combination of radicals especially pentadecane radicals hinders their addition to nanotubes.

This method provides a simple way to directly incorporate organic moieties onto the nanotubes surface leading to pentadecane-grafted MWCNTs with a grafting density as high as 1.46 mmol/g at 150 °C. At higher temperatures, the grafting density decreases because the β-scission reaction of cumyloxyl radical increases as the temperature increases, leading to the formation of methyl radicals. These latter preferentially react by combination whereas cumyloxyl radicals are more prone to hydrogen abstraction from pentadecane. Pentadecane-grafted MWCNTs have exhibited good dispersibility in various organic solvents and we showed that a grafting density of 1.464 mmol/g leads to a solubility of 19.2 mg/mL in dichlorobenzene.

In order to suppress the combination of radicals we used TEMPO as a radical scavenger in second part of the model compound study. The use of TEMPO proved beneficial as it enhanced the grafting density up to 16 wt % (from 30 to 36 wt %). We used Raman spectroscopy to qualitatively monitor the changes in the chemistry of nanotubes. The extent of grafting was calculated through TGA and verified by elemental analysis.

Solubility analysis showed three states of dispersion: sedimented—as in case of p-MWCNTs in all solvents despite sonication; swollen—as in case of cumyloxyl-g-MWCNTs and penta-g-MWCNTs in chloroform and THF; and dispersed—as in case of penta-g-MWCNTs in DMF, toluene, DCB and xylene. The stability of pentadecane-grafted MWCNTs is disturbed in polar solvents such as acetone, chloroform and THF, however, pretty good solubility in DMF, toluene, DCB and xylene.

After establishing and optimised model for PE grafting we performed this procedure to graft PE onto nanotubes. The results were interesting however the degree of PE grafting remained lower than the model — 22% as compared to 30% in case of pentadecane. End functionalised PE can also be used for PE grafting onto nanotubes. To exploit this option we obtained TEMPO and thiol end functionalised PE. These end functionalised nanotubes were then grafted onto nanotubes in DCB solvent. TEM pictures showed a layer of considerable thickness around the periphery of the nanotubes demonstrating successful functionalisation.

In order to follow the same strategy for nanotubes functionalisation with PP. We selected tetramethylpentadecane as a model compound for PP and we grafted it to nanotubes along the similar way. We successfully grafted 8 wt % of tetramethylpentadecane on to nanotubes which was characterised by IR and Raman spectroscopy. TMP grafted MWCNTs exhibited dispersibility in various organic solvents with solubilities varying from 4.8 mg/mL in ethanol to 23.2 mg/mL in acetone. SEM images of the PP-*g*-MWCNTs nanocomposites with filler loadings of 3 wt% in PP matrix did not show a significant improvement in MWCNTs dispersion within the PP matrix although sizes of the aggregates were slightly reduced.

6.2 Perspective

This method is believed to provide ease in fabricating polyolefin/nanotubes composites for various applications. We have performed this procedure in a glass reactor; however, as we envisaged, this process needs to be carried out in an extruder. Experiments are underway in this connection. Secondly, dispersion is one of the critical factors that control the properties of the composite. We have seen qualitatively through solubility and TEM analysis that nanotubes were not in form of agglomerates after functionalisation. However this needs to be verified quantitatively through rheological measurement. Another interesting idea is to mix PE grafted nanotubes into polymer matrix.

In summary, future study would involve performing this procedure in an extruder. We expect that we will have to optimise this procedure for extrusion where mixing conditions and time limits will be different.

Résumé de thèse en français

Introduction

Les nanotubes de carbone (NTCs) sont des charges particulièrement intéressantes car ils présentent des facteurs de forme (longueur/diamètre) très élevés, jusqu'à 10 000. Ainsi, ils permettent la formation de chemins conducteurs pour des concentrations inférieures à 5 % alors que des valeurs supérieures à 20 % sont nécessaires pour des charges de noir de carbone. Cependant, le développement de ces applications à haute valeur ajoutée a été freiné par les problèmes de mise en œuvre des NTCs (résultant de la difficulté de les disperser dans un milieu polymère) et par la formation d'agrégats de nanotubes en « fagots », ne permettant pas l'obtention de mélanges homogènes. La solution réside dans la fonctionnalisation des nanotubes avec des chaînes polymères afin de réduire l'effet des interactions entre NTCs et d'assurer une meilleure comptabilisation avec le polymère hôte au cours du mélange. Ici, nous nous sommes intéressés à la fonctionnalisation des nanotubes de carbone par des polyoléfines en utilisant une procédure de greffage radicalaire de type « grafting onto ». La réaction radicalaire a été effectuée en présence de peroxyde de dicumyle qui est utilisé en tant qu'abstracteur d'atomes d'hydrogène. L'inconvénient majeur du greffage radicalaire est sa non sélectivité liée à une durée de vie très courte des radicaux ce qui engendre des réactions secondaires de couplage et de β-scission. Dans un premier temps, nous avons donc fait une étude modèle en milieu pentadécane pour faciliter l'analyse du milieu réactionnel par des techniques conventionnelles.

1. Greffage de pentadécane sur nanotubes de carbone

Le système modèle permettant une étude du greffage radicalaire du polyéthylène sur nanotubes de carbone est donc défini par une chaîne hydrocarbonée linéaire (le pentadécane) et des nanotubes de carbone multi-walled en présence d'un amorceur radicalaire (le peroxyde de dicumyle, DCP) (Figure 1).

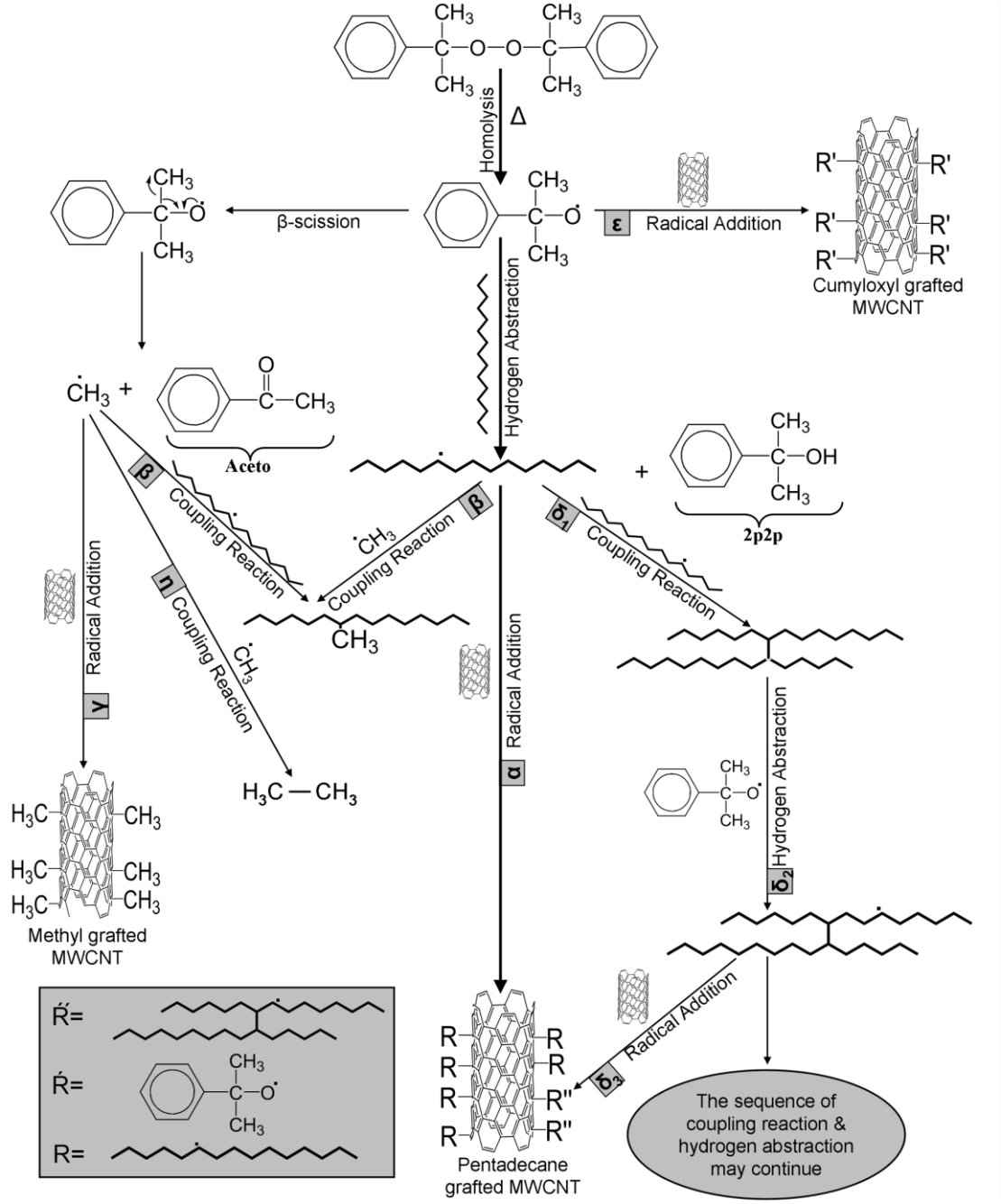

Figure 1 : Principales réactions chimiques impliquées lors du greffage radicalaire du pentadécane sur nanotubes de carbone

La nature chimique des radicaux générés par la décomposition de l'amorceur joue un rôle essentiel dans la sélectivité des réactions radicalaires. Tandis que les radicaux alcoxyles ont tendance à arracher des atomes d'hydrogène, les radicaux centrés sur le carbone comme les radicaux méthyles s'additionnent davantage à une double liaison et/ou se recombinent avec d'autres radicaux. Le DCP a été choisi en fonction des conditions du procédé d'extrusion, où la température est relativement

élevée, de 150 à 200°C. Les deux principaux facteurs à considérer sont le temps de demi-vie et la nature chimique de l'amorceur radicalaire. Le temps de demi-vie ($t_{1/2}$) de l'amorceur, doit être idéalement court par rapport au temps de séjour dans l'extrudeuse. Si le temps de séjour vaut cinq fois le temps de demi-vie, alors la consommation de l'amorceur est supérieure à 97%. Notre choix s'est donc porté sur le peroxyde de dicumyle ($t_{1/2}$=1min à 178°C). Le tableau 1 résume les principales expériences qui ont été réalisées.

Tableau 1: Conditions expérimentales du greffage de pentadécane sur MWCNTs.

Echantillon	Constituants	Température, Temps	Produit attendu
A	MWCNTs (50mg) +DCP(0.23g) +Pentadecane (7.69g)	150°C for 6 hours	Penta-g-MWCNTs
B-1	Blank experiment: DCP(0.23g) +Pentadecane (7.69g)	150°C for 6 hours	Interlinked pentadecane
B-2	Blank experiment: MWCNTs (50mg) +DCP(0.23g) + DMF (5 mL)	150°C for 6 hours	Cumyloxyl-g-MWCNTs
C	MWCNTs (50mg) +DCP(0.23g) +Pentadecane (7.69g)	At different temperatures for 6 hours	Penta-g-MWCNTs
D	MWCNTs (50mg) +DCP(different ratios) +Pentadecane (7.69g)	150°C for 6 hours	Penta-g-MWCNTs

Il est à noter que l'analyse GC-MS de l'échantillon B-1 (Tableau 1) a mis en évidence la formation de Aceto et 2p2p (Figure 1) et de chaînes pentadecane branchées caractéristiques de la présence de réactions de couplage radicalaire. L'ajout dans le milieu réactionnel de nanotubes de carbone (échantillon A, Tableau 1) a diminué la quantité de 2p2p formé c'est à dire que la réaction de B-scission a été défavorisée au profit d'une addition radicalaire de radicaux cumyloxy sur les MWCNTs (Figure 1). Le greffage radicalaire de pentadecane sur les nanotubes de carbone a été mis en évidence de façon qualitative par spectroscopie Raman et l'analyse quantitative par analyse élémentaire et analyse thermogravimétrique a permis de calculer une densité de greffage de 1,42mmol/g.

Nous avons aussi étudié l'effet de la température sur la densité de greffage. Nous avons donc fait varier la température de la réaction de 140°C à 180°C et, pour

une concentration en DCP de 3% en poids, nous avons observé que les densités de greffage variaient de 1,18 à 1,63 mmol/g pour des températures respectives de 140°C et 150°C (Tableau 2). Pour des températures supérieures à 160°C, la densité de greffage diminue jusqu'à 0,47mmol/g à 180°C avec formation d'insolubles (Tableau 2). Ces résultats indiquent que la réaction de B-scission des radicaux cumyloxy est favorisée à haute température au détriment de la réaction d'abstraction d'atomes d'hydrogène sur le pentadécane.

Tableau 2: Effect de la temperature de reaction sur la densité de greffage avec 3% en poids de DCP.

échantillon	T (°C)	A_{2p2p}/A_{Aceto}	A_{Penta}/A_{2p2p}	Percent grafting[a] (perte de poids en ATG)	Nombre de chaines par CNT[b]	densité de greffage[b]	
						(mg.m^{-2})	mmol.g^{-1}
C1	140	~9	~4	25	62800	0.108	1.180
C2	150	~10	~4	31	77900	0.134	1.463
C3	160	~9	~5	27	67800	0.117	1.278
C4	170	~4	~9	16	40200	0.069	0.754
C5	180	~3	~15	10	25100	0.043	0.470

[a] Basé sur les resultats ATG
[b] Basé sur un calcul en utilisant les données suivantes : CNT longueur = 5µm and diamètre de 13nm.

En considérant une température optimale de réaction de 150°C, nous avons ensuite étudié l'influence de la concentration en DCP sur la réaction de greffage. En faisant varier la concentration en DCP de 0,5% en poids à 5% en poids, nous avons observé que la densité de greffage du pentadecane diminuait de 1,46mmol/g à 0,37mmol/g par augmentation de la concentration en DCP de 3% en poids à 5% en poids. Cette tendance a été attribuée à l'augmentation des réactions de couplage inter-radicaux par augmentation de la concentration en radicaux dans le milieu. Les conditions expérimentales optimales pour le greffage du pentadécane sur NTCs sont donc : DCP=3w% et T=150°C.

La stabilité des suspensions de nanotubes de carbone greffés pentadécane dans des solvants tels que le DMF, le Toluène, le Dchlorobenzène et le Xylène a aussi

été appréhendée. Pour une densité de greffage de 1,46mmol/g, les solubilités ont varié de 1.1mg/mL (dans l'acétone) à 19.2mg/mL dans le dichlorobenzène.

L'état de dispersion des nanotubes de carbone fonctionnalisés a été exploré par microscopie électronique à transmission et les clichés montrent une diminution de la taille des agrégâts après le greffage de pentadécane (Figures 2 et 3).

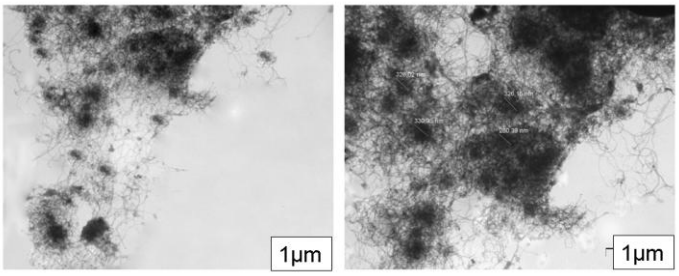

Figure 2 : Cliché MET des MWCNTs nus

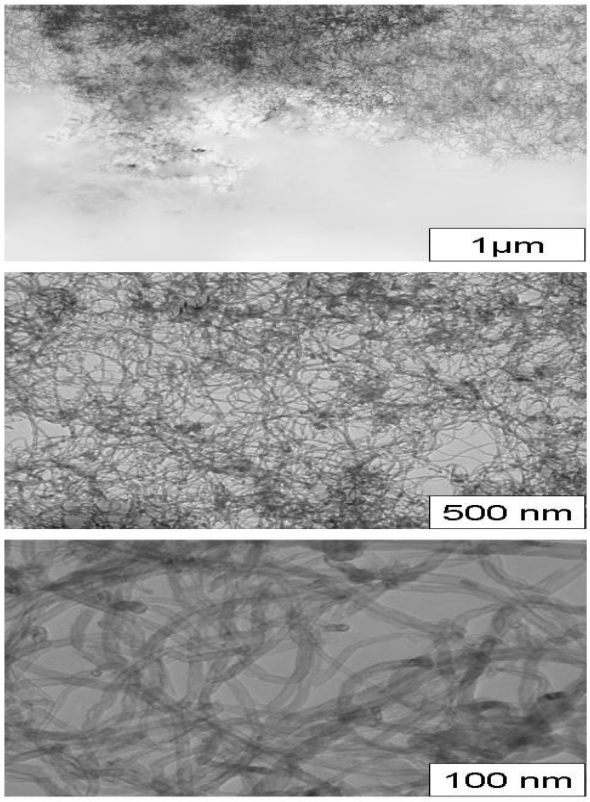

Figure 3 : Clichés MET des MWCNTs greffés pentadécane

L'étape suivante a été d'essayer de maitriser les réactions secondaires observées lors de la réaction de greffage radicalaire en introduisant dans le milieu des pièges à radicaux de type nitroxyde.

2. Greffage de pentadécane sur nanotubes de carbone en présence de radicaux nitroxyles

L'introduction de radicaux nitroxyles (TEMPO) au cours de la réaction de greffage du pentadecane sur les NTCs a été effectuée afin de diminuer les réactions de combinaison entre les radicaux de manière à augmenter la densité de greffage. L'utilisation de la chromatographie en phase gazeuse couplée à la spectrométrie de masse a permis de confirmer le rôle de piège à radicaux du TEMPO avec la formation d'espèces H_3C-TEMPO et la présence d'une très faible quantité d'espèces branchées (Figure 4).

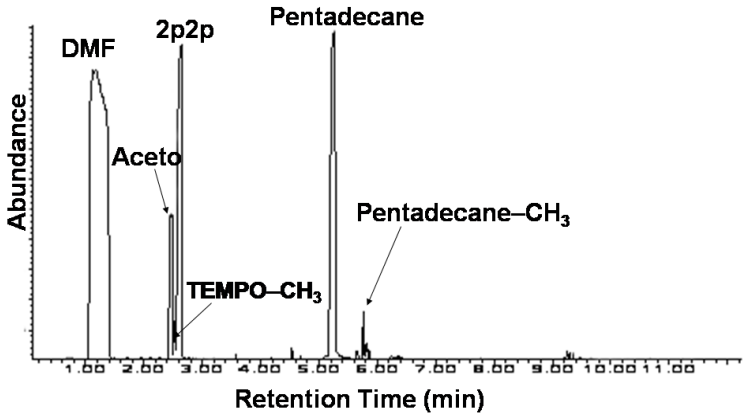

Figure 4 : Chromatogramme GC-MS du filtrat de la reaction de greffage du pentadecane en présence de TEMPO à T=160°C

Contrairement aux réactions en l'absence de TEMPO, la température optimale de greffage a été d'ici de 160°C pour une densité de greffage de 1,18mmol/g.

La présence de groupes TEMPO greffés sur les nanotubes de carbone a aussi été montrée par des tests de solubilités dans le THF. En effet, les suspensions de NTCs ne sont stables dans le THF que si la réaction de greffage du pentadécane a été

effectuée en présence de TEMPO c'est à dire que la polarité des groupes TEMPO fixés sur les NTCs les stabilise (Figure 5).

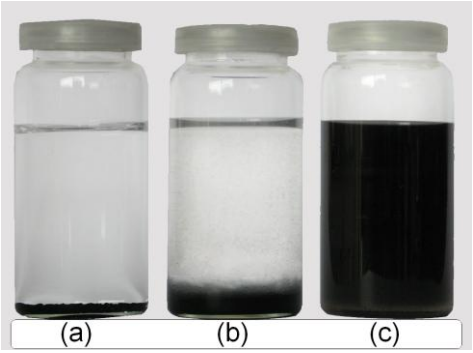

Figure 5: Stabilité des suspensions de MWNTCs dans le THF: MWCNTs nus après 5 min (a); pentadécane greffé sur MWCNTs après une semaine (b); pentadécane et TEMPO greffés sur MWCNTs après un mois (c).

3. Greffage radicalaire de polyéthylène (PEBD) sur nanotubes de carbone par diffrentes voies

Suite à l'étude modèle, nous avons exploré trois voies de greffage de PEBD sur NTCs :

1) fonctionnalisation radicalaire des NTCs par le PEBD sans TEMPO (échantillon 2, Tableau 3),

2) greffage radicalaire de PEBD en présence de TEMPO (échantillon 3, Tableau 3, Figure 6),

3) greffage radicalaire en présence d'oligomères de PE fonctionnels (échantillons 4-5, Tableau 3, Figure 7).

Tableau 3: Liste des échantillons et descriptif des conditions expérimentales

Echantillon	Description	Acronyme	Composition des réactifs
1	Crosslinked LDPE	PE_c	LDPE: 1g DCP: 0.03g Solvent: DCB 50ml
2	MWCNTs functionalisation by LDPE using DCP	PE-g-MWCNTs	MWCNTs: 50mg LDPE: 1g DCP: 0.03g Solvent: DCB 50ml
	Samples 2-A and 2-B were prepared with PE having mol. wt. ~1400 and 700 $g.gmol^{-1}$ respectively instead of LDPE.		
3	MWCNTs functionalisation by LDPE using DCP and TEMPO	PE.TEMPO-g-MWCNTs	MWCNTs: 50mg LDPE: 1g DCP: 0.03g TEMPO: 0.25g Solvent: DCB 50ml
4	MWCNTs grafted via TEMPO functionalised PE	$PE_{f\text{-}TEMPO}$-g-MWCNTs	MWCNTs: 50mg $PE_{f\text{-}TEMPO}$: 1g Solvent: DCB 50ml
5	MWCNTs grafted via SH functionalised PE	$PE_{f\text{-}SH}$-g-MWCNTs	MWCNTs: 50mg DCP: 0.03g $PE_{f\text{-}SH}$: 1g Solvent: DCB 50ml

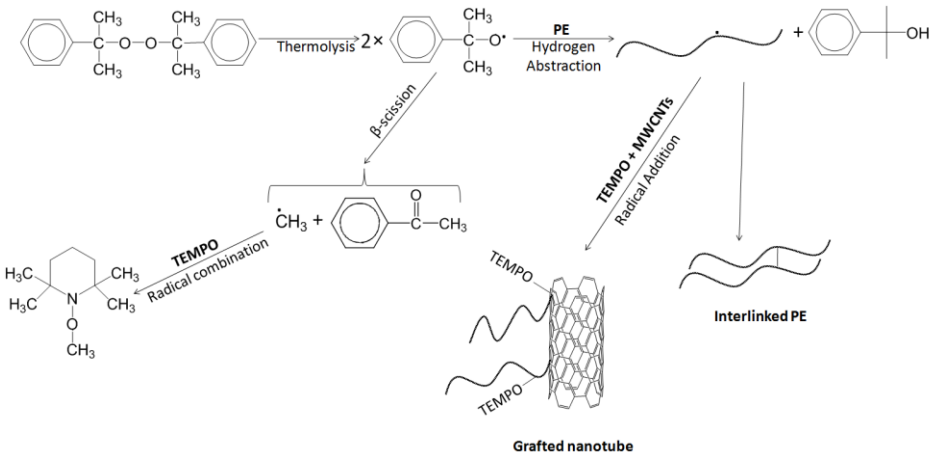

Figure 6: Greffage radicalaire de PEBD sur MWCNTs en présence de TEMPO

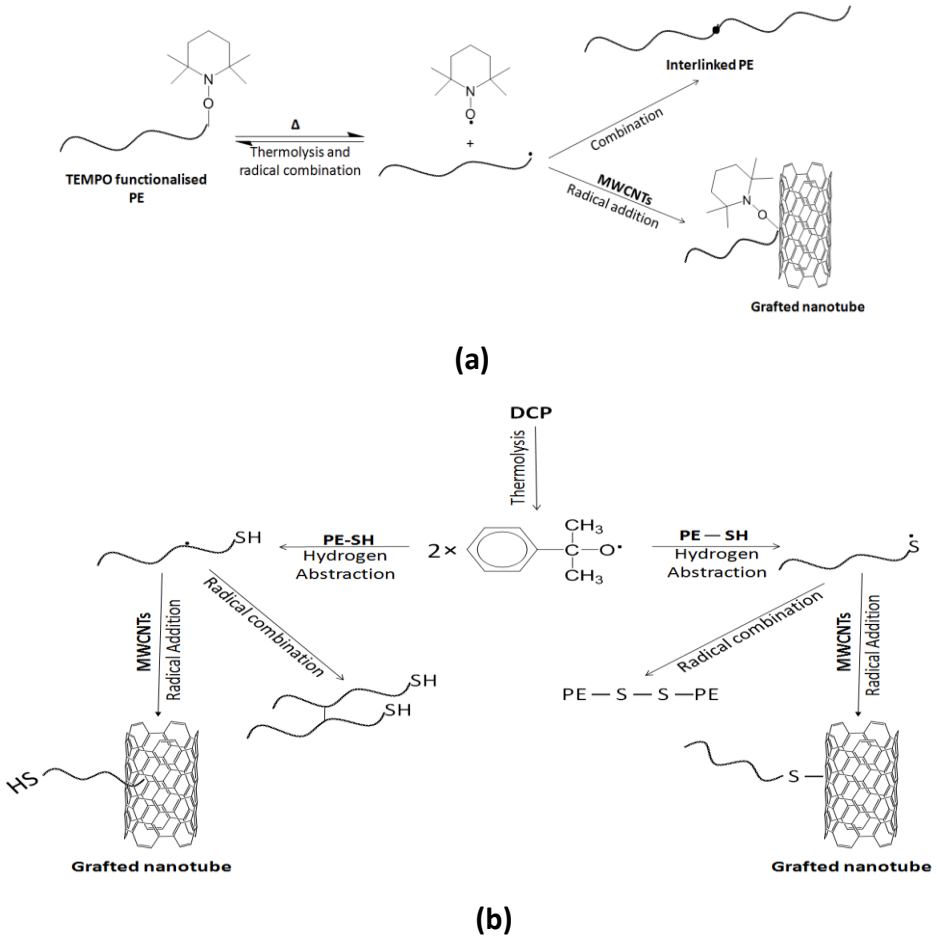

Figure 7: Reaction scheme for end functionalised PE grafting onto MWCNTs: (a) via PE-TEMPO; (b) via PE-SH

La reaction de greffage du PE sur NTCs a été montrée qualitativement par spectroscopie raman pour tous les échantillons concernés.

L'analyse quantitative a été réalisée par analyse thermogravimétrique et par analyse élémetaire. Les densités de greffage obtenues sont rassemblées dans le tableau 4.

Tableau 3. Effect of the grafting procedure on the degree of PE grafting.

Echantillon	Analyse élémentaire wt%	Densité de geffage du PE (TGA)		
		wt%	$mg.m^{-2}$	$\mu mol.m^{-2}$
2 PE-g-MWCNTs	H: 3.9	20	1.1	0.012
3 PE.TEMPO-g-MWCNTs	N: 0.5 H:4.9	24	1.4	0.015
4 $PE_{f\text{-}TEMPO}$ -g- MWCNTs	N: 0.3 H: 4.8	36	2.5	1.78
5 $PE_{f\text{-}SH}$-g-MWCNTs	S: 0.8 H: 3.8	34	2.3	2.8

N.B. Analyse élémentaire des MWCNTs shows: N, 0.78%; O, 0.89%; H, 0.30%; P, 1.81%.; S, <0.2%. Densités de greffage en $mg.m^{-2}$ basées sur l'utilisation d'une surface spécifique de 225 $m^2.g^{-1}$ pour les MWNTCs.

Les densités de greffage obtenues varient de 1,1$mg.m^{-2}$ ou 0.015$\mu mol.m^{-2}$ (échantillon 2, Tableau 3) à 2,5$mg.m^{-2}$ (échantillon 4, Tableau 3). L'incorporation de TEMPO dans le milieu réactionnel de l'échantillon 2 permet d'augmenter légèrement sa densité de greffage à 1,4 $mg.m^{-2}$ (échantillon 3, Tableau 3). Par contre, l'utilisation d'oligomères de polyéthylène à terminaison de type nitroxyde et de type thiol permet d'améliorer la densité de greffage du PE d'environ un facteur 2.

Des expériences de pyrolyse couplées à la GC-MS (Figure 8) sur les échantillons 3,4 et 5 (Tableau 3), ont permis de montrer la présence de fragments à base de TEMPO dans les échantillons 3 et 4 et de souffre dans l'échantillon 5.

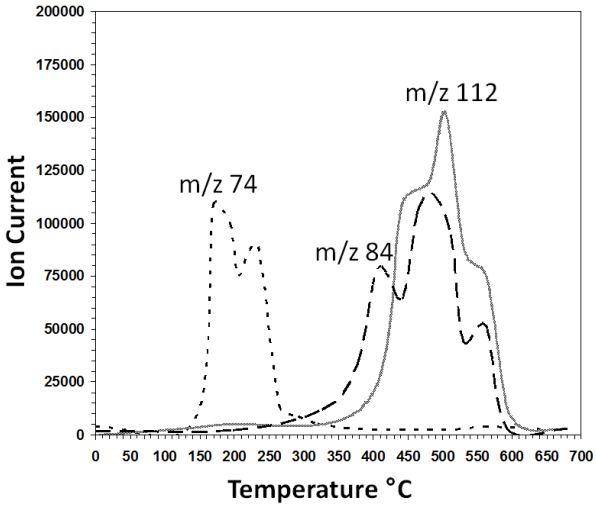

Figure 8 : Pyrogramme du PE.TEMPO-g-MWCNTs (échantillon 3, Tableau 3) dans la gamme de température 100-600°C . Ion current vs time pour m/z 74, 84, et 112 correspondants au TEMPO, C4H8 et C5H10 respectivement.

Par ailleurs, les images MET (Figure 9) ont clairement clairement indiqué, quelque soit l'échantillon, que les NTCs ont été uniformément recouverts de la couche de polyéthylène, formant des structures de type cœur NTCs-écorce PE avec une épaisseur variant de 1,5 nm à 4.1nm.

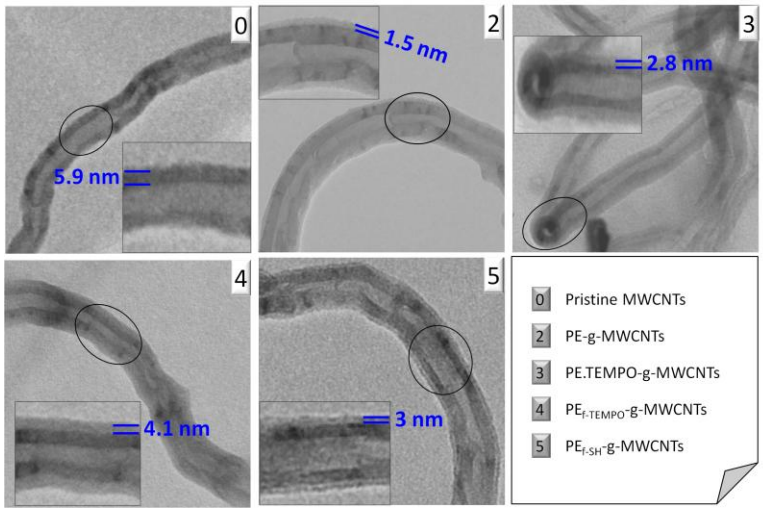

Figure 9: TEM pictures of p-MWCNTs (0); PE-g-MWCNTs (2); PE.TEMPO-g-MWCNTs (3) ; PEf-TEMPO-g-MWCNTs (4); PEf-SH-g-MWCNTs (5).

Selon la même procédure de greffage radicalaire, le polypropylène a été greffé sur les NTCs.

4. Greffage radicalaire de polypropylène (PP) sur nanotubes de carbone

En utilisant la même stratégie que celle utilisée pour le greffage de PE sur NTCs, nous avons étudié le greffage de PP sur NTCs. La première étape a été de réaliser une étude modèle en simulant le polypropylène par du tétraméthylpentadecane (TMP) (Figure 10).

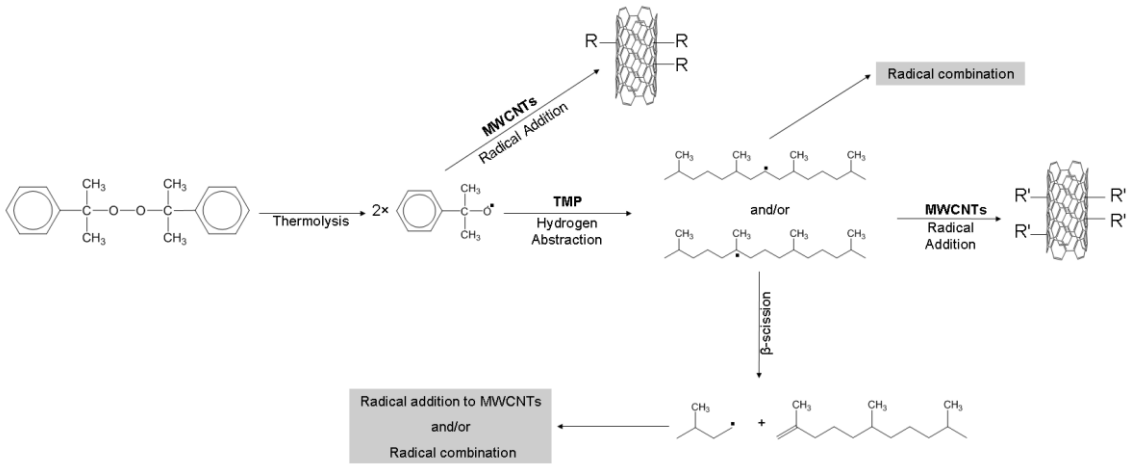

Figure 10: Greffage du TMP sur NTCs en présence de DCP.

Les conditions optimales de greffage du TMP ont été obtenues avec une température de 160°C et une concentration en DCP de 12% en poids. La densité de greffage obtenue dans ces conditions expérimentales a été de 0,78mg.m^{-2}. Néanmoins, afin de limiter la dégradation très probable du PP (réaction de B-scission)en présence d'une forte concentration en DCP, nous avons choisi de poursuivre l'étude avec une concentration classique en DCP de 1,5% en poids.

L'effet de solvant sur la réaction de greffage du TMP a été appréhendé dans le diméthylformamide (DMF), le dichlorobenzène (DCB) et le TMP (procédé « en masse »). Les densités de greffage obtenues ont été de 0,43 mg.m^{-2}, 0,75mg.m^{-2} et de 0,92mg.m^{-2}, respectivement. L'addition des radicaux issus du TMP sur les NTCs est donc défavorisée en milieu dilué.

L'utilisation du dodécanethiol (DT) à la place du TMP pour générer des radicaux localisés sur les bouts de chaîne après une réaction de transfert n'a pas permis d'amélorer la densité de greffage et bien au contraire. En effet, dans ce cas nous avons obtenu une densité de greffage voisine de 0,2 $mg.m^{-2}$. Cette faible valeur montre que l'addition des radicaux soufrés sur les NTCs est moins efficace que celle des radicaux carbonés ce qui a déjà été démontré sur C_{60}.

Le comportement des NTCs greffés TMP, DT et DCP en solution a ensuite été étudié dans différents solvants (Figure 11).

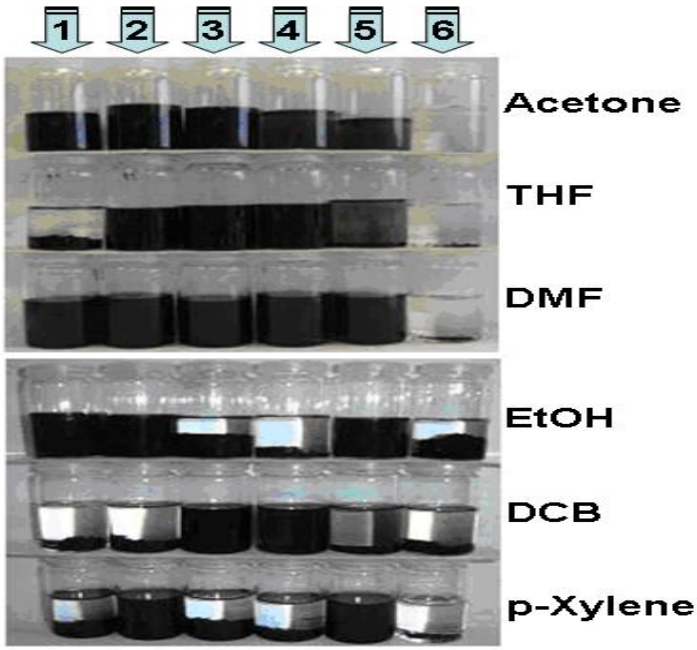

Figure 11 : Comportement des suspensions de (1) DT-g-MWCNTs, (2) DCP-g-MWCNTs, (3) TMP-g-MWCNTs (0.92 mg m^{-2}), (4) TMP-g-MWCNTs (0.75 mg m^{-2}), (5) TMP-g-MWCNTs (0.43 mg m^{-2}), (6) MWCNTs dans différents solvants.

Les NTCs nus donnent des suspensions instables dans la plupart des solvents mais les NTCs greffés TMP donnent des suspensions stables dans l'acetone, le THF, le DMF et le DCB (Figure 11). Contrairement aux NTCs greffés TMP, les NTCs greffés DT ont donné des suspensions stables dans l'éthanol suggérant que l'atome de souffre présent augmente la polarité des NTCs. L'insatbilité des suspensions de NTCs greffés DT dans le THF et le DCB peut être attribuée à la plus faible densité de greffage du DT par rapport à celle du TMP (0,20 mg m^{-2} et 0,43 mg m^{-2}, respectivement). La

haute densité de geffage du TMP sur les NTCs (0.92 mg m^{-2}) a permis d'obtenr des valeurs de solubilité de 8,7 ; 23,2 et 20,9 mg mL^{-1} dans le DMF, l'acetone et le THF, respectivement alors que le pentadecane greffé NTCs a une solubilité de 1.1 mg mL^{-1} dans l'acetone et n'est pas soluble dans le THF.

Pour la première fois, le PP a ensuite été greffé sur les NTCs à 160°C en présence de 1,5% en poids de DCP dans une solution de DCB. L'analyse ATG des NTCs greffés PP (purifiés par une extraction au soxlhet de DCB) n'a pas permis d'obtenir des résultats reproductibles. Cependant, nous avons quand même étudié la morphologie de ces NTCs greffés PP par microscopie électronique à transmission (Figure 12).

Les images MET révèlent la présence de nanotubes de carbone individualisés pour les NTCs greffés TMP ainsi que ceux greffés PP ce qui montre que l'étape de fonctionnalisation permet de désagréger les NTCs initiaux. De plus, les images indiques la présence de « bosses » sur les NTCs ce qui est carctéristique de la présence de groupes organiques sur les NTCs.nL'étude par microscopie électronique à balayage (SEM) de nanocomposites PP-*g*-MWCNTs dispersés à 3t% en poids n'a pas montré une amélioration significative de la dispersion des NTCs dans la matrice PP même si la taille des agrégâts de NTCs a été réduite (Figures 13a et 13b).

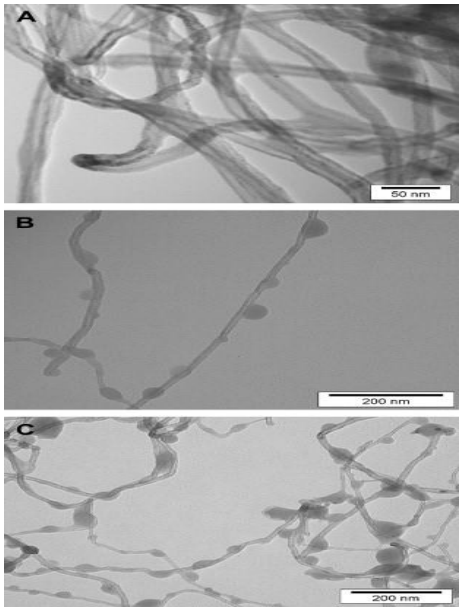

Figure 12: Images MET de (A) MWCNTs nus, (B) *TMP*-g-MWCNTs, (C) PP-g-MWCNTs.

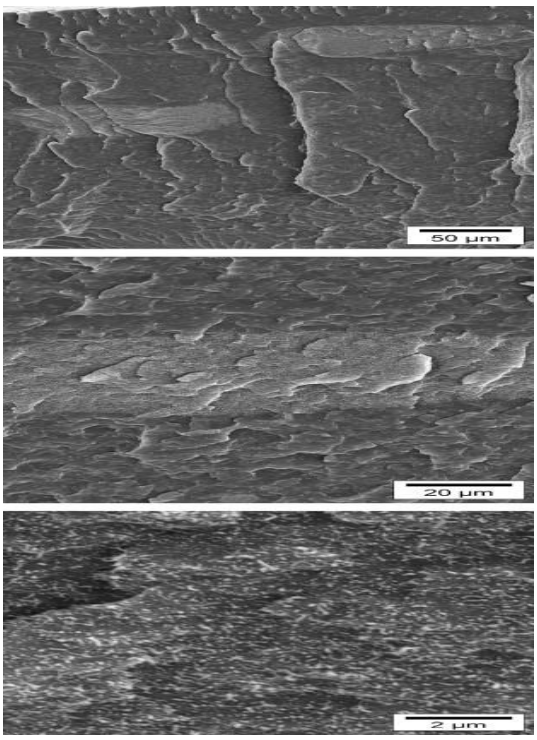

Figure 13a: images SEM de composites PP/MWCNTs avec 3w% de MWCNTs

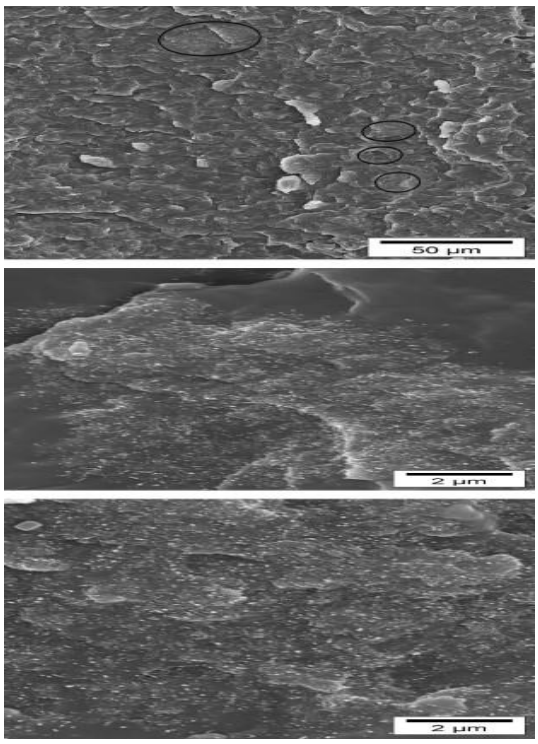

Figure 13b: images SEM de composites PP/PP-g-MWCNTs avec 3w% de MWCNTs

Conclusions

L'idée de greffer le PE et le PP sur les nanotubes de carbone (NTCs) en présence peroxyde de dicumyle (DCP) pendant une opération d'extrusion est un challenge. Nous avons envisagé que les radicaux cumlyoxly issus de la thermolyse du DCP seraient capables d'arracher des atomes d'hydrogène sur les chaînes de polyoléfine pour générer des macroradicaux susceptibles de s'additionner sur les NTCs. L'intérêt majeur de cette voie radicalaire est que la durée de vie très courte des radicaux est compatible avec un temps de séjour faible en extrudeuse. Par contre, la faible chimiosélectivité des espèces radicalaires formées impliquent la présence de nombreuses réactions secondaires (coupure de chaînes, réticulation, combinaison).

Pour optimiser la réaction de greffage de PE sur NTCs, nous avons donc réalisé une étude modèle en sélectionnant le pentadecane pour simuler le PE. L'étude GC-MS des produits formés au cours de la réaction de greffage ont permis d'optimiser les conditions expérimentales de greffage qui nous ont permis d'obtenir une densité de greffage du pentadecane sur NTCs de 1.46 mmol/g at 150 °C. A des températures plus élevées, nous avons constaté une diminution de la densité de greffage à cause de la réaction de β-scission reaction des radicaux cumyloxy. L'addition de radicaux nitroxyles dans le milieu réactionnel pour contrôler les réactions secondaires (et en particulier la réaction de combinaison des radicaux) a permis d'améliorer sensiblement la densité de greffage du pentadecane sur NTCs. De plus, les NTCs greffés pentadécane ont montré une bonne stabilité dans divers solvants et nous avons obtenu une solubilité de 19.2 mg/mL dans le dichlorobenzene pour une densité de greffage de 1.46mmol/g.

Le greffage de PE sur NTCs dans les mêmes conditions expérimentales que celles utilisées pour le pentadecane a été moins efficace que celui du pentadécane même si nous avons pu former des structures de type cœur NTC-écorce PE. Nous avons aussi sondé le greffage radicalaire d'oligomères de PE fonctionnels sur NTCs. Des oligomères de PE terminés TEMPO et thiol ont donc été greffés avec succès sur les NTCs avec une densité de greffage nettement supérieure à celle obtenue à partir d'un PE commercial.

Avec la même stratégie, nous avons simulé le greffage du PP sur NTCs à partir du tétraméthylpentadécane (TMP). Nous avons obtenu des solubilités variant de 4.8 mg/mL dans l'éthanol à 23.2 mg/mL dans l'acétone. En ce qui concerne le greffage de PP sur NTCs nous n'avons pas pu donner de valeur de densité greffage faute de reproductibilité des résultats. L'étude par microscopie électronique à balayage (SEM) de nanocomposites PP-*g*-MWCNTs dispersés à 3t% en poids n'a pas montré une amélioration significative de la dispersion des NTCs dans la matrice PP même si la taille des agrégâts de NTCs a été réduite.

Il reste maintenant à étudier cette méthode de greffage radicalaire de polyoléfines sur NTCs dans une extrudeuse sachant que nous avons montré que cette technique de fonctionnalisation est une bonne approche pour désagréger les NTCs et améliorer leurs stabilité en milieu solvant. Il restera aussi à étudier les propriétés mécaniques et électriques des composites correspondants.

RESUME en français

Les nanotubes de carbone (NTCs) sont des charges particulièrement intéressantes car ils présentent des facteurs de forme (longueur/diamètre) très élevés. Cependant, le développement de ces applications à haute valeur ajoutée a été freiné par les problèmes de mise en œuvre des NTCs. Cependant, le développement de ces applications à haute valeur ajoutée a été freiné par les problèmes de mise en œuvre des NTCs (résultant de la difficulté de les disperser dans un milieu polymère) et par la formation d'agrégats de nanotubes en « fagots », ne permettant pas l'obtention de mélanges homogènes. La solution réside dans la fonctionnalisation des nanotubes avec des chaînes polymères afin de réduire l'effet des interactions entre NTCs et d'assurer une meilleure comptabilisation avec le polymère hôte au cours du mélange. Ici, nous nous sommes intéressés à la fonctionnalisation des nanotubes de carbone par des polyoléfines en utilisant une procédure de greffage radicalaire de type « grafting onto ».

TITRE en anglais

Radical grafting of polyolefins onto multi-walled carbon nanotubes: Model study and application to manufacture PE & PP composites

RESUME en anglais

Carbon nanotubes (CNTs) as filler are particularly interesting because they possess very high aspect ratio (length/diameter), typically up to 10,000. Hence, they can form conductive path in polymer matrix at much lower concentrations (below 5%), whereas in case of carbon black filler more than 20wt% loading is needed. However, the development of applications based on nanotubes with high value addition has been hampered by processing limitations resulting from the difficulty of dispersing in a polymeric medium. The formation of aggregates or bundles of nanotubes into host polymer do not allow obtaining homogeneous mixtures. The solution lies in the functionalisation of nanotubes with polymer chains to reduce the effect of interactions between CNTs and better compatibility with the host polymer in the mixture. Here, in this study, we aim to functionalise carbon nanotubes by using a polyolefin grafting procedure involving radical 'grafting onto'.

DISCIPLINE

MATERIAUX POLYMERES ET COMPOSITES

MOTS-CLES

Polyéthylène, polypropylène, nanotubes de carbone, composites, pentadecane, greffage radicalaire, TGA, EA, GC-MS, TEM, Raman spectroscopie

INTITULE ET ADRESSE DE L'U.F.R. OU DU LABORATOIRE :

Ingénierie des Matériaux Polymères CNRS UMR 5223: Laboratoire des Matériaux Polymères et Biomatériaux, 15 boulevard Latarget, F-69622 Villeurbanne, France